

DISSERTATION

**BIODEGRADABLE POLYESTERS FROM
SOLID-STATE PRECURSORS**

**– BASIC COMPONENTS OF A
BIOMEDICAL MATERIALS CONCEPT**

ZUR ERLANGUNG DES DOKTORGRADES DES FACHBEREICHS CHEMIE
DER UNIVERSITÄT HAMBURG

VORGELEGT VON

KARSTEN SCHWARZ

AUS MARNE

HAMBURG 2001

Die vorliegende Arbeit entstand im Zeitraum Oktober 1997 bis April 2001 im Institut für Anorganische und Angewandte Chemie des Fachbereichs Chemie der Universität Hamburg.

1. Gutachter: Prof. Dr. M. Epple
2. Gutachter: Prof. Dr. D. Rehder

Tag der mündlichen Prüfung: 25.06.2001

"Health, Wealth, Love - and the time to enjoy it !"

Spanish Toast

Meiner Familie und meinen Freunden zum Dank

Table of Contents

<u>General introduction</u>		<u>Page</u>
GI.1	Polyesters as biomaterials.....	1
GI.2	Conventional vs. solid-state chemical synthesis of polyglycolide.....	6
GI.3	Bone and bone substitution.....	10
GI.4	Aim of this work.....	15
<u>Part A: Polyesters from solid-state precursors</u>		
AI. The formation of polyglycolide from sodium chloroacetate		
AI.0	Introduction.....	16
AI.1	Results and discussion.....	20
	<i>Identity of solid-state chemically prepared PGA.....</i>	<i>20</i>
	<i>Reaction extent.....</i>	<i>24</i>
	<i>Chain growth and degree of polymerization.....</i>	<i>26</i>
	<i>Development of crystallinity.....</i>	<i>30</i>
	<i>Porosity of the formed polyglycolide.....</i>	<i>31</i>
AI.2	Concluding remarks.....	34
AI.3	Materials and methods.....	35
AII. The <i>in vitro</i> degradation of polyglycolide from solid-state reaction		
AII.0	Introduction.....	41
AII.1	Results and discussion.....	48
	<i>Geometric stability.....</i>	<i>50</i>
	<i>Morphology and degradation mechanism.....</i>	<i>53</i>
	<i>Development of average molecular weight.....</i>	<i>55</i>
	<i>Water uptake and mass loss (erosion).....</i>	<i>56</i>
	<i>Degree of crystallinity.....</i>	<i>58</i>
	<i>Mechanical testing: Young`s modulus and fracture toughness.....</i>	<i>59</i>
AII.2	Concluding remarks.....	60
AII.3	Materials and methods.....	61

AIII.	The transposition to higher homologues: 3-Cl-butyrate and Cl-pivalate	
AIII.0	Introduction.....	64
AIII.1	Results and discussion.....	70
	<i>Metal 3-Chloro-butyrate</i>	70
	<i>Na 3-Cl-butyrate</i>	73
	<i>Ag 3-Cl-butyrate</i>	84
	<i>Na Cl-pivalate</i>	87
AIII.2	Concluding remarks.....	91
AIII.3	Materials and methods.....	91

Part B: Composites of polyglycolide and calcium phosphate

B.0	Introduction.....	98
B.1	Results and discussion.....	104
	<i>Fabrication of composite bodies with calcium phosphates</i>	104
	<i>Adjustment of external pH-value of composite bodies</i>	105
	<i>Testing for biocompatibility with murine osteoblasts</i>	109
	<i>Structuring of composite bodies</i>	115
B.2	Concluding remarks.....	119
B.3	Materials and methods.....	120

<u>General conclusion</u>	125
--	-----

Appendix

Zusammenfassung (Summary in German).....	130
Kurzzusammenfassung (Short summary).....	136
Sicherheit und Entsorgung (Toxicity).....	138
Danksagungen (Acknowledgements).....	142
List of publications.....	144
Lebenslauf (Biography).....	148
Erklärungen (Declarations).....	149

List of acronyms (in alphabetical order)

AgClAc	- silver chloroacetate	mp.	- melting point
BSE	- bovine spongiform encephalopathy	MS	- mass spectrometry
CACP	- carbonated amorphous calcium phosphate	NaBrAc	- sodium bromoacetate
calc.	- calculated	NaClAc	- sodium chloroacetate
CaP	- calcium phosphates	NaIAc	- sodium iodoacetate
CAP	- carbonated apatite	NMR	- nuclear magnetic resonance
CsClAc	- cesium chloroacetate	orig.	- original
DIN	- Deutsche Industrie Norm	PBS	- phosphate buffered saline
DSC	- differential scanning calorimetry	PBT	- poly(butylene terephthalate)
DTA	- differential thermal analysis	PCL	- poly(ϵ -caprolactone)
EA	- elemental analysis	PDS	- poly(p-dioxanone)
ECM	- extracellular matrix	PEO	- poly(ethylene oxide)
EI	- electron ionization	PET	- poly(ethylene terephthalate)
eq.	- equation	PGA	- poly(glycolic acid)
EXAFS	- extended X-ray absorption fine structure	PHB	- poly(hydroxybutyric acid)
FAB	- fast atom bombardment	PHV	- poly(hydroxyvaleric acid)
FDA	- American Food and Drug Administration	PLA	- poly(lactic acid)
fig.	- figure	PVA	- poly(vinyl alcohol)
GI.	- general introduction	RbIAc	- rubidium iodoacetate
HAP	- hydroxyapatite	ref.	- reference
HFIP	- hexafluoroisopropanol	SAXS	- small angle X-ray scattering
HIV	- human immune-deficiency virus	SBF	- simulated body-fluid
ICI	- Imperial Chemical Industries	SEC	- size exclusion chromatography
IR	- infrared spectroscopy	SEM	- scanning electron microscopy
IUPAC	- International Union of Pure and Applied Chemistry	TCP	- tricalcium phosphate
LiBrAc	- lithium bromoacetate	TG	- thermogravimetry
LiClAc	- lithium chloroacetate	theor.	- theoretical
LiIAc	- lithium iodoacetate	THF	- tetrahydrofuran
magn.	- magnification	TXRD	- temperature-resolved X-ray powder diffraction
MALDI-TOF	- matrix-assisted laser desorption ionization time of flight	vs.	- versus
MEM	- minimum essential medium	WAXS	- wide angle X-ray scattering
		XRD	- X-ray powder diffraction

Foreword

During evolution many organisms from plants and bacteria to human beings developed highly optimized hybrid material constructs that serve purposes like protection, mechanical stability, orientation, compartmentation or as element storage systems. Prominent examples for such constructs are snail-houses, mussel-shells, teeth and of course the human skeleton. The formation and maintenance is a result of complex multi-dimensional phenomena like tissue architecture, diffusion control, genetic protein targeting and cell activity. Bulk materials (e.g., calcium carbonate, calcium phosphate) are combined with macromolecules to composites with unique properties. To understand these processes and apply the principles to the design of synthetic products requires interdisciplinary efforts. The analysis and reconstruction of hard tissues is a challenge to different scientists to uncover nature`s strategies in material functionalization.

General introduction

GI.1 Polyesters as biomaterials

Aliphatic polyesters gained attention in the second half of the twentieth century when scientists and companies became aware of the advantageous properties of this polymer family¹ for some applications starting with the substitution of natural collagen fibers (“catgut”) as suture material for wound closure². It was speculated about applications where the chemical and biological degradability³ of the polyesters (i.e., susceptibility towards hydrolysis, enzymatic breakdown), hitherto regarded as a strong disadvantage for material storage and use, could be exploited to address specific purposes. From an ecological point of view, biodegradable polyesters are ideal materials for example for mulch films, seed or fertilizer capsules in agriculture⁴ or packaging purposes like shampoo bottles⁵. Hydrolytic degradation and subsequent metabolization by microorganisms lead to carbon dioxide and water as “residues”. This reduces the amount of persistent garbage on municipal solid waste disposals. Despite these properties, the substitution of commodity polymers like polyolefins is restricted because of the comparatively high production price of aliphatic polyesters^{1,4,6}.

The main field of application of biodegradable polyesters is therefore found in biomedical technology and pharmaceuticals where the price is secondary compared to desired material properties. **Fig.GI.1-1** gives a compilation of the most important homopolyesters in biomedical technology. For the sake of brevity the compounds are given with their ubiquitous trivial names and acronyms. The IUPAC nomenclature of the corresponding polymers can be found in ref.⁷.

Various combinations of copolymers have been synthesized, mainly of the systems PGA/PLA, PLA stereo-copolymers and PHB/PHV to alter the properties of the

¹ M. Vert, G. Schwarch, J. Coudane “Present and future of PLA polymers”, *J.M.S.- Pure Appl. Chem.* **1995**, A32(4), 787-796.

² E.J. Frazza, E.E. Schmitt “A new absorbable suture”, *J. Biomed. Mater. Res. Symp.* **1971**, 43(1), 43-58.

³ J.P. Singhal, H. Singh, A.R. Ray „Absorbable suture materials: Preparation and properties“, *J.M.S.- Rev. Macrom. Chem. Phys.* **1988**, C28(384), 475-502.

⁴ P.J. Hocking “The classification, preparation, and utility of degradable polymers”, *J.M.S.- Rev. Macrom. Chem. Phys.* **1992**, C32(1), 35-54.

⁵ D. Seebach, A. Brunner, B.M. Bachmann, T. Hoffmann, F.N.M. Kühnle, U.D. Lengweiler “Biopolymers and –oligomers of (R)-3-hydroxyalkanoic acids – Contributions of synthetic organic chemists“, *Lectures of the Ernst Schering Foundation* **1995**, 28.

⁶ J.-U. Ackermann, W. Babel “Approaches to increase the economy of the PHB production”, *Polym. Degrad. Stab.* **1998**, 59, 183-186.

⁷ A.D. Jenkins, K.L. Loening “Nomenclature” in *Comprehensive polymer science*, vol. 1, Pergamon, Oxford, New York, Beijing, Frankfurt, Sao Paulo, Sydney, Tokyo, Toronto, 1989, 13-55.

homopolymers in the desired way.

Among the biodegradable polyesters poly(α -hydroxy esters) like polyglycolide or polylactide play a predominant role in clinical application. The American Food and

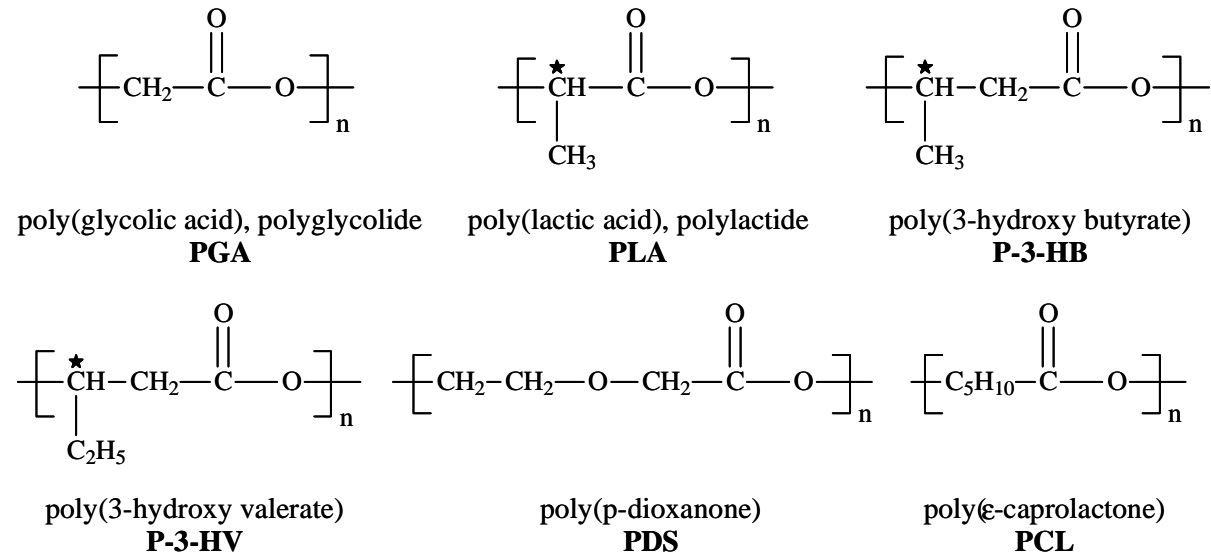


Fig.GI.1-1 Prominent homopolyesters in biomedical technology

Drug Administration (FDA) has approved poly(α -hydroxy esters) for human clinical use as resorbable sutures and drug carriers⁸. There is a consensus that these polymers can be termed biocompatible. Biocompatibility has been defined⁹ as the ability of a material, prosthesis, artificial organ, or biomedical device to perform with an appropriate host response in a specific application. Vert et al.¹⁰ more explicitly summed up the criteria for a material *in vivo* to be biocompatible:

- no systemic toxic effects of the material itself, degradation products or by-products
- no or minimal adverse reaction or inflammation (macrophages, giant cells)
- no cytotoxicity with respect to cell proliferation and function
- no carcinogenicity or thrombogenicity of the material and its metabolites

These definitions can be regarded as ideal requirements. PGA and PLA meet these requirements in most documented cases although the discussion is still controversial. In some studies inflammation, necrotic surrounding tissue, or other complications were

⁸ S.L. Ishaug, M.J. Yaszemski, R. Bizios, A.G. Mikos "Osteoblast function on synthetic biodegradable polymers", *J. Biomed. Mater. Res.* **1994**, 28, 1445-1453.

⁹ J.M. Anderson "Biocompatibility of tissue engineered implants" in *Frontiers in tissue engineering*, Pergamon, Oxford, New York, Tokyo, **1998**, 152-165.

¹⁰ M. Vert, S.M. Li, G. Spenlehauer, P. Guerin "Bioresorbability and biocompatibility of aliphatic polyesters", *J. Mater. Sci.: Mater. In Med.* **1992**, 3, 432-446.

reported¹¹. The opportunity and acceptance to use polyesters *in vivo* offered a variety of applications of which the core fields are described in the following passages:

Polyester matrices are used for controlled drug release¹² where a drug (e.g., proteins, hormones, antibiotics, vitamins) is loaded into a compact or structured polymeric material. The release profile is a function of parameters like interdiffusion (contact angle, accessibility for water, porosity), bonding between drug and matrix as well as degradation mechanism and behavior¹³. The ultimate goal for this application is the design of matrix/drug constructs with controlled release rate to provide the appropriate dosage over a fixed time period¹⁴. In most projects fully or partially amorphous polyesters like poly(lactide-co-glycolide) were used. Release kinetics up to 4 months were reported^{12,15}. As another example, polyglycolide¹⁶ was mixed with an active substance, processed into pellets and annealed at temperatures from 40-120 °C. Release rates differed from 2 hours to 1 day for complete washout.

A prerequisite for successful controlled drug release is the choice of polyester and the investigation of the degradation *in vitro* in media like water or (better) body fluid-simulating solutions. As a consequence of the variety of parameters affecting release performance, variations in polymer characteristics (e.g., crystallinity, average chain length, dispersity, porosity, thermal transition points) can lead to different matrix properties.

A relatively new interdisciplinary research field emerged and developed in the last decade: the reconstruction and replacement of damaged tissues and organs – Tissue Engineering. The *terminus technicus* ‘tissue engineering’ is defined as “*the application of the principles and methods of engineering and the life sciences towards the fundamental understanding of structure-function relationships in normal and pathological mammalian tissues and the development of biological substitutes that*

¹¹ K.A. Athanasiou, G.G. Niederauer, C.M. Agrawal “Sterilization, toxicity, biocompatibility and clinical applications of polylactic acid/polyglycolic acid copolymers”, *Biomaterials* **1996**, *17*, 93-102.

¹² R. Langer “Drug delivery and targeting”, *Nature* **1998**, *392*, 5-10.

¹³ M.A. Tracy, K.L. Ward, L. Firouzabadian, Y. Wang, N. Dong, R. Qian, Y. Zhang “Factors affecting the degradation rate of poly(lactide-co-glycolide) microspheres *in vivo* and *in vitro*”, *Biomaterials* **1999**, *20*, 1057-1062.

¹⁴ R.T. Bartus, M.A. Tracy, D.F. Emerich, S.E. Zale “Sustained delivery of proteins for novel therapeutic products”, *Science* **1998**, *281*, 1161-1162.

¹⁵ M.R. Kreitz, J.A. Domm, E. Mathiowitz “Controlled delivery of therapeutics from microporous membranes. II. *In vitro* degradation and release of heparin-loaded poly(D,L-lactide-co-glycolide)”, *Biomaterials* **1997**, *18*, 1645-1651.

restore, maintain, or improve tissue function”¹⁷. Aims of this technology comprise *in vitro* seeding, proliferation and differentiation of cells on scaffold materials. The cultivated cells have to be autologous by nature to circumvent adverse reactions after implantation in the host organism. Most of the current research is focused on the evaluation of suitable matrices in conjunction with seeding and incubation techniques for different cell phenotypes to generate “artificial” tissue. PGA/PLA homo- and copolymers proved to be appropriate scaffold materials for that purpose¹⁸. From the pool of biodegradable polymers, highly porous foams, meshes or membranes made from the named polyesters are predominantly used⁸. They are reported to allow cell attachment, high proliferation rates, undisturbed differentiation and the development of cell functions¹⁹. For cell association, the scaffold acts as the synthetic counterpart of guiding extracellular matrix (ECM) molecules in living tissues²⁰.

Although this new technique fights with restrictions and drawbacks, the successes in practical application are striking and encouraging. This is underlined by reports in mass media of skin or cartilage implantation after serious injuries. Biodegradable polyester scaffolds as carrier substances are closely linked to the development of this fast developing research complex.

In clinical surgery, polyesters presumably play the most important role in connection with the fixation, augmentation and replacement of bone. Devices like screws, plates, anchors, or pins serve for positioning and fixation of bone fragments²¹ after bone loss or damage through trauma or bone surgery. The idea to use biodegradable, biocompatible polyesters for such applications is based on the fact that in contrast to metallic implants a second operation for removal is not necessary²². Reduced costs for the public health system and less discomfort for patients are a consequence. In addition to this second operation, another important point is in favor of polymeric fixation

¹⁶ R. Ries, F. Moll “Matrix formation of polyglycolic acid tablets by annealing”, *Eur. J. Pharm. Biopharm.*, **1994**, 40(1), 14-18.

¹⁷ C.W. Patrick jr., A.G. Mikos, L.V. McIntire “Prospectus of tissue engineering” in *Frontiers in tissue engineering*, Pergamon, Oxford, New York, Tokyo, **1998**, 3.

¹⁸ K.J.L. Burg, S. Porter, J.F. Kellam “Biomaterial developments for bone tissue engineering”, *Biomaterials* **2000**, 21, 2347-2359.

¹⁹ K.C. Dee, R. Bizios “Mini-Review: Proactive biomaterials and bone tissue engineering”, *Biotechnol. Bioeng.* **1996**, 50, 438-442.

²⁰ H.L. Wald, G. Sarakinos, M.D. Lyman, A.G. Mikos, J.P. Vacanti, R. Langer “Cell seeding in porous transplantation devices”, *Biomaterials* **1993**, 14(4), 270-278.

²¹ W.S. Pietrzak, D. Sarver, M. Verstyne “Bioresorbable implants – Practical considerations”, *Bone* **1996**, 19(1), 109S-119S.

devices: the mechanical integration of the implant in the bone tissue. The comparatively stiff metal pins and screws lead to stress shielding and subsequent weakening of the surrounding bone²³. Processing of polymers offers a wider range of material properties adjustment. An example for a clinically extensively tested product is a screw made from polyglycolide developed by a research group from Finland²⁴. Rokkanen et al. employed a fiber spinning technique to fabricate a material termed 'self-reinforced' with values of bending strength and modulus close to human cortical bone. The structure of this woven fabric is shown in **fig.GI.1-2**.

The filling of defects in bone is another application for biodegradable polyesters. A common strategy forms the background for the incorporation of biodegradable materials into bone: the implant is designed for temporary function to allow a healing

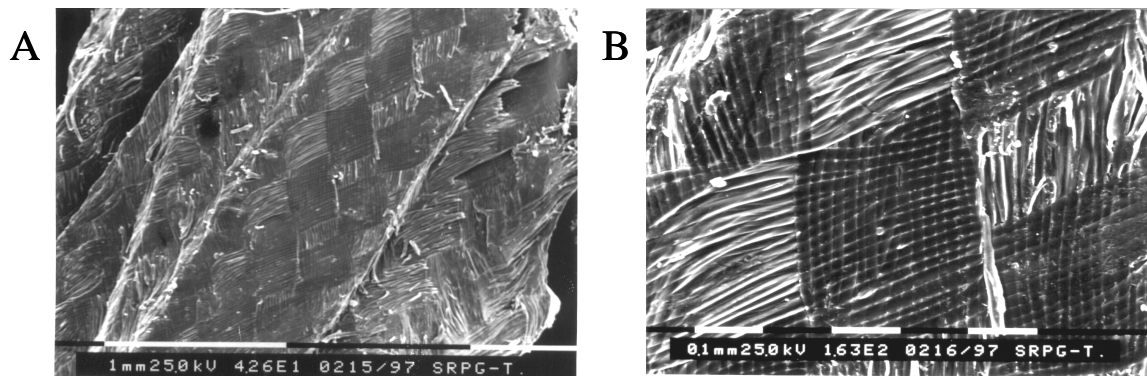


Fig.GI.1-2 Fiber-structure of a self-reinforced PGA screw (A: 43x, B: 163x)

process and to retain strength during the early stages after operation. The loss of strength and modulus of the implant should be in harmony with the increasing strength of the injured tissue²⁵. Proceeding degradation creates space for restoring processes to fill the gap with ingrown vital host tissue.

Presently, no filling material is available that fits this profile satisfactorily to form new homogeneous bone in large defects²⁶. The interaction of host tissue and implant is of extremely complex nature and up to now no complete picture exists. Therefore there is

²² J.M. Rueger "Knochenersatzmittel – Heutiger Stand und Ausblick", *Der Orthopäde* **1998**, 27, 72-79.

²³ J. Viljanen, J. Kinnunen, S. Bondestam, A. Majola, P. Rokkanen, P. Törmälä "Bone changes after experimental osteotomies fixed with absorbable self-reinforced poly-L-lactide screws or metallic screws studied by plain radiographs, quantitative computed tomography and magnetic resonance imaging", *Biomaterials* **1995**, 16, 1353-1358.

²⁴ N. Ashammakhi, P. Rokkanen "Absorbable polyglycolide devices in trauma and bone surgery", *Biomaterials* **1997**, 18, 3-9.

²⁵ P. Törmälä, P. Rokkanen "Biodegradable polymers in orthopaedics: experimental and clinical", *Mat. Clin. Appl.* **1995**, 639-651.

a strong need for the development or modification of biomaterial concepts. Again, aliphatic polyesters are, probably as constituents of composite materials, candidates to contribute to a solution of this serious medical problem.

GI. 2 Conventional vs. solid-state chemical synthesis of polyglycolide

The review of conventional synthesis of polyesters is concentrated on PGA as the simplest poly(α -hydroxy ester), because PGA represents the basic compound in this thesis. Some of the reaction principles can be transferred to higher homologues (e.g., polylactide). A short link is given to the biotechnologically produced poly(hydroxy alkanates) like poly(3-hydroxy butyrate).

The synthesis of PGA is possible by the simple polycondensation of glycolic acid from the melt with Sb_2O_3 present as initiator (**fig. GI.2-1 eq. (1)**) at elevated temperature and reduced pressure. Reaction water is removed from the reaction vessel under those conditions. The resulting polymer has a low molecular weight, and optimum properties are not obtained²⁷. The preferred route to PGA is the ring-opening polymerization of the cyclic diester glycolide using antimony, zinc, lead, or preferably tin salt catalysts²⁷ (**eq. (3)**). The reaction can be carried out either as a bulk polymerization in the molten stage (mp. glycolide 80°C), in suspension or in solution. Dilution of the monomer enables a better reaction and heat flow control²⁸. The obtained chains have an average molecular weight around 10^5 g mol^{-1} (i.e., about 1700 monomer units). The educt itself is prepared in the same way as in eq. (1) with the difference that extended pyrolysis (250°C) of the PGA oligomers leads to glycolide formation (**eq. (2)**). The cyclic diester sublimes and can be obtained as white crystals²⁷. The mechanism of polymerization, as well as dispersity and average chain length vary as a function of reactions conditions, catalyst and additives. Cationic, anionic and coordination-insertion mechanisms have been proposed for different setups²⁹. A recent approach used the conventional method of heating glycolic acid to obtain oligomers of PGA (**eq. (4)**) with subsequent annealing and post-polymerization in the solid-state.

²⁶ J.M. Rueger "Knochenersatzmittel", *Unfallchir.* **1996**, 99, 228-236.

²⁷ D.K. Gilding, A.M. Reed "Biodegradable polymers for use in surgery – polyglycolic/poly(lactic acid) homo- and copolymers: 1", *Polymer* **1979**, 20, 1459-1464.

²⁸ A. Lendlein "Polymere als Implantatwerkstoffe", *Chem. Unserer Zeit* **1999**, 5, 279-295.

²⁹ F.E. Kohn, J.G. van Ommen, J. Feijen "The mechanism of the ring-opening polymerization of lactide and glycolide", *Eur. Polym. J.* **1983**, 19(12), 1081-1088.

PGA with an average molecular weight of $91.000 \text{ g mol}^{-1}$ resulted (in the range of ring-opening polymerization products)³⁰. Alternative educts for the production of

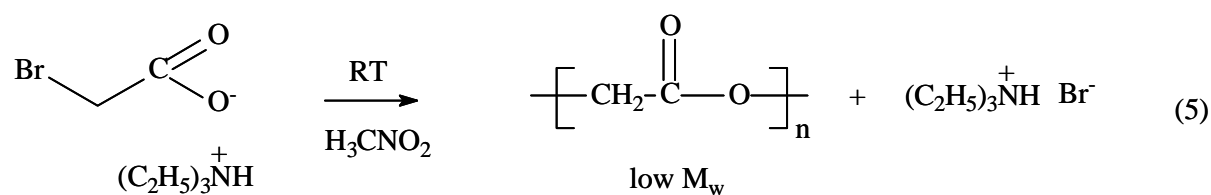
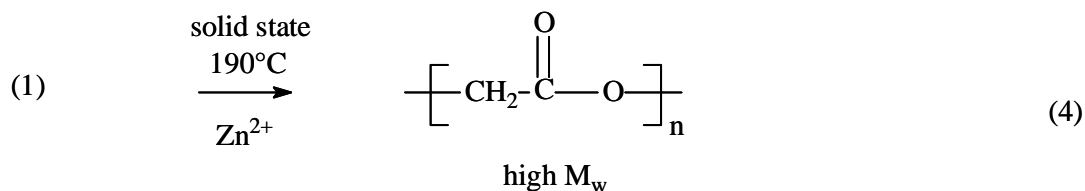
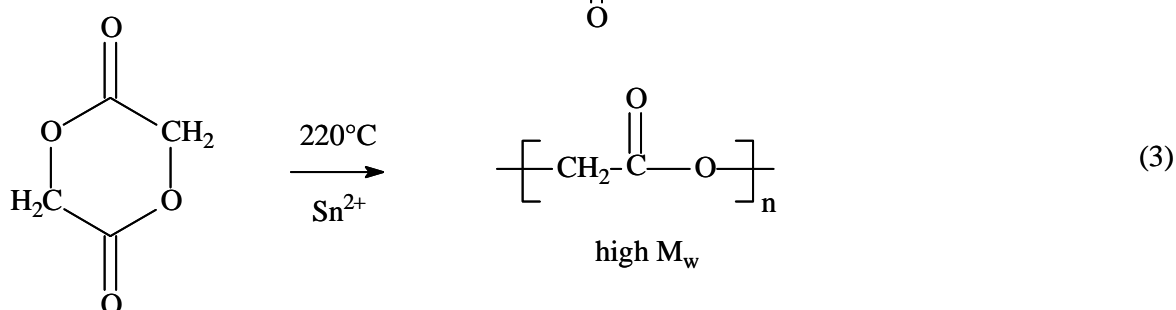
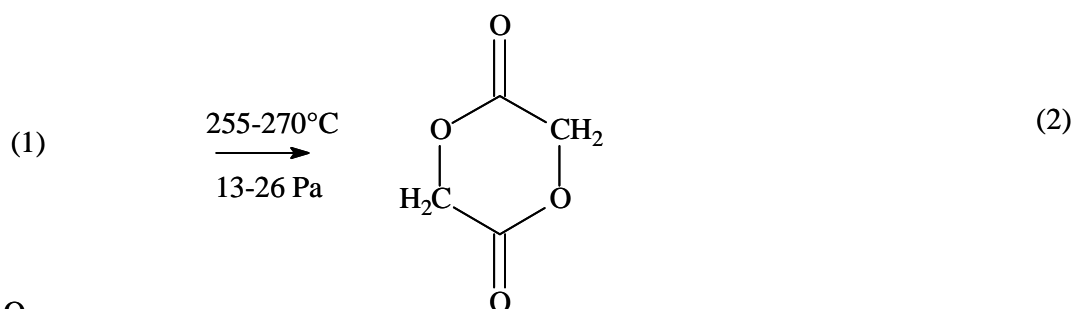
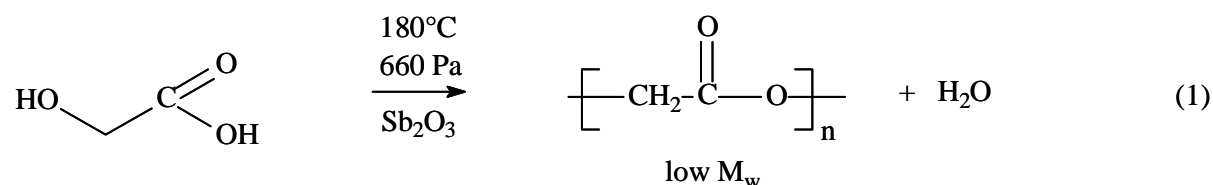


Fig.GI.2-1 Conventional syntheses of polyglycolide

glycolide and PGA are halogenoacetates. Upon heating sodium chloroacetate NaCl is eliminated and glycolide can be isolated as the pyrolyzation product³¹. Pinkus et al. isolated PGA after aging triethylammonium bromoacetate at ambient temperature in

³⁰ K. Takahashi, I. Taniguchi, M. Miyamoto, Y. Kimura "Melt/solid polycondensation of glycolic acid to obtain high-molecular weight poly(glycolic acid)", *Polymer* **2000**, *41*, 8725-8728.

³¹ K. Chujo, H. Kobayashi, J. Suzuki, S. Tokuhara, M. Tanabe "Ring-opening polymerization of glycolide", *Macrom. Chem* **1967**, *100*, 262-266.

nitromethane with triethylammonium bromide as coproduct³² (eq. (5)).

In the case of the dominant ring-opening polymerization, the educt glycolide has to be extensively purified to obtain a polymer of high molecular mass³⁰. Another disadvantage of conventional synthesis is the contamination of the product with residual monomer, solvents and catalysts making necessary washing and other purification steps²⁸. This is a problem with respect to the high quality requirements for materials in biomedical use. At least, the cleaning and post-treatment contribute to the high price of polyglycolide production. The polymers are obtained in the bulk state with crystallinities between 40 and 55% and melting points around 230°C²⁸. PGA proved to be insoluble in most organic solvents at low temperatures except for hexafluoroacetone and 1,1,1,3,3,3 - hexafluoroisopropanol.

Some higher aliphatic polyesters (e.g., P-3-HB/P-3-HV homo- and copolymers) can be produced biotechnologically. Numerous microorganisms accumulate this poly(hydroxy alkanoates) as an energy storage source up to dry mass-contents of 80%⁵. Variation in the monomer ratios of the feedstock⁴ can influence the composition of the polyesters. The products from this route face the same isolation and impurity problems as the synthetically produced PGA.

The route to PGA via solid-state reaction first appeared about 150 years ago. Hoffmann³³ and Kekulé³⁴ obtained KCl besides an insoluble compound after heating potassium chloroacetate to 110°C. The polymeric character of the organic component was not recognized at that time. Instead it was assumed that a cyclic diester, glycolide, was present. Further experiments along this line were carried out by Heintz³⁵, who prepared sodium chloroacetate, Norton and Tcherniak, who developed a method to prepare PGA from sodium chloroacetate³⁶ and Beckurts and Otto, who prepared it from silver chloroacetate³⁷. By heating sodium chloro- and bromoacetate, Bischoff and Walden systematically investigated this elimination³⁸ and were the first to postulate

³² A.G. Pinkus, R. Subramanyam "New high-yield, one-step synthesis of polyglycolide from haloacetic acids", *J. Polym. Sci.: Polym. Chem. Edit.* **1984**, 22, 1131-1140.

³³ R. Hoffmann "Über Monochloressigsäure", *Liebigs Ann. Chem.* **1857**, 102, 1.

³⁴ A. Kekulé "Bildung von Glycolsäure aus Essigsäure", *Liebigs Ann. Chem.* **1857**, 105, 288.

³⁵ W. Heintz in *Poggendorfs Ann. Chem. Phys.* **1862**, 115, 452.

³⁶ J.H. Norton, J. Tcherniak "Recherches sur le glycolide", *C. R. Acad. Sci. Paris* **1878**, 86, 1332.

³⁷ H. Beckurts, R. Otto "Studien über das Verhalten der Silbersalze von halogensubstituierten Säuren der Reihe C_nH_{2n}O₂ beim Erhitzen mit Wasser und für sich", *Chem. Ber.* **1881**, 14, 576.

³⁸ C.A. Bischoff, P. Walden "Über Derivate der Glycolsäure", *Liebigs Ann. Chem.* **1894**, 279, 45.

the polymeric nature of the product, following a suggestion of Anschütz³⁹.

Up until the nineties of the last century, when Epple et al. started the research in this field with modern solid-state chemical techniques, no studies were carried out to gain insights into the underlining principles of the reaction with respect to its energetics, kinetics or product morphology.

The explorations revealed, that the thermal decomposition of sodium chloroacetate (**fig.GI.2-2**), to form PGA and NaCl, proceeds as a one-step reaction in the solid state without detectable intermediates.

This is supported by combined *in-situ* small- and wide angle X-ray scattering (SAXS-WAXS)⁴⁰, *in-situ* EXAFS⁴¹ and *in-situ* ²³Na and ¹³C solid-state NMR spectroscopy⁴²

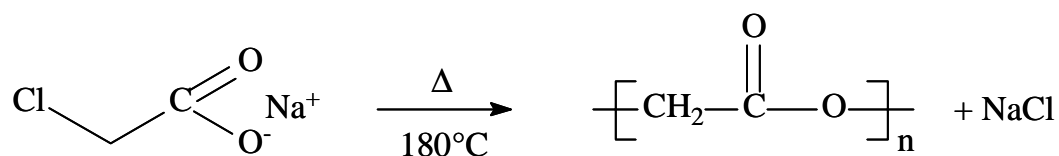


Fig.GI.2-2 Polyglycolide from sodium chloroacetate

measurements. The consumption of sodium chloroacetate occurs simultaneously with the formation of sodium chloride and crystalline PGA. The product mixture consists of bulk PGA with small inclusions of metal salt cubicles. The incorporated salt can be washed out with water, leaving behind a porous polymer matrix with an interconnected pore system. **Fig.GI.2-3** shows salt cubicles integrated in the surface of PGA and the porous polymer after washing treatment. Systematic studies to replace chloride for other halogens (i.e., bromide, iodide) and different cations (i.e., Li, K, Rb, Ag, Cs, NH₄) for sodium indicated that in most cases the reaction principle can be transposed to other halogenoacetates⁴³. The precursor choice strongly effects the reaction parameters and product morphology. Onset temperatures of the exothermic

³⁹ R. Anschütz "Über die Molekulargröße von Salicylid und Homosalicylid", *Liebigs Ann. Chem.* **1893**, 273, 97.

⁴⁰ O. Herzberg, R. Gehrke, M. Epple "Combined *in-situ* small and wide-angle synchrotron X-ray scattering (SAXS-WAXS) applied to a solid-state polymerization reaction", *Polymer* **1999**, 40, 507-511.

⁴¹ M. Epple, G. Sankar, J.M. Thomas "Solid-state polymerization reaction by combined *in-situ* X-ray diffraction and X-ray absorption spectroscopy", *Chem. Mater.* **1997**, 9, 3127-3131.

⁴² A.E. Aliev, L. Elizabé, B.M. Kariuki, H. Kirschnick, J.M. Thomas, M. Epple, K.D.M. Harris "In-situ monitoring of solid-state polymerization reactions in sodium chloroacetate and sodium bromoacetate by ²³Na and ¹³C solid-state NMR spectroscopy", *Chem. Eur. J.* **2000**, 6, 1120-1126.

⁴³ M. Epple, O. Herzberg "Polyglycolide with controlled porosity: an improved biomaterial", *J. Mater. Chem.* **1997**, 7(6), 1037-1042.

reaction peak range from 25 (CsClAc) to 204°C (NaIAc), reaction enthalpies from -23.4 (NaBrAc) to -72.0 kJ mol⁻¹ (NaIAc). The morphology is affected by pore numbers per surface area and average pore diameters after salt removal. Calculated theoretical porosities lie between 42 (AgClAc) and 62% (RbIAc)⁴⁴.

Bearing in mind that solid-state reaction are complex phenomena, the synthesis of PGA in the solid state is a function of several influencing factors. To control the

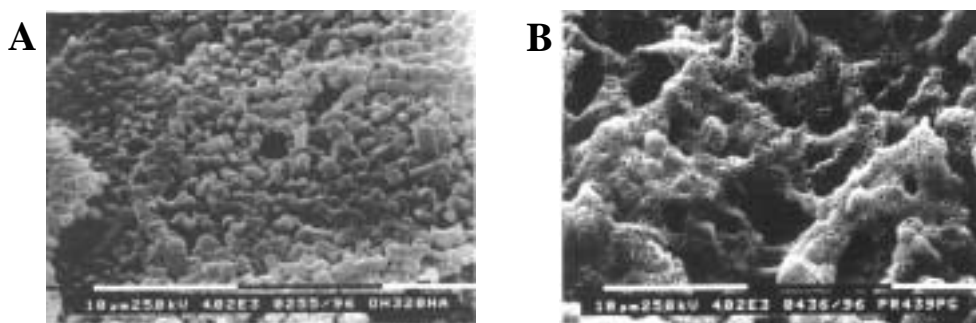


Fig. GI.2-3 A: PGA as received with NaCl inclusions, B: porous PGA after salt removal, (4020x).

reaction course itself requires knowledge of how parameters like reaction time and temperature affect the properties of the resulting polyester. Previous work showed, however, that physical processes continue after the reaction is chemically finished. This can include ordering processes in the polymer or ripening of the included salt crystals⁴⁰.

The intrinsic interconnected structure of the solid-state chemically prepared PGA offers perspectives for the functionalization of an established biomaterial. In addition, it is conceivable to expand the reaction type to other halogenocarboxylic acids to open up new synthetic pathways.

GI. 3 Bone and bone substitution

The term bone as an organ refers to a family of materials, which all have a basic constitution in common: mineralized fiber constructs out of collagen I. Single collagen fibers are arranged to higher aggregates and different structural motifs⁴⁵. At the molecular level, triple helices of tropocollagen molecules are assembled into microfibrils with small gaps between the ends of the fibrils. These fibrils, with a

⁴⁴ M. Epple, O. Herzberg "Porous polyglycolide", *J. Biomed. Mater. Res.* **1998**, *43*, 83-88.

⁴⁵ S. Weiner, H.D. Wagner "The material bone: structure-mechanical function relations", *Annu. Rev. Mater. Sci.* **1998**, *28*, 271.

specific tertiary structure (67 nm periodicity, 40 nm gap diameter), further self-assemble to form the microscopic units of bone. Hierarchical levels of organization form a matrix which is able to generate a surface with potential nucleation sites for inorganic materials. Controlled mineral nucleation and growth are accomplished within the microcompartments (gaps) formed by the collagen matrix⁴⁶. The collagen moiety makes up to one third of the dry mass of bone.

The mineral phase of bone (about 70% of the dry mass) consists of calcium phosphate, in particular low crystalline hydroxyapatite (HAP, stoichiometric formula $\text{Ca}_{10}(\text{PO}_4)_6(\text{OH})_2$). The nucleation of thin, platelet-like apatite crystals occurs within the discrete spaces of the collagen fibrils, thereby limiting the possible growth of the mineral crystals, and forcing the crystals to be discrete and discontinuous⁴⁶. **Fig.GI.3-1** gives a schematic illustration of the apatite deposits inside collagen gaps (A) and the natural appearance in mineralized turkey tendon (B).

In contrast to the naturally occurring *ex-vivo* hydroxyapatite, a highly ordered crystalline bulk mineral, the crystals in bone are nanocrystalline and highly disordered. In the apatite lattice each of the three ions Ca^{2+} , PO_4^{3-} , and OH^- can be substituted by other ions. Most relevant examples are the substitution of

- F^- for OH^- to give fluoroapatite, a mineral phase in teeth enamel of some animals⁴⁷
- Pb/Cd for Ca as an accumulation of toxic heavy metals in bone mineral or ion exchangers⁴⁸
- CO_3^{2-} for OH^- (A-type carbonated apatite) and PO_4^{3-} (B-type carbonated apatite), as present in bone to an extent of 4-8 wt%⁴⁹

The latter example significantly contributes to the amorphous and disordered character of bone mineral⁵⁰. In conclusion, the bone mineral can be described as nanocrystalline and X-ray-amorphous HAP with noticeable carbonate contents. In the following, the calcium phosphate phase in bone is designated as carbonated apatite (CA). The

⁴⁶ L.T. Kuhn, D.J. Fink, A.H. Heuer "Biomimetic strategies and material processing" in *Biomimetic Materials Chemistry*, VCH Publishers, Weinheim, New York, Cambridge, **1996**, 41.

⁴⁷ H.A. Lowenstam, S. Weiner "On Biomineralization", Oxford University Press, Oxford, New York, **1989**.

⁴⁸ N.C. Blumenthal, V. Cosma, D. Skyler, J. LeGeros, M. Walters "The effect of cadmium on the formation and properties of hydroxyapatite *in vitro* and its relation to cadmium toxicity in the skeletal system", *Calcif. Tissue Int.* **1995**, *56*, 316-322.

⁴⁹ Y. Doi, T. Shibusaki, Y. Moriwaki, T. Kajimoto, Y. Iwayama "Sintered carbonate apatites as bioresorbable bone substitutes", *J. Biomed. Mater. Res.* **1998**, *39*, 603-610.

⁵⁰ C. Rey, B. Collins, T. Goehl, I.R. Dickson, M.J. Glimcher "The carbonate environment in bone mineral: a resolution-enhanced Fourier transform infrared spectroscopy study", *Calcif. Tissue Int.* **1989**, *45*, 157-164.

material bone is not of static nature in that it just grows and remains unchanged. Instead, dynamic cellular processes regulate bone mass and structure⁵¹.

The formation, maintenance, resorption and adaptation of bone are mediated by three

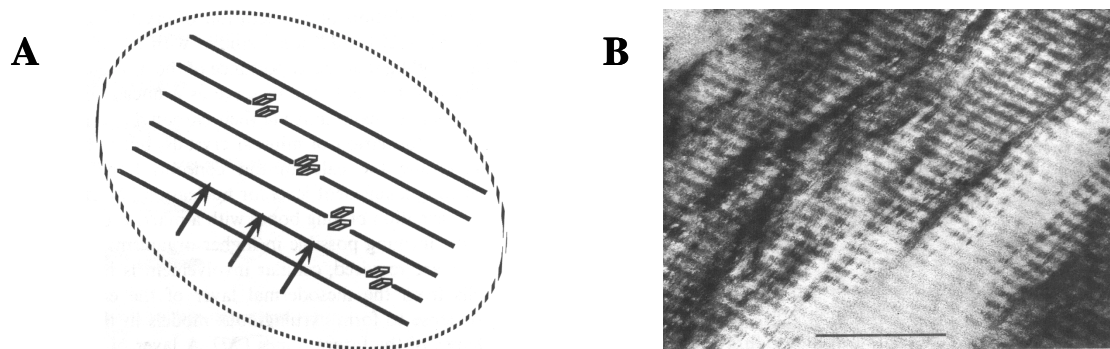


Fig. GI.3-1 A: schematic illustration of apatite deposits in collagen gaps, B: SEM micrograph of mineralized turkey tendon (scale bar 0.5 μm).

cell phenotypes: Osteoblasts are able to build up collagenous extracellular matrix and to mineralize the generated fibrils. In the process of mineralization the osteoblasts integrate themselves in the newly-formed bone and differentiate to osteocytes, which are assumed to sense and signal mechanical stress⁵². Resorption of bone is performed by multinucleated osteoclasts⁵¹. The mechanism of collagen mineralization and the role of osteoblasts in this process is not clarified in detail⁵³. One proposed explanation is the formation of calcified matrix vesicles inside osteoblasts. The vesicles are excreted from the cell to attach to collagen fibers. Once in place, the calcium phosphate self assembles with the spatial collagen structures to form a mineralized matrix⁵⁴.

The interaction of the involved cells (i.e., cytokines, signal transduction, differentiation pathways) and the overall regulatory system is currently under intense investigation to uncover the interdependencies of cell activity^{55,56}. This especially

⁵¹ G. Vaes "Cellular biology and biochemical mechanism of bone resorption", *Clin. Orthop. Rel. Res.* **1988**, Section III – Basic science and pathology, 239-271.

⁵² K. Terai, T. Takano-Yamamoto, Y. Ohba, K. Hiura, M. Sugimoto, M. Sato, H. Kawahata, N. Inaguma, Y. Kitamura, S. Nomura "Role of osteopontin in bone remodeling caused by mechanical stress", *J. Bone Miner. Res.* **1999**, 14(6), 839-849.

⁵³ T. Schinke, M.D. McKee, G. Karsenty "Extracellular matrix calcification: where is the action ?", *Nature Genetics* **1999**, 21, 150-151.

⁵⁴ U. Plate, S. Arnold, U. Stratmann, H.P. Wiesmann, H.J. Höhling "General principle of ordered apatitic crystal formation in enamel and collagen rich hard tissues", *Connective Tissue Res.* **1998**, 38(1-4), 149-157.

⁵⁵ K.M. Eyster "Introduction to signal transduction", *Biochem. Pharmacol.* **1998**, 55, 1927-1938.

accounts for the understanding and therapy of bone diseases and malfunctions of the skeletal system (e.g., osteoporosis)⁵⁷. The natural process of bone mass regulation by osteoblasts and osteoclasts is called remodeling. Bone structure and constitution provide a guiding network for cell activity by different noncollagenous extracellular matrix molecules that mediate cell adhesion, differentiation or mineralization sites⁵⁸. Vital bone can be termed osteoinductive, because it provides necessary factors and the “infrastructure” for dynamic cell remodeling. The material bone, with respect to mechanical properties, can be regarded as a composite of flexible collagenous matrix that is enforced by carbonate apatite nanocrystals. Both, the structural composite architecture and the dynamic regulation and maintenance processes, make bone a highly optimized, unique functional biological material.

This brief description of bone gives an imagination of the difficulty to substitute such a highly sophisticated tissue in clinical routine after trauma or tissue removal. A variety of strategies and materials coexist for various indications, all with their specific advantages and disadvantages. A uniform strategy to solve the problem does not yet exist. The following classification of bone substitution materials and concepts was proposed by Rueger⁵⁹.

Four categories with examples:

I. biological, organic substances

⇒ demineralized bone matrix, bone matrix extracts, bone growth factors,

II. synthetic, inorganic materials

⇒ calcium phosphate phases, HA of coralline origin, thermally treated bovine bone, glass ceramics and bioglasses, calcium phosphate cements

III. synthetic, organic substances

⇒ homo- and copolyesters, poly(amino acids), poly(ortho esters)

IV. Composites

⇒ combinations of the above listed materials

⁵⁶ D. Corral, M. Amling, M. Priemel, E. Loyer, S. Fuchs, P. Ducy, R. Baron, G. Karsenty “Dissociation between bone resorption and bone formation in osteopenic transgenic mice”, *Proc. Natl. Acad. Sci.* **1998**, 13835-13840.

⁵⁷ M. Amling, M.W. Hentz, M. Priemel, G. Delling “Transgenic and knockout animals in skeletal research” in *Novel approaches to treatment of osteoporosis*, Springer Verlag, Berlin, **1998**, 123-156.

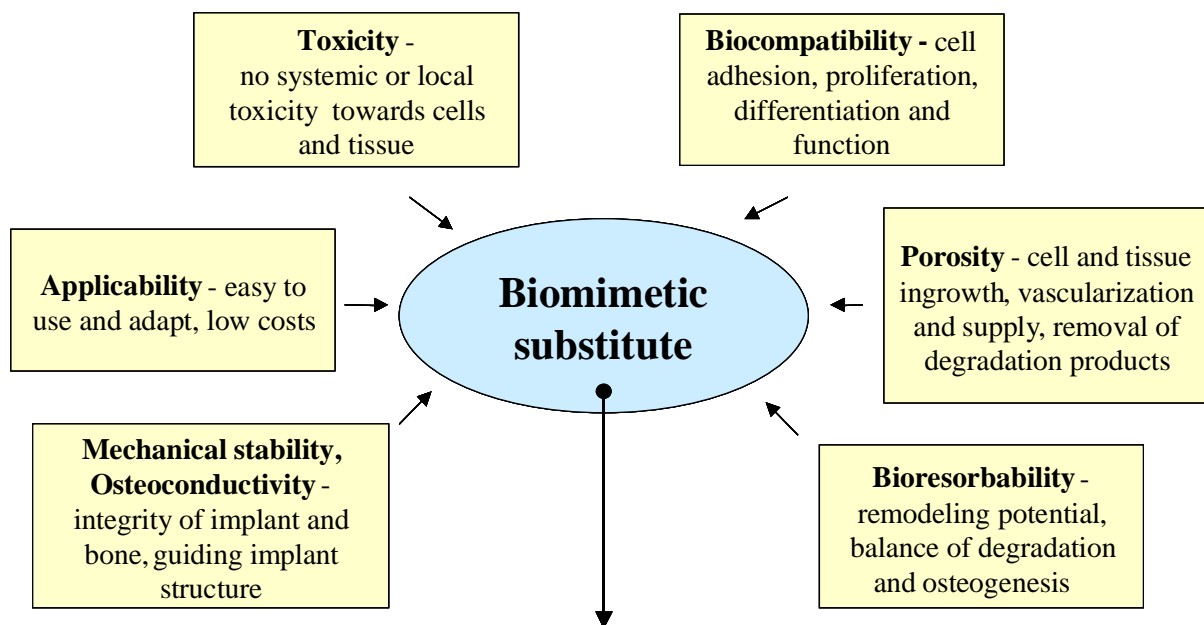
⁵⁸ Y. Ayukawa, F. Takeshita, T. Inoue, M. Yoshinari, M. Shimono, T. Suetsugu, T. Tanaka “An immunoelectron microscopic localization of noncollagenous bone proteins (osteocalcin and osteopontin) at the bone-titanium interface of rat tibiae”, *J. Biomed. Mater. Res.* **1998**, 41, 111-119.

Besides this classification of material origin, other distinctions can be applied to material properties, e.g. resorbable/non-resorbable implants.

The predominant treatment for bone defects at the moment is (still) the transposition of autologous bone from reservoirs of the patient's own body⁵⁷. Clinical experience relies on the fact that autologous bone material ensures

- osteoconduction and osteoinduction, providing a self-similar structure and biology,
- remodeling potential through osteoinduction,
- vascularization and vitalization,
- no risk of adverse reaction, low risk of infections

in most cases. These attributes make autologous bone the “golden standard” for defect treatment. The disadvantages, however, are a second operation site (instability, infect



Composites of porous polyesters and carbonated apatite

Fig. GI.3-2 Requirement-profile for a synthetic bone substitution material

risk, pain) and limited availability. To overcome the latter restriction, allogeneous (same species, material stored in bone banks) and xenogeneous (different species, e.g. of porcine or bovine origin) are conceivable. Implantations of that kind bear the additional risk of adverse reaction and disease transmittance (e.g., HIV, BSE).

In the light of the present discussion, it can be concluded that the transplantation of

⁵⁹ J.M. Rueger “Knochenersatzmittel – Heutiger Stand und Ausblick”, *Orthopäde* **1998**, 27, 72-79.

autologous bone must be regarded as a “golden standard” not because of ideal viability, but rather as a consequence of lacking alternatives⁵⁷.

Requirements for a synthetic substitution material as an alternative are comprised in **fig.GI.3-2**. Composites of biodegradable, porous polyesters and carbonated apatites are proposed to represent a biomimetic bone substitution material.

GI. 4 Aim of this work

Aim of the present thesis is the characterization and evaluation of PGA from solid-state reaction as a biomaterial in a composite concept for potential use as a bone substitution material. The composite design should account for important requirements for an implant material to serve the requested functions mentioned above.

The thesis is subdivided in two main parts:

Part A comprises the monitoring and characterization of the PGA synthesis from NaClAc in AI, the degradation behavior of compact and porous PGA pellets in water and cell nutrition medium in AII, and the transposition of the solid-state reaction principle to the higher halogeno carboxylates 3-Cl-butyric acid and Cl-pivalic acid in AIII. The variation of the polyester component in the composite concept may open different component combinations and related composite properties.

Part B reports the development and optimization of PGA/calcium phosphate composite bodies with respect to component composition, stability, porosity and external pH-value in media. The optimized composite pellets were tested for biocompatibility by cell seeding with murine osteoblastic cells to analyze the material suitability and influence on cell attachment, proliferation, differentiation and function.

The philosophy of the introduced composite concept is the rational design of a biodegradable material that can be converted into bone by natural body functions with subsequent remodeling activity.

Part A: Polyesters from solid-state precursors

AI. The formation of polyglycolide from sodium chloroacetate

AI.0 Introduction

Polyglycolide can be synthesized by thermally induced polycondensation of halogenoacetates. The products of this reaction are PGA chains with inclusions of metal halide¹. Solid-state precursors as starting materials yield solid products after a heating process. This raises the question whether the reaction takes place entirely in the solid state, i.e. without liquid intermediates. If a solid-state reaction is present, structural orientations of the educt molecules and other topological factors like crystallinity or crystal regularity determine the reactivity of the parent compound and the topochemistry of the reaction². Together with static factors, dynamic ones (e.g., heat production and flows or density changes after reaction start) can influence the character and course of a reaction. Therefore the characterization of a solid-state reaction is a challenge with the aim to understand and control the reaction itself and the properties of the products. Although some metal halogenoacetates undergo the polycondensation reaction, the investigations were mostly focused on the parent

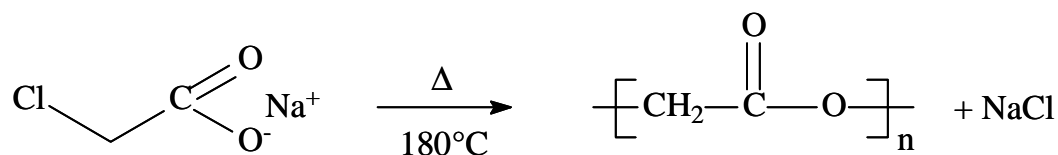


Fig.AI.0-1 Synthesis of PGA from sodium chloroacetate

compound sodium chloroacetate:

Thermal analysis^{3,4} revealed an onset temperature for the polymerization $T_{onset} = 198^\circ\text{C}$ and a reaction enthalpy $\Delta_r H = -25.2 \text{ kJ mol}^{-1}$ (DSC, heating rate $\beta = 5 \text{ K min}^{-1}$). The thermal elimination takes place between 185 and 215°C with no detectable mass loss throughout the exothermic reaction indicating that no liquid or gaseous intermediates evaporate from the reaction vessel. Upon further heating, exothermic combustion of

¹ M. Epple, O. Herzberg "Polyglycolide with controlled porosity: an improved biomaterial", *J. Mater. Chem* **1997**, 7(6), 1037-1042.

² G.R. Desiraju, *Organic solid state chemistry*, Elsevier, Amsterdam, **1987**.

³ M. Epple, H. Kirschnick "The thermally induced solid-state polymerization reaction in halogenoacetates", *Chem. Ber.* **1996**, 129, 1123-1129.

the formed PGA occurs between 250 and 400°C accompanied by CO₂ and H₂O mass signal detection. The mass loss of 49.3 % is in good accordance with the calculated value (49.8 %) for the total burn-up of PGA and NaCl as residue (TG-DTA-MS, 50 cm³ min⁻¹ air flow, $\beta = 5$ K min⁻¹). The exothermic polycondensation and the combustion are well separated, so that the products can be isolated without decomposition when the reaction temperature is controlled.

In situ temperature-resolved X-ray diffractometry^{3,4} was carried out to follow the course of consumed and formed crystalline components involved in the reaction and possible non-amorphous intermediates. Quantitative evaluation resulted in a reaction extent that can be fitted with a sigmoidal curve (corroborated by *ex situ* argentometric titration of formed chloride, monitoring of precursor decrease by ¹H NMR and quantitative X-ray absorption spectroscopy). Compared to the consumption of sodium chloroacetate, the formation of crystalline PGA and NaCl appeared delayed. It can be assumed that the eliminated Na⁺ and Cl⁻ ions have to migrate and accumulate first to reach a cluster size that develops a detectable long-range order to give a noticeable diffraction. The PGA reflexes have, compared to precursor and NaCl, low intensities and high peak width. This indicates an initially disordered, partly amorphous and therefore poorly crystalline material. No other crystalline compounds could be detected during reaction. Concerning kinetics it can be stated that a sharp onset-temperature for the polymerization does not exist^{3,4}. The observed values range from 130°C upward with corresponding reaction times. The reaction start and dynamics can be affected by numerous parameters like heating rate, heat flows, precursor crystallinity and grain size distribution, precursor mass and powder geometry or surrounding atmosphere. For instance, it was noted that the reaction was accelerated by *in situ* irradiation with X-rays compared to DSC measurements under the same heating profile³.

To check for the occurrence of amorphous intermediates, X-ray absorption spectroscopy (EXAFS) on the chlorine K-edge was employed⁴. The intensity of the Cl-C coordination shell decreased continuously during the reaction, and the structure of a cubic NaCl lattice developed. The determined distance between Cl and Na in the

⁴ M. Epple, L. Tröger "Study of a solid-state polymerization reaction: thermal elimination of NaCl from sodium chloroacetate", *J. Chem. Soc., Dalton Trans.* **1996**, 11-16.

formed NaCl of 2.81 Å is identical with the nearest-neighbor distance in bulk NaCl. The measured Cl-C and Cl-Na distances remain constant within 0.02 Å throughout the reaction. These data suggest that intermediate compounds are unlikely because of almost constant shell distances for educt and product without detectable appearance of transitional shell distances.

To gain more insights into the formation of the PGA during the reaction and subsequent ordering processes, combined small- and wide angle X-ray scattering (SAXS-WAXS) was applied using synchrotron radiation⁵. The high intensity of synchrotron radiation enables diffraction experiments at very small Bragg angles with sufficient reflex resolution and intensity. The SAXS measurements showed, compared to the corresponding WAXS reflexes of disappearing precursor, a delayed evolution of the PGA long period reflex indicating structural ordering processes leading to a superstructure with a d -value of 96 Å. Apparently, the formation of a PGA superstructure is kinetically hindered and needs sustained thermal activation.

The mentioned results were further corroborated by *in situ* solid-state NMR-spectroscopy with ²³Na and ¹³C as probed nuclei⁶. NMR is an appropriate tool to visualize changes in the chemical environment of a nucleus. ²³Na was chosen to analyze the conversion of NaClAc to NaCl and consequently ¹³C for the conversion of the precursor to PGA. The reaction temperature was set to 140°C for 47 h, leading to a reaction extent of 42 % (assessed from the sodium chloroacetate peak). Again, only two signals were detected, a multiplet caused by the coordinational coupling of Na in the precursor lattice and a sharp single signal referring to NaCl. Consumption of NaClAc lead to the corresponding formation of NaCl to the same extent.

A structure determination of the starting material is a prerequisite to make suggestions about the reaction mechanism and to have a structural basis for the interpretation of precursor reactivity. It proved to be difficult to obtain suitable single crystals of NaClAc in size and regularity for an X-ray diffraction analysis with conventional

⁵ O. Herzberg, R. Gehrke, M. Epple "Combined in-situ small and wide-angle synchrotron X-ray scattering (SAXS-WAXS) applied to a solid-state polymerization reaction", *Polymer* **1999**, *40*, 507-511.

⁶ A.E. Aliev, L. Elizabé, B.M. Kariuki, H. Kirschnick, J.M. Thomas, M. Epple, K.D.M. Harris "In-situ monitoring of solid-state polymerization reactions in sodium chloroacetate and sodium bromoacetate by ²³Na and ¹³C solid-state NMR spectroscopy", *Chem. Eur. J.* **2000**, *6*, 1120-1126.

crystal growth techniques like slow solvent cooling or gel diffusion⁷. The latter technique was successfully applied to the slow crystallization of AgClAc. The structure determination yielded an orthorhombic crystal system with the space group $Pbc2_1$ ⁸. The structure consists of stacks of silver chloroacetate dimers parallel to the x axis with two carboxylate groups bridged almost symmetrically by two silver ions. The distance between Ag and Cl was calculated to be 2.903 Å, comparable to the distance in silver chloride of 2.775 Å, indicating a considerable attraction already in the precursor structure. It was concluded that the polymerization proceeds along the x

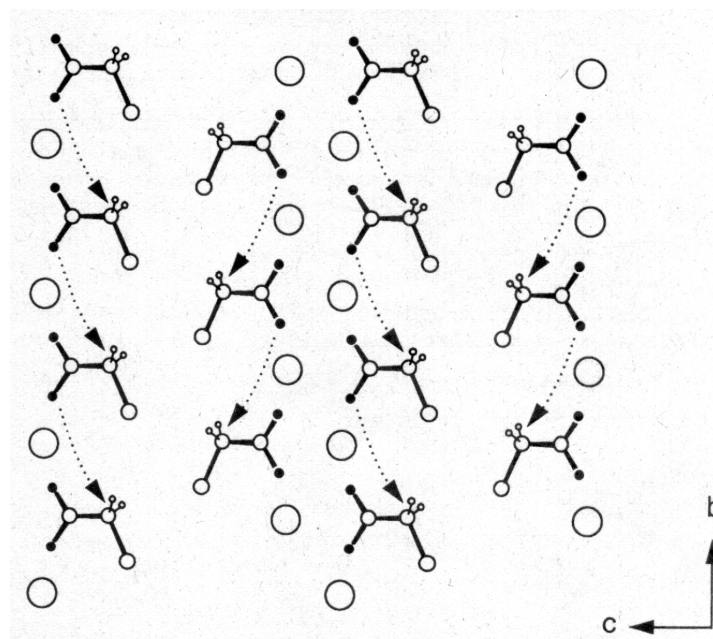


Fig. AI.0-2 Section of the structure of NaClAc with arrows indicating the propagation of the polymerization reaction within rows of chloroacetate ions along the b axis⁹

axis with the proximity of Cl and Ag favoring an elimination. Ag^+ and Cl^- can migrate through formed channels besides the growing PGA chains. In the case of NaClAc the structure was determined from powder diffraction data applying synchrotron radiation and a Monte Carlo structure solution algorithm⁹. A two-dimensional section of the structure is displayed in **fig.AI.0-2**. Rows of chloroacetate anions are

arranged along the b axis. Na^+ coordinates to the oxygen atoms of the chloroacetate with six oxygens associated around each sodium cation. The C-O distance of neighboring molecules is shortest in the b direction (4.61 Å) together with an ideal O-C-Cl angle of 168° for a "back-side attack" trajectory make a polymerization along

⁷ O. Herzberg, M. Epple "A single crystal study of a solid-state polymerization reaction", *J. Therm. Anal. Cal.* **1999**, 57, 151-156

⁸ M. Epple, H. Kirschnick "Silver chloroacetate: crystal structure and thermal polymerization mechanism", *Chem. Ber./Recueil* **1997**, 130, 291-294.

⁹ L. Elizabe, B.M. Kariuki, K.D.M. Harris, M. Tremayne, M. Epple, J.M. Thomas "Topochemical rationalization of the solid-state polymerization reaction of sodium chloroacetate: structure from powder diffraction data by the Monte Carlo method", *J. Phys. Chem. B* **1997**, 101(44), 8827-8831.

the b axis even more conceivable. The structural findings derived from crystal structure data support a topochemical polymerization, where the relative orientation of functional groups and the vibrational activation of the lattice determine the reactivity of the solid material. To investigate whether the crystal structure of the precursor is transposed to the reaction products in an oriented way, a NaClAc single crystal of lower quality was reacted⁷. X-ray diffraction measurements (Bragg rotating crystals pictures) indicated polycrystalline products without predominant orientations. The loss of structural integrity could be caused by heat evolution gradients, local density changes and competing nucleation at different sites in the crystal.

The previous studies about the thermochemistry and structural course of the polycondensation describe the reaction as a solid-state reaction without liquid or solid intermediates that leads to polycrystalline PGA of low crystallinity. The aim of the present work is the determination of the reaction extent under variation of the temperature (160 and 180°C) to get an idea about the kinetics of the reaction for different thermal activation. The resulting product PGA is further characterized by mass spectroscopy, X-ray powder diffraction and thermal analysis to exclude the dimer glycolide as a possible intermediate and to prove the identity of the solid-state polymerization mechanism in contrast to the conventional ring-opening oligomerization via glycolide, mentioned in the General Introduction.

Aliquots of the reaction mixture were taken under isothermal conditions to evaluate developing chain growth (degree of polymerization), crystallinity and resulting porosity after removal of NaCl. A set of methods (NMR, XRD, DSC, viscosimetry, mercury porosimetry, TG-DTA-MS, mass spectrometry) was applied to obtain a detailed characterization of the reaction dynamics outlined in the following sections.

AI.1 Results and discussion

Nature of solid-state chemically prepared PGA

Fig.GI.2-1 of the General Introduction shows the conventional synthesis for PGA with glycolide as an intermediate or educt for the formation of polyglycolide chains of different length. To exclude an involvement of glycolide in the solid-state chemical reaction and to support the derived polycondensation mechanism, PGA from solid-

state reaction was characterized compared to glycolide. The analyzed PGA was obtained by heating sodium chloroacetate for 3 h at 180°C followed by NaCl extraction with cold water (4°C, 6 h). PGA was filtered off and dried in oil-pump vacuum prior to characterization¹⁰.

Commercially available glycolide was provided by Boehringer.

Fig. AI.1-1 displays XRD measurements of isolated PGA from solid-state reaction in comparison with diglycolide. It is clearly

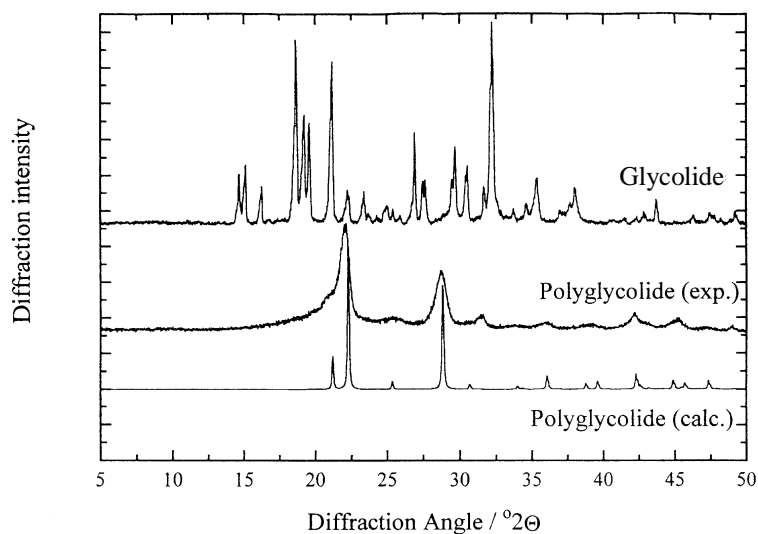


Fig. AI.1-1 X-ray powder diffraction patterns of glycolide and PGA from solid-state reaction. For comparison, the calculated pattern from single crystal data reported by Chatani et al.¹¹ is attached.

visible that the two compounds are of different crystallographic nature and that no traces of the cyclic dimer are detectable. In 1967 Chatani et al.¹¹ determined the PGA structure on a stretched fiber-like single crystal. Based on that data the third pattern was computed. As expected, the measured diffraction peaks are much broader due to structural disorder and lower crystallinity. The peak positions are in accordance with

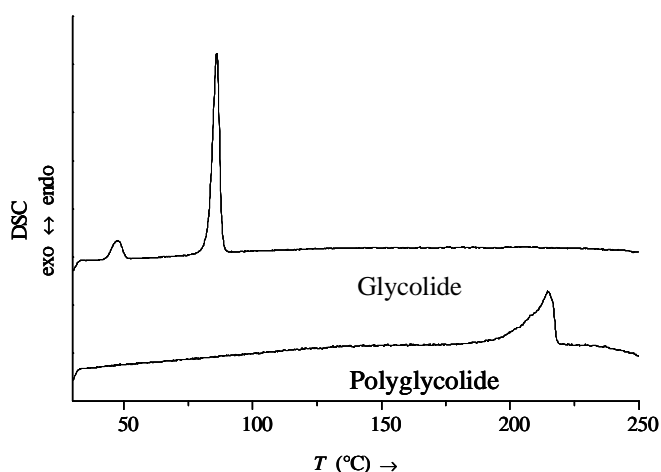


Fig. AI.1-2 Comparison of DSC thermograms of glycolide and PGA from solid-state reaction. ($\beta = 5 \text{ K min}^{-1}$). Glycolide shows an endothermic phase transition from monoclinic α - to orthorhombic β -phase at 43°C, followed by an endothermic melting process occurring at 82°C¹².

¹⁰ K. Schwarz, M. Epple "A detailed characterization of polyglycolide prepared by solid-state polycondensation reaction", *Macromol. Chem. Phys.* **1999**, 200, 2221-2229.

¹¹ Y. Chatani, K. Suehiro, Y. Okita, H. Tadokoro, K. Chujo "Structural studies of polyesters I - crystal structure of polyglycolide", *Macrom. Chem.* **1968**, 113, 215-229.

¹² E.J. Frazza, E.E. Schmitt "A new absorbable suture", *J. Biomed. Mater. Res. Symp.* **1971**, 43(1), 43-58.

the calculated reference. No additional reflexes are visible indicating a poorly crystalline but phase-pure PGA.

The results of a DSC analysis are shown in **fig.AI.1-2**. The melting of PGA is expressed as a broad endothermic signal suggesting a certain distribution of chain length. Below 180°C no signal appears. Crystalline PGA oligomers, as well as glycolide would show-up as endothermic signals in addition to the melting enthalpy of PGA with longer chains. The DSC measurements confirm that the formed PGA exhibits a degree of polymerization higher than a few monomer units and that it does not contain glycolide. To rule out the removal of contaminations in the washing step, as received PGA was refluxed for 2h with d_6 -acetone to extract soluble glycolide and short oligomers of PGA. NMR gave no evidence for a presence of these compounds. For mass spectroscopy analysis three different techniques were employed. PGA from NaClAc and glycolide were subjected to electron ionization (EI), fast atom bombardment (FAB) and MALDI-TOF. The methods can be distinguished by their way of ionizing the probed substances. The mass spectroscopy data for the three *modi* with the detected fragments is summarized in **table AI.1-1**.

Table AI.1-1 Mass spectroscopy of glycolide and PGA: fragments detected with EI, FAB and MALDI-TOF, [m/e]

	EI	FAB	MALDI-TOF
Glycolide	117 (M+1u) 116 (molecular peak) 88, 72, 56	same as EI	same as EI
PGA	523 (n = 9 +1u) 479, 464 (n = 8), 421, 420, 348 (n = 6), 332, 274, 232 (n = 4), 216, 158, 117, 116 (n = 2), 100, 73, 72, 61	589 , 330, 318	1102 , 928, 748, 573, 484, 394, 354, 269, 217, 178, 140, 96, 39

M = molecular mass, n = degree of polymerization, u = atomic weight unit

For EI the sample is heated under reduced pressure to evaporate the sample molecules. Heating to 400° C at 10^{-6} Torr was necessary to obtain a spectrum for PGA. Under these conditions, a high degree of fragmentation in the gas phase is inevitable, besides the risk of pyrolyzation in the solid/molten state. Glycolide was probed under the same pressure at 25°C. For glycolide the molecular peak (116 u) gives the most intense signal with some detectable fragments below $m/e = 100$. Despite the applied

evaporation conditions PGA signals are detectable up to 523 u, which refers to a $n = 9$ fragment. The spectrum is in good agreement with the data reported by Jacobi et al.¹³ for polyglycolide pyrolyzed at 250°C. The FAB measurements were carried out in a matrix of *m*-nitrobenzylalcohol. Detected masses reach up to 589 u.

MALDI-TOF is a more gentle technique to ionize fragile macromolecules. The probed substance is dissolved in a matrix-solution and ionized by exposition to laser-light. PGA was dissolved in hexafluoroisopropanol and mixed with 3-hydroxypicolinic acid/ammonium citrate in H₂O/acetonitrile. Unfortunately, segregation of the liquids occurred to some extent, bearing the risk of the beam hitting the polymer directly. Fragments slightly more intensive than the noise are visible up to a mass of 2000 u. Clear assignment is possible for $m/e = 1100$ u. From this results it may be stated that polymer units with at least 20 monomers in the chain are present.

The additional characterization of PGA from solid-state polycondensation proved that no short oligomers are present after the reaction. The average degree of polymerization is therefore higher than approximately 20 monomeric units. The cyclic diester glycolide could not be found as a pyrolyzed side-product of the reaction.

¹³ E. Jacobi, I. Lüderwald, R.C. Schulz, "Strukturuntersuchung von Polyestern durch direkten Abbau im Massenspektrometer - Polyester und Copolyester der Milchsäure und Glycolsäure, *Macromol. Chem.* **1978**, *179*, 429-436.

Monitoring of the properties of polyglycolide during solid-state polycondensation*Reaction extent*

Two polycondensation experiments were carried out at 160 and 180°C in round-bottom flasks immersed in a heated oil bath. To realize a homogeneous temperature profile, the reaction was stirred with a magnetic stirrer. Nitrogen was passed over the reacting material to prevent extensive contact with oxygen.

The reaction extent α was determined on aliquots by X-ray powder diffraction, DSC, ^1H NMR spectroscopy and gravimetric analysis. XRD was quantitatively evaluated

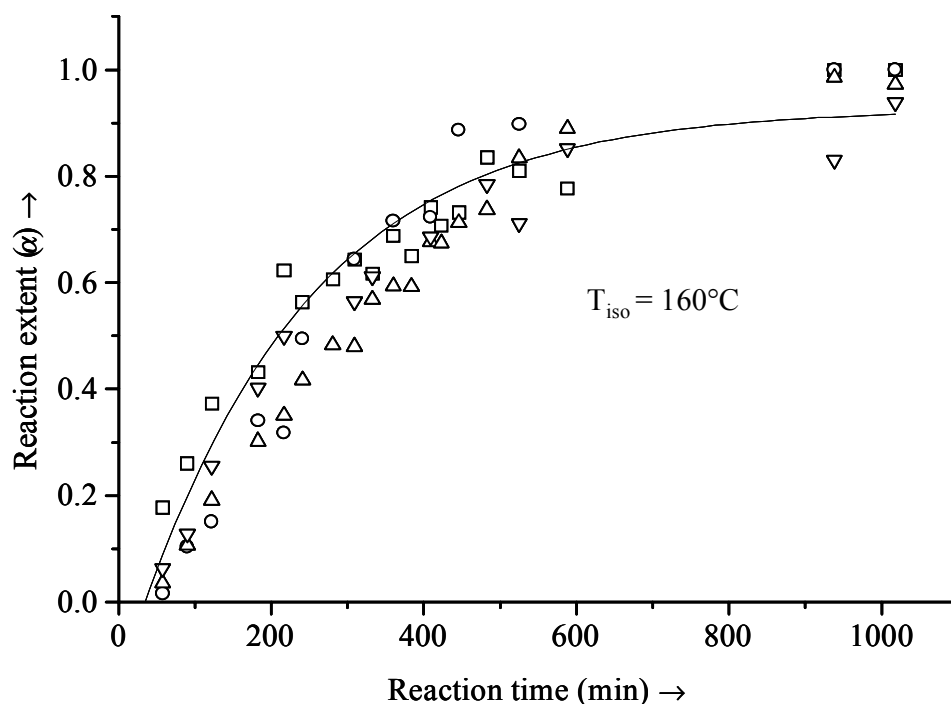


Fig. AI.1-3 Reaction extent α for the solid-state polycondensation of PGA at 160°C determined with different methods. () ^1H NMR; (○) DSC; (∇) XRD; (Δ) gravimetry. At $t = 588$ min the reaction was interrupted and cooled down for 12 h to be heated up again later (see materials and methods).

with respect to precursor decrease and product evolution (NaCl and PGA), DSC and ^1H NMR for precursor decrease and gravimetry for the formation of PGA after removal of water-soluble NaCl and residual NaClAc (**fig.AI.1-3**). The destination temperatures were reached after a 30 minutes heating period. This time point was defined as the reaction start in both cases ($t = 0$). At each time point an aliquot of ca. 2 g material was taken off the reaction vessel. Despite some scatter, it is evident that all methods yield the same values for α over time. A significant delay of the measured reaction extent is not observed for a particular method. Sodium chloroacetate is

consumed with the same rate as NaCl and PGA are formed. Consequently, there are no detectable intermediates. The time for a turn-over of 50 % ($\alpha = 0.5$) is about 280 min.

Fig.AI.1-4 shows the calculated reaction extent for the two reaction temperatures. The values for α were averaged for all four applied methods. At 180°C, the reaction occurs

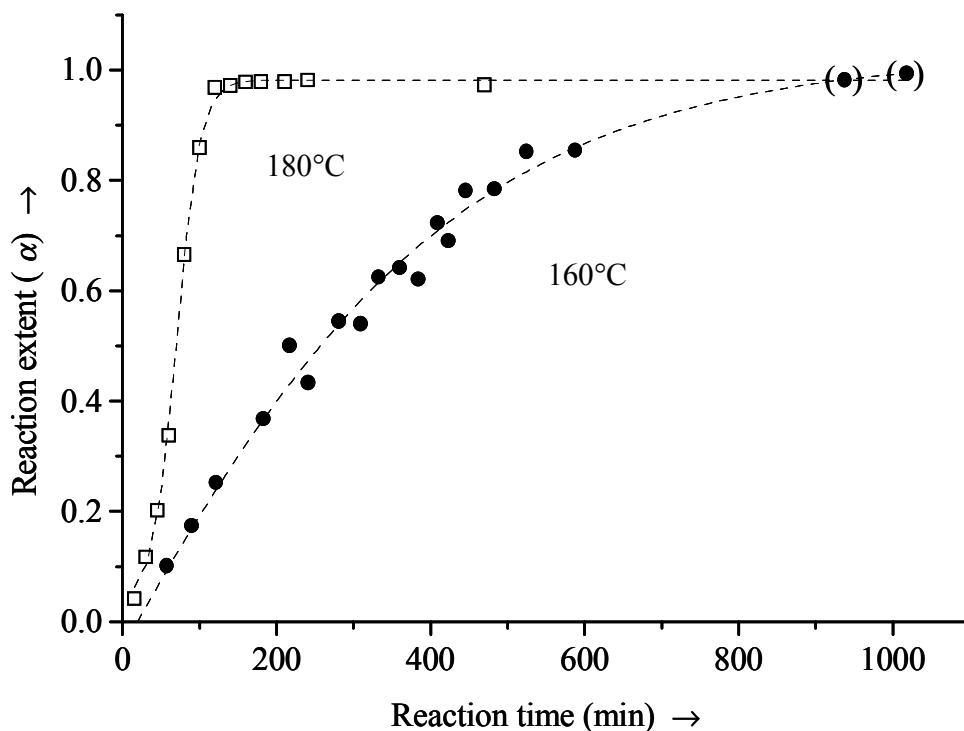


Fig. AI.1-4 Comparison of the reaction extent α for 160 (●) and 180°C (□) as an averaged value from ^1H NMR, DSC, XRD and gravimetry. Values in parentheses were obtained after a cooling period (see materials and methods).

much faster with a half turn-over at ca. 70 min where 50 % of the sample had reacted. After 120 min, the reaction is complete with α approaching 1. The data can be fitted with a sigmoidal curve in both cases, although values for short time periods are difficult to obtain because of low reaction extent and lack of measurable products. Apparently, the reaction has an induction period followed by an increase of reaction velocity. This is more strongly expressed for 180°C, probably due to self-heating by the exothermic reaction. In other experiments with higher heating rate and/or higher destination temperature, the heat evolution lead to extensive pyrolysis of the sample mass. The results clearly show that variation of surrounding temperature strongly affects the reaction extent. Control of heat production and removal is critical to the course of the reaction and a first step towards reproducible conditions.

Chain growth and degree of polymerization

An important parameter for the properties of the reaction product is the average chain length and the chain length distribution (dispersity). Methods to determine the average

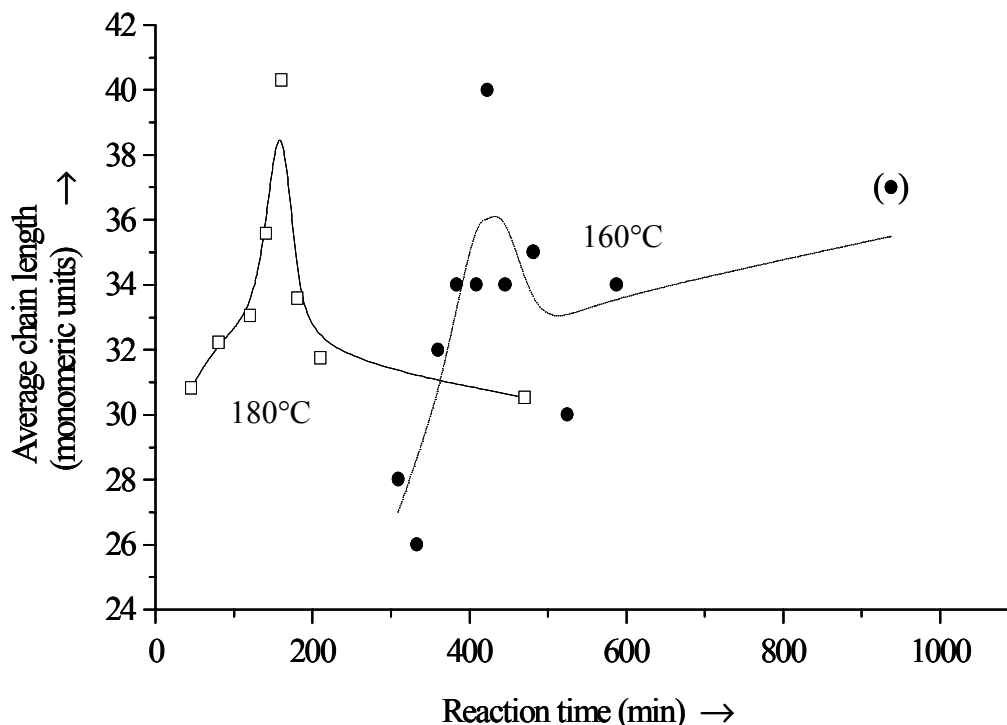


Fig. AI.1-5 Average chain length n of polyglycolide as determined by viscosimetry measurements in 1,1,1,3,3,3-hexafluoroisopropanol employing the Ubbelohde capillary technique. was determined on aliquots taken from the reaction at 160 (●) and 180°C (□). The value in parenthesis was obtained after a cooling period (see Materials and Methods).

degree of polymerization have been developed on the basis of the generated viscosity changes of polymer solution with different concentrations. A feasible method to obtain information about the chain length distribution is the Size Exclusion Chromatography (SEC), where molecules in solution are separated by their size in a more or less porous gel column compared to the elution times for a standard with known dispersity. Unfortunately, PGA is insoluble in almost all solvents except for 1,1,1,3,3,3-hexafluoroisopropanol (HFIP), which is highly volatile, toxic and expensive. A SEC apparatus operating on hexafluoroisopropanol was not available to determine the dispersity of PGA from solid-state reaction. The alternative to determine the degree of polymerization from CH_2 endgroup analysis in the ^1H NMR spectrum was obstructed by overlapping HFIP signals. Instead, viscosimetry measurements were carried out using an Ubbelohde capillary viscosimeter to obtain average molecular weights. The

relationship between the viscosity-average of the molecular weight \bar{M}_v and the intrinsic viscosity (Staudinger index) is given by the *Mark-Houwink equation*

$$[\eta] = K_\eta \cdot \bar{M}_v^a$$

with K_η and a being values that are characteristic of the corresponding polymer, the solvent and the measuring conditions¹⁴. Unfortunately, no Mark-Houwink equation is available for the system PGA/HFIP in the literature, therefore an exact determination of \bar{M}_v was not possible. Published values for K_η and a exist for polylactide and some of its copolymers in various solvents¹⁰. The exponent a (form factor) is generally in the range of 0.6-0.85, while the preexponential factor K_η is of the order of $5 \cdot 10^{-3}$ to 10^{-1} . To compute \bar{M}_v , the intrinsic viscosimetry together with the two corresponding constants have to be applied. For consistency, the determined $[\eta]_{\text{HFIP}}$ values were converted into $[\eta]_{\text{THF}}$ values following an empirical equation by Kenley et al.¹⁵, who gave a relationship for the intrinsic viscosity of poly(D,L-lactide-co-glycolide) ($n : n \approx 50 : 50$) in both THF and HFIP:

$$[\eta]_{\text{THF}} = 3.2(53) + 0.405(53) \cdot [\eta]_{\text{HFIP}} \quad ([\eta] \text{ in ml g}^{-1})$$

The corresponding constants for the copolymer were obtained by averaging five published values for PDLLA/PGA copolymers¹⁰, giving $K_\eta = 4.8 \cdot 10^{-2}$ and $a = 0.73$. The average number of monomers (degree of polymerization n) was calculated by dividing \bar{M}_v by 58, the monomer mass. Typical values for $[\eta]_{\text{HFIP}}$ were 20 ml g^{-1} , resulting in typical values for $[\eta]_{\text{THF}}$ of 12 ml g^{-1} .

Fig.AI.1-5 shows the degree of polymerization as a function of the reaction time for the two experiments at 160 and 180°C, respectively. Interestingly, \bar{M}_v increases with time up to a maximum of approximately 40 monomer units in both cases. The maximum in chain length corresponds to a molecular weight of $\approx 2300 \text{ g}$ which is in accordance with the data received from MALDI-TOF measurements. At both temperatures, the maximum in average degree of polymerization is reached before the

¹⁴ P.A. Lovell "Dilute solution viscosimetry" in *Comprehensive polymer science, vol. 1*, Pergamon, Oxford, New York, Beijing, Frankfurt, Sao Paulo, Sydney, Tokyo, Toronto, 1989, 173-197.

¹⁵ R.A. Kenley, M.O. Lee, T.R. Mahony, L.M. Sanders "Poly(lactide-co-glycolide) decomposition kinetics in vivo and in vitro", *Macromolecules* **1987**, 20, 2398.

reaction is finished ($\alpha = 1$). This points to at least two coexisting phenomena: the propagating polycondensation reaction increases the molecular weight and thermal degradation that sets in at this comparatively high temperature, decreasing the

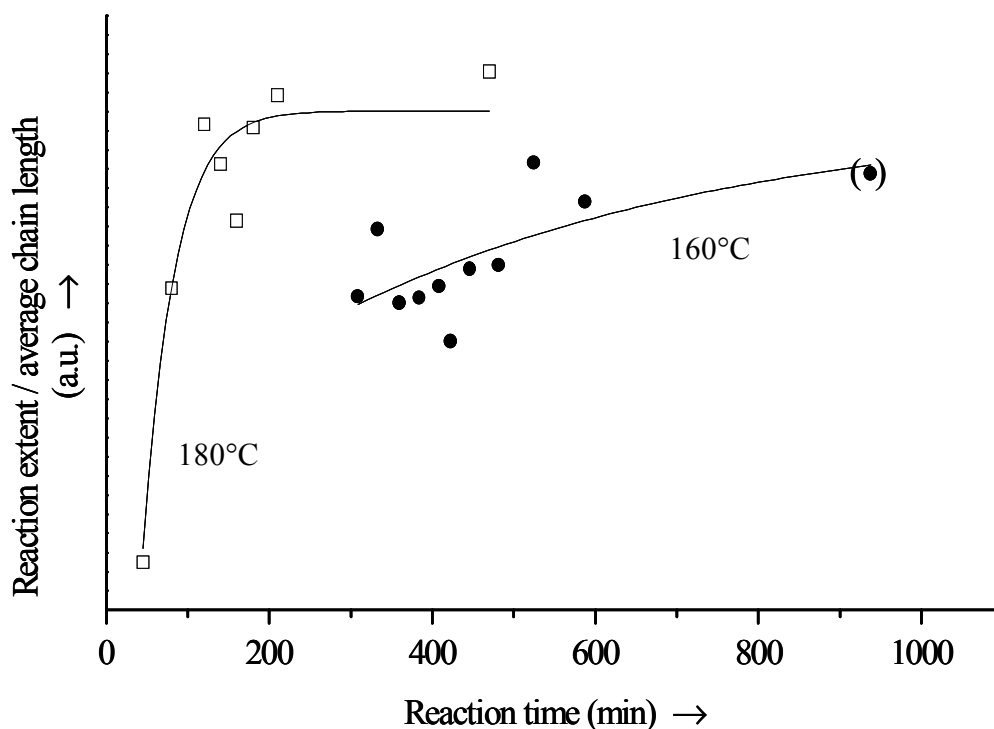


Fig. AI.1-6 The ratio of the reaction extent α to the average chain length n as a function of the reaction time for the two reaction temperatures 160 (●) and 180°C (□). The ratio is proportional to the number of chains present. The value in parenthesis was obtained after a cooling period (see materials and methods).

molecular weight. If a high degree of polymerization is desired, the reaction should be stopped after the precursors is completely converted at the latest to prevent loss of chain length due to thermal fragmentation. This accounts for different temperatures as lower reaction temperature is compensated by longer reaction times. For a temperature of 140°C (data not shown) a full conversion can be expected after approximately 6 d. Given the fact that the derived relationships to calculate the average degree of polymerization, themselves empirically determined, do not strictly account for PGA in HFIP and that the Mark-Houwink equation is computed with values for a PDLLA/PGA copolymer, it must be noted that the accuracy for absolute values has a substantial systematic error probably in the range of 30-50%. In contrast, the precision of the experiment itself is estimated to $\pm 1\%$. Therefore, the values for \bar{M}_v as displayed in **fig.AI.1-5** exhibit a considerable absolute error, but their relative magnitude, especially the occurrence of a maximum, is significant. Considering the absolute level

of the resulting polymer chains, it has to be stated that one can talk of oligomers with high degree of polymerization or a polymer with short chains compared to PGA from conventional ring-opening polymerization. The possibility to obtain molecules of higher molecular mass is restricted by the fact that the necessary temperature to initiate a solid-state reaction leads to parallel thermal degradation.

For the mechanism of chain growth, it is of interest whether the reaction pathway has more the character of a polycondensation (with a continuous increase in M as a function of the reaction extent α) or of a polymerization (with constant M). The definitions are designed to describe growth mechanism for reactions in solution. For solid-state reactions, structural limitations of the reactants and other anisotropic phenomena like crystal defects can trigger mixed mechanisms. An estimate of the number of polymer chains present in the sample is given by the ratio of the reaction extent α to the average chain length n . This is shown in **fig.AI.1-6**, where the number of chains increases sharply at the beginning of the reaction and remains mostly constant thereafter (again, more expressed for 180°C). With respect to the increase of the measured \overline{M}_v at the beginning, the following mechanism can be ruled out: The polymerization starts at potential nuclei (crystal defects), where a fast polymerization of neighboring molecules occurs, leading to a mixture of long polymer chains and residual unreacted precursor molecules. The unreacted sodium chloroacetate would have been removed by washing with water, and therefore the degree of polymerization would be independent of the reaction extent. In contrast to that scenario, the polymer chains grow steadily (except for the thermal fragmentation). It appears, that the reaction resembles more a polycondensation than a polymerization. Further information to resolve this question would be provided by a determination of the molecular weight distribution. The extraction experiments with hot acetone to identify possible low molecular weight oligomers and the melting behavior of PGA from NaClAc strongly suggest a relatively homogeneous molecular weight distribution. The absence of very short chains supports the proposed polycondensation mechanism.

Development of crystallinity

The crystallinity of the solid-state chemically prepared PGA was determined on aliquots of polyglycolide from the reactions by DSC. The melting enthalpy was

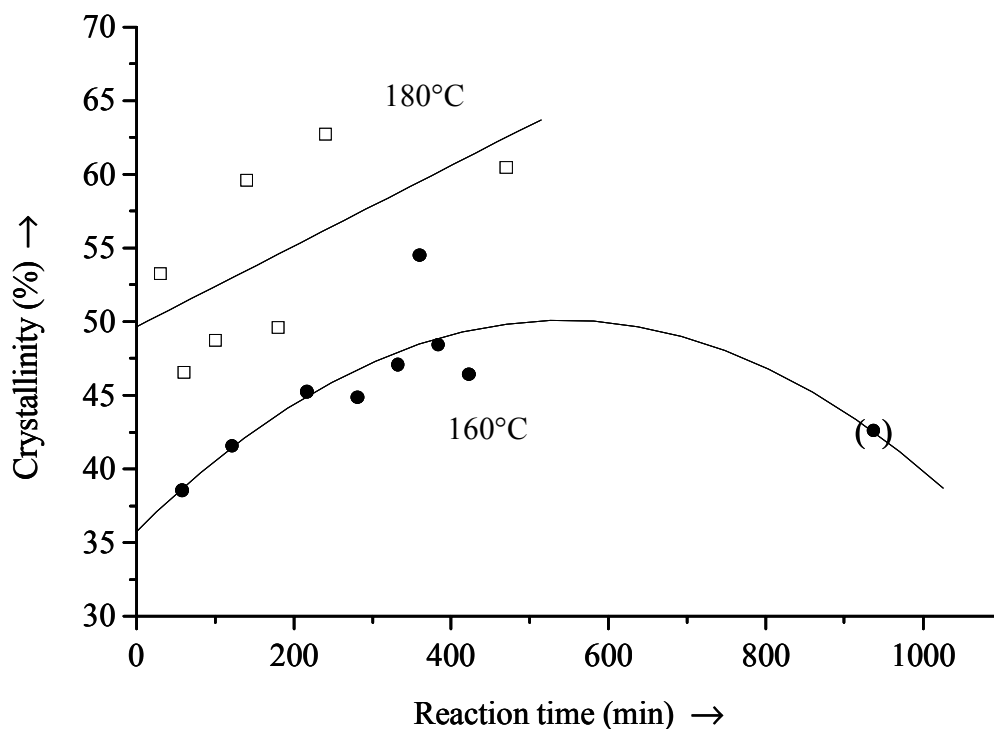


Fig. AI.1-7 Crystallinity of polyglycolide from NaClAc for reaction temperatures of 160 (●) and 180°C (□) as a function of reaction time. Crystallinity values were determined on the melting enthalpy by DSC compared to 100% crystalline polymer. The data point in parenthesis was obtained after a cooling period (see material and methods).

measured and related to the value for 100% crystalline polymer. Two literature values from were averaged to obtain a relative crystallinity. Ginde and Gupta¹⁶ published 11.96 kJ mol⁻¹ (monomer equivalents) and Lebedev¹⁷ et al. 11.75 kJ mol⁻¹, giving an average value of 11.86 kJ mol⁻¹. The heating rate was 5 k min⁻¹ with sample masses of 5-8 mg. Division of the measured enthalpy of fusion by the averaged value for fully crystalline PGA gives an estimate of the degree of crystallinity. **Fig.AI.1.-7** displays the development of the crystallinity for the two temperatures. For both temperatures, the crystallinity increases with time. The data point in parentheses was obtained after cooling (quenching process with possible changes in crystallinity) and renewed

¹⁶ R. Ginde, R. Gupta "In vitro chemical degradation of poly(glycolic acid) pellets and fibers", *J. Appl. Polym. Sci.* **1987**, 33, 2412-2429.

¹⁷ B.V. Lebedev, A.A. Yevstropov, Y. G. Kiparisova, V.I. Belov "The thermodynamics of glycolide, polyglycolide and of polymerization of glycolide in the temperature range of 0-550°K", *Polym. Sci. USSR* **1978**, 20, 32-42.

heating and should therefore be disregarded for the interpretation. At 180°C the values are about 10% higher than at 160°C. Apparently, annealing provides the activation energy for an ordering process. The measured crystallinity (37-62%) is in the range of reported values for conventionally prepared PGA¹⁸.

Porosity of the formed polyglycolide

The polycondensation mechanism comprises the elimination of NaCl. At the very beginning after the emergence, the atoms have to be present as ion-pairs accumulating to small clusters to minimize the interfacial energy. In a previous study, the formation

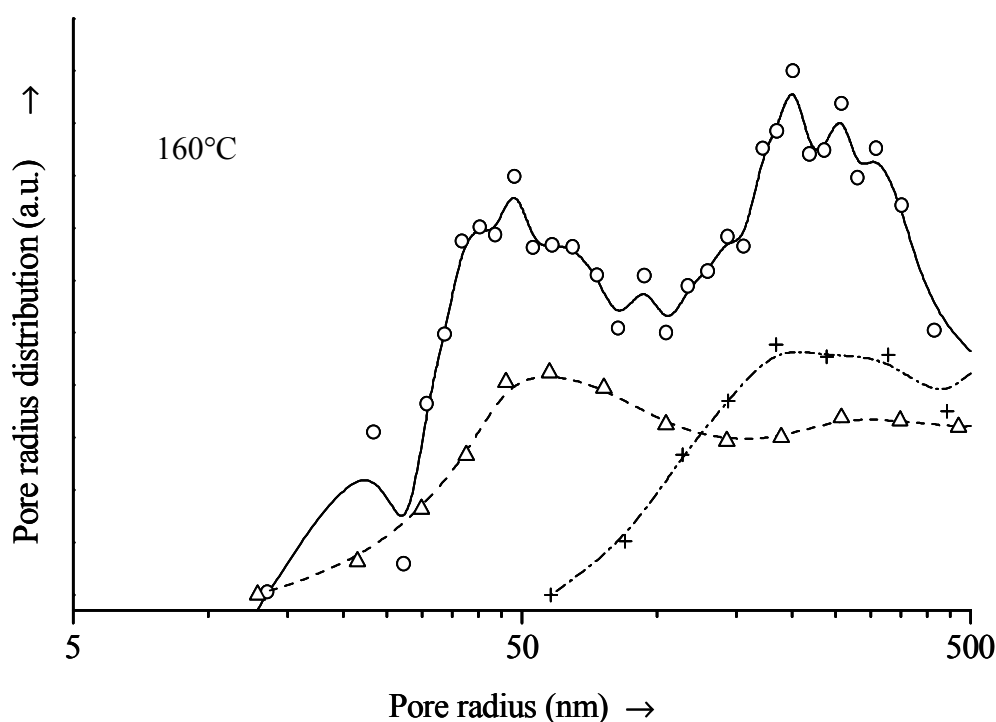


Fig. AI.1-8 Pore radius distribution of PGA reacted at 160°C determined by mercury porosimetry. Measured samples were taken after 90 min (O), 180 min (Δ) and 380 min (+), respectively.

of PGA from sodium bromoacetate was followed by *in situ* XRD¹⁹. The average crystallite size of the formed NaBr was approximated by evaluation of the line width applying the Scherrer equation²⁰. The crystallites grow almost linearly with temperature from detectable 200 Å at 100°C to 1600 Å at 170°C. Concerning the

¹⁸ D.K. Gilding, A.M. Reed "Biodegradable polymers for use in surgery – polyglycolic/poly(lactic acid) homo- and copolymers: 1", *Polymer* **1979**, 20, 1459-1464.

¹⁹ M. Epple, G. Sankar, J.M. Thomas "Solid-state polymerization reaction by combined in-situ X-ray diffraction and X-ray absorption spectroscopy (XRD-EXAFS)", *Chem. Mater.* **1997**, 9, 3127-3131.

²⁰ E.F. Kaelble, *Handbook of X-rays*, McGraw-Hill, New York, **1967**.

reaction extent, the reaction was finished at 120°C. These results underscore the assumption that the thermally driven coalescence process of the NaBr crystals continues after the precursor is totally consumed. As the porosity of the formed polymer is generated with the removal of the included salt, the average crystallite size should have an influence on the pore size distribution and the number of pores. The latter parameters were determined from SEM micrographs for surfaces (two dimensional evaluation) of PGA from different precursors by counting and measuring¹. For NaClAc the total number of pores was 260 per 100 μm^2 and the average pore diameter was determined to be 0.3 μm . The overall porosity is fixed by stoichiometry and the density of the products¹, giving a value of about 42.6 vol.% for PGA from NaClAc.

To determine a 3-dimensional pore size distribution, mercury porosity is an appropriate tool. Hg is pressed into a porous structure under high pressure. If the intruded mercury volume and the applied pressure are known, the corresponding pore diameter can be computed using the *Washburn equation*²¹

$$\Delta p \cdot r = -2 \cdot \gamma \cdot \cos \Theta$$

with Δp (as pressure difference), r (pore diameter), γ (surface tension of mercury) and Θ (contact angle of mercury with the porous material). The right hand side of the equation consists of two constants. Therefore, r can be calculated for a measured pressure profile. The evaluation was carried out with the program "MI.Le.S.TO.NE. 100" by Carlo Erba Instruments. The resulting pore radius distributions are displayed in **fig.AI.1-8** and **-9**. Three aliquots were analyzed for each temperature. At 160°C, the time points correspond to reaction extents of 17% (90 min), 37% (180 min) and 68% (380 min), respectively. At 180°C, the values are 5% (15 min), 20% (45 min) and 98% (240 min). For both temperatures, a shift to larger pores with reaction time is visible. At 160°C, a bimodal distribution with maxima at 40 nm and at 250 nm is detected. The first maximum (smaller pore sizes) had vanished after 380 min ($\alpha = 0.65$), indicating the growth of NaCl crystals with reaction extent. The same observations, but less pronounced can be made for 180°C. After 240 min of reaction and 98% reaction extent, no pore radii were measured below 150 nm. (Note that the distribution above $r = 400$ nm should be disregarded, because of the filling of

interstitial grain voids at low Hg-pressures).

The maxima of the last measured values (r in the range of 200-250 nm) are in good agreement with the two-dimensional evaluation from SEM micrographs, where an average pore diameter of $\underline{d} = 300$ nm was determined¹. The mercury porosimetry experiments confirm the data obtained from *in situ* XRD: annealing leads to the

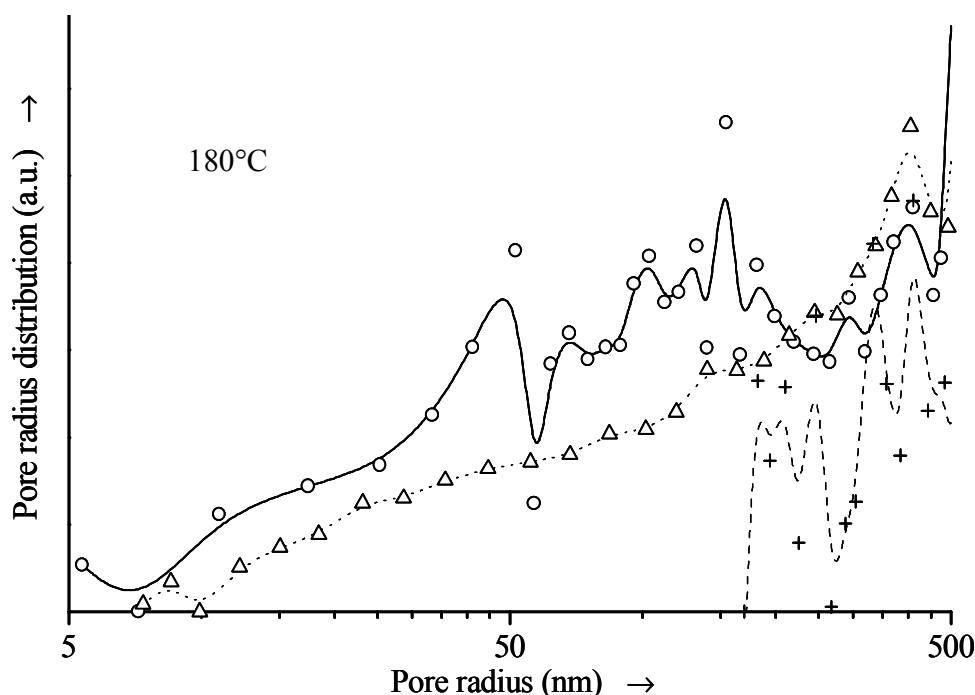


Fig AI.1-9 Pore radius distribution of PGA reacted at 180°C determined by mercury porosimetry. Measured samples were taken after 15 min (o), 45 min (Δ) and 240 min (+).

formation and growth of the NaCl crystals. As small cavities seem to disappear with prolonged reaction, it is obvious that small clusters aggregate to bigger crystals.

An approach to explain the bimodal distribution could be as follows: around the crystals corresponding to the second (and final?) maximum the distance is too far for other crystals (of comparable size) to migrate and fuse with the parent one. A saturation in the growth mechanism is achieved. The maximum corresponding to smaller average pore radius refers to "newly reacted" spaces, where further fusion is slowed down, limited by the diffusion of already aggregated crystals of a certain size, but still possible.

This implies, on an atomic scale, that there is a considerable diffusion of NaCl within the solid material. It would be of interest to clarify the migration mechanism and the

²¹ E.W. Washburn, *Phys. Rev.* **1921**, 17, 273.

routes of lowest energy for NaCl to travel through the growing polymer chains and the fully reacted bulk material.

AI.2 Concluding remarks

The solid-state reaction of sodium chloroacetate to polyglycolide was studied with a number of techniques to characterize the formed polyester and to monitor the parameters reaction extent, degree of polymerization, crystallinity and pore radius distribution *ex situ* during the reaction. The results can be summarized as follows to complement previous investigations:

- The reaction takes place in one step without detectable intermediates. The reaction course can be displayed as a sigmoidal curve with an induction period at the beginning, followed by a fast propagation. Approaching $\alpha = 1$, the reaction slows down, due to the consumption of precursor. The reaction time is about 2 h at 180°C and approximately 15 h at 160°C.
- The reaction is strongly enhanced by an increase in reaction temperature.
- The average degree of polymerization increases with reaction time, reaches a maximum of about 40 monomer units in the chain, and decreases again as a consequence of parallel thermal degradation. The value for \bar{M}_v is low compared to conventionally prepared PGA. The molecular weight distribution, although not measured, has to be relatively homogeneous as no short oligomers could be detected. The obtained data speaks in favor of a polycondensation mechanism.
- The crystallinity increases as a function of reaction time and is comparable to conventional PGA.
- The eliminated NaCl is formed as small crystals at the beginning of the reaction (diameter ca. 40 nm). With time, larger crystals grow at the expense of smaller crystals, leading to an increase of average pore diameter after removal of the occluded salt with water (diameter ca. 400 nm).

The intrinsic porosity makes PGA from solid-state reaction an even more interesting biomaterial compared to conventional compact polyglycolide. A significant restriction for the synthesis of the biomaterial PGA is the thermal degradation at elevated temperatures, limiting the average molecular weight of the product. The structural investigations point to a topochemically determined reaction. The relative

intermolecular orientation and the vibrational activation are critical to the start and propagation of the reaction. Bearing this in mind, experiments appear worthwhile to initiate the reaction with infrared radiation of appropriate energy and dosage to reduce thermal stress and heat accumulation.

A main goal of reaction control is the reproducibility of the reaction itself and the products. The described solid-state reaction is influenced by a number of parameters, which are impossible to coordinate all at once. Note that the monitoring of the PGA properties at two temperatures for two experiments has to be interpreted *ceteris paribus* - with other factors kept constant, except for the external temperature. The characterization of the reaction made it clear that dynamic processes continue after the polycondensation is chemically finished: the formed polyglycolide crystallizes upon prolonged annealing accompanied by thermal fragmentation and NaCl undergoes a diffusion mediated crystallite growth comparable to Ostwald ripening for crystals in solution with the minimization of the surface energy as the driving force.

AI.3 Materials and Methods

Chloroacetic acid and sodium hydroxide were purchased from Merck in "pro analysis" quality.

Sodium chloroacetate

NaClAc was synthesized by neutralization of chloroacetic acid (101.92 g, 1.08 mol) with NaOH (42.93 g, 1.08 mol) in ethanol. Chloroacetic acid was dissolved in 300 ml solvent. Under ice-cooling and stirring NaOH, dissolved in 100 ml ethanol, was slowly added. NaClAc precipitates as a white powder. After 30 min, about half of the solvent was removed in vacuum and the precipitate was filtered off. The product was washed with cold ethanol and ether followed by drying in oil-pump vacuum. 100.7 g (0.86 mol) product were obtained, 81% of the theoretical yield.

Characterization:

Elemental analysis: C: 20.69% (calc. 20.6%), H: 1.86% (calc. 2.0%)
IR (KBr): $\tilde{\nu}$ [cm⁻¹] = 3010 (w, C-H), 2975 (w, C-H), 1601 (s, C=O), 1419 (s, COO⁻, C-H), 1250 (s, C-O), 932 (m),

770 (m), 674 (m), 578 (m), 426 (m)

 $^1\text{H NMR}$ (360 MHz, D_2O): δ [ppm] = 4.06 (s, 2H)XRD (main reflections): Diffraction angle [$^\circ 2\Theta$] = 8.24 (001), 33.2 (004)DSC ($\beta = 5 \text{ K min}^{-1}$) $\Delta_{\text{R}}H$ [kJ mol^{-1}] = -24.9

Polycondensation

Sodium chloroacetate was ground prior to reaction. For both temperatures, 30 g of precursor were reacted in a round-bottom flask under nitrogen atmosphere. It took 30 min to reach the final temperatures of 160 and 180°C, respectively. The time points were defined as $t = 0$. From 120°C on, the reactions were stirred every 5 min with a spatula. Aliquots of 2 g substance were taken from the vessels every 30 to 40 min for 160°C and about every 20 min for 180°C. In the case of the longer reaction time at 160°, the reaction was cooled to room temperature after 588 min for 12 h to be reheated to 160°C for another 440 min, giving a total reaction time of 1028 min.

The aliquots were analyzed by gravimetry, DSC, XRD and $^1\text{H NMR}$. For mercury porosimetry, crystallinity and viscosimetry the samples were washed with water as described above to obtain the porous polymer.

Determination of the reaction extent

From XRD

X-ray powder diffractometry was carried out with a Philips PW 1050/25 diffractometer (Ni-filter, Cu K_α -radiation, $\lambda = 154.178 \text{ pm}$, proportional detector) in

$$\alpha = \frac{I_t}{I_{(t=\infty)}}$$

Bragg-Brentano geometry. The peak intensity was measured by integration. The reaction extent α was determined on the one hand by dividing the peak integrals of the

$$\alpha = 1 - \frac{I_t}{I_{(t=0)}}$$

parent compound (sodium chloroacetate) by those at $t = 0$:

On the other hand, the reaction extent was calculated by extrapolation to complete reaction concerning the products PGA and NaCl:

No strong differences were found for the three components, except for a small time lag in the formation of PGA ascribed to delayed crystallization. The following, non-overlapping reflections were used for integration:

sodium chloroacetate: $2\Theta = 8.24$ (001), 33.2 (004)

NaCl: $2\Theta = 31.76$ (200), 45.48 (220)

PGA: $2\Theta = 22.20$ (011), 27.44 (200) (Miller indices assigned)

From DSC

Differential scanning calorimetry was carried out with a Mettler TA 4000 instrument in sealed aluminum crucibles. The heating rate was generally 5 K min^{-1} , applied for an

$$\alpha = 1 - \frac{n(\text{NaClAc})_t}{n(\text{NaClAc})_{(t=0)}} = 1 - \frac{\Delta_R H_t}{\Delta_R H_{(t=0)}}$$

interval from 30-300°C and the average sample mass was in the range 5-8 mg. The reaction extent was determined by the reaction enthalpy $\Delta_R H$ for the polycondensation of the parent sample.

The fraction of NaClAc in the mixture with NaCl and PGA undergoes the exothermic polymerization. The measured enthalpy is proportional to the amount of unreacted precursor. It is divided by $\Delta_R H$ for a pure sample of NaClAc ($-25.2 \text{ kJ mol}^{-1}$) determined by multiple runs³.

From ¹H NMR

NMR spectroscopy was carried out with a Varian Gemini 200 instrument (200 MHz). Aliquots of partially reacted sodium chloroacetate were dissolved in D₂O. The insoluble PGA was allowed to precipitate in the NMR tube. Addition of a constant amount of sodium acetate gave a standard for the amount of NaClAc in solution:

$$\alpha = 1 - \frac{n(\text{NaClAc})_t}{n(\text{NaClAc})_{(t=0)}} \quad \text{with} \quad n(\text{NaClAc})_t = n(\text{NaAc}) \cdot X$$

$$X = \frac{I_{4.06 \text{ ppm}}}{I_{1.88 \text{ ppm}}} \cdot \frac{3}{2}$$

$$\text{and} \quad n(\text{NaClAc})_{(t=0)} = \frac{m_{\text{sample}}}{M_{\text{NaClAc}}}$$

The factor X correlates the proton signal integrals of the standard sodium acetate ($\delta = 1.88$ ppm, 3H) and NaClAc ($\delta = 4.06$ ppm, 2H).

From gravimetry

Sodium chloroacetate and NaCl are soluble in water, whereas polyglycolide is completely insoluble. This fact is exploited for the derivation of the reaction extent from gravimetry. The weight of parent aliquot fractions was determined prior to washing with water. With NaCl and remaining precursor removed, the mass of PGA can be measured after drying in vacuum. The reaction extent can be computed as follows:

$$\alpha = \frac{m(PGA)_t}{m(PGA)_{(t=\infty)}} \quad \text{with} \quad m(PGA)_{(t=\infty)} = \frac{m_{\text{sample}} \cdot M(PGA)_{\text{monomer}}}{M(\text{NaClAc})}$$

$m(PGA)_t$ is obtained as the dry-mass of the polymer and $m(PGA)_{(t=\infty)}$ is fixed by the sample mass.

Mass spectroscopy

The following instruments were employed for different ionization modi:

Electron ionization (EI): Varian, "MAT 311A"

Fast Atom Bombardment (FAB): VG Analytical, "70-250 s" (Xenon)

MALDI-TOF: Finnigan, "MAT Vision 2000" (5 keV ion source, 20 kV acceleration, N₂-Laser, 337 nm)

Viscosimetry

Viscosimetry was carried out with an Ubbelohde capillary viscosimeter (DIN 51562), immersed in a water bath of 25°C. 90 mg of PGA were dissolved in previously dried 1,1,1,3,3,3-hexafluoroisopropanol (30 ml) and stirred for 3 days at room temperature. The concentration was therefore 3 mg ml⁻¹ throughout all experiments. The resulting solution was of yellowish color and transparent without visible solid residues. The solutions were filtered prior to measurement. 7-10 runs were carried out with each sample and the results were averaged. In the light of the very expensive and volatile solvent, the reduced viscosity was measured instead of the intrinsic viscosity. The

determination of the intrinsic viscosimetry would require several measurements per sample with different concentrations to extrapolate the data for infinitely diluted solution. In a preliminary experiment this was done for a different PGA sample with concentrations of the same range. The reduced viscosity changed only little in the probed concentration range (1.3-5 mg ml⁻¹), therefore it appeared justified to sacrifice absolute accuracy for practicability.

In the experiment, the time is measured for a fixed solution volume to flow through the capillary under hydrostatic pressure. The relative viscosimetry can be computed by the ratio of the averaged flow times for the probed solution and the pure solvent:

$$\eta_r = \frac{\eta}{\eta_0}$$

The reduced viscosimetry can be further determined according to the following relation:

$$\eta_{red} = \frac{\eta_r - 1}{c}$$

The measured values were used for the intrinsic viscosimetry to determine \bar{M}_v with the *Mark-Houwink equation* (after conversion to THF-relevant values following Kenley et al.) as described in the results and discussion section.

Crystallinity

The degree of crystallinity of porous PGA was determined with DSC under the same conditions as for the reaction extent. The enthalpy of fusion was measured for the probed samples. The crystallinity was related to the averaged values for 100% crystalline PGA^{16,17} ($\Delta_f H_{(100\%)} = 11.86 \text{ kJ mol}^{-1}$):

$$\text{crystallinity}[\%] = \frac{\Delta_f H_t}{\Delta_f H_{(100\%)}} \cdot 100$$

Mercury porosimetry

The measurements were carried out with a "Porotec 200" porosimeter and a "Macropore-120-Unit" Hg-filling station from Carlo Erba Instruments. Mercury was purified by extensive filtration. The measurements are automated and the data

evaluation was executed by the program "MI.Le.S.TO.NE" provided by Carlo Erba Instruments. The sample mass was about 100 mg. The parameters required for the application of the *Washburn equation* were taken from literature (contact angle Hg/PGA $\Theta = 132^\circ$, Hg surface tension $\gamma = 4.85 \cdot 10^{-3} \text{ N cm}^{-1}$)²².

²² L.E. Freed, J.C. Marquis, A. Nohria, J. Emmanuel, A.G. Mikos, R. Langer "Neocartilage formation *in vitro* and *in vivo* using cells cultured on synthetic biodegradable polymers", *J. Biomed. Mater. Res.* **1993**, 27, 11-23.

AII. The *in vitro* degradation of polyglycolide from solid-state reaction

AII.0 Introduction

The physico-mechanical properties of aliphatic polyesters depend on intrinsic and extrinsic factors²³. Chemical structure and reactivity, degree of crystallinity and polymerization, affinity to other compounds/solvents and thermodynamic characteristics vary with the type of polyester²⁴. Environmental temperature, thermal treatment and fabrication (with respect to isotropic/anisotropic chain alignment, macroscopic architecture), exposition to chemicals or radiation and applied mechanical stress contribute as external parameters to the performance of polyester devices. The main applications for poly(α -hydroxy acids), namely as scaffolds for tissue engineering, matrices for drug delivery and devices for bone substitution and fixation, rely on the initial and predictable properties of the polyesters in use. The individual function is closely linked to the mechanical, chemical and biological performance over time.

Due to the polarized functional ester group, polyesters are susceptible to nucleophilic chain cleavage. In aqueous media, hydrolysis by the nucleophil water leads to the degradation of polymer chains:

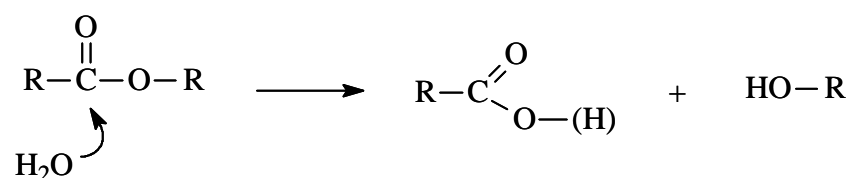


Fig. AII.0-1 Hydrolytic chain cleavage generating acidic endgroups.

In the body, implant materials are exposed to body-fluids. Body-fluids are aqueous solutions containing proteins, enzymes and salts. Polymeric materials are likely to be affected by this environment in various ways such as wetting and swelling, adsorption and hydrolysis. Polymers may be degraded by hydrolysis due to the aqueous medium

²³ I. Engelberg, J. Kohn "Physico-mechanical properties of degradable polymers used in medical applications: a comparative study", *Biomaterials* **1991**, 12, 292-304.

²⁴ J.P. Singhal, H. Singh, A.R. Ray "Absorbable suture materials: preparation and properties", *JMS-Rev. Macromol. Chem. Phys.* **1988**, C28(384), 475-502.

and/or by enzymes. Many bacteria employ depolymerases²⁵ to digest higher poly(hydroxy acids) for metabolization.

The experimental efforts to investigate the contribution of these two types in polyester degradation *in vivo* and *in vitro* were reviewed by Vert et al.²⁶, who reported a consensus that enzymatic breakdown plays an inferior role compared to hydrolytic degradation for the main systems PGA, PLA and copolymers. The activity of esterases is restricted to the last stages of bulk and chain degradation, when mono- and oligomers are metabolized. The overall degradation kinetics is independent from the presence or absence of depolymerases. These conclusions were supported by a study by Doi et al.²⁷ who analyzed the impact of proteinase-K exposition to single crystals of poly(L-lactic acid). Degradation was observed to little extent at the crystal edges of disordered chain-packing regions without a significant reduction in molecular weight distribution. Doi proposed an enzymatic activity on single polyester chains sticking out of the inaccessible bulk material. Hydrolysis is therefore the dominating mechanism to affect polyester properties in aqueous media.

The chain scission itself is a random process for equal positions in the chain, assuming comparable exposition to water²⁸. As a consequence, hydrophilicity, porosity structure and ordering state of the polymer contribute to the degradation rate.

Although PGA was the subject of various degradation studies, most of the work was done with polylactides of different stereo-compositions, and copolymers of the two polymers²⁹. The persistence of the investigated polyesters (i.e., molecular weight, crystallinity, mechanical stability, geometry conservation) strongly depends on the stereo-regularity and the initial degree of crystallinity. The time for a total mass loss

²⁵ D. Seebach, A. Brunner, B.M. Bachmann, T. Hoffmann, F.N.M. Kühnle, U.D. Lengweiler "Biopolymers and -oligomers of (R)-3-hydroxyalkanoic acids – Contributions of synthetic organic chemists", *Lectures of the Ernst Schering Foundation* **1995**, 28.

²⁶ M. Vert, S.M. Li, G. Spenlehauer, P. Guerin "Bioresorbability and biocompatibility of aliphatic polyesters", *J. Mater. Sci.: Mater. In Med.* **1992**, 3, 432-446.

²⁷ T. Iwata, Y. Doi "Morphology and enzymatic degradation of poly(L-lactic acid) single crystals", *Macromolecules* **1998**, 31, 2461-2467.

²⁸ N. Ashammakhi, P. Rokkanen "Absorbable polyglycolide devices in trauma and bone surgery", *Biomaterials* **1997**, 18, 3-9.

²⁹ S. Li "Hydrolytic degradation characteristics of aliphatic polyesters derived from lactic and glycolic acids", *J. Biomed. Mater. Res.* **1999**, 48, 342-353.

ranges from about 15 weeks for amorphous poly(D,L-lactic acid)³⁰ and more than 4 years for highly crystalline poly(L-lactic acid)³¹. For polyglycolide samples, the duration of stability was reported to be a few weeks, with material disintegration at 6 weeks and a total dissolution at about 15 weeks^{16,32}. The periods published for total degradation range from 3-9 months²⁸. All poly(α -hydroxy acids) have in common that amorphous regions of the material degrade much faster than crystalline ones, so that for semi-crystalline polyesters the average crystallinity of the residual bulk increases at first and decreases in the final stages of degradation³³. Due to a higher hydrophilicity and a more strongly polarized ester group, polyglycolide degrades *ceteris paribus* faster than polylactide. This fact was underscored by results from degradation of poly(lactide-co-glycolide)³⁴. The preferential degradation of PGA sections leads to an enrichment of PLA sequences and to crystallization. Van der Elst et al. observed such a behavior in a long-term animal model with PLA and copolymer pins, which were implanted in the femora of sheep³⁵. After 30 months of implantation, the copolymer disappeared in some femora, while in others the implant was present as an disintegrated bulk. The PLA pins retained their compact appearance with surface cracks in some cases. Tracy et al. executed a comparative *in vitro/in vivo* study on copolymer microspheres for sustained drug release³⁶. The relative degradation with respect to reduction of molecular weight *in vivo* (Sprague-Dawley rats, subcutaneous injection) was 1.7-2.6 times faster than *in vitro*. An exponential decrease in molecular

³⁰ S.M. Li, H. Garreau, M. Vert "Structure-property relationships in the case of the degradation of massive aliphatic poly-(α -hydroxy acids) in aqueous media, Part 1: Poly(D,L-lactic acid)", *J. Mater. Sci.:Mater. Med.* **1990**, *1*, 123-130.

³¹ S.M. Li, H. Garreau, M. Vert "Structure-property relationships in the case of the degradation of massive aliphatic poly-(α -hydroxy acids) in aqueous media, Part 3: Influence of the morphology of poly(L-lactic acid)", *J. Mater. Sci.:Mater. Med.* **1990**, *1*, 198-206.

³² W.D. Holder, H.E. Gruber, A.L. Moore, C.R. Culberson, W. Anderson, K.J.L. Burg, D.J. Mooney "Cellular ingrowth and thickness changes in poly-L-lactide and polyglycolide implanted subcutaneously in the rat", *J. Biomed. Mater. Res.* **1998**, *41*, 412-421.

³³ E.A.R. Duek, C.A.C. Zavaglia, W.D. Belangero "In vitro study of poly(lactic acid) pin degradation", *Polymer* **1999**, *40*, 6465-6473.

³⁴ S.M. Li, H. Garreau, M. Vert "Structure-property relationships in the case of the degradation of massive aliphatic poly-(α -hydroxy acids) in aqueous media, Part 2: Degradation of lactide-glycolide copolymers: PLA37.5GA25 and PLA75GA25", *J. Mater. Sci.:Mater. Med.* **1990**, *1*, 131-139.

³⁵ M van der Elst, C.P.A.T. Klein, J.M. de Blicke-Hogervorst, P. Patka, H.J.T.M. Haarman "Bone tissue response to biodegradable polymers used for medullary fracture fixation: A long term *in vivo* study in sheep femora", *Biomaterials* **1999**, *22*, 121-128.

³⁶ M.A. Tracy, K.L. Ward, L. Firouzabadian, Y. Wang, N. Dong, R. Qian, Y. Zhang "Factors affecting the degradation rate of poly(lactide-co-glycolide) microspheres *in vivo* and *in vitro*", *Biomaterials* **1999**, *20*, 1057-1062.

weight was observed. After 25 days, no polymer bulk material was left. Parallel to the untreated samples, zinc carbonate was added to the microspheres to change the water affinity. A second variation was the capping of endgroups as ethyl esters. In all cases, the degradation developed parallel to the extent of water uptake. The capping of the chain ends lead to a delay in water uptake and an extended stability. Samples with zinc carbonate and capped endgroups retained residual mass for more than 50 days. For uncapped samples, the addition of the salt had no effect. Note that *in vivo* an implanted material is usually exposed to permanent mechanical stress. Such conditions can contribute to an increase in surface area, material desintegration and a accelerated degradation.

Understanding degradation requires the distinction between the two main parameters mass loss and reduction of average molecular weight. While the process of chain scission is defined as degradation, the mass loss of the sample is denoted erosion, the removal of soluble degradation products from the polymer mass³⁷. Following these definitions, a considerable degradation can take place without a decrease in sample mass. For the degradation of bulk PLA/PGA polymers, a special mechanism was repeatedly observed: a faster degradation for the inner parts of the polymer bodies compared to other regions³⁸. Such an inhomogeneous surface/interior differentiation exhibits shorter chains (and more acidic endgroups) in the center, a cracked and roughened surface and a less affected area in between³⁹. Prolonged degradation leads to hollow structures via a state of pasty/glassy consistency in the center. Hollow structures form after the erosion of highly degraded oligomers (**fig.AII.0-3**). Nowadays, the heterogeneous degradation is accepted as a general mechanism for the behavior of compact polyesters in aqueous media⁴⁰. The common explanation is the entrapment of acidic degradation products, caused by limited diffusion and exchange in bulk polymers. The lowering of local pH leads to further hydrolysis that triggers an autocatalytic cycle. This phenomenon of accumulated oligomers is more pronounced

³⁷ A. Göpferich, R. Langer "Modeling of polymer erosion", *Macromolecules* **1993**, 26, 4105-4112.

³⁸ M. Vert, G. Schwarch, J. Coudane "Present and future of PLA polymers", *J.M.S.-Pure Appl. Chem.* **1995**, A32(4), 787-796.

³⁹ P. Mainil-Varlet, R. Curtis, S. Gogolewski "Effect of *in vivo* and *in vitro* degradation on molecular and mechanical properties of various low-molecular-weight polylactides", *J. Biomed. Mater. Res.* **1997**, 36, 360-380.

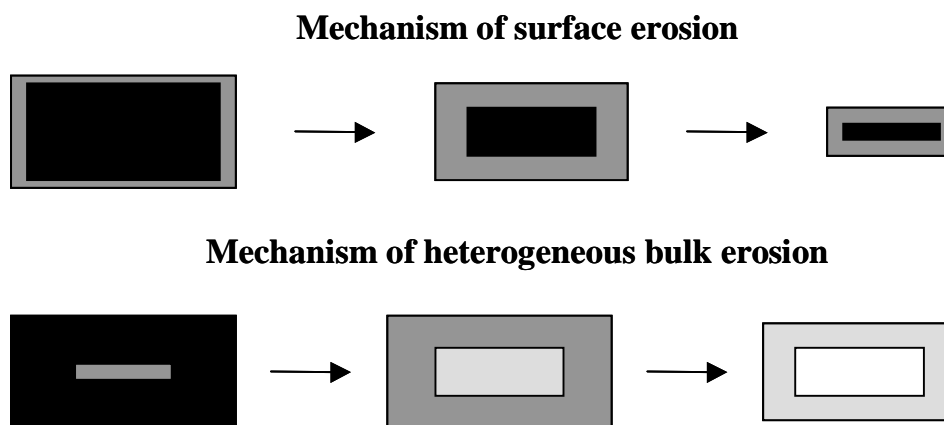


Fig. AII.1-2 Schematic illustration of surface vs. heterogeneous bulk erosion

in the center region. For porous PLLA, the influence of pore wall thickness on the degradation speed was investigated⁴¹. It was found that thicker walls significantly decrease the half-lives based on average molecular weight. This was ascribed to the local autocatalytic effect. In contrast, Grizzi et al. showed that small-sized devices such as thin films or fibers degraded homogeneously and therefore slower, due to absence of autocatalysis⁴². From these results, it can be derived that the porosity and the internal surface to volume ratio of a polyester has a considerable influence on the sustainability of the implant. The generation of acidity and the described heterogeneous mechanism during degradation have important implications and consequences for the *in vivo* application of polyesters.

In most tissues of the body, the pH is buffered at the physiological level of 7.2 to 7.5. This homeostasis is a prerequisite for cell function and healing processes of damaged tissue like bone. Deviations from the physiological range can lead to tissue necrosis and cell death. As a vital cell activity is necessary for the restoration of bone at the implant site, the control of local pH is critical for a successful bone substitution. This is especially valid for the phase of beginning erosion from the implant. The "acidic burst" caused by the elution of former entrapped oligomers has a negative effect on the

⁴⁰ S. Li, S. McCarthy "Further investigations on the hydrolytic degradation of poly(DL-lactide)", *Biomaterials* **1999**, *20*, 35-44.

⁴¹ L. Lu, S.J. Peter, M.D. Lyman, H.-L. Lai, S.M. Leite, J.A. Tamada, J.P. Vacanti, R. Langer, A.G. Mikos "In vitro degradation of porous poly(L-lactic acid) foams", *Biomaterials* **2000**, *21*, 1595-1605.

⁴² I. Grizzi, H. Garreau, S. Li, M. Vert "Biodegradation of devices based on poly(lactic-co-glycolic acid): size-dependence", *Biomaterials* **1995**, *16*, 305-311.

biocompatibility and can even lead to osteolysis of the surrounding bone^{43,44}.

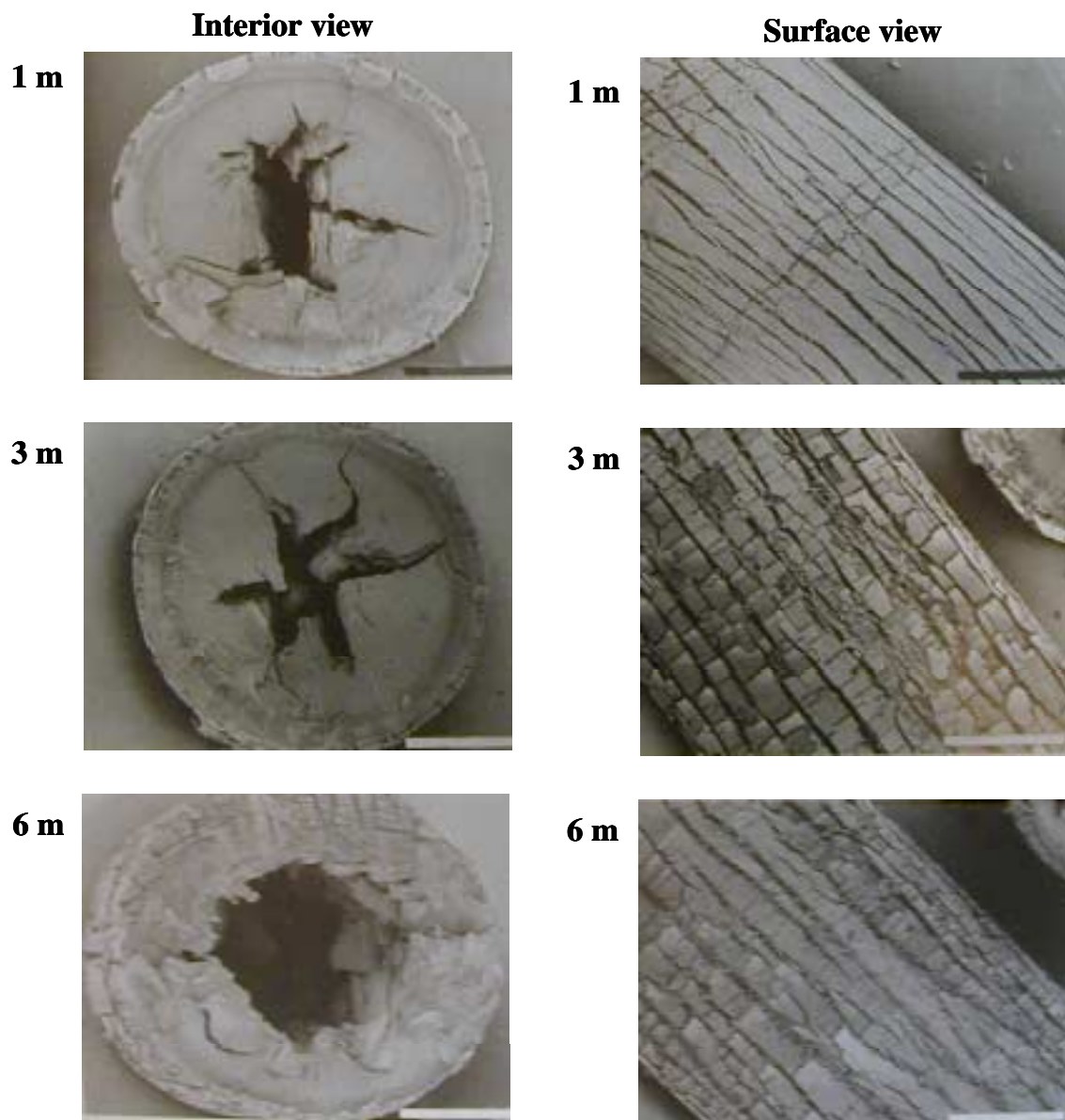


Fig. AII.0-3 Heterogeneous bulk erosion observed for a pin of poly(D,L-lactic acid) after 1, 3 and 6 months incubation in PBS. Degradation leads to hollow pins with a cracked surface³⁹.

To prevent this acidosis phenomenon, accumulation of acid products has to be avoided, so that the natural exchange in body-fluids can keep the concentration below

⁴³ O.M. Böstmann "Osteolytic changes accompanying degradation of absorbable fracture fixation implants", *J. Bone Joint Surg.* **1991**, 73B, 679-682.

⁴⁴ O. Böstmann, U. Pääväranta, E. Partio, J. Vasenius, M. Manniner, P. Rokkanen "Degradation and tissue replacement of an absorbable polyglycolide screw in the fixation of rabbit femoral osteotomies", *J. Bone Joint Surg.* **1992**, 74A, 1021-1031.

the threshold of cytotoxicity⁴⁵. Porosity might be a key factor to ensure biocompatible degradation. Other important aspects to consider *in vivo* are adverse effects like macrophage activity due to crystalline particles of degrading polymer⁴⁶ and formation of fibrous tissue (neomembranes⁴⁷), separating the implant from the healthy bone matrix. Such reactions can strongly disturb the healing process. The minor role of enzymatic degradation, comparable results for *in vitro/in vivo* studies and the care for animal life suggest *in vitro* set-ups for the testing of polymer devices to estimate the *in vivo* performance. A variety of media have been employed to simulate the effects of body-fluids on polyester degradation. The compositions of the media are mostly oriented at the constituents of body-fluids saline, blood or cellular fluids. Prominent examples for degradation media are:

- *Phosphate Buffered Saline*, PBS, (physiologically buffered solution)
- *Simulated Body-fluid*, SBF (salt concentration of the human blood plasma)
- *Minimum Essential Medium*, MEM (cell nutrition medium)
- Various buffer systems (e.g., HEPES-, Hanks-, Sørensen-buffer)

Guideline for the media constitution is the biomimetic simulation with respect to pH-value, osmolarity, ionic strength and chemical reactivity. An important parameter for the polyester degradation is the pH of the incubation medium. Ginde and Gupta¹⁶ investigated PGA degradation as a function of external pH. Sample mass retainment decreased with increasing pH from 4.7 to 10.6, proving that alkaline medium has a higher potential for polyester cleavage. However, most of the experiments are carried out at physiological pH.

In the following study, PGA from solid-state reaction is tested for the degradation behavior in a physiologically buffered medium in comparison to unbuffered water. Hanks-Buffer was chosen as incubation medium with a pH-value of 7.4. The buffer was modified in the buffer components $\text{H}_2\text{PO}_4^-/\text{HPO}_4^{2-}$ to increase the capacity as a response to the rapid acidic degradation of PGA. The pH in the water-incubated samples was allowed to float freely. PGA bodies were prepared by hot pressing as

⁴⁵ M.S. Taylor, A.U. Daniels, K.P. Andriano, J. Heller "Six bioabsorbable polymers: *In vitro* acute toxicity of accumulated degradation products", *J. Appl. Biomater.* **1994**, 5, 151-157.

⁴⁶ E. Dawes, N. Rushton "Response of macrophages to poly(L-lactide) particulates which have undergone various degrees of artificial degradation", *Biomaterials* **1997**, 18, 1615-1623.

pellets and rods. To investigate the role of microporosity on degradation, compact and porous bodies were incubated. Propagating degradation was monitored with respect to retainment of geometric stability, morphology changes, crystallinity, average molecular weight and sample mass. In addition, the polymer rods were cut and subjected to mechanical testing of the fracture toughness and the elasticity modulus.

The experiment is designed to compare the behavior of PGA from NaClAc with its inherent characteristics to references for conventional polyglycolide, to estimate the stability of polymer bodies at simulated *in vivo* conditions and to check the

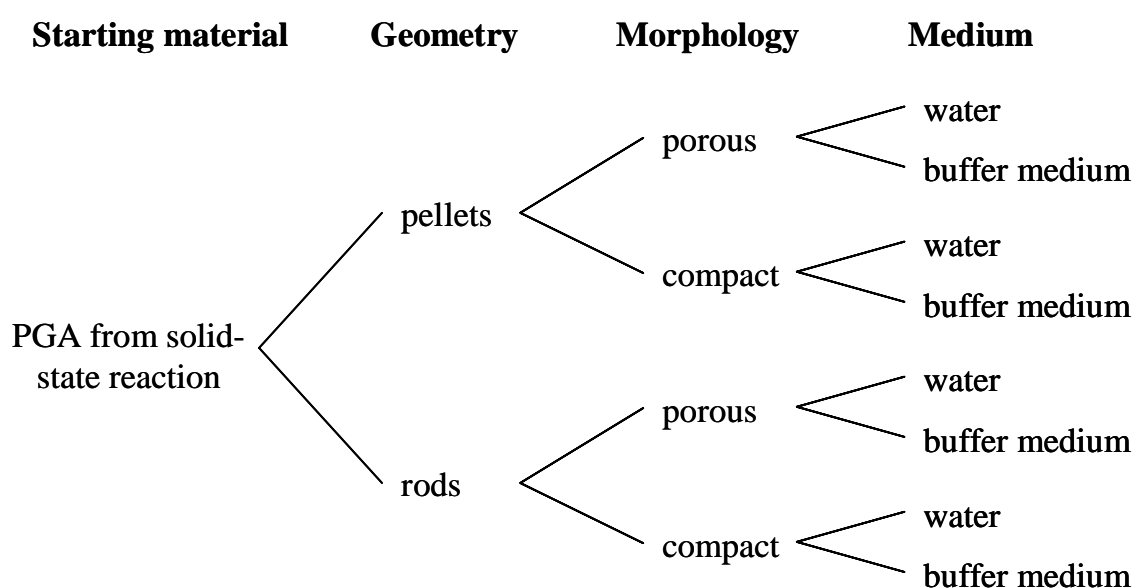


Fig. AII.1-1 Categories of sample degradation conditions

degradation mechanism for compact and porous samples.

AII.1 Results and discussion

Variation of sample geometry, morphology and degradation medium leads to 8 categories of degradation series:

The different samples were incubated in 100 ml solution at 37°C, using 200 ml PE-flasks. Samples were placed on glass wool to ensure an equal exposition to the surrounding medium of all sides. Samples were taken out of the medium after 1 day, 1 week, 2 weeks etc. up to 9 weeks, giving 10 time points per category. To prevent contamination with microorganisms, 1%- penicillin/streptomycin was added to both

⁴⁷ N.A. Ashammakhi "Neomembranes: A concept review with special reference to self-reinforced polyglycolide membranes", *J. Biomed. Mater. Res. (Appl. Biomater.)* **1996**, 33, 297-303.

water and Hanks-Buffer.

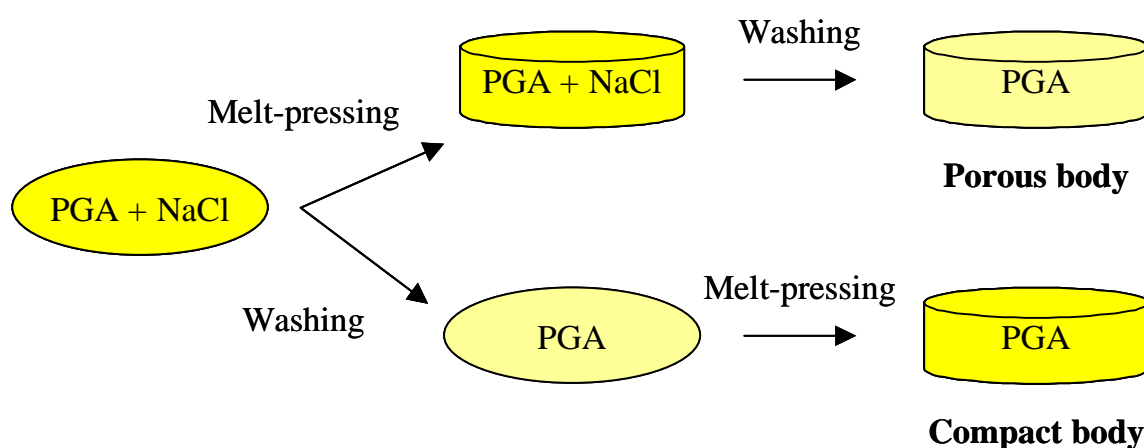


Fig. AII.1-2 Processing of PGA to porous and compact bodies

The processing steps from raw product to porous and compact samples are displayed in **fig.AII.1-2**. The initial mass was 1.3 g for salt loaded bodies, giving a resulting polymer mass for porous bodies of 0.65 g after wash-out. Compact bodies were fabricated from 1.12 g of porous PGA. To analyze the influence of the processing steps on the properties of the polymer, the material was characterized with respect to crystallinity, average molecular weight and fracture toughness. The characterization scheme is depicted in **table AII.1-1**. Rods were analyzed with SEM and subjected to mechanical testing. Degradation was assumed to be equal for pellets and rods of the same porosity and time. Therefore, chemical characterization was carried out with pellets only. The degradation medium was changed weekly and controlled for the pH-value. For Hanks-Buffer, the values ranged from 6.8 to 7.6 throughout the whole experiment.

Table AII.1-1 Characterization scheme for bodies of various degradation states

Body Geometry	Characterization Technique	Characterization Aspects
Pellets	digital photography	- geometric stability - outer appearance
Pellets	weighing	- water uptake, swelling - mass loss, erosion
Pellets	DSC	- degree of crystallinity
Pellets	viscosimetry	- average molecular weight
Rods	SEM	- morphology, degradation mechanism
Rods	mechanical testing	- fracture toughness, Young`s-modulus

Fig.AII.1-3 displays the development of the pH value for porous and compact bodies in water. A drop in pH to 3.5 is observed after 1 d of incubation for both

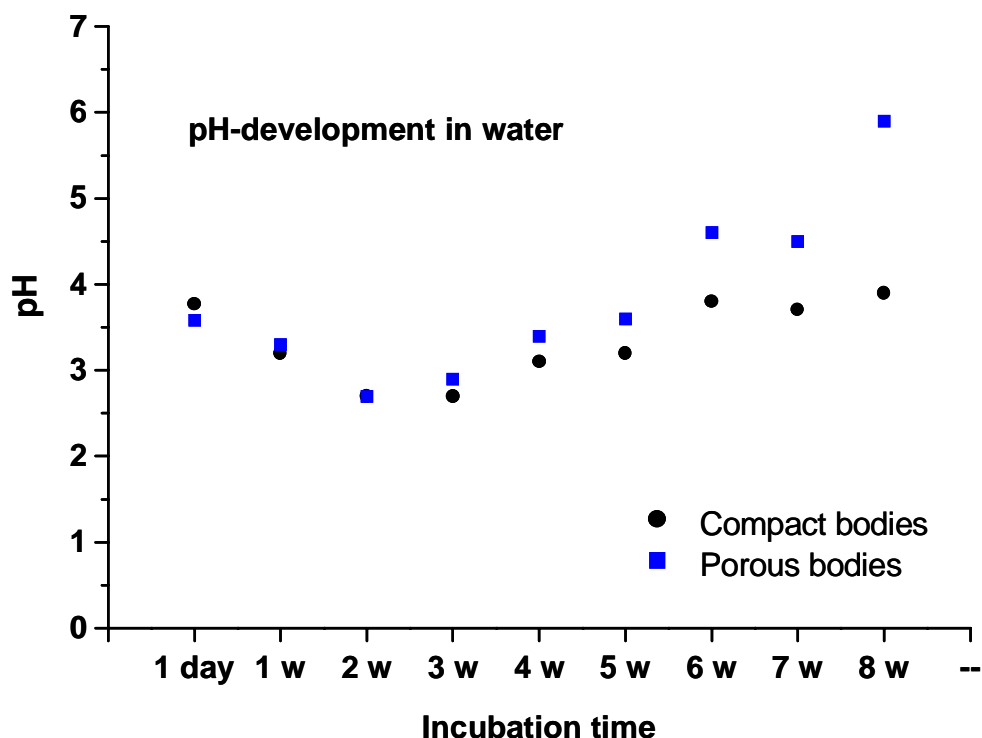


Fig. AII.1-3 pH-values for compact and porous bodies in water

morphologies. The values reach a minimum of 2.5 after 2-3 weeks in water. At later time points an increase in pH occurs to 5.8 for porous and 4 for compact samples. It can be stated that for longer incubation times, compact samples generate a more acidic medium than porous ones. The increase probably occurs due to repeated medium change, sample mass loss and a saturation of water uptake. The results show that PGA from solid-state reaction develops an acidic environment after just one day with sustained acidic potential over a period of 8 weeks in water. Thinking about an *in vivo* application of the polymer as a pure compound evokes the problems associated with cytotoxic pH and degradation products. Despite the buffering capacity of body-fluids, a significant drop in local pH seems unavoidable.

Geometric stability

For documentation of the retainment of geometry of porous and compact PGA, the bodies were photographed prior to removal from the incubation vessel. **Fig.AII.1-4** gives a comparison of compact and porous pellets in water over a period of 8 weeks incubation (the pictures at 1 d were taken in the dry state). Apparently, porous bodies retain a higher stability than compact ones. Porous pellets retain their initial geometry

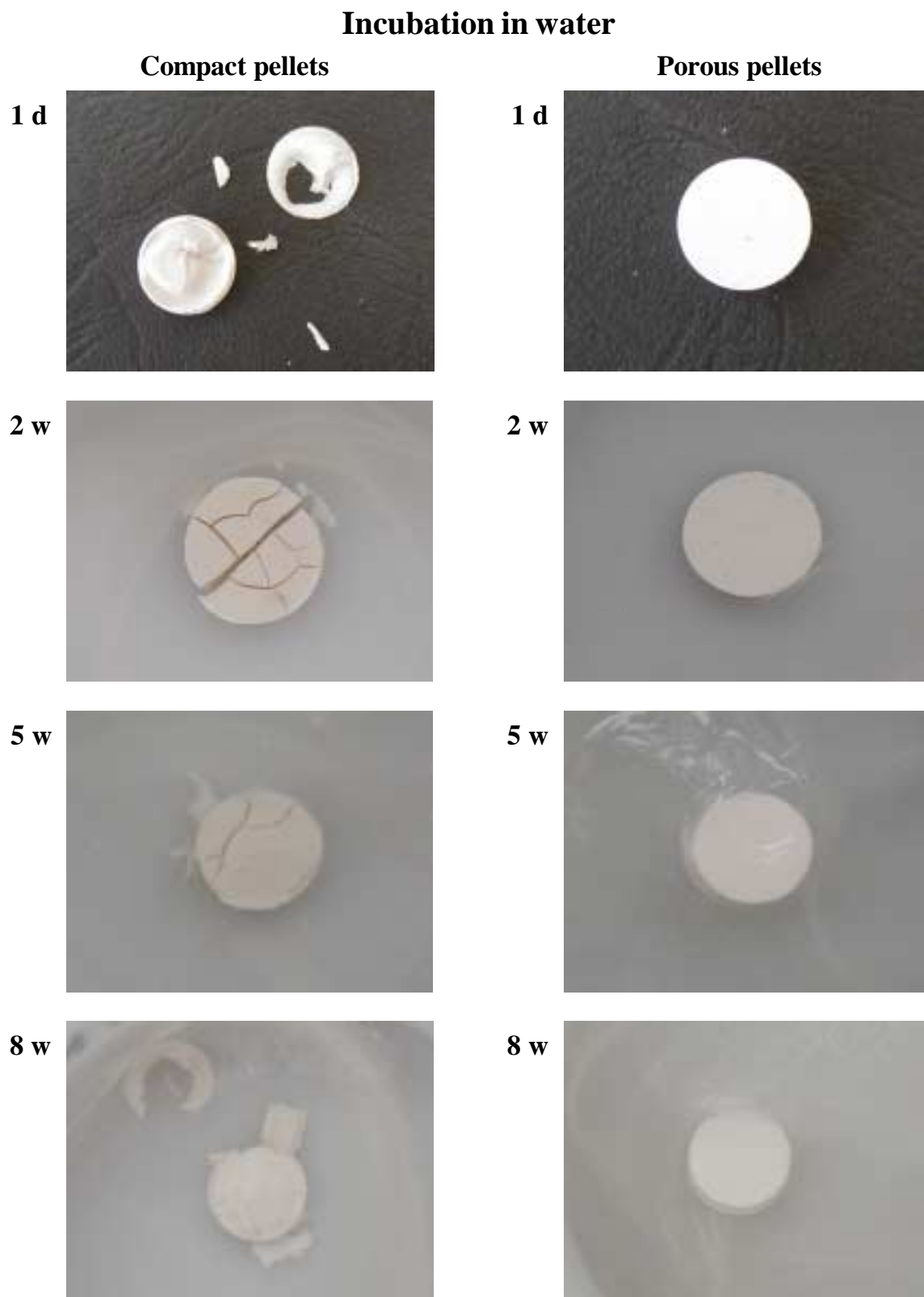


Fig. AII.1-4 Geometric stability of water-incubated PGA pellets – comparison of compact and porous bodies over a period of 8 weeks.

throughout the experimental period. A compact pellet shows a fractured surface layer after recovery from a one-day incubation. After 2 weeks, the pellets is fractured

overall. The following pictures at 5 and 8 weeks show cracked bodies with a rougher surface compared to the sample after 2 weeks indicating surface degradation. The results for incubation in modified Hanks-Buffer are displayed in **fig.AII.1-5**. In contrast to the incubation in water, the samples are generally less stable in buffered

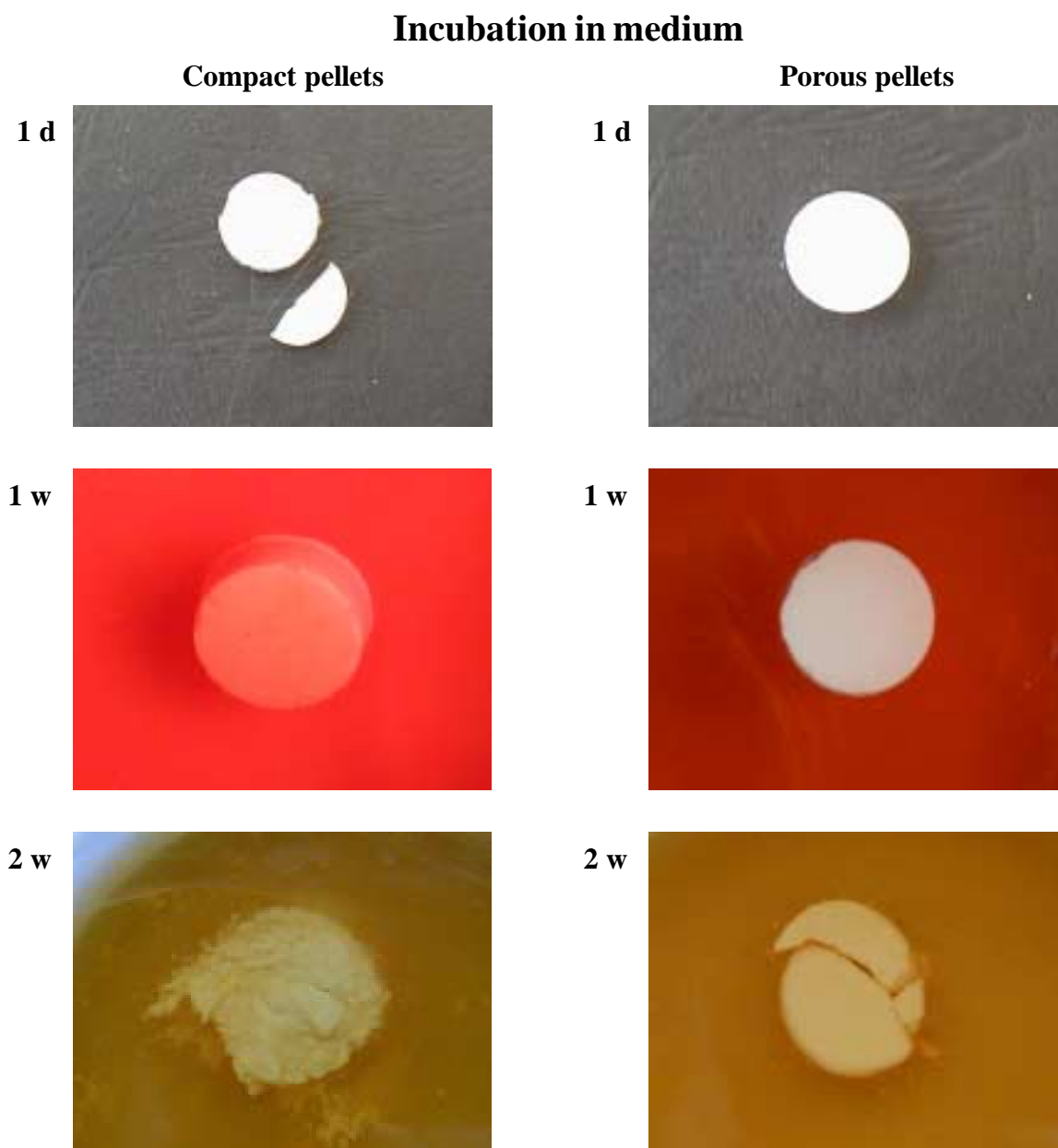


Fig. AII.1-5 Geometric stability of medium-incubated PGA pellets – comparison of compact and porous bodies over a period of 2 weeks.

medium. Compact bodies show a total disintegration after 2 weeks. Again, porous bodies inhibit a higher stability, although fracturing occurs as early as 2 weeks. The sample shows a roughened surface.

A possible explanation for the lower stability of compact bodies could be the lack of

flexibility towards the strain caused by swelling of the polymer. It is likely that the generated strain due to local volume increase leads to cracks in the pellet. The porous polymer is obviously able to dissipate the tension due to the flexible pore system. The reasons why samples are more stable in acidic water than in physiologically buffered medium are speculative. A chemical interaction of the dissolved ions cannot be excluded.

Morphology and degradation mechanism

The morphology of degrading sample was further analyzed by scanning electron

Porous PGA rods in medium

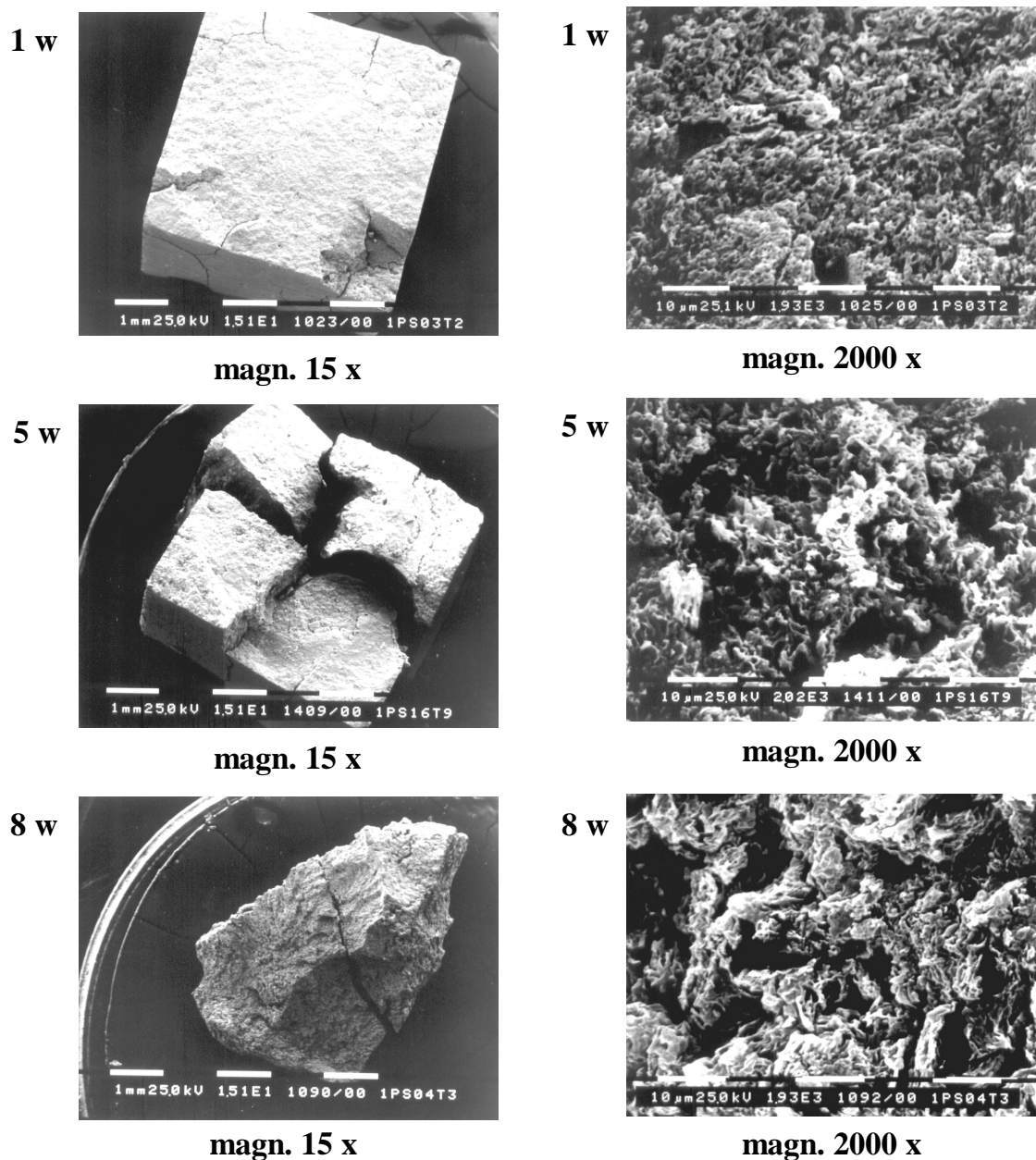


Fig. AII.1-6 SEM micrographs of degraded PGA in medium over a period of 8 weeks

microscopy. For porous rods in water (data not shown), the impressions from the digital photographs were confirmed. Bodies retain their geometry throughout the experiment. The rod after 8 weeks was fractured in two parts. A comparison at higher magnification (2000x) showed no significant differences in the microstructure of the polymer. Compact rods in medium (data not shown) were disintegrated as early as after 2 weeks. After 1 week the body showed a roughened surface. One week later, the residual polymer was a shapeless mass.

A typical degradation is shown in **fig.AII.1-6** for porous rods in modified Hanks-Buffer. The cut rod is fractured into quarters after 5 weeks of incubation. At the end of

Compact PGA rods in water

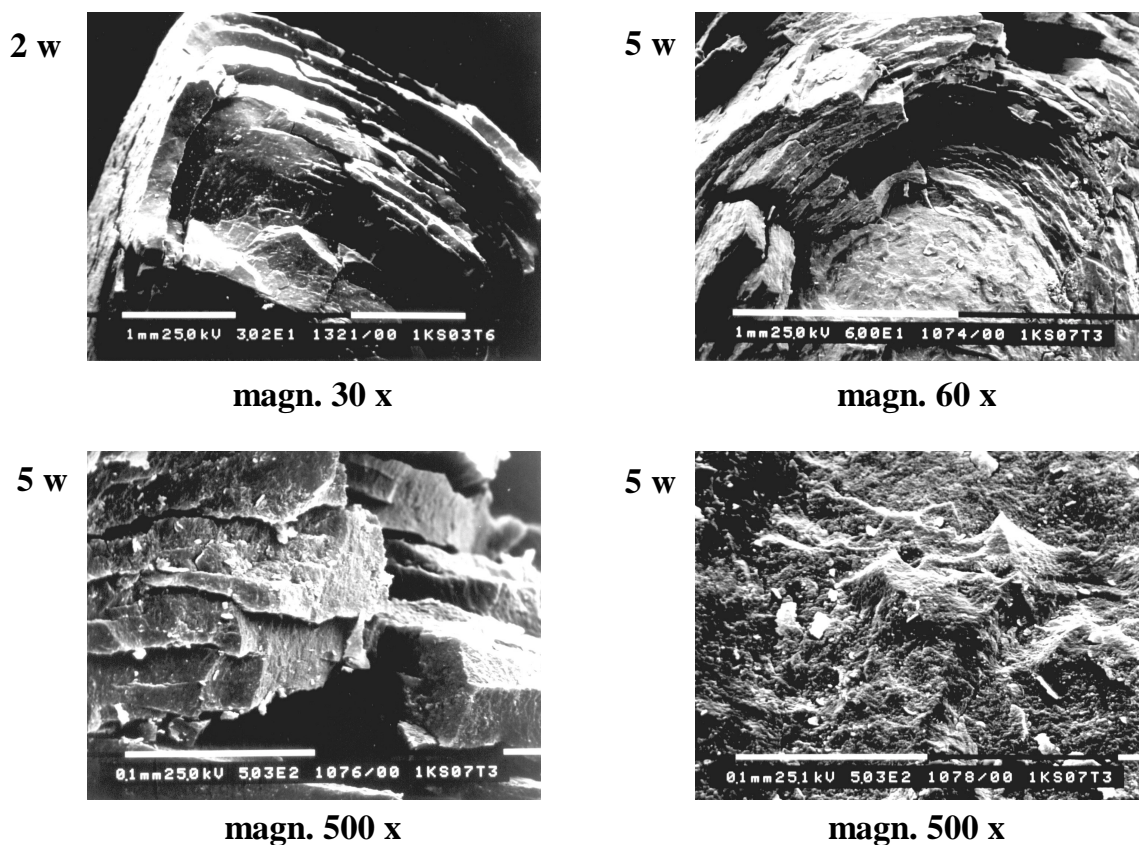


Fig. AII.1-7 SEM micrographs of degraded compact PGA incubated in water for 2 and 5 weeks. The samples show a „onion-like“ degradation mechanism: a layered structure propagating to the center of the body with time. Outer layers split off the body during degradation.

the experiment, strongly degraded fragments of irregular shape were recovered. At higher magnification (2000x) the polymer seems to be more roughened with larger cavities in the surface. A surprising mechanism was observed for compact samples in water (**fig.AII.1-7**). The material develops a layered structure that resembles an onion-

peel. The layered structure seems to propagate from the surface to the center with time. Due to loosening of contact between the layers, outer layers split off the bulk at later time points. Perpendicular to the layer direction (lower right picture), the surface has the typical appearance of compact PGA. It might be speculated that the layers pre-formed during the melt-pressing procedure. Propagating swelling from the surface to the center leads to tension between the layers and a loss of contact.

Strikingly, a surface/interior differentiation cannot be confirmed for solid-state chemically prepared PGA. In none of the four investigated cases, a hollow structure was visible. It has to be stated, however, that the degradation is rapid, especially for compact samples, and that the instability of most bodies could restrict the development of hollow structures.

Development of average molecular weight

The average degree of polymerization was determined on dry sample (dried in oil-pump vacuum) employing viscosimetry. The obtained average molecular weight was converted to the average number of monomers per chain. The results for the 4 incubation conditions are displayed in **fig.AII.1-8**. The pre-incubation processing steps are included to complete the history of the material. The compact samples show an increase in chain length after the washing step and after melt-pressing. The first increase could only be explained with the removal of shorter chains and the second with a post-polymerization under the conditions of high pressure and temperature to some extent. The expected behavior of chain pyrolysis due to thermal treatment was not observed. For porous samples the degree of polymerization increases as well after the melt-pressing, followed by a decrease after exposition to water. During incubation, the chain length drops almost linearly in all cases except for porous pellets in water, where the value remains nearly constant at 27 monomer units. The last value for compact bodies in water with an increase to 32 units after 8 weeks of incubation cannot be explained. Generally, the values start at ca. 50 and drop to 25. Compared to compact samples, the breakdown is much faster for porous bodies. A value of 25 is reached after only one day in both cases. The compact samples are more stable with respect to chain stability. This indication is not surprising taking into account the porous structure and the internal surface. Note that one cleavage per ester chain will

Degree of polymerization

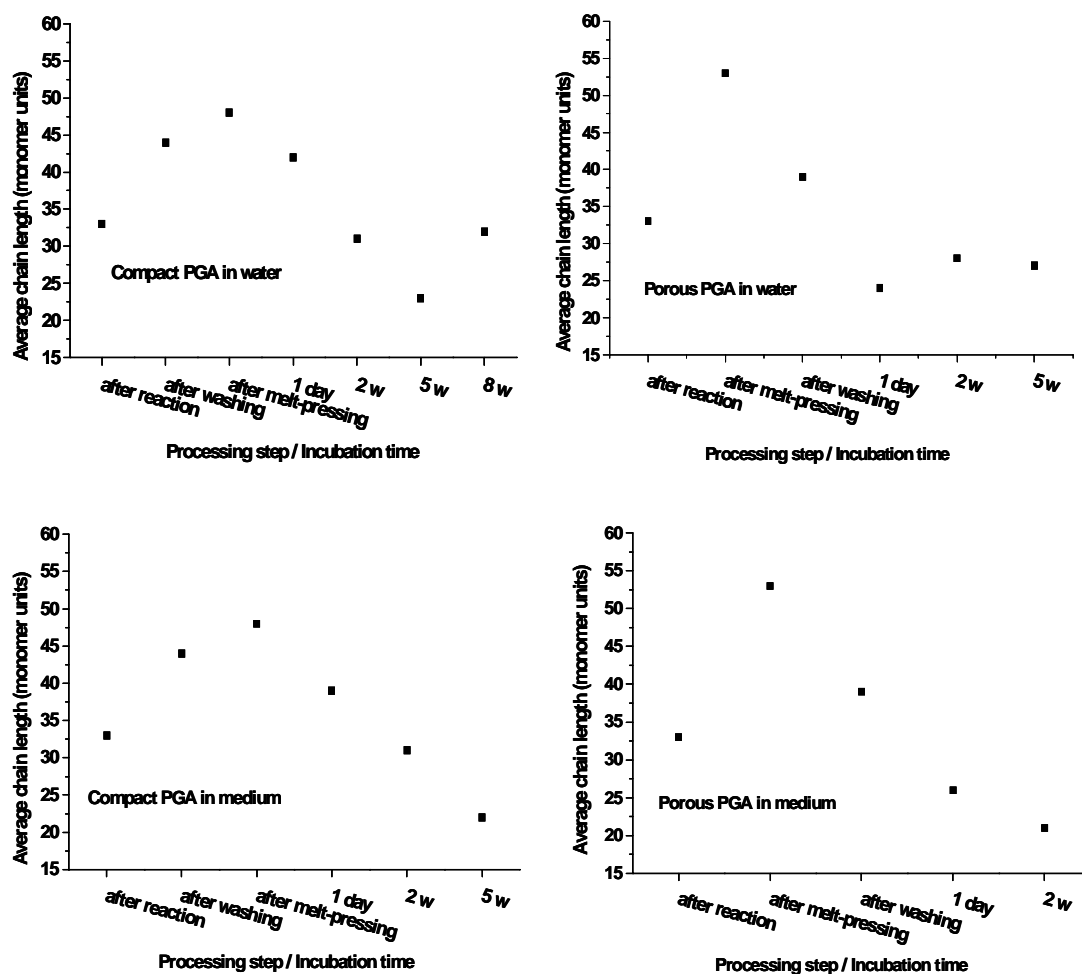


Fig. AII.1-8 Average number of monomer units per chain for pre-incubation processing steps and incubation time points.

halve the average chain length. The overall development after incubation is in agreement with the reported decay of chain length in the literature. The decrease is mostly described as a linear or exponential reduction in molecular weight³⁶.

Water uptake and mass loss (erosion)

Water uptake was measured as the difference between wet- and dry-mass (samples dried in a desiccator) of the recovered bodies. The residual dry-mass is displayed relative to the initial mass of the body (set to 100%) in **fig.AII.1-9**. Bodies in medium degraded so rapidly that only 2 values each could be obtained (after 1 d and after 1 w) with a suitable geometry to be measured without a significant systematic error.

Compact pellets in water show a linear water uptake in the first three weeks up to 27% of the corresponding dry-mass. After that time point a saturation is observed at about

25%. The mass of the compact samples decreases to 72% after 8 week of incubation. The relationship between the two parameters is clearly visible. An increase in water uptake is parallel to a reduction in mass loss. For the porous bodies, the water uptake is significantly higher, as it could be expected because of the porous structure and the hydrophilic nature of the polymer. Again, the two parameters are inversely related. Water uptake is 55% after 1 d already and reaches 90% at the end of the experiment. The mass loss is comparable to the values for compact polymer. After 8 week the resulting dry-mass was 67% of the initial mass. The values for medium-incubated samples are summarized in **table AII.1-2**:

Compact PGA medium	Water uptake [%]	Relative dry-mass [%] ($t_0 = 100\%$)
1 day	2.2	97.6
1 w	5.0	70.3

Porous PGA medium	Water uptake [%]	Relative dry-mass [%] ($t_0 = 100\%$)
1 day	55.1	83.5
1 w	69.3	77.9

The compact bodies show water uptake to a little extent after the first week of incubation. In contrast, the mass decreased to 70% after 1 week. The porous samples

Water uptake / mass loss

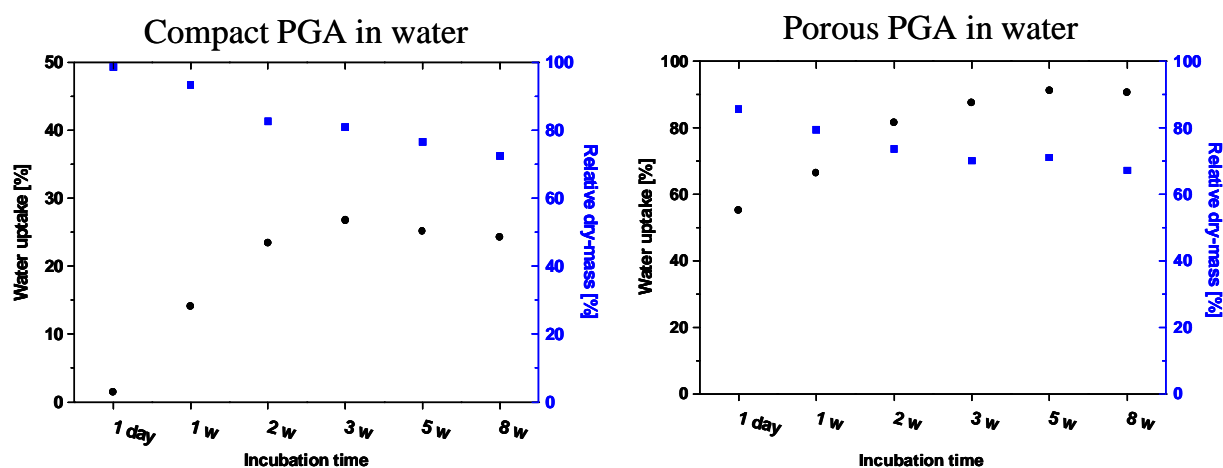


Fig.AII.1-9 Water uptake and relative mass for water incubated samples

had high values for water uptake and lost 22% of the dry-mass. The strong decrease in sample mass leads to the desintegration of the medium-buffered bodies one week later. All measured samples show a continuous decrease in mass. A sudden change in the

mass value was not observed, so that an "acidic burst" caused by massive erosion of degradation products could be ruled out. It has to be noted that such a behavior is unlikely for porous bodies because of continuous exchange through the porous structure. The medium incubated samples do not allow an interpretation of the erosion mechanism because of very short incubation time.

Degree of crystallinity

The degree of crystallinity was determined by DSC measurements from the enthalpy of fusion for the crystalline polymer as described in chapter AI. **Fig.AII.1-10** graphs

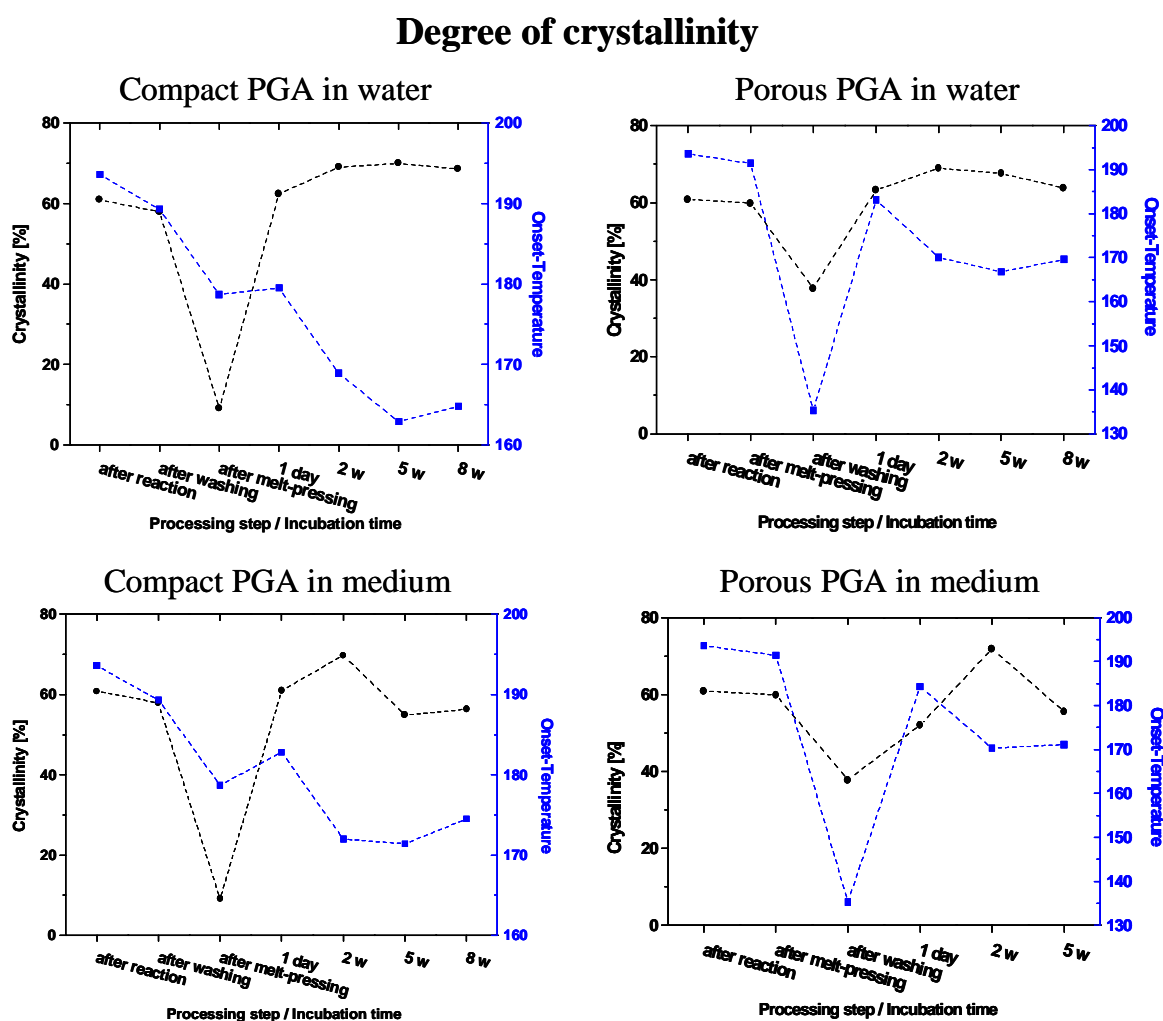


Fig. AII.1-10 Degree of crystallinity determined by DSC

the results for the 4 categories over periods of 8 and 5 weeks, respectively. Pre-incubation processing steps were integrated in the plots. The initial crystallinity was 60%. After the washing step the crystallinity was unchanged in all cases. The melt-pressing procedure and subsequent quenching drastically lowers the values below 15%

in all cases. After 1 d of incubation the crystallinity was restored to 60%. The average crystallinity remained relatively constant at that level until the end of the experiment. The constant crystallinity underscores the theory of faster degrading amorphous moieties increasing the crystallinity parallel to amorphization caused by degradation lowering the crystalline content. The onset-temperatures decrease for all categories, suggesting shorter chains and probably smaller crystallites. Values fall from initially 190 to 165°C (compact PGA in water) and 175°C (compact PGA in medium).

Mechanical testing: Young`s-modulus and fracture toughness

Mechanical testing was carried out with cut rods in a Zwick-apparatus. The samples were crushed with a constant speed and the force was measured. **Fig.AII.1-11** displays

Young`s - modulus / Fracture toughness

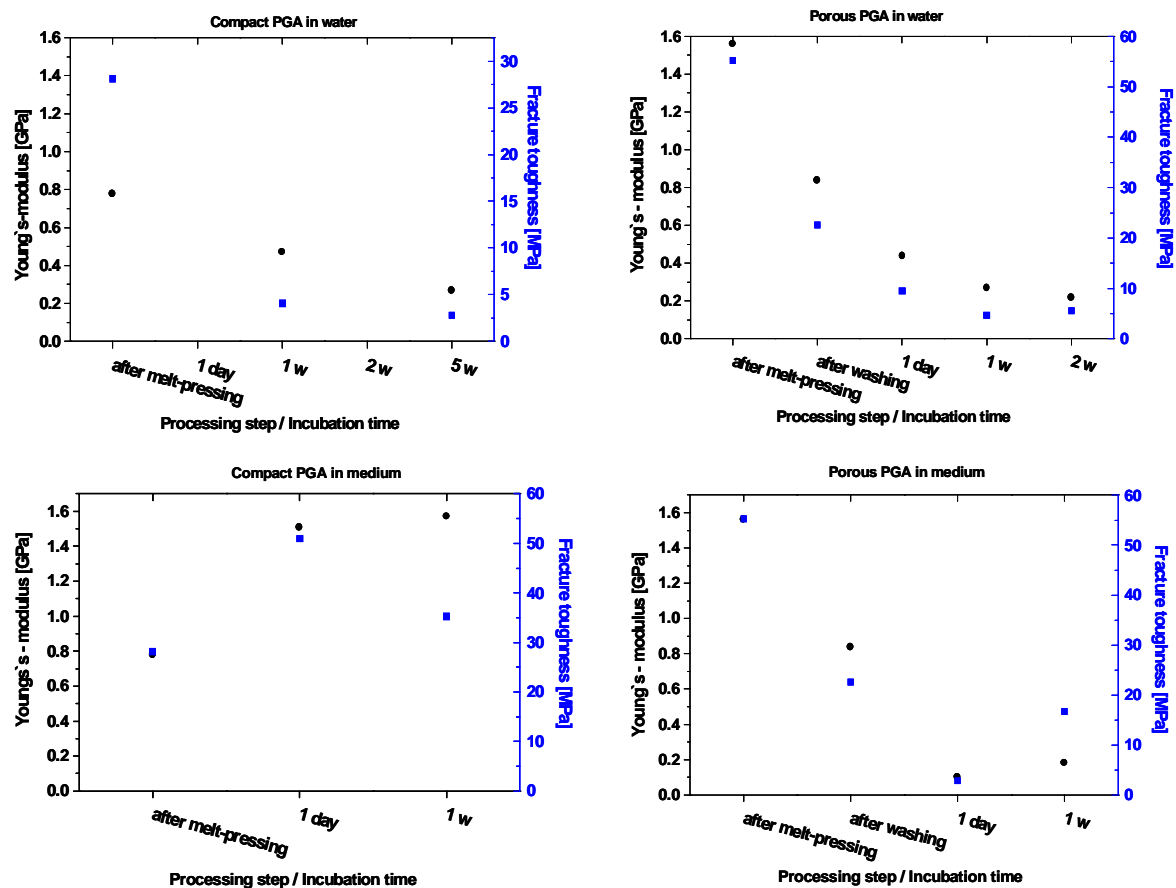


Fig. AII.1-11 Determination of Young`s - modulus and fracture toughness for PGA rods

the received values for fracture toughness and Young`s modulus. Pre-incubation states are displayed also for salt-loaded body, porous and compact rods. Except for compact samples in medium both values decrease parallel with incubation time. The values for

the Young's modulus typically decrease from 0.8 GPa to 0.2. The fracture toughness decreases for porous bodies from 55 MPa to 5 (porous PGA in water) and 17 (in medium), respectively. Both determined parameters indicate a rapid and strong loss of mechanical properties during degradation for all four categories. Values were determined on intact fragments cut from rods of 14 mm length. Note that the washing step for porous bodies leads to a significant decrease of fracture toughness prior to incubation.

AII.2 Concluding remarks

The following conclusions can be drawn from the results obtained in the present study.

- PGA from solid-state reaction generates an acidic pH (2.5 to 6) in water over a period of 8 weeks incubation. Modified Hanks-buffer is a suitable medium for keeping the pH at a physiological level.
- Bodies of porous PGA retained their geometry during the whole experiment (eight weeks). In contrast, compact pellets fractured after 1 day of incubation. Surprisingly, the exposition to modified Hanks Buffer causes a disintegration of porous and compact bodies after only 2 weeks. The incubation in physiologically buffered medium leads to a faster erosion compared to acidic aqueous medium.
- SEM-micrographs documented the fragmentation of PGA bodies analogous to the digital photographs. At high magnifications, no differences in microstructure could be detected for the probed time-points and sample categories. Compact samples in water show a degradation mechanism which revealed a layered structure that propagates to the center of the body with incubation time.
- All categories exhibit a comparable decrease in average molecular weight.
- The water uptake increases parallel to mass decrease for porous samples. A saturation in water uptake is observed for compact pellets at about 25% relative to dry-mass, and about 90% for porous samples, respectively.
- The crystallinity was determined to be relatively constant at a level of 60% relative to 100% crystalline polymer.
- Samples lose mechanical strength (Young's-modulus and fracture toughness) rapidly after incubation in media.
- A heterogeneous mechanism with an inner/outer differentiation resulting in hollow

structures was not observed.

Taking into account the intrinsic acidic degradation and the lacking mechanical stability, PGA from solid-state reaction is disqualified for an *in vivo* application as a pure bulk material for bone substitution. The solution realized by Tormälä et al. (see General Introduction) to fabricate self-reinforced fiber constructs out of high molecular weight PGA is optimal concerning mechanical properties. However, the acidic degradation remains a serious restriction.

AII.3 Materials and Methods

Pre-incubation procedure

Polyglycolide was obtained from solid-state reaction of NaClAc (180°C, 180 min) as described in AI. Part of the received product was washed with cold water for 12 h to remove the included NaCl. PGA was filtered off and dried in vacuum. The porous PGA was compressed in the melt-press to form compact bodies. Characterization was carried out for the product, after the washing step and for the compact bodies prior to incubation. For porous bodies, PGA + NaCl was subjected to melt-pressing with subsequent removal of NaCl in cold water ($T = 4^{\circ}\text{C}$). The removal of NaCl was controlled by dry-weight and morphology (regions with NaCl still included appear darker than porous ones). It took almost 10 d for melt-pressed PGA to extract all NaCl. Characterization was carried out before and after the melt-processing and for the porous bodies prior to incubation. Due to mass loss in the melt-pressing step, a repeated mass determination was necessary. For porous bodies, the resulting mass was measured in dry condition after the wash-out step to give the initial mass of the sample.

Melt-pressing

Hot pressing was carried out with a melt-press “PW 10” by Paul-Otto Weber GmbH with a temperature control unit “TG2E/PT100”. About 1.3 g of salt-loaded PGA and 1.12 g of pure PGA were subjected to melt-pressing. The rod-shaped molding form had basis dimensions of 30 mm length and 5 mm width. The diameter of the pellet form was 13 mm. Samples with included salt were pressed with 10 kN at a

temperature of 150°C for 10 min. Compact samples were pressed under the same conditions, but at a lower temperature of 120°C. Pressing parameters are summarized in **table AII.3-1**. Sample were removed from the form in hot state and cooled down to room temperature.

Table AII.3-1 Press-conditions for pellets and rods

Body Geometry	Basis Dimension	Force	Pressure
Pellet-Form Ø 13 mm	133 mm ²	10 kN	75.2 MPa (752 bar)
Rod-Form 30·5 mm	150 mm ²	10 kN	66.7 MPa (667 bar)

Incubation medium

Water

Ion-exchanged water was used for incubation (with 1vol% penicillin/streptomycin). Medium change was carried out weekly and the pH-value was measured. No buffering components were added.

Hanks-buffer

Standard Hanks-buffer was modified in the buffering phosphate components. **Table AII.3-2** lists the composition of standard and modified Hanks-buffer:

Component	Standard Hanks-buffer [g l ⁻¹]	Modified Hanks-buffer [g l ⁻¹]
CaCl ₂	0.14	0.14
KCl	0.40	0.40
KH ₂ PO ₄	0.06	9.08*
MgCl ₂ ·6H ₂ O	0.10	0.10
MgSO ₄ ·7H ₂ O	0.10	0.10
NaCl	8.00	8.00
Na ₂ HPO ₄ ·7H ₂ O	0.09	11.88*
D-glucose	1.00	1.00
phenol red	0.01	0.01

* modified concentrations

The components were dissolved in 1 l solution and adjusted to pH = 7.4 with NaOH-solution. Phenol red is included as an indicator for pH-value. If the pH drops below 7, the indicator changes from red to orange color. Medium change was scheduled weekly. 1 vol% penicillin/streptomycin was added to the medium to prevent growth of microorganisms. The pH was checked daily for both media.

Incubation procedure

Before removal from the incubation dish, the samples were photographed to document the geometric stability. pH measurements were carried out daily during incubation and after removal of a body from the medium. To determine the wet-mass, bodies were wiped dry with tissue paper to avoid the influence of adherent surface water. Dry-mass was determined after two day storage in a desiccator over P₂O₅. The dry polymer from compact and porous pellets was subjected to DSC and viscosimetry measurements. For mechanical testing, rods were cut to a length of about 14 mm. Residual pieces were sputter-coated with gold and analyzed with SEM.

Instruments and methods

Digital photography

Digital photographs were taken with a Olympus "Camedia C-920 Zoom" digital Camera.

pH-Meter

pH-values were measured with a Hanna "Piccolo Plus - ATC Temp" pH-meter.

DSC

DSC measurements were carried out on a Netzsch "DSC 204" at a heating rate of 5 K min⁻¹ in open aluminum crucibles.

Viscosimetry

Viscosimetry was carried out as described in chapter AI with 100-200 mg of polymer dissolved in 25 ml HFIP.

SEM

Scanning electron microscopy was performed with a Philips "SEM 515" instrument operating at 25 kV with gold-sputtered samples.

Mechanical testing

Measurements were carried out with an "Z2.5/TN1S" testing apparatus from Zwick. Data evaluation was executed with the corresponding software "testXpert v.3.0".

AIII. The transposition to higher homologues: 3-Cl-butyrate and Cl-pivalates

AIII.0 Introduction

The polycondensation to obtain PGA from halogenoacetates described in **AI** is a twofold interesting reaction: First it represents a synthesis of a polymer from a solid-state precursor, and furthermore it produces a biomaterial with inherent porosity, which is definitely advantageous for certain aspects of *in vivo* biomaterial application⁴⁸. The reaction is reported for various combinations of metal halogenoacetates, having a carboxylate group and a halogen function in common. This fact suggests the possibility to transpose this reaction to other carboxylates with a halogen function in the molecule. Such efforts offer the prospect of obtaining polyesters with a porous structure. This property could be exploited for the design of implant materials, namely, influencing degradation behavior, biocompatibility or mechanical performance.

Some studies have been carried out so far that point in that direction. Epple and Kirschnick investigated the reactivity of three chlorocarboxylic acids⁴⁹. The parent compounds and products are displayed in **fig.AIII.0-1**. The compounds were prepared as sodium salts and characterized with thermal analysis, ¹H NMR and size exclusion chromatography to determine the degree of polymerization. It turned out that all three components showed the characteristic exothermal reaction enthalpy corresponding to the elimination of NaCl at about 150°C. Generally, an exothermic elimination with only little mass loss is followed by evaporation and combustion of the organic part of the molecule. In all cases, a viscous yellow oil was obtained, indicating that the reactions do not take place in the solid state. Instead, liquefaction occurred leading to oligomers. NMR endgroup analysis and SEC revealed oligomers of n = 4-6 for sodium 3-Cl-propionate and sodium 2-Cl-butyrate. Sodium 2-Cl-propionate showed a bimodal distribution with high molecular mass (n = 520) polylactide and oligomers (n = 11). The reactions can be described as oligomerization in the liquid state with partial polymerization in the latter case. Two side reactions were observed accompanying the desired polycondensations: in all three cases the corresponding hydroxy acids formed

⁴⁸ A.G. Mikos, G. Sarakinos, M.D. Lyman, D.E. Ingber, J.P. Vacanti, R. Langer "Prevascularization of porous biodegradable polymers", *Biotechnol. Bioeng.* **1993**, 42, 716-723.

⁴⁹ M. Epple, H. Kirschnick "Oligomerization and polymerization in sodium salts of chlorocarboxylic acids", *Liebigs Ann./Recueil* **1997**, 81-85.

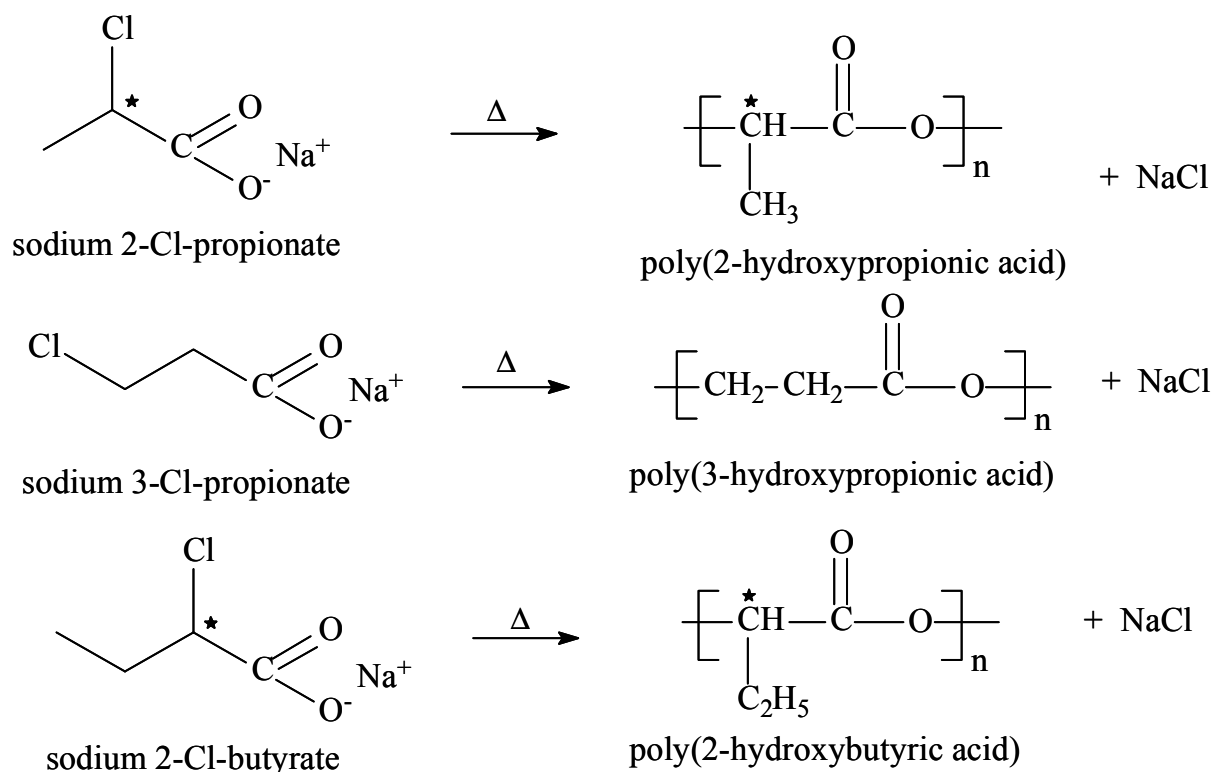


Fig. AIII.0-1 Attempted polymerizations of sodium chlorocarboxylates

probably due to partial (10-20%) hydrolysis. For the compound with the chlorine group in the β -position, sodium 3-Cl-propionate, the elimination of HCl was a strongly competing reaction (30%), which led to acrylic acid as the elimination product.

It can be stated that the reaction courses are different from the formation of PGA. Chain growth is likely to proceed in the liquid state depending on annealing temperature and time. The crystal structure is not decisive for the reactivity. A homogeneous polymeric product was not obtained.

In further studies alkali salts of *m*- and *p*-halogenomethylbenzoic acids were heated to obtain the corresponding poly(hydroxymethylbenzoic acids)⁵⁰. The Li-salts did not show the expected reaction. The *p*-halogenomethylbenzoates all tend to form solvate crystals with either the solvent (ethanol) or *p*-halogenomethylbenzoic acid. However, the products were the desired polyesters in all cases. In most isothermal experiments, no liquefaction was observed, therefore a solid-state polymerization appears likely. In some cases of high reaction temperature, temporary melting occurred due to self-

⁵⁰ O. Herzberg, M. Epple "Thermally induced polymerization in *m*- and *p*-halogenomethylbenzoates to poly(hydroxymethylbenzoic acid)", *Macromol. Chem. Phys.* **1999**, 200, 2662-2666.

heating. The degree of polymerization, determined by ^1H NMR endgroup analysis and viscosimetry, varied from short oligomers to long chains with no detectable endgroup signals. For the *para* salts, the resulting polymer was partially crystalline, the *meta* salts gave amorphous polymers. SEM micrographs were obtained from salt-loaded and porous poly(hydroxymethylbenzoic acid) after washing with water similar to the morphology of PGA from solid-state reaction.

Further investigations on structural aspects of the halogenomethylbenzoates with solid-state ^{13}C NMR spectroscopy and crystal structure determination from synchrotron X-ray powder diffraction data confirmed a solid-state reaction for the Na and K salts leading to the desired polyesters⁵¹. The structures could only be determined for the non-reacting Li-salts, because of polymorphism of the Na and K compounds. The two Li salts (Cl and Br as the halogen function) are isostructural, with a monoclinic lattice. The molecules adopt a layer-like packing, with the halogen atoms pointing together and the Li ions tetrahedrally coordinated by four oxygen atoms from four different carboxylate groups. The structure is very similar to those of the isostructural LiClAc, LiBrAc and LiIAc, which themselves do not polymerize. It was concluded that the small, strongly polarizing Li cation leads to kinetic inhibition of the polymerization reaction by coordination to four oxygen atoms.

The mentioned examples underscore the prospect of a successful transposition to higher homologues and related molecules in some cases to open up a new synthetic pathway to various polyesters.

The high activity in the field of research and development of biodegradable polyesters and other macromolecules reflects their potential and the need for *in vivo* application⁵². Different polymer materials and strategies are currently developed and tested for degradation behavior, cell interaction, bone bonding ability or stability aspects *in vitro* or at various implantation sites. Although homo- and copolymers of poly(α -hydroxy acids) are the dominating substrates, many alternative approaches can be found in the literature. A few examples are given in the following passages.

Attawia et al. introduced poly(anhydride-*co*-imides) for orthopedic applications with

⁵¹ O. Herzberg, H. Ehrenberg, S.J. Kitchin, K.D.M. Harris, M. Epple "Structural aspects of the solid-state polycondensation reaction in alkali 4-halogenomethylbenzoates", *J. Solid State Chem.* **2001**, 156, 61-67.

⁵² A. Lendlein "Polymere als Implantatwerkstoffe", *Chem. unserer Zeit* **1999**, 5, 279-295.

the intention to provide a material suitable for weight bearing situations⁵³. The study provided evidence of normal osteoblast function on the material surface. The bone forming cells retained their osteoblastic phenotype over three weeks of interaction with the polymer. Chinn et al. proposed modifications for poly(ethylene terephthalate) to moderate the inflammatory response and to prevent thrombosis⁵⁴ as blends with a fluoropolymer (FluoropassivTM) or RGD-sequence containing peptides. The modifications reduced fibroblast (connective tissue forming cells) proliferation into the porous polymer and inhibited thrombus accumulation in contact with baboon blood compared to unmodified PET. Domb⁵⁵ published the synthesis of a degradable poly(amide anhydride) based on alanine and sebacic acid that degraded with a constant rate *in vitro* (phosphate buffer, pH = 7.4, 37°C) within 5-10 d. L-lactide was copolymerized with ϵ -caprolactone to reduce Young's modulus of poly-L-lactide for an application as suture material by Tomihata et al⁵⁶. The new filament showed histopathological findings and properties comparable to commercially available sutures with respect to mass loss profile, strength retention and foreign-body reaction. Peter et al. used poly(propylene fumarate) besides PLA/PGA copolymers as scaffolds for tissue engineering⁵⁷ and Scotchford et al. cultured osteoblasts on collagen/PVA bioartificial polymers under variation of the cross-linking method for the stabilization of collagen⁵⁸. It was shown that dehydrothermal treatment was superior to glutaraldehyde cross-linking with respect to cell adhesion, proliferation and morphology.

A well characterized and extensively tested copolymer-system was developed by van Blitterswijk and coworkers for bone-graft substitution and bone defect filling. The group synthesized polyester block-copolymers with different ratios of poly(ethylene

⁵³ M.A. Attawia, K.M. Herbert, K.E. Uhrich, R. Langer, C.T. Laurencin "Proliferation, morphology, and protein expression by osteoblasts cultured on poly(anhydride-co-imides)", *J. Biomed. Mater. Res. – Appl. Biomater.* **1999**, *48*, 322-327.

⁵⁴ J.A. Chinn, J.A. Sauter, R.E. Phillips, Jr., W.J. Kao, J.M. Anderson, S.R. Hanson, T.R. Ashton "Blood and tissue compatibility of modified polyester: Thrombosis, inflammation, and healing". *J. Biomed. Mater. Res.* **1998**, *39*, 130-140.

⁵⁵ A.J. Domb "Biodegradable polymers derived from amino acids", *Biomaterials* **1990**, *11*, 686-689.

⁵⁶ K. Tomihata, M. Suzuki, T. Oka, Y. Ikada "A new resorbable monofilament suture", *Polym. Degrad. Stab.* **1998**, *59*, 13-18.

⁵⁷ S.J. Peter, M.J. Miller, A.W. Yasko, M.J. Yaszemski, A.G. Mikos "Polymer concepts in tissue engineering", *J. Biomed. Mater. Res. – Appl. Biomater.* **1998**, *43*, 422-427.

⁵⁸ C.A. Scotchford, M.G. Cascone, S. Downes, P. Giusti "Osteoblast responses to collagen-PVA bioartificial polymers in vitro: the effects of cross-linking method and collagen content", *Biomaterials* **1998**, *19*, 1-11.

oxide) (PEO) and poly(butylene terephthalate) (PBT), which are commercialized under the tradename Polyactive®. The polymers inhibit soft (PEO) and hard (PBT) segments with a swelling ability dependant on the constituent ratio. An *in vitro*⁵⁹ study revealed the surface precipitation of carbonated apatite from metastable calcification solution (SBF). A covering layer of 100 µm thickness formed after 4 d of incubation. An *in vivo* study in cortical bone of goats documented an increase in water uptake, calcification and bone bonding area (70% of the material surface in direct contact to bone after one year of implantation for a ratio of 70/30 w%) with an increase of the PEO moiety⁶⁰. The polymers with ratios of 40/60 and 30/70 showed no calcification of the interface and therefore no bone bonding. In a later study, the polymer was implanted with interconnected pores (300 ± 150 µm pore diameter) in a rabbit femur model⁶¹. After 8 weeks the defect was bridged by new calcified bone which almost completely filled the pores of the polymer. The study confirmed that the 70/30 proportion was the most suitable material. Addition of allogenic bone marrow did not enhance bone formation, but instead led to inflammation and delay of bone ingrowth. The cited examples give an impression of the opportunities in polymer development and clinical use, and parallel of the complexity of host/implant interactions.

The current chapter deals with the synthesis of metal salts of 3-Cl-butyric acid and Cl-pivalic acid and their thermochemic reactivity, displayed in **fig.AIII.0-2**. The expected polymers would be poly(3-hydroxybutyrate) and poly(pivalolactone). Poly(3-hydroxybutyrate) (P-3HB) is the most prominent polyester of the poly(hydroxyalkanoic acids) family⁶². Poly(hydroxyalkanoic acids) are biopolymers that are accumulated by many bacteria with access to carbon sources for nutrition, lacking other nutrients containing e.g. nitrogen, sulfur, phosphate, iron or magnesium. The polyester is harvested from cultures either by extraction with solvents, destruction

⁵⁹ P. Li, D. Bakker, C.A. van Blitterwijk "The bone bonding polymer Polyactive® 80/20 induces hydroxycarbonate apatite formation *in vitro*", *J. Biomed. Mater. Res.* **1997**, 34, 79-86.

⁶⁰ A.M. Radder, H. Leenders, C.A. van Blitterswijk "Interface reactions to PEO/PBT copolymers (Polyactive®) after implantation in cortical bone", *J. Biomed. Mater. Res.* **1994**, 28, 141-151.

⁶¹ R. Kuijjer, S.J.M. Bouwmeester, M.M.W.E. Drees, A.A.M. Surtel, E.A.W. Terwindt-Rouwenhorst, A.J. van der Linden, C.A. van Blitterwijk, S.K. Bulstra "The polymer Polyactive™ as a bone-filling substance: an experimental study in rabbits", *J. Mater. Sci.: Mater. Med.* **1998**, 9, 449-455.

⁶² A. Spyros, R. Kimmich, B.H. Briese, D. Jendrossek "¹H NMR imaging study of enzymatic degradation in poly(3-hydroxybutyrate) and poly(3-hydroxybutyrate-co-3-hydroxyvalerate). Evidence for preferential degradation of the amorphous phase by PHB depolymerase B from *Pseudomonas lemoignei*", *Macromolecules* **1997**, 30, 8218-8225.

of other cell components with alkaline hypochlorite solution or enzymatic digestion of such "by-products", leaving behind the isolated insoluble polymer⁶³. The

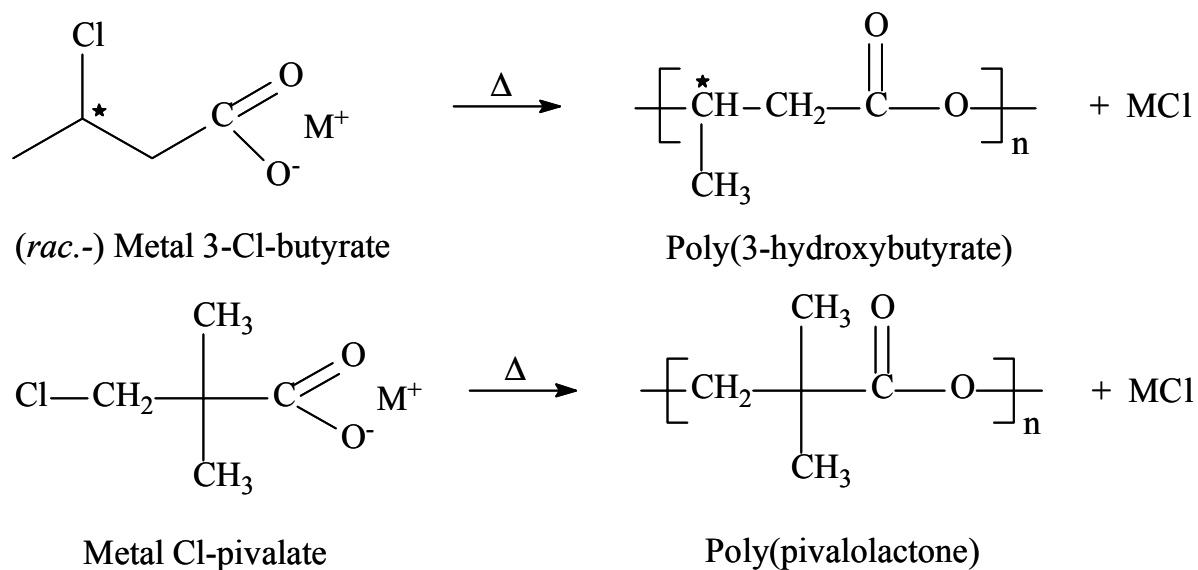


Fig. AIII.0-2 Attempted polycondensation reactions of 3-Cl-butyrate and Cl-pivalates

biotechnologically produced P-3-HB has (R)-configuration exclusively for the stereogenic center. In contrast to PGA or PLA, the predominant degradation mechanism is enzymatic⁶⁴, hydrolytic degradation is a comparatively slow process. Microorganisms possess several depolymerases to metabolize the polymer⁶². P-3-HB has properties similar to those of polypropylene. ICI produced a copolymer with 3-hydroxyvalerate (BiopolTM) and fabricated packages for commodity goods. The polymer is a promising candidate for biomedical application, because of proven biocompatibility and high degradation resistance^{62,65}.

Poly(pivalolactone) is a less prominent polymer with a reported melting range of 230-240°C⁷⁶. The two methyl groups in the close vicinity of the ester function should provide an even higher stability towards hydrolytic break-down.

Successful polycondensation in the solid state could provide degradable, biocompatible and porous biomaterials and an interesting alternative synthetic route.

⁶³ A. Steinbüchel "Polyhydroxyfettsäuren - thermoplastisch verformbare Polyester aus Bakterien", *Nachr. Chem. Tech. Lab.* **1991**, 39(10), 1112-1124.

⁶⁴ M. Uefuji, K. Kasuya, Y. Doi "Enzymatic degradation of poly[(R)-3-hydroxybutyrate]: secretion and properties of PHB depolymerase from *Pseudomonas stutzeri*", *Polym. Degrad. Stab.* **1997**, 58, 275-281.

⁶⁵ C. Doyle, E.T. Tanner, W. Bonfield "In vitro and in vivo evaluation of polyhydroxybutyrate and of polyhydroxybutyrate reinforced with hydroxyapatite", *Biomaterials* **1991**, 12, 841-847.

AIII.1 Results and discussion

Metal 3-Chloro-butyrate

The corresponding acid for the neutralization to form the desired precursor salts, 3-Cl-butyric acid, is not commercially available and needs to be synthesized. Among the various reaction pathways with the acid as an intermediate or target molecule is the exposition of concentrated hydrochloric acid to crotonic acid, leading to the addition of HCl to the α/β double bond. Cloves⁶⁶ reported the conversion into 3-Cl-butyric acid after 3 days of incubation in a closed glass vessel in excess of HCl gas saturated hydrochloric acid at -10°C , isolation of the formed product (with unreacted crotonic acid still present) and repeated incubation for another 3 days under the same conditions. Lovén and Johansson⁶⁷ obtained the same result at higher temperature and shorter incubation time. In the first step the crotonic acid/hydrochloric acid mixture was heated to $70\text{-}80^{\circ}\text{C}$ for "a few hours", the tube was opened, the product isolated and reincubated for another four hours with saturated acid at 100°C . Apparently, temperature plays a decisive role for the addition/elimination equilibrium. The addition of HCl to the double bond yields racemic 3-Cl-butyric acid with the Cl-function in the β -position only⁶⁶ as illustrated in **fig.AIII.0-3**:

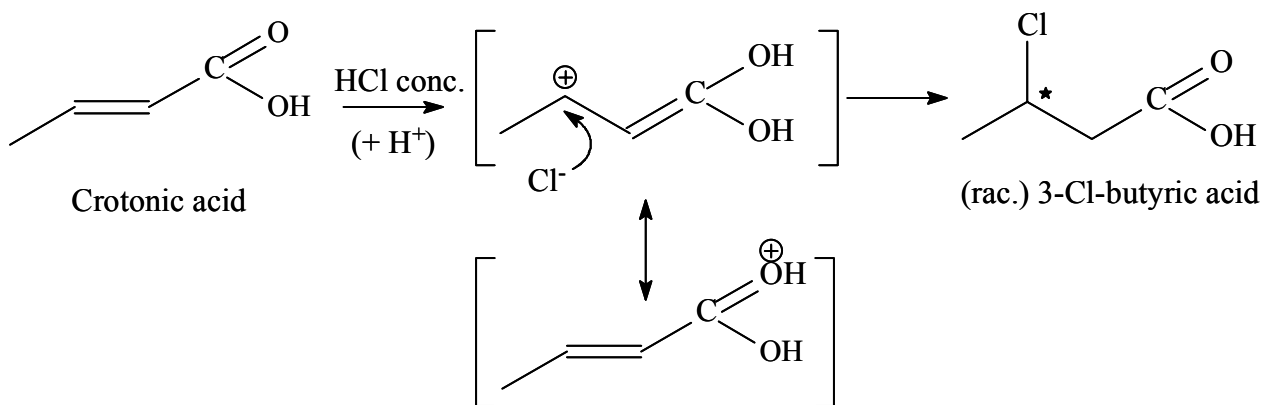


Fig.AIII.1-1 The addition of HCl to crotonic acid with Cl in the β -position

Intramolecular proton transfer leads to the formation of the acid after the attack of the chloride ion. The acid separates from the aqueous phase on cooling.

As an alternative, Sato et al. obtained the acid in quantitative yield after addition of dry

⁶⁶ A.M. Cloves "Die Darstellung der halogensubstituierten Buttersäuren und der δ -halogensubstituierten Valeriansäuren", *Ann. Chem.* **1901**, 319, 357-368.

HCl gas in ether at 0°C for three days⁶⁸.

The treatment of crotonic acid in concentrated hydrochloric acid was chosen here for the synthesis of 3-Cl-butyric acid. The reaction was not carried out in a closed vessel, because of security considerations. Instead, the vessel was equipped with a pressure

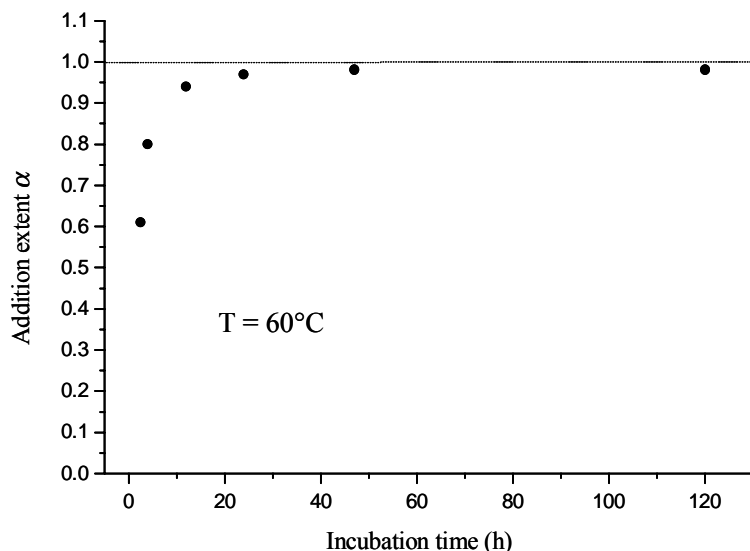


Fig.AIII.1-2 Addition kinetics for the addition of HCl to crotonic acid

gauge (nitrogen bubbler) to slow down the evaporation of HCl and the depletion of the hydrochloric acid. The apparatus was placed in a oven at a reaction temperature of 60°C. Hydrochloric acid was used in a 10 to 20-fold excess. To monitor the kinetics of the addition, aliquots of the reaction mixture were taken from the vessel. The product was extracted with dichloromethane, isolated at reduced pressure and analyzed with ¹H NMR to compare the integrated signals of educt and product (C4 methyl protons in both cases). **Fig.AIII.1-2** displays the conversion as a function of incubation time.

The addition proceeds very fast during the first hours of incubation and slows down thereafter. The reaction extent remains unchanged after 24 h with a final value of 0.98. From these results it can be deduced that the addition is not quantitative without repeated HCl gas saturation in a completely closed reaction vessel. Under the applied conditions the reaction reaches an equilibrium of addition/elimination at $\alpha = 0.98$. Kaufler discussed the problem of complete addition to crotonic acid in 1929⁶⁹ and

⁶⁷ J.M. Lovén, H. Johansson "Einige schwefelhaltige β -Substitutionsderivate der Buttersäure", *Chem. Ber.* **1915**, 48, 1254-1262.

⁶⁸ K. Sato, Y.-S. Lin, T. Amakasu "The acid-catalyzed reaction of aromatic compounds with β -chlorocarboxylic acids", *Bull. Chem. Soc. Jp.* **1969**, 42, 2600-2604.

⁶⁹ F. Kaufler "Beiträge zur Kenntnis der Crotonsäure", *Monatsh. Chem.* **1929**, 53/54, 119-126.

previous studies showed a substantial decomposition of 3-Cl and 3-Br-butyric acid after distillation at reduced pressure⁷⁰. A second incubation with fresh hydrochloric acid did not change the ratio of product and educt. Heating the reaction vessel from room temperature to 60°C led to escape of HCl through the bubbler so that the final pressure is lower compared to a closed flask. The reaction was carried out several times and in some attempts of comparable scale, crotonic acid signals were not detectable by NMR. It has to be concluded that elevated HCl gas pressure is necessary for a complete addition. **Fig.AIII.1-3** shows the ¹H NMR of the obtained 3-Cl-butyric acid. Chromatographic techniques were employed to separate the traces of crotonic

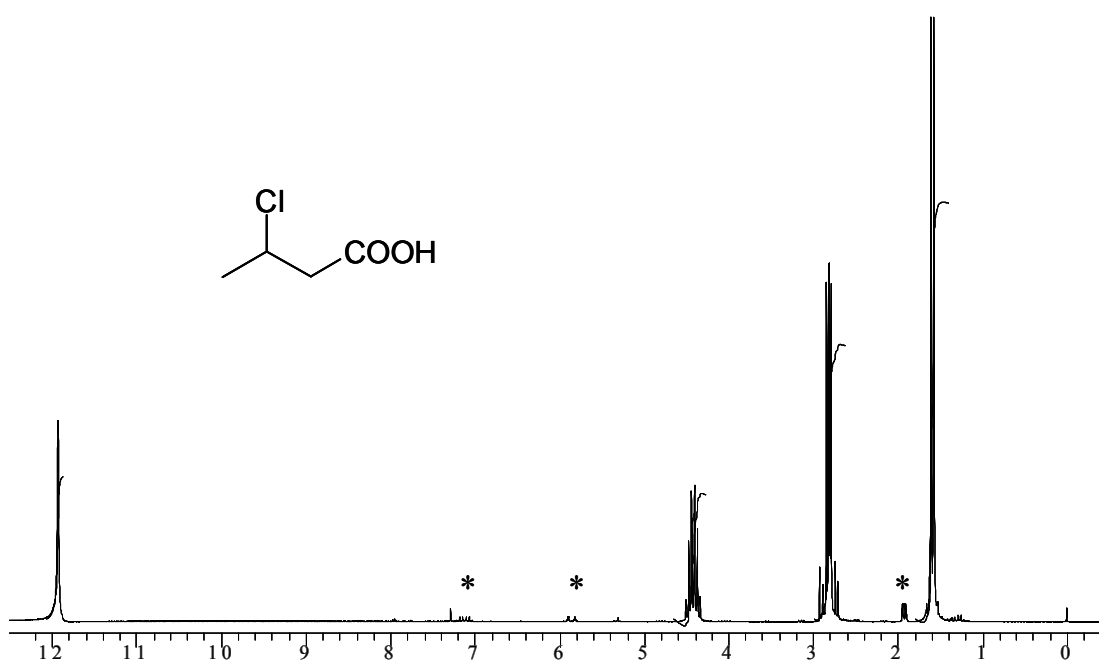


Fig.AIII.1-3 ¹H NMR (CDCl₃) of 3-Cl-butyric acid. Signals referring to traces of crotonic acid are marked with an asterisk (*).

acid from the product without success, because of very similar polarity of the two compounds. As a consequence, 3-Cl-butyric acid was obtained in ≈ 98% purity by this procedure and used for the subsequent neutralizations.

⁷⁰ K. Schwarz, diploma thesis "Thermisch initiierte Synthese von Polyestern aus Halogencarboxylaten und Füllung von porösem Polyglycolid mit Mineralien", 1997.

Na 3-Cl-butyrate

Na 3-Cl-butyrate was synthesized by neutralization of 3-Cl-butyric acid by two different procedures using two different bases:

1st method: neutralization with Na-*tert*-butylate in tetrahydrofuran (THF)

2nd method: neutralization with NaOH in methanol

The reactions are displayed in **fig.AIII.1-4**.

In both cases the base was dissolved and added to the acid-solution (same solvent) under ice-cooling. The conditions of the first variant were chosen to avoid the

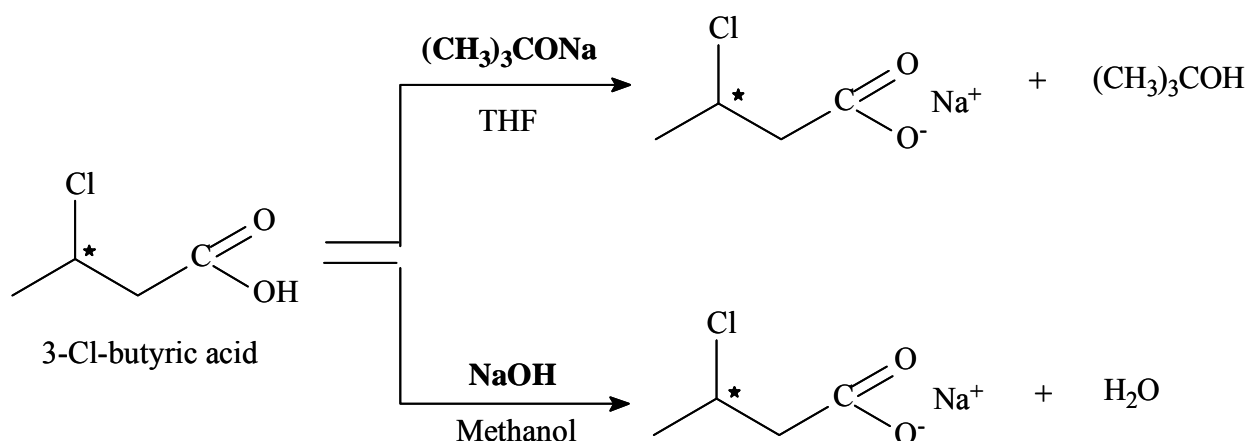


Fig.AIII.1-4 Neutralization procedures for 3-Cl-butyric acid

formation of water as a very polar solvent and to force a precipitation of the formed salt. The first variant led to the rapid voluminous precipitation of Na 3-Cl-butyric after about one fourth of the base-solution was added. In the second approach, the NaOH solution was added completely without a precipitation of the product. Therefore the salt was filtered off, washed with cold ether and dried for isolation in the first variant. In the latter case, the reaction mixture was dried with Na_2SO_4 to bind the reaction water. The product was isolated by evaporation of the methanol under oil-pump vacuum, washed with cold ether and dried again. For the work with Na 3-Cl-butyrate in solution, some competing side reactions have to be considered for a successful synthesis. The possible side reactions are collected in **fig.AIII.1-5**.

Increasing temperature increases the risk of HCl elimination. As mentioned, purification attempts by distillation of 3-Cl-butyric acid led to crotonic acid to a significant extent and the heating of Na 3-Cl propionate in the solid state caused the formation of an acrylic acid moiety in the polymerization product. Being aware of the elimination risk, the neutralization was carried out under ice-cooling. The temperature

in the vessel was controlled during the addition of the base-solution to prevent warming by the neutralization heat. The corresponding product for Na 3-Cl-butyrate would be sodium crotonate.

The substitution of the halogen function by nucleophiles like water represents another unwanted side-reaction. In earlier experiments the addition of HCl to crotonic acid in an open vessel at 70°C led to the formation of about 30% 3-hydroxybutyric acid after

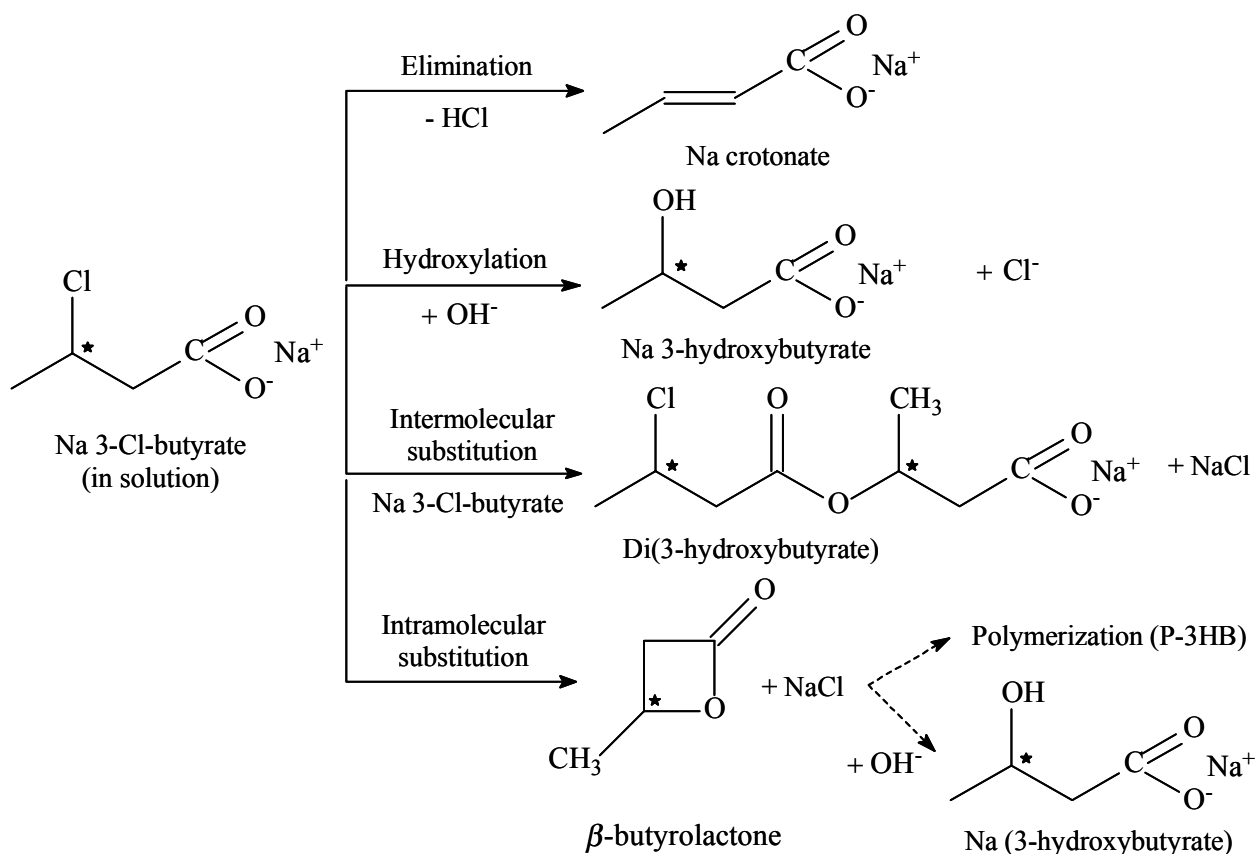


Fig.AIII.1-5 Possible side-reactions for Na 3-Cl-butyrate in solution

10 days and progressive depletion of the hydrochloric acid. Furthermore, the carboxylate group can act as a nucleophile itself leading to inter- and intramolecular substitution of the chloride function. The first route would give the same product as in the envisioned solid-state reaction with NaCl as the condensation by-product, but in solution. Dimers and possibly oligomers of poly(3-hydroxybutyric acid) would be the result of such an intermolecular substitution. Intramolecular substitution leads to cyclization and generation of β-butyrolactone. In 1915 Johansson⁷¹ introduced the heating (40-50°C) of Na 3-Br-butyrate in aqueous solution as a way to obtain β-

⁷¹ H. Johansson "Über β-butyrolactone ", *Chem Ber.* **1915**, 48, 1262-1266.

butyrolactone. 3-Br-butyric acid was neutralized with Na_2CO_3 to obtain the educt salt. The lactone was immediately and repeatedly extracted with ether. The author reported a yield of 40% with respect to the initial amount of educt and postulated the lactone as an intermediate compound in the formation of 3-hydroxybutyrate. The findings were confirmed eight years later by Salkowski Jr.⁷²

The four-membered ring is a precursor for the synthetic production of P-3-HB with ring-opening polymerization initiated by various catalysts⁷³. A polymerization of the generated lactone molecules is rather unlikely under the applied conditions. More likely is ring-opening by nucleophilic attack. The lactone is susceptible to hydrolysis leading to 3-hydroxybutyrate. The work of Johansson showed that the lactone can be isolated without the rapid formation of 3-hydroxybutyrate. However, higher temperature and longer exposition time in aqueous solution favor the conversion of 3-Cl to 3-OH-butyrate. Therefore water should be excluded.

Fig.AIII.1-6 shows the infrared spectra of the parent compound 3-Cl-butyric acid in comparison to the obtained Na salts for the two neutralization procedures. The spectra

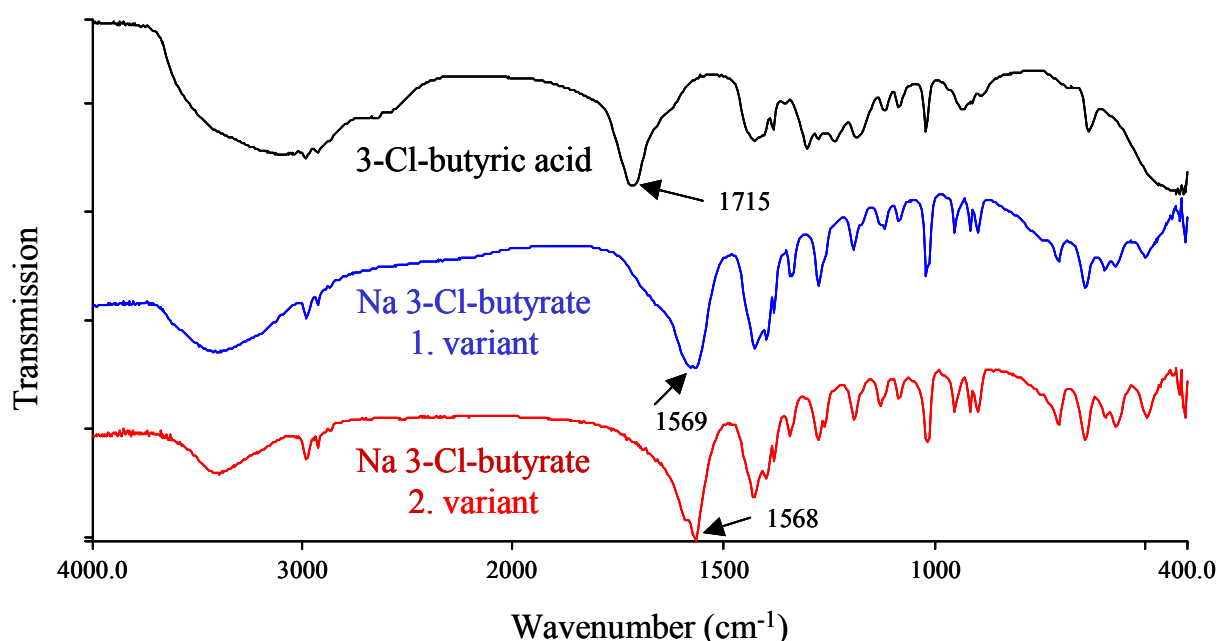


Fig.AIII.1-6 Comparative IR spectra of 3-Cl-butyric acid, Na 3-Cl-butyrate obtained by neutralization with Na *tert.*-butanol in THF (1.variant) and obtained by neutralization with NaOH in methanol (2.variant).

⁷² H. Salkowski Jr. "Über die β -Lactone der β -Oxybuttersäure und ihrer Alkylderivate, sowie die Anhängigkeit der β -Lactonsplattung von der Konstitution", *Chem Ber.* **1923**, 56, 253-265.

for the two variants are very similar and show the characteristic C=O vibration band at 1570 cm^{-1} . Bands of residual acid are not expressed. On a closer look, the bands at 3400 cm^{-1} and the broadening of the C=O vibration (more pronounced in the first variant) point to the partial protonation of the carboxylate groups that should not be present. It can be assumed that solvates formed in part either with acid or solvent molecules, water or *tert.*-butanol.

The NMR spectra of the obtained salts are almost identical. **Fig.AIII.1-7** shows the ^1H NMR for the product of the first variant. Both spectra show very little crotonic acid

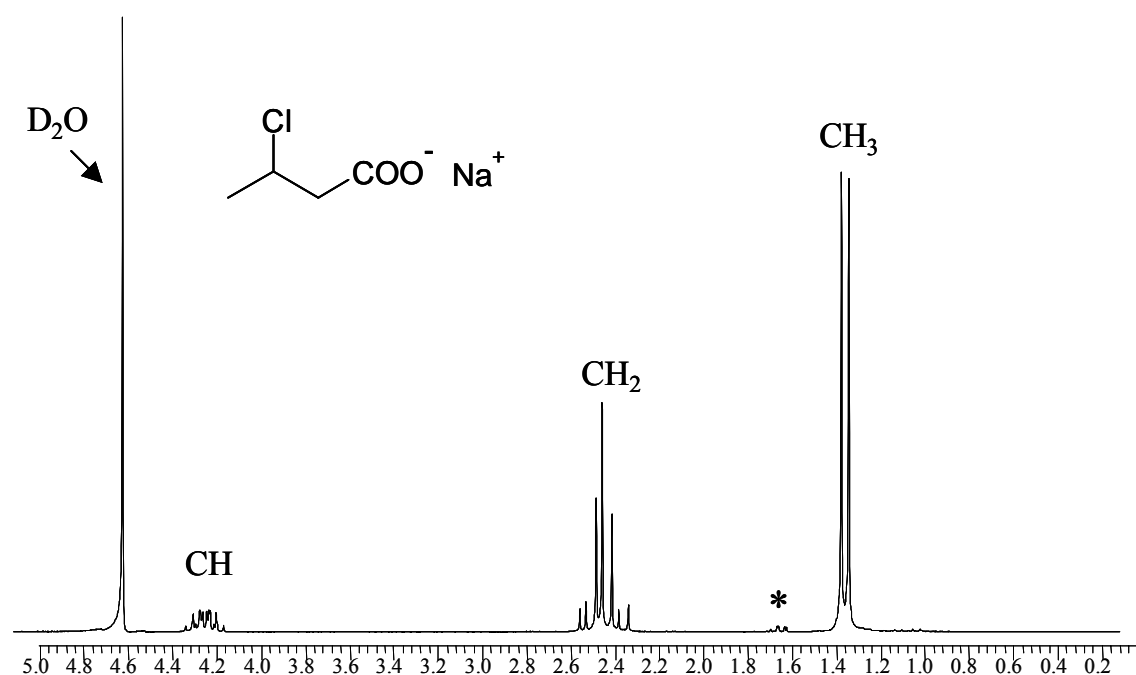


Fig.AIII.1-7 ^1H NMR (D_2O) of Na 3-Cl-butyrate synthesized by neutralization with *tert.*-butanolate in THF. Methyl protons of crotonic acid are marked with an asterisk.

(estimated 1%) and therefore prove that the neutralization conditions are rather a purification step than a destabilizing procedure with respect to HCl elimination. Surprisingly, no other signals than product, crotonic acid or solvent signals are detected. If solvates or solvent inclusions are present, the intensities are below the detection threshold of the NMR spectrometer.

The thermal behavior was measured with DSC and combined TG-DTA-MS. The DSC thermograms of the obtained salts from the two variants were similar in the occurrence of the same signals. The thermogram of the second approach is shown in **fig.AIII.1-8**.

⁷³ C.W. Lee, R. Urakawa, Y. Kimura "Copolymerization of γ -valerolactone and β -butyrolactone", *Eur. Polym. J.* **1998**, 34(1), 117-122.

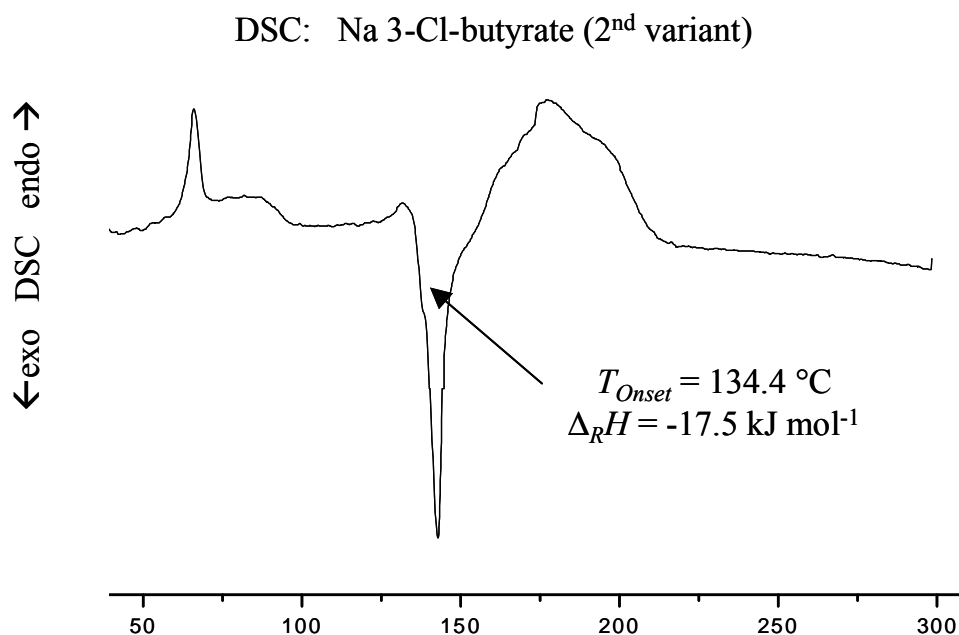


Fig.AIII.1-8 DSC of Na 3-Cl-butyrate (NaOH in methanol, $\beta = 5\text{ k min}^{-1}$)

The diagram shows two overlaying endothermic signals in the range 60-90°C. The signals refer to the evaporation of methanol. It could not be clarified why two different signals occur. It can be speculated that methanol is bond in two different ways (e.g., as inclusion or solvate molecule). Traces of residual water may contribute to the signal as well. The following exothermic signal has an onset-temperature of 134.4°C and corresponds to the decomposition of the precursor. The exothermic signal is not separated from a successive endothermic signal. In the DSC of the first variant (data not shown) the signals (solvent evaporation, precursor decomposition, endothermic signal) are closer together and less well separated. The solvent evaporation peaks are more pronounced and of comparable intensity to the other signals indicating a stronger tendency to form solvates in the first variant. An accurate quantification was not possible. The evaporation peaks are assumed to correspond to THF and *tert.*-butanol. Further analyses and polymerization attempts were focused on the second approach.

Fig.AIII.1-9 displays the TG-DTA measurement and adds the corresponding mass losses. The solvent evaporation is accompanied by a 4.4 % mass loss. Exothermic decomposition peak and following endothermic peak proceed in a one-step mass loss of 54.3%. The total mass loss of 56.8 % (corrected for solvent evaporation) is in good agreement with the theoretical mass of the organic moiety of the precursor with NaCl as residue (58.8 %). The decomposition leads to the formation of NaCl in an

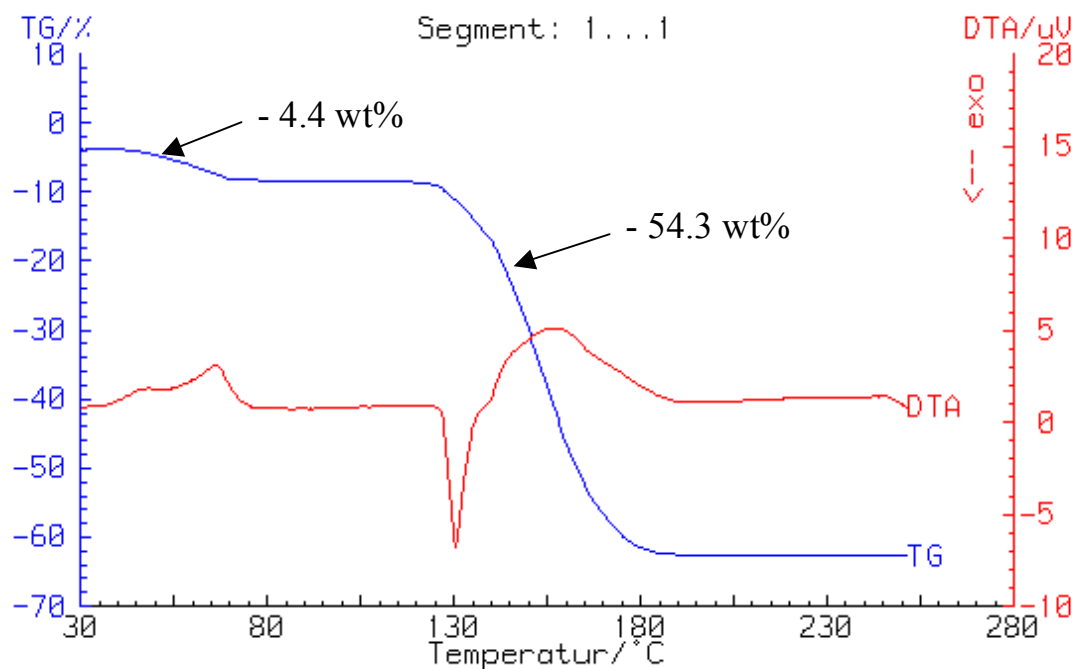


Fig.AIII.1-9 TG-DTA of Na 3-Cl-butyrate (2.variant), $\beta = 5 \text{ K min}^{-1}$, air atmosphere

exothermic process (with mass loss) and a subsequent endothermic evaporation of organic matter. Detected mass fragments were 14 (CH_2^+), 15 (CH_3^+), 28 (CO^+) for the solvent evaporation and 14 (CH_2^+), 15 (CH_3^+), 28 (CO^+), 36 (H^{35}Cl^+), 44 (CO_2^+) during the second mass loss.

The problem of solvent incorporation was approached with thermal treatment of the precursor on the one hand and with recrystallization from different solvents on the other hand. DSC measurements suggest the possibility of solvent removal at elevated temperatures. Heating to 60°C under oil-pump vacuum led to a decrease of solvent content after 1, 2 and 3 days (decrease of OH-vibration band in IR, decrease in relative DSC signal intensity). A total removal was not achieved. Instead an increase in crotonic acid/Na crotonate (9% after 3 days) was detected by NMR. Prolonged heating for one week led to the occurrence of an ester vibration band at 1730 cm^{-1} indicating a partial intermolecular substitution. Despite the measured onset-temperature of over 130°C , longer heating periods can cause the formation of ester bonds at much lower temperatures. Short heating to 90°C for 30 min resulted in a better ratio of solvent removal and crotonic acid formation. An ester vibration band did not occur. It was concluded that the post-synthetic removal of the incorporated solvent was not feasible by thermal treatment without significant decomposition of the precursor. As a

consequence of the heating experiments, it was tried to recrystallize Na 3-Cl-butyrate from different solvent mixtures. For that purpose, aliquots of the reaction mixture were taken from the vessel and mixed with an excess of solvents with different polarity (chloroform, dichloromethane, diethylether, THF, acetone, pentane), to induce a slow crystallization. The preparation tubes were stored in a freezer at -25°C . After two weeks, no crystals had developed in any mixture.

For further measurements and polymerization attempts the precursor was used as characterized above with inclusions of methanol. The thermal decomposition was monitored with temperature-resolved X-ray powder diffraction (TXRD). **Fig.AIII.1-**

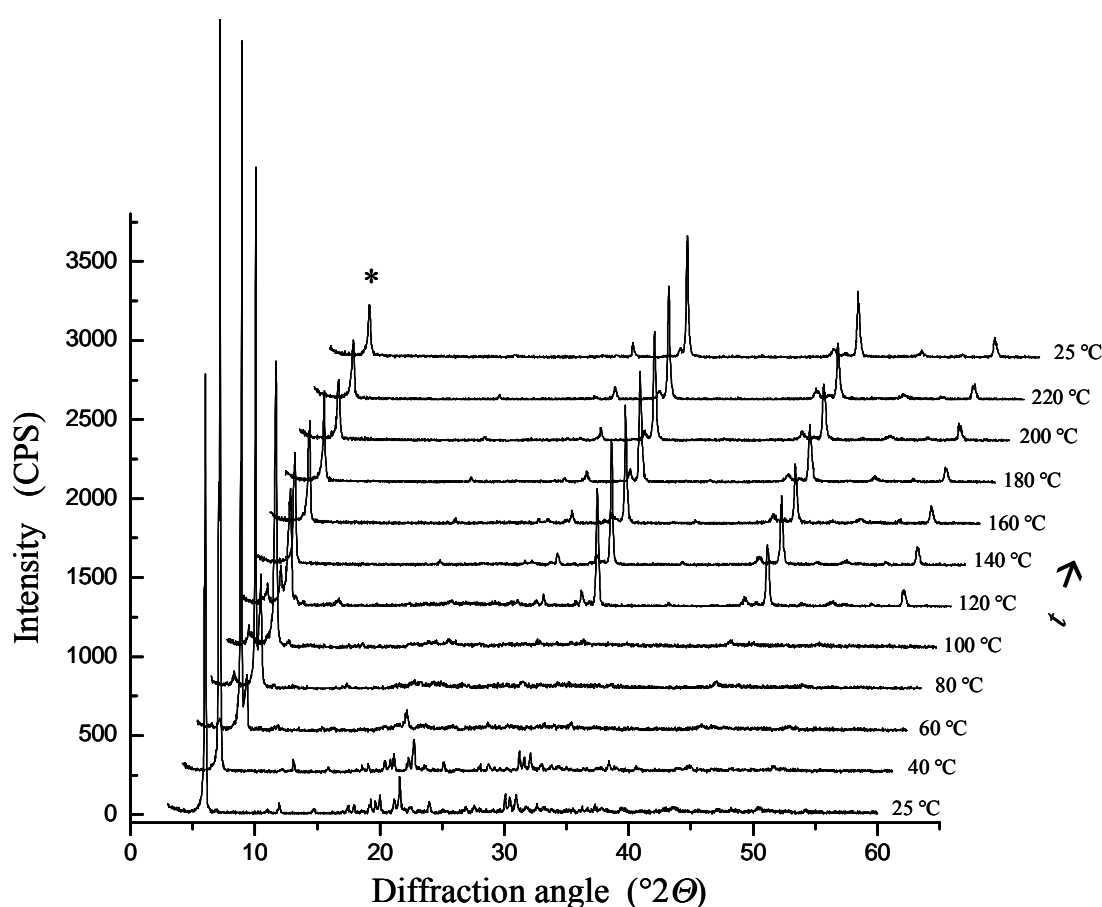


Fig.AIII.1-10 Temperature resolved XRD of Na 3-Cl-butyrate, $\beta = 1 \text{ K min}^{-1}$, 20 K interval. The main reflection of sodium crotonate is marked with an asterisk (*).

10 shows the results of the TXRD measurements. The sample was heated with 1 K min^{-1} to 220°C and cooled to room temperature. Measurements were carried out at 25°C , at 40°C , every 20 K to 220°C and after the cool-down period at 25°C . The precursor undergoes a reorientation upon heating to 100°C leading to a decrease in reflex intensities for higher diffraction angles. The intensity of the reflex at $6.1^{\circ} 2\theta$ increases in the low-temperature region. The formation of NaCl ($2\theta = 27.2, 31.6,$

45.1, 56.0) is detected from 120°C upwards. The reaction starts at lower temperatures under X-ray irradiation compared to the measured onset-temperature in DSC as reported earlier for the influence of synchrotron radiation⁴. Besides NaCl reflections peaks of Na crotonate ($2\theta = 6.2, 18.0, 30.6, 43.3, 50.5, 53.5$) develop at higher temperature than 120°C. The starting reaction led in part to the formation of the crotonate salt. Na crotonate is reported to be thermally stable up to 250°C. At higher temperature the compound undergoes a dimerization⁷⁴. Cooling down to room temperature after the heating procedures did not result in the formation of additional reflexes. Other crystalline products are therefore not detectable during and after the decomposition of the precursor. The presence of crystalline NaCl and Na crotonate indicates that the residual mass in thermogravimetry is made up of these two

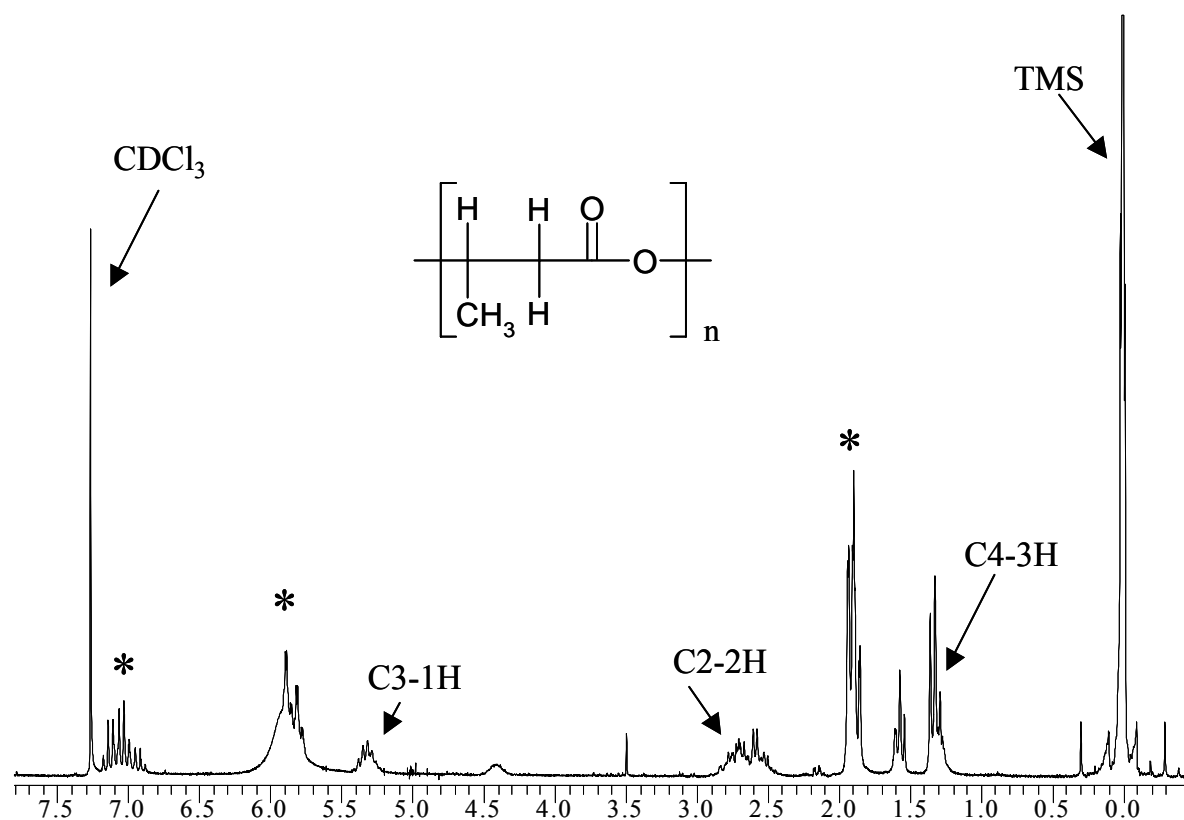


Fig.AIII.1-11 ¹H NMR (CDCl₃) of the reaction mixture obtained from heating Na 3-chlorobutyrate to 120°C for one hour. Signals of Na crotonate/crotonic acid are marked with an asterisk (*).

compounds.

The polymerization attempts were carried out in a rotary evaporator that was heated

⁷⁴ K. Naruchi, M. Miura "Thermal dimerization of alkali-metal salts of crotonic acid in the solid state", *J. Chem. Soc. Perkin Trans. II* **1987**, 113-116.

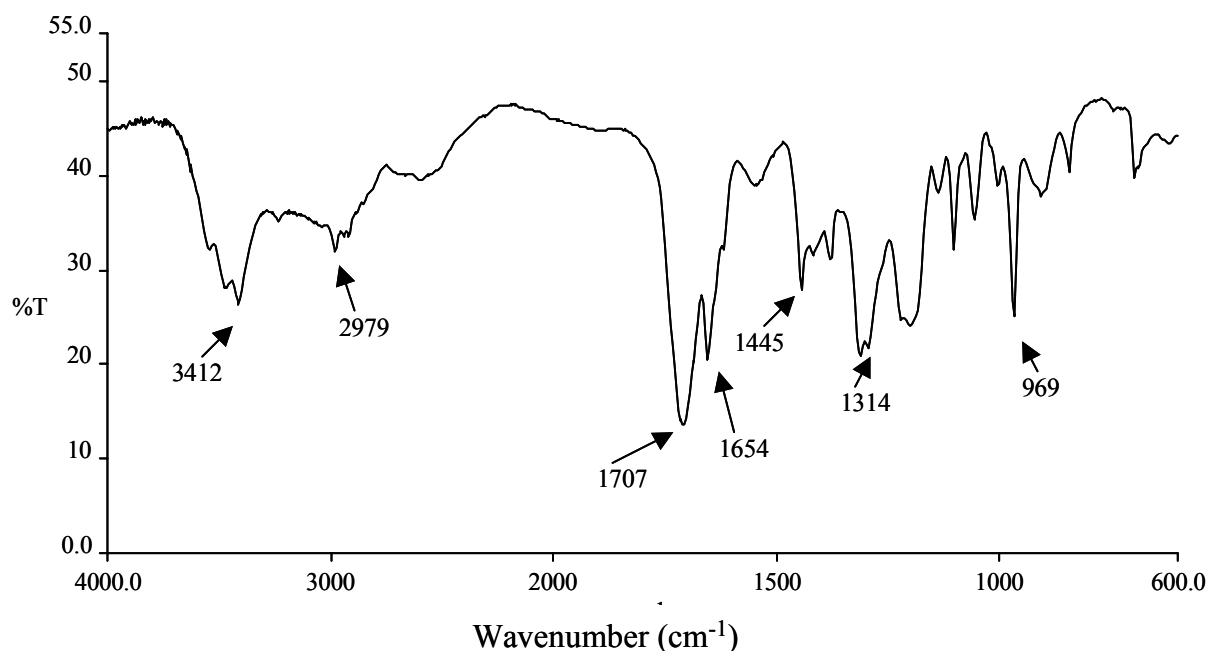


Fig.AIII.1-12 IR spectrum of the reaction mixture obtained from heating Na 3-Cl-butyrate with an oil-bath. The oil-bath was heated slowly to the polymerization temperature of 120°C. The reaction start and course were controlled by *ex situ* IR measurements. Liquefaction indicated the start of the reaction. The precursor change from the solid state to a viscous oil. The evolution of HCl (as white smoke that caused an acidic reaction on wet indicator paper) was visible shortly after initiation of the reaction. The IR spectra did not change after one hour. The resulting mixture was characterized by IR and ¹H NMR spectroscopy. **Fig.AIII.1-11** displays the ¹H NMR spectrum of the reaction mixture recorded in CDCl₃. The spectrum contains signals that can be assigned to poly- or oligomers of the desired product P-3-HB⁵. The main product is Na crotonate and/or crotonic acid, respectively. The corresponding signals are marked with an asterisk. Additional signals at δ [ppm] = 1.57, 3.50, and 4.42 could not be clearly assigned. Possible consecutive reaction could be the partial hydrolysis of the precursor or intermediate products as observed before⁴⁹ or the formation of crotyl-endgroups. The signal at 3.5 is like to be a solvent contamination. The IR spectra of the obtained product (**fig.AIII.1-12**) strongly resembles the spectrum for pure crotonic acid as the dominating compound. The following conclusions can be drawn from the synthetic efforts to obtain poly(3-hydroxybutyric acid) in a solid-state polycondensation:

Heating Na 3-Cl-butyrate to 120°C and above triggers at least three processes. One

side reaction is the elimination of hydrochloric acid leading to Na crotonate as shown by temperature resolved XRD. The fragility of the chlorine function in β -position, as observed for Na 3-Cl-propionate⁴⁹, is confirmed for the higher homologue Na 3-Cl-butyrate. Na crotonate is stable up to 250°C without thermal events in the measured temperature region⁷⁴ and contributes to the residual mass after evaporation of the organic matter at 200°C.

The second occurring reaction is most likely the condensation of NaCl followed by an intramolecular proton exchange from C2 to the acid function. Products of such a decomposition are NaCl and crotonic acid. **Fig.AIII.1-13** shows the evaluated thermal behavior of Na 3-Cl-butyrate. The third reaction type has the character of the desired polycondensation. Part of the precursor undergoes an intermolecular substitution. The resulting signals in the corresponding NMR are weak compared to the elimination products but match the characterization in the literature⁵.

The latter reaction occurs parallel to the liquefaction of the precursor and the described

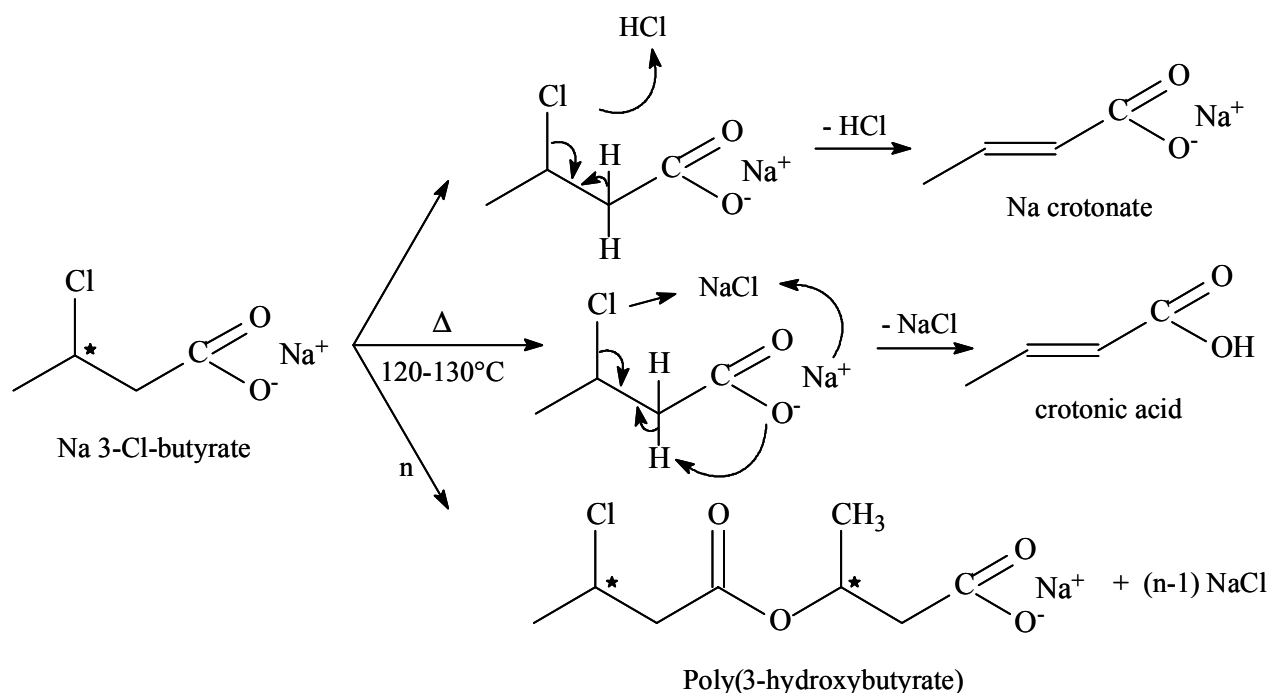


Fig.AIII.1-13 Decomposition reactions observed for Na 3-Cl-butyrate

exothermic side reactions. The generated enthalpy contributes to the acceleration of the multiple decomposition. The complex processes do not allow a determination of the degree of polymerization or possible post-polymerization eliminations to crotyl endgroups.

Experiments with different heating rates ($1-10 \text{ K min}^{-1}$), different reaction

temperatures (60-140°C) and the corresponding reaction times failed to separate the condensation process from the subsequent mass loss and to suppress the elimination in the α/β -position.

A solid-state polycondensation of the acetate type seems to be not transposable to Na 3-Cl-butyrate. The fact that a high reaction temperature promotes the elimination in the α/β -position suggested further experiments with the more reactive silver salt to improve the yield of the desired P-3HB.

Ag 3-Cl-butyrate

The synthesis of Ag 3-Cl-butyrate was carried out according to Paal and Schiedewitz⁷⁵. 3-Cl-butyric acid was neutralized with calcium carbonate in an ethanol/water mixture. The calcium salt was converted into a silver salt by the addition of AgNO₃ solution. The insoluble Ag 3-Cl-butyrate precipitates from the mother liquor. The flask with the isolated compound was wrapped in aluminum foil to prevent light-initiated decomposition and stored in a freezer at -25°C. Characterization with IR and NMR spectroscopy (see materials and methods) revealed associative O-H vibrations and a crotonic acid content of about 1%. Further solvent signals were not detected in the NMR spectrum. The DSC analysis (**fig.AIII.1-14**) shows three thermal events: The endothermic evaporation of solvent molecules (ethanol/water) from 40-

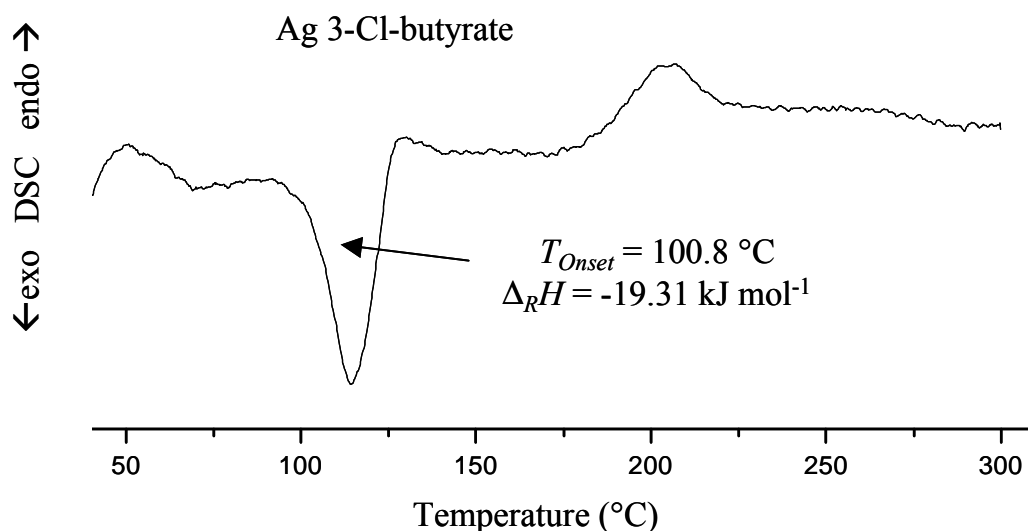


Fig.AIII.1-14 DSC diagram of Ag 3-Cl-butyrate, $\beta = 5 \text{ K min}^{-1}$

70°, the exothermic decomposition signal of the precursor at an onset-temperature of 100°C and again an endothermic signal at 184°C. The lower reaction temperature compared to the Na salt indicates a higher reactivity of the Ag compound. In contrast to the Na salt, the exothermic signal is well separated from other thermal events. In TG-DTA-MS, the events are accompanied by the following three mass loss steps: 1st step (40-80°C) $\Delta m = -4.1\%$, $m/z = 14 (\text{CH}_2^+)$, $17 (\text{OH}^+)$, 2nd (80-130°C) $\Delta m = -8.1\%$, $m/z = 15 (\text{CH}_3^+)$, $37 (^{37}\text{Cl}^+)$ und $44 (\text{CO}_2^+)$, 3rd step (130-240°C) $\Delta m = -21.2\%$, $m/z = 15 (\text{CH}_3^+)$, $37 (^{37}\text{Cl}^+)$ und $44 (\text{CO}_2^+)$. The total mass loss (corrected for solvent

evaporation) up to 240°C is 35.2 %, in good agreement with the fraction of the organic part of the precursor (34.6%). It can be deduced at this point that AgCl remains in the crucible as residue.

Fig.AIII.1-15 shows the results of the thermal behavior measured with temperature resolved XRD. Reflections of the precursor Ag 3-Cl-butyrate ($^{\circ}2\theta = 7.5, 15.0, 21.9$)

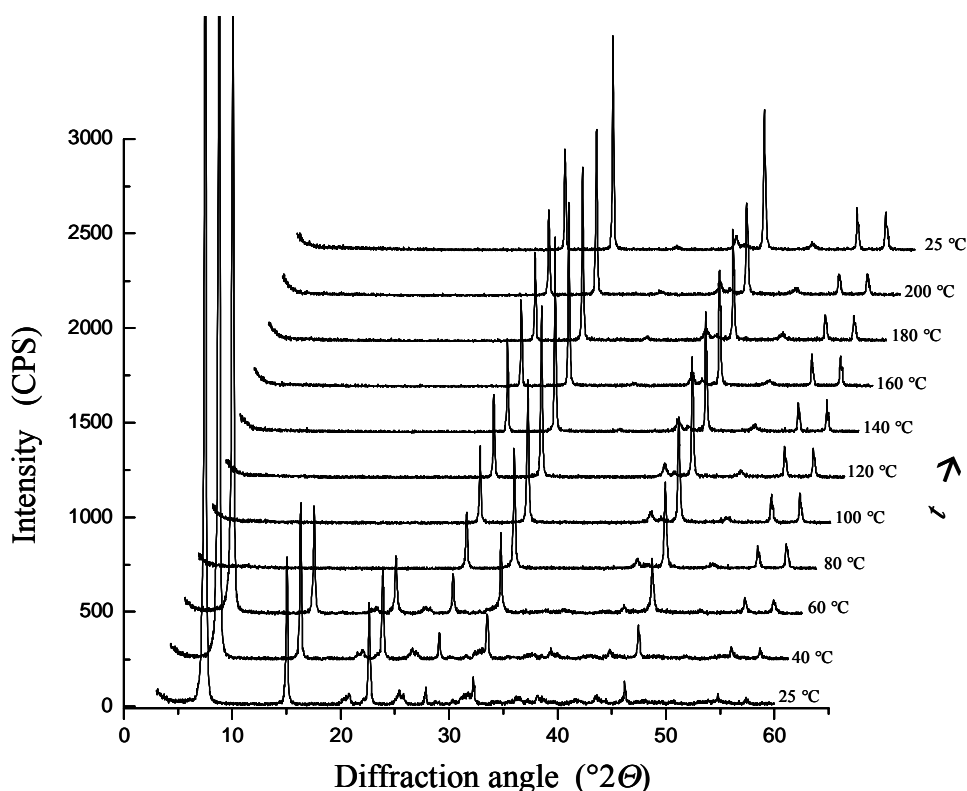


Fig.AIII.1-15 Temperature resolved XRD of Ag 3-Cl-butyrate, $\beta = 1 \text{ K min}^{-1}$, 20 K interval

are visible up to 60°C. The decomposition reaction takes place within the temperature interval 60-80°C. Reflections of AgCl ($^{\circ}2\theta = 27.5, 32.0, 45.8, 54.3, 57.0$) are visible from the first measurement at 25°C on. It has to be concluded that the X-radiation induces the polycondensation already at room temperature. Reflections of AgCl were not detected in the XRD characterization prior to the heating experiments. The reaction, however, takes place within 20 min. Again, the exposition to radiation lowers the onset by about 30 K. Apart from AgCl peaks, reflections are detected at $^{\circ}2\theta = 38.0, 44.3, 50.4$ that refer to the sample-holder. Other possible intermediates and products in a crystalline state are not detected. The IR-spectrum of the obtained reaction mixture (data not shown) clearly shows a strong ester vibration at 1741 cm^{-1}

⁷⁵ C. Paal, H. Schiedewitz "Über das Verhalten der α - und β -Chlor-buttersäuren bei der katalytischen Hydrierung", *Chem. Ber.* **1929**, 62, 1935-1939.

indicating an inverse ratio of wanted polycondensation and unwanted eliminations compared to the Na salt. This assumption is corroborated by the ^1H NMR of the obtained product (**fig.AIII.1-16**). The signals referring to crotonic acid are far less

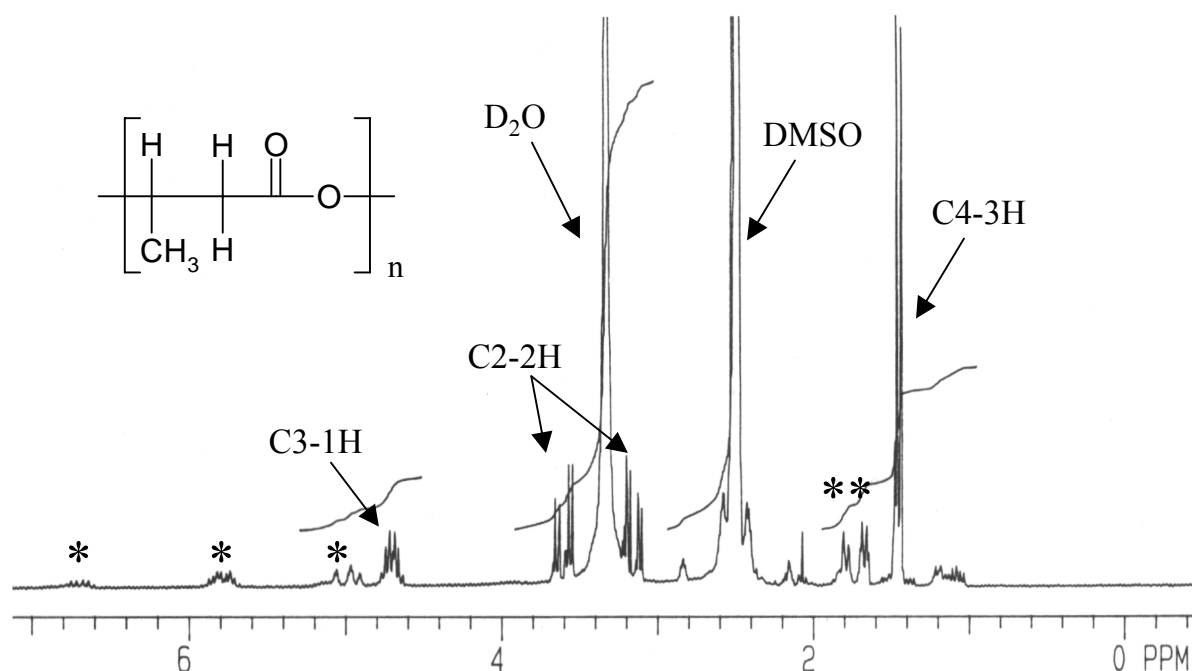


Fig.AIII.1-16 ^1H NMR (DMSO) of the reaction mixture obtained from heating Ag 3-Cl-butyrate to 100°C for one hour. Signals of crotonic acid and crotyl endgroups are marked with an asterisk (*).

intense than in the Na case. Chains of the desired product poly(3-hydroxybutyric acid) are the main product. The assigned signals are in good agreement with data reported by Seebach et al.⁷⁶. The signals at 1.7 and 5 ppm could refer to protons of crotyl endgroups, which have undergone elimination after intermolecular substitution or methyl protons of the 3-hydroxy acid⁷⁶. The obtained product mixture is solid at room temperature. The product was not further analyzed with respect to degree of polymerization.

It can be concluded that lower polymerization temperatures suppress the elimination in the α/β -position. Instead, the precursor shows a polycondensation leading to oligomers of poly(3-hydroxybutyric acid). Further investigations are necessary to optimize precursor synthesis, reaction conditions and to measure the molecular weight distribution of the resulting product.

⁷⁶ D. Seebach, A. Brunner, B.M. Bachmann, T. Hoffmann, F.N.M. Kühnle, U.D. Lengweiler "Biopolymers and -oligomers of (R)-3-hydroxyalkanoic acids – Contributions of synthetic organic chemists", *Lectures of the Ernst Schering Foundation* **1995**, 28.

Na Cl-pivalate

Na Cl-pivalate was synthesized following the same procedures as described for Na 3-Cl-butyrate (see materials and methods). The parent acid, Cl-pivalic acid, was purchased from Aldrich in the quality 99%+ and was used as received for neutralization. Characterization of the two obtained salts with IR and NMR spectroscopy revealed results comparable to the synthesis for Na 3-Cl-butyrate. Bands pointing to solvent inclusions are stronger in the first variant with *tert.*-butanolate in THF. Signals of THF, *tert.*-butanol, and of Cl-pivalic acid are detectable in the NMR spectrum. No such solvent signals appear in the spectrum of the second variant obtained from neutralization with NaOH in methanol. Thermal analyses, TXRD and product characterization are therefore focused on the second variant. Efforts to remove the included methanol were more successful than with the butyrate compound. Short-time heating (30 min) to 100°C resulted in a significant loss in solvent mass moiety. The masses (measured after heating periods of 10, 20, 30 and 40 min) converged to a final mass loss of about -3%. Solvent signals in DSC decreased significantly. Removal of solvent molecules seems to be feasible by thermal pretreatment in the case of

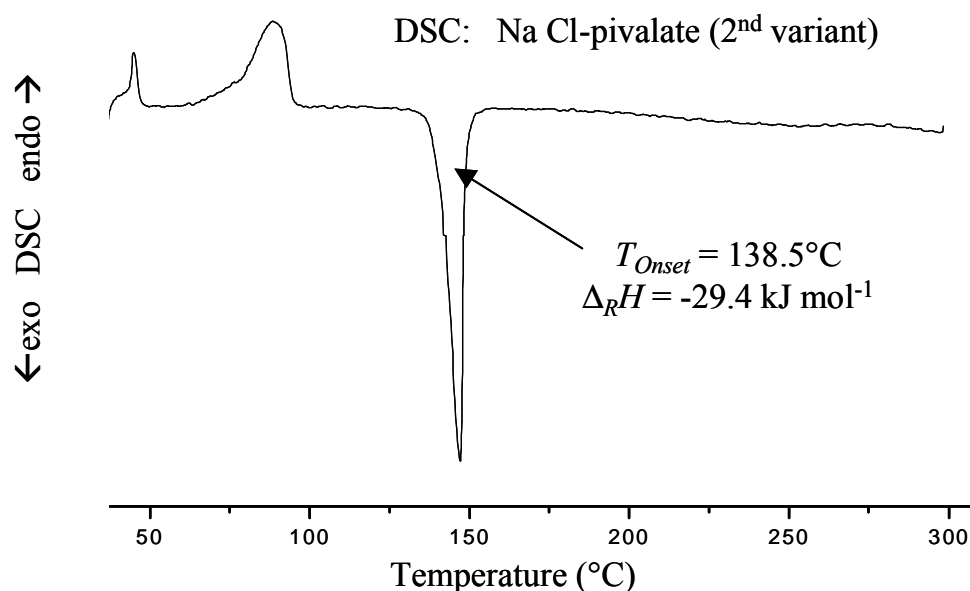


Fig.AIII.1-17 DSC of Na Cl-pivalate (NaOH in methanol, $\beta = 5 \text{ K min}^{-1}$)

pivalate. A decomposition was not noticed. An elimination is not possible without rearrangements or destruction of the carbon chain. For that aspect, pivalates are intrinsically more stable than the fragile β -substitute butyrates.

The DSC diagram of the second variant is displayed in **fig.AIII.1-17** above. Three

thermal events are visible. The first at 40-46°C corresponds to the melting of unreacted Cl-pivalic acid (mp.: 42-45°C). The second represents the enthalpy of methanol evaporation. The third and last visible signal documents the exothermic polycondensation reaction. The onset-temperature is comparable to the one for the butyrate salt. In contrast, the signal is well separated from other thermal events, suggesting an undisturbed product isolation.

Fig.AIII.1-18 shows a reduction in sample mass in two steps. The first 3% are accompanied by the evolution of 14 (CH_2^+) and 17 (OH^+) mass fragments identifying

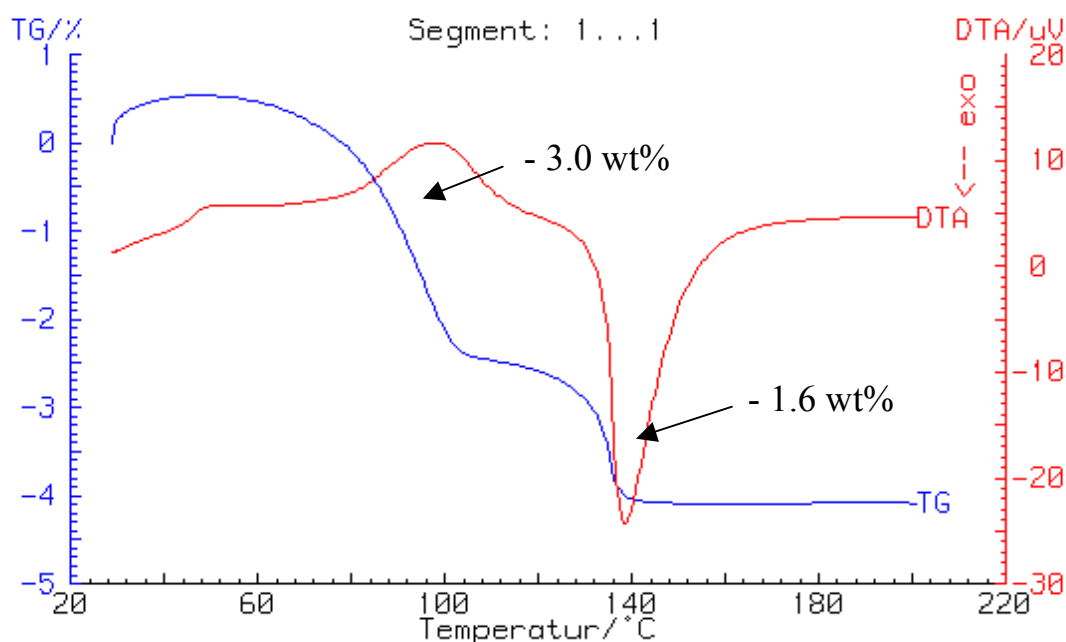


Fig.AIII.1-18 TG-DTA measurement of Na Cl-pivalate, $\beta = 5 \text{ K min}^{-1}$, air flow

methanol evaporation (60-100°C). The second mass loss occurs parallel to the polycondensation reaction. The mass fragments 17 (OH^+) and 18 (H_2O^+) prove an incomplete interception of water by sodium sulfate. The reaction itself occurs without a further mass loss up to 200°. A TG measurement of a pre-treated sample showed no mass loss over the whole range, proving that the solvent molecules are responsible for mass losses alone.

The strongest reflections (**fig.AIII.1-19**) of the precursor were detected at $2\theta = 6.3, 12.6, 16.8, 25.6, 30.2, 39.0, 43.6$ at the beginning of the measurement at 25°C. The polycondensation reaction occurs in the temperature region 80-120°C with the formation of NaCl. Other visible reflections are an amorphous halo (10-25 2θ) that develops above 120°C and peaks at 43.3, 44.2, and 50.4 resulting from the sample-

holder. These reflections are already visible in the initial diagram at room temperature. The amorphous halo may be assigned to an initially amorphous poly(pivalolactone) that starts to crystallize under thermal activation. After cooling to room temperature, crystallization leads to the formation of weak reflections of the polymer at $2\theta = 11.4, 15.5, 17.7$ (ref.⁷⁷: 11.4, 15.3, 17.8). A DSC measurement of the cooled reaction mixture gave an endothermic melting signal from 170-220°C. The melting range for poly(pivalolactone) is reported to be 240-270°C⁷⁶. The lower melting temperature can be related to significantly shorter chains in the present case of a solid-state polycondensation.

The polymerization attempts were carried out in a rotary evaporator at a reaction temperature of 130°C for one hour. The obtained product was characterized with IR and NMR spectroscopy. The analysis of the XRD measurements is confirmed by the results from NMR spectroscopy.

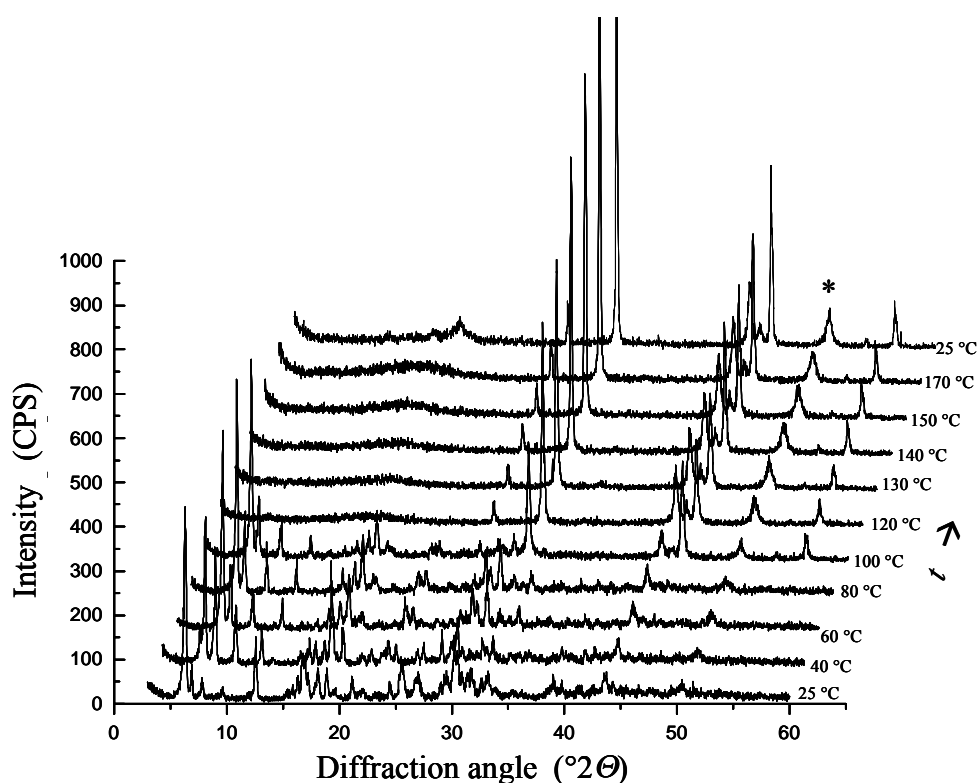


Fig.AIII.1-19 Temperature-resolved XRD of Na Cl-pivalate, $\beta = 1 \text{ K min}^{-1}$, 20 K interval. The reflection marked with an asterisk refers to the sample-holder.

⁷⁷ R.E. Prud'Homme, R.H. Marchessault "La fusion et la cristallisation du polypivalolactone", *Macromol. Chem.* **1974**, 175, 2705-2718.

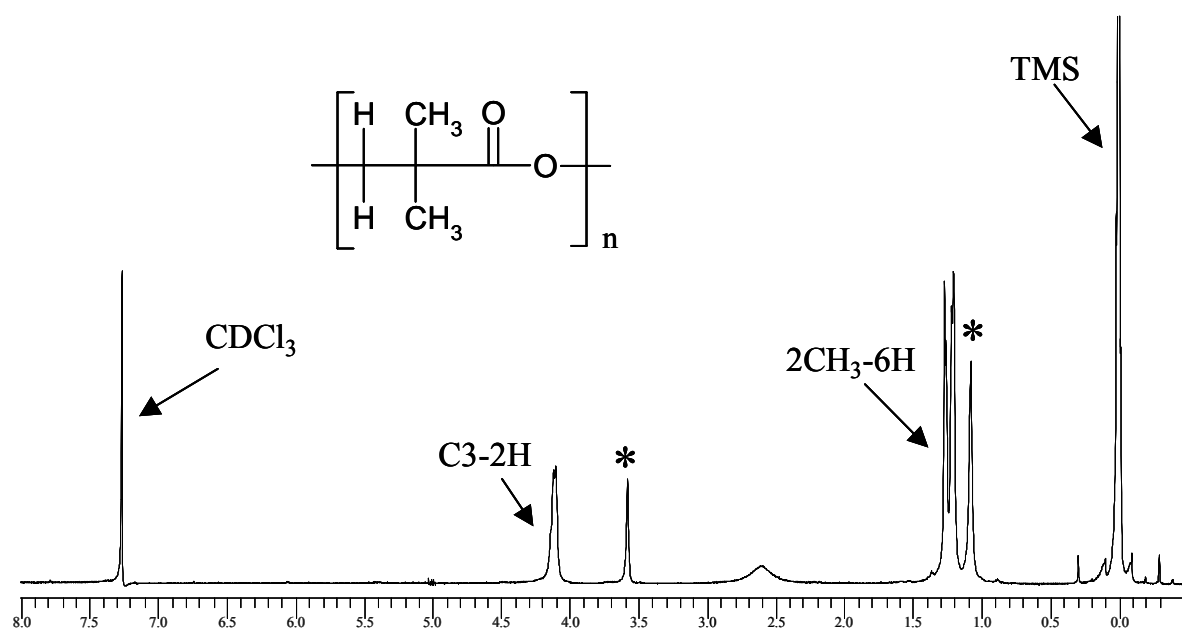


Fig.AIII.1-20 ¹H NMR (CDCl₃) of the reaction product from Na Cl-pivalate. Signals of hydroxypivalic acid/sodium hydroxypivalate are marked with an asterisk (*).

The spectrum in **fig.AIII.1-20** shows signals of poly(pivalolactone) at 1.3 and 4.1 ppm. The split of the signals could refer to steric fixation, due to the two methyl groups in the close vicinity of the ester function.

The signals at 1.1 and 3.6 could result from partial hydrolysis of the precursor during

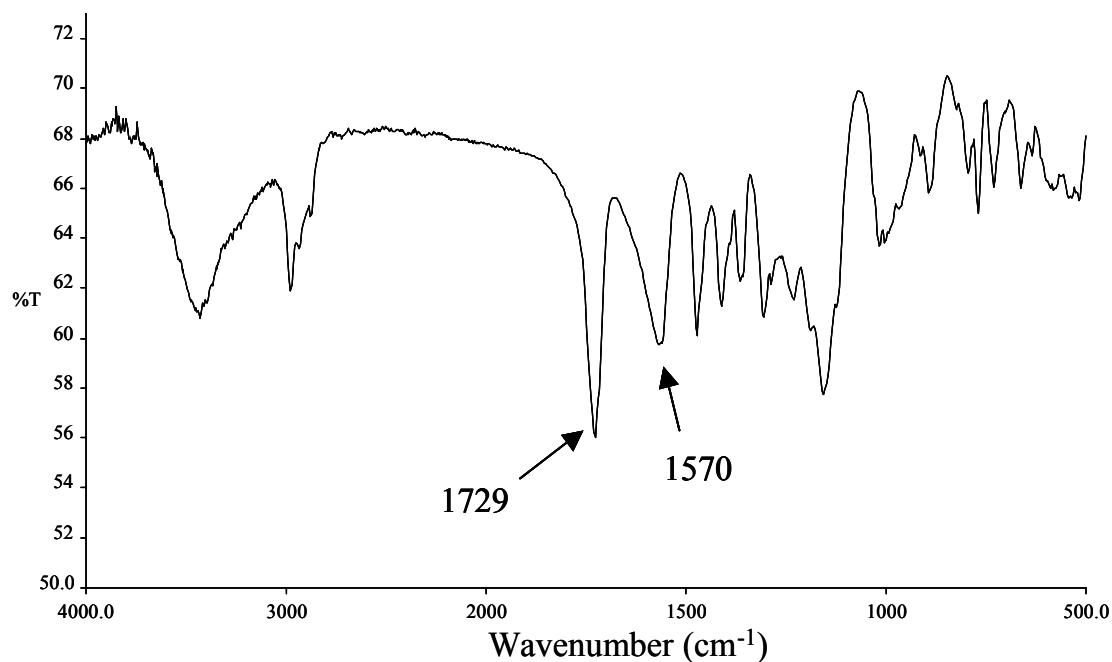


Fig.AIII.1-21 IR-spectrum of the polycondensation of Na Cl-pivalate

reaction and match the data for hydroxypivalic acid (AIST database, Japan) The absence of noticeable endgroup signals suggests comparatively long chains for the

formed polymer. In the IR-spectrum in **fig.AIII.1-21** a strong ester vibration band at 1729 cm^{-1} is visible. The band at 1570 cm^{-1} indicates the formation of sodium hydroxypivalate as a side-product.

AIII.2 Concluding remarks

β -halogeno substituted butyrates are intrinsically unstable with respect to elimination in the α/β -position. The risk of elimination increases with temperature. The heating of Na 3-Cl-butyrate with a reaction onset of about 120°C leads to elimination as the main process. At lower temperature, as in the case of Ag 3-Cl-butyrate with an onset of 20 K lower, polycondensation becomes the main reaction leading to intermolecular substitution and the formation of poly(3-hydroxybutyric acid) oligomers. Possibilities for optimization are offered by the educt synthesis without traces of crotonic acid, the solvate-free precursor synthesis and the control over the polycondensation itself. A tempting idea is the stereo-specific synthesis of metal 3-halogeno-butyrate, its thermal behavior and the resulting product character.

The second investigated system, poly(pivalolactone) from Na Cl-pivalate is a promising candidate to realize and to further analyze another solid-state polycondensation. A synthetic restriction is the strong tendency to solvate formation. The present investigations showed that the precursor is stable enough for a thermal removal of solvent molecules. A closer look onto the crystallographic phase composition and phase transitions appears worthwhile to explain the persistence of a precursor phase above 200°C while most of the compound reacts. It can be assumed that structural orientation may be responsible for the thermal behavior. A determination of the molecular weight distribution for different reaction conditions would help to clarify the potential of the investigated carboxylate systems to yield degradable polymers from solid-state precursors.

AIII.3 Materials and methods

3-chloro-butyric acid

Typical reaction: 30 g (0,35 mol) crotonic acid and 200 ml (≈ 2.4 mol HCl) 37 %-hydrochloric acid were placed in a 500 ml-flask equipped with a nitrogen bubbler. The

set-up was heated to 60°C in an oven for 30 h. At 60°C the crotonic acid was completely dissolved. After 30 h the product phase had separated from the aqueous phase as a yellow oil. The reaction mixture was extracted two times with dichloromethane. The united extracts were dried with Na₂SO₄. The dichloromethane was first partly removed on the rotary evaporator at 40°C and 400 mbar and finally at oil-pump vacuum at room temperature and self-cooling. The work-up yielded 33.5 g (0.27 mol), which is 77 % of the theoretical yield. The acid is a viscous yellow oil. 3-Cl-butyrac acid was characterized with infrared and NMR spectroscopy.

¹H-NMR (200 MHz, CDCl₃ + TMS): δ [ppm] = 1.6 (d, 3 H, C-4, ³J_{4,3} = 6.59 Hz), 2.8 (m, 2 H, C-2), 4.4 (sextett, 1 H, C-3), 12.0 (s, 1 H, -COOH), (Crotonic acid): δ [ppm] = 2,0 (dd, 3 H, C-4, ³J_{4,3} = 6,84 Hz, ⁴J_{4,2} = 1,71 Hz), 5.9 (d, 1 H, C-2, ³J_{2,3} = 7.2 Hz), 6.6 (m, 1 H, C-3), IR (NaCl plates): $\tilde{\nu}$ [cm⁻¹] = 2999, 2931 (m, C-H), 1715 (s, C=O), 1429, 1383 (m, -CH₃-CH₂-), 636 (m, C-Cl), (Crotonic acid): $\tilde{\nu}$ [cm⁻¹] = 2977, 2920 (m, C-H), 1704 (s, C=O), 1654 (m, C=C), 1446 (m, -CH₃-CH₂-), 636 (m, C-Cl)

Na 3-Cl-butyrate

1st variant

31.6 g (0.26 mol) 3-Cl-butyrac acid were dissolved in 50 ml of THF. 24.8 g (0.26 mol) Na-*tert*-butylate were dissolved in an ultrasonic bath in 50 ml of THF and added drop wise to the acid-solution under ice-cooling. The product precipitated during the addition of the base-solution, was filtered off, washed with cold ether and dried in oil-pump vacuum. The isolation yielded 37.1 g (0.26 mol) Na 3-Cl-butyrate, 99 % of the theoretical yield. The compound was stored in a freezer at -25°C. The salt was characterized with elemental analysis, IR, NMR and XRD.

EA: C: 35.06 % (theor. 33.24 %), H: 4.33 % (theor. 4,19 %), IR (NaBr pellet): $\tilde{\nu}$ [cm⁻¹] = 2984, 2929 (m, C-H), 1569 (s, C=O), 1427, 1398, 1380 (m, -CH₃-CH₂-), 707, 644 (m, C-Cl), ¹H NMR (D₂O, 200 MHz): δ [ppm] = 1.2 (d, 3 H, C-4, ³J_{4,3} = 6.59 Hz), 2.3 (m, 2 H, C-2), 4.1 (m, 1 H, C-3), D₂O: 4.5 (s, HDO), XRD (Cu-K_α, λ = 154.178 pm, Bragg-Brentano geometry): (main reflections) diffraction angle [°2θ] = 6.0, 6.7, 20.5, 24.0, 30.0, 30.4, (crotonic acid) [°2θ] = 11.5, 14.1, 22.7, 23.2, 24.1, 24.9, 27.7, 35.8, 36.4, 37.0.

2nd variant

33.5 g (0.27 mol) 3-Cl-butyric acid were dissolved in 50 ml of methanol. Na₂SO₄ was added to the solution in ten-fold excess to intercept the generated reaction water. 10.9 g (0.27 mol) NaOH were dissolved in an ultrasonic bath in 100 ml of methanol and added drop wise to the acid-solution under ice-cooling. The product did not precipitate from the neutralized solution. The sodium sulfate was filtered off and the solvent was removed in oil-pump vacuum. Washing with cold ether was followed by repeated drying. The work-up yielded 38.5 g (0.27 mol), which is 99 % of the theoretical yield. The compound was stored in a freezer at -25°C. The salt was characterized with EA, IR, NMR, DSC, TG-DTA-MS, and XRD.

EA: C: 34.56% (theor. 33.24 %), H: 4.27% (theor. 4.19 %), IR (NaBr pellet): $\tilde{\nu}$ [cm⁻¹] = 2982, 2929 (m, C-H), 1567 (s, C=O), 1429, 1399, 1380 (m, -CH₃-CH₂-), 707, 644 (m, C-Cl), ¹H NMR (D₂O, 200 MHz): δ [ppm] = 1.2 (d, 3 H, C-4, ³J_{4,3} = 6,59 Hz), 2.3 (m, 2 H, C-2), 4.1 (m, 1 H, C-3), DSC (5 K min⁻¹, open aluminum crucibles): exothermic decomposition peak: onset-temperature 134.4°C, reaction enthalpy -17.5 kJ mol⁻¹, endothermic post-decomposition peak: onset-temperature 155.6°C, enthalpy 265.5 J g⁻¹, TG-DTA-MS (5 K min⁻¹, aluminum oxide crucibles, air flow 50cm³ s⁻¹): mass loss in two steps, 1. step (40°C < T < 90°C): Δm = -4.4%, m/z = 14 (CH₂⁺), 15 (CH₃⁺), 28 (CO⁺), 2. step (120°C < T < 200°C): Δm = -54.3%, m/z = 14 (CH₂⁺), 15 (CH₃⁺), 28 (CO⁺), 36 (H³⁵Cl⁺), 44 (CO₂⁺), total mass loss 58.7% (theor. mass loss with NaCl as residue 58.8%), XRD (Cu K_α λ = 154.178 pm, Bragg-Brentano geometry): (main reflections) diffraction angle [°2θ] = 6.0, 6.7, 20.5, 24.0, 30.0, 30.4. (crotonic acid) [°2θ] = 11.5, 14.1, 22.7, 23.2, 24.1, 24.9, 27.7, 35.8, 36.4, 37.0).

Ag 3-Cl-butyrate

The synthesis of Ag 3-Cl-butyrate was carried out according to Paal and Schiedewitz⁷⁶. 20 g (0.16 mol) 3-Cl-butyric acid were dissolved in an ethanol/water mixture (volume ratio 2/5) and cooled with ice. The solution was neutralized with 8 g of (0.08 mol) calcium carbonate powder. 160 ml of AgNO₃ solution (1 m) were added to the formed Ca 3-Cl-butyrate solution. The metal exchange lead to the precipitation of silver 3-Cl-butyrate. The product was filtered off and dried in vacuum.

The work-up yielded 32.9 g (0.14 mol) of Ag 3-Cl-butyrate, which is 88% of the

theoretical yield. The compound was wrapped in aluminum foil to prevent light-initiated decomposition and stored in a freezer at -25°C . The salt was characterized by EA, IR, NMR, DSC, TG-DTA-MS, and XRD.

EA: C: 20.77 % (theor. 20.94 %), H: 2.66 % (theor. 2.64 %), IR: (NaBr pellet): $\tilde{\nu}$ [cm^{-1}] = 2985, 2927 (m, C-H), 1580 (s, C=O), 1415, 1337 (m, $-\text{CH}_3, -\text{CH}_2-$), 729, 639 (m, C-Cl), ^1H NMR (acetone- d_6 , 200 MHz): δ = 1.0 (m, 3 H, C-4), 2.0 (m, 2 H, C-2), 3.5 (m, 1 H, C-3), (β -butyrolactone) (200 MHz, CDCl_3): δ [ppm] = 1.6 (d, 3 H, $-\text{CH}_3$, $^3J = 6,1$ Hz), 3.1 (dd, 1a H, α -C, $^3J_{\alpha\beta} = 16,36$ Hz, $^4J = 4.15$), 3.6 (dd, 1b H, α -C, $^3J_{\alpha\beta} = 16.36$ ppm, $^4J = 4.15$ Hz), 4.8 (m, 1 H, β -C), DSC (5 K min^{-1} , open aluminum crucibles): exothermic decomposition peak: onset-temperature 100.8°C , reaction enthalpy -19.3 kJ mol^{-1} , endothermic post-decomposition peak: onset-temperature 184.2°C , enthalpy 35.7 J g^{-1} , TG-DTA-MS (5 K min^{-1} , aluminum oxide crucibles, air flow $50\text{ cm}^3\text{ s}^{-1}$): mass loss in three steps, 1. step ($40^{\circ}\text{C} < T < 80^{\circ}\text{C}$): $\Delta m = -4.1\%$, $m/z = 14$ (CH_2^+), 17 (OH^+), 2. step ($80^{\circ}\text{C} < T < 130^{\circ}\text{C}$): $\Delta m = -8.1\%$, $m/z = 15$ (CH_3^+), 37 ($^{37}\text{Cl}^+$), 44 (CO_2^+), 3. step ($130^{\circ}\text{C} < T < 240^{\circ}\text{C}$): $\Delta m = -21.2\%$, $m/z = 15$ (CH_3^+), 37 ($^{37}\text{Cl}^+$), 44 (CO_2^+), total mass loss is 33.8% (theor. mass loss with AgCl as residue 34.6%), XRD (Cu K_{α} $\lambda = 154.178\text{ pm}$, Bragg-Brentano geometry) (main reflections) diffraction angle [$^{\circ}2\theta$] = 7.5, 15.0, 21.9, 27.7, 31.8, 45.8, 55.1, 58.1.

Na Cl-pivalate

The synthesis of Na Cl-pivalate was carried out analogous to the procedures for Na 3-Cl-butyrate with Na *tert.*-butylate and NaOH as basis. Cl-pivalic acid was purchased from Aldrich in the quality 99%+ and used as received for neutralization.

1st variant (Na *tert.*-butylate in THF)

Quantities: 14.5 g (0.11 mol) 3-Cl-pivalic acid, 10.2 g (0.11 mol) Na *tert.*-butylate

The addition of base-solution lead to the rapid precipitation of little 3-Cl-pivalic acid. The precipitated acid was removed from the vessel by filtration. The product Na-Cl-pivalate crystallized from the solution over a period of 3-5 days. The product was isolated several times by filtration, washed with cold ether and dried in vacuum. The isolation yielded 15.7 g (0.10 mol) Na Cl-pivalate, 90 % of the theoretical yield. The compound was stored in a freezer at -25°C . The salt was characterized with EA, IR,

NMR, DSC and XRD.

EA: C: 38.64 % (theor. 37.88 %), H: 4.88 % (theor. 5.09 %), IR (NaBr pellet): $\tilde{\nu}$ [cm^{-1}] = 2978, 2937, 2874 (m, C-H), 1566 (s, C=O), 1479, 1429, 1404, 1370 (m, -CH₃-CH₂-), 724, 638 (m, C-Cl), (Cl-pivalic acid) $\tilde{\nu}$ [cm^{-1}] = 2977, 2937, 2877 (m, C-H), 1705 (s, C=O), 1433, 1406, 1364 (m, -CH₃-CH₂-), 729, 639 (m, C-Cl), ¹H NMR (acetone-d₆, 200 MHz): δ [ppm] = 1.2 (s, 6 H, -CH₃), 3.8 (s, 2 H, -CH₂Cl), (further signals) δ [ppm] = 1.4 (s, *tert*-butanol), 2.0 (m, THF, -CH₂-), 2.8 (s, acetone), 4.2 (s, THF, -CH₂O), (3-Cl-pivalic acid, D₂O) δ [ppm] = 0.9 (s, 6 H, -CH₃), 3.4 ppm (s, 2 H, -CH₂Cl), DSC (5 K min⁻¹, open aluminum crucibles): exothermic decomposition peak: onset-temperature 129.6°C, reaction enthalpy -11.9 kJ mol⁻¹, XRD (Cu K _{α} λ = 154.178 pm, Bragg-Brentano geometry): (main reflections) diffraction angle [$^{\circ}2\theta$] = 6.7, 12.9, 16.3, 25.2, 30.9.

2nd variant (NaOH in methanol)

Quantities: 30.0 g (0.22 mol) 3-Cl-pivalic acid, 8.79 g (0.22 mol) NaOH, 40.0 g sodium sulfate. Sodium sulfate was filtered off after complete addition of the NaOH solution. The product Na 3-Cl-pivalate did not precipitate from the solution. The product was isolated in oil-pump vacuum. The isolation yielded 34.1 g (0.22 mol) product, 99 % of the theoretical yield. The compound was stored in a freezer at -25°C. The salt was characterized with EA, IR, NMR, DSC, TG-DTA-MS, and XRD.

EA: C: 39.54 % (theor. 37.88 %), H: 5.56 % (theor. 5.09 %), IR (NaBr pellet): $\tilde{\nu}$ [cm^{-1}] = 2978, 2937, 2874 (m, C-H), 1566 (s, C=O), 1479, 1429, 1404, 1370 (m, -CH₃-CH₂-), 724, 638 (m, C-Cl), ¹H NMR (acetone-d₆, 200 MHz): δ [ppm] = 1.2 (s, 6 H, -CH₃), 3.8 (s, 2 H, -CH₂Cl), the NMR spectrum is identical to the one obtained from the product of the 1. variant, but with no additional solvent signal present., DSC (5 K min⁻¹, open aluminum crucibles): exothermic decomposition peak: onset-temperature 138.5°C, reaction enthalpy -29.4 kJ mol⁻¹, TG-DTA-MS (5 K min⁻¹, aluminum oxide crucibles, air flow 50cm³ s⁻¹): mass loss in two steps, 1. step (60°C < T < 100°C): Δm = -3.0%, m/z = 14 (CH₂⁺), 17 (OH⁺), 2. step (110°C < T < 150°C): Δm = -1.6%, m/z = 17 (OH⁺), 18 (HO₂⁺), total mass loss 4.6% (theor. mass loss with NaCl as residue 63.1%), XRD (Cu K _{α} λ = 154.178 pm, Bragg-Brentano geometry): (main reflections) diffraction angle [$^{\circ}2\theta$] = 6.7, 12.9; 16.3, 25.2, 30.9.

Polymerization attempts

The polymerizations were carried out in a rotary evaporator that was heated with an oil-bath. The baths were heated slowly to the destination temperatures for the corresponding precursors: Na 3-Cl-butyrate 120°C, Ag 3-Cl-butyrate 100°C, Na Cl-pivalate 130°C. The reactions were controlled with *ex situ* IR spectroscopy. Reaction time was about one hour in all cases. The precursors liquefied to viscous oils in the cases of Na 3-Cl-butyrate and Na Cl-pivalate shortly after reaction initiation. The resulting mixtures were characterized with IR, ¹H NMR and temperature resolved XRD.

Precursor Na 3-Cl-butyrate

IR (NaBr pellet): $\tilde{\nu}$ [cm⁻¹] = 3412, 2979 (m, C-H), 1707 (s, C=O), 1654 (s, C=C), 1445, 1379 (m, -CH₃, -CH₂-), 969, 699 (m, C-Cl), ¹H NMR (200 MHz, CDCl₃ + TMS): δ [ppm] = 1.3 (m, 3 H, -CH₃), 2.6 (m, 2 H, -CH₂-), 5.3 (m, 1 H, CH), (Crotonic acid): δ [ppm] = 2.0 (dd, 3 H, C-4, ³J_{4,3} = 6.84 Hz, ⁴J_{4,2} = 1.71 Hz), 5.9 (d, 1 H, C-2, ³J_{2,3} = 7.2 Hz).

Precursor Ag 3-Cl-butyrate

IR (NaBr pellet): $\tilde{\nu}$ [cm⁻¹] = 2992, 2941, 2878 (m, C-H), 1741 (s, C=O), 1658 (m, C=C), 1566 (m, C=O), 1445, 1414, 1382 (m, -CH₃, -CH₂-), 1272, 1184, 1018, ¹H NMR (D₂O, 200 MHz): δ [ppm] = 1.4 (d, 3H, C4), 3.4 (dd, 2H, C2), 4.7 (m, 1H, C3), (Crotonic acid): δ [ppm] = 2.0 (dd, 3 H, C-4, ³J_{4,3} = 6.84 Hz, ⁴J_{4,2} = 1.71 Hz), 5.9 (d, 1 H, C-2, ³J_{2,3} = 7.2 Hz).

Precursor Na Cl-pivalate

IR (NaBr pellet): $\tilde{\nu}$ [cm⁻¹] = 3434 (m, O-H), 2981 (m, C-H), 1729 (s, COOR), 1570 (m, COO⁻), 1474, 1413, 1366 (m, -CH₃, -CH₂-), 1308, 1233, 1157, 1018, 894, 771, ¹H NMR (CDCl₃, 200 MHz): δ [ppm] = 1.3 (dd, 6 H, -CH₃), 4.1 (d, 2 H, -CH₂-), (hydroxypivalic acid): δ [ppm] = 1.1 (s, C2, 6H), 3.6 (s, C3, 2H).

*Instruments and methods*Infrared spectroscopy

IR spectroscopy was carried out with a FT-IR spectral photometer 1720 from Perkin Elmer. Solid samples were mixed with KBr, liquid samples were measured between plates of NaCl.

¹H NMR spectroscopy

¹H NMR spectroscopy was carried out with a Varian Gemini 200 instrument (200 MHz).

DSC

DSC measurements were carried out on a Mettler TA 4000 instrument at a heating rate of 5 K min⁻¹ in open aluminum crucibles. Average sample mass was 5-8 mg.

TG-DTA-MS

Combined thermogravimetry-differential thermal analysis-mass spectroscopy was carried out with a Netzsch STA 409 system, employing dynamic air atmosphere (50 ml min⁻¹) and a heating rate of 5 K min⁻¹. Open alumina crucibles served as sample holders. Typical sample masses were 30-50 mg.

Temperature resolved XRD

Measurements were carried out on a Siemens D-5000 instrument (Cu-K_α λ = 154.178 pm) with a heating rate of 1 K min⁻¹ in the diffraction angle range 5° < 2 θ < 70°. Scans were carried out at 25°C, 40°C, every 20 K to 220°C and after cooling to room temperature again.

Part B: Composites of polyglycolide and calcium phosphate

B.0 Introduction

Part A of the present work dealt with the synthesis and degradation of porous polyglycolide from solid-state reaction and the logical approach to higher homologues. Part B continues with the evaluation of the porous biomaterial PGA in composite with calcium phosphates (CaP) as a potential bone substitution material.

The surgical incidence of bone loss, fractures or instabilities is treated with a variety of strategies and materials being biogenic or synthetic, autogenic or allogenic, permanent or temporary, resorbable or non-resorbable^{1,2}. The fact that bone owes its unique properties to its composite character and to its complex regulatory system suggests the development of synthetic composite materials that can serve as a substitute with remodeling potential. The mimicking aspect of bone implant design was appropriately formulated by de Groot et al.³: *"To produce an excellent bone substitute material, it is necessary to emphasize several compositional and structural characteristics of natural bone. The mineral of bone is nonstoichiometric hydroxyapatite with carbonate substitution. Its low crystallinity and nanometer size make it different from synthetic ceramic. [...]. Moreover, on the histological level, natural bone has an interconnected porous structure"*. This statement points to the specific nature of the calcium phosphate forming the bone mineral. This very special nature of nanometer-sized, X-ray amorphous crystals with heteroion substitution makes bone apatite an excellent constituting material in the cellular remodeling process. The coordinative assembly of nano-crystallites embedded in a collagen matrix stabilizes the crystals (which exhibit a high surface energy) and prevents compositional changes and ripening processes to some extent⁴. Osteoclastic resorption is mediated by cell adhesion to the CaP substrate and acidic dissolution of the crystals in a large surface membrane compartment ("ruffled border")^{5,6}. Due to the structural disorder, a comparatively high solubility for

¹ G.O. Hofmann "Biodegradable implants in traumatology: a review on the state-of-the-art", *Arch. Orthop. Trauma Surg* **1995**, *114*, 123-132.

² J.M. Rueger "Knochenersatzmittel – Heutiger Stand und Ausblick", *Der Orthopäde* **1998**, *27*, 72-79.

³ C. Du, F.Z. Cui, Q.L. feng, X.D. Zhu, K. de Groot "Tissue response to nano-hydroxyapatite/collagen composite implants in marrow cavity", *J. Biomed. Mater. Res.* **1998**, *42*, 540-548.

⁴ R. Legros, N. Balmain, G. Bonel "Age-related changes in mineral of rat and bovine cortical bone", *Calcif. Tissue Int.* **1987**, *41*, 137-144.

⁵ S.L. Teitelbaum, M.M. Tondravi, F.P. Ross "Osteoclasts, macrophages, and the molecular mechanism of bone resorption", *J. Leukocyte Biol.* **1997**, *61*, 381-388.

CaP and a high surface to volume ratio, bone mineral can be effectively resorbed by osteoclasts to enable a dynamic remodeling process⁷. Synthetic solutions for CaP implants are always a compromise between the advantages and disadvantages of specific requirements. Biogenic materials like bovine bone (e.g., endobon[®] from Merck Biomaterials) or corals (e.g., algipore[®] from Friadent) were thermally or hydrothermally treated to remove immunogenic factors, to retain the unique porous structure and to profit from the integrational bone bonding ability⁸. The (chemical)

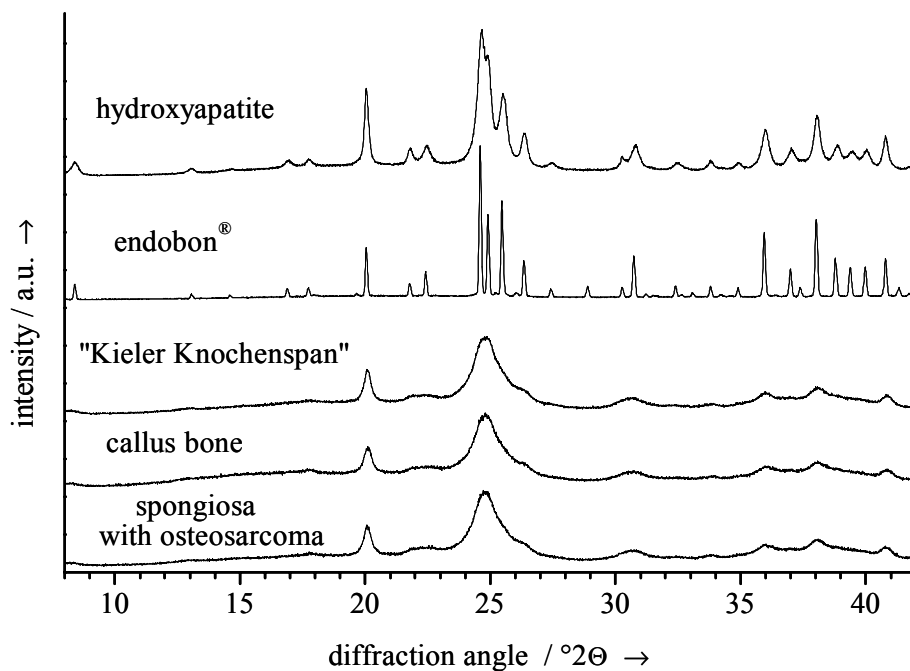


Fig.B.0-1 Comparative XRD diagrams of synthetic hydroxyapatite ("hydroxyapatite for bioceramics", Merck Biomaterials), endobon[®] (Merck Biomaterials), "Kielers Knochenspan" (bovine bone) and two samples of natural human bone.

price for such a treatment with temperatures up to 1100°C in the case of endobon[®] is displayed in **fig.B.0-1**⁹. XRD diagrams of synthetic hydroxyapatite, endobon[®], "Kielers Knochenspan" ("Kiel bone", bone of bovine origin that underwent thermal treatment at lower temperature of about 400°C without complete removal of organic material) and

⁶ G. Vaes "Cellular biology and biochemical mechanism of bone resorption", *Clin. Orthop. Rel. Res.* **1988**, Section III – Basic science and pathology, 239-271.

⁷ Y. Doi, T. Shibusaki, Y. Moriwaki, T. Kajimoto, Y. Iwayama "Sintered carbonate apatites as bioresorbable bone substitutes", *J. Biomed. Mater. Res.* **1998**, 39, 603-610.

⁸ G. Daculsi, R.Z. Legeros, M. Heughebaert, I. Barbioux "Formation of carbonate-apatite crystals after implantation of calcium phosphate ceramics", *Calcif. Tissue Int.* **1990**, 46, 20-27.

⁹ F. Peters, K. Schwarz, M. Epple "The structure of bone studied with synchrotron X-ray diffraction, X-ray absorption spectroscopy and thermal analysis", *Thermochim. Acta* **2000**, 361, 131-138.

¹⁰ W. Linhart, N.M. Meenen, J.M. Rueger "Knochenersatzmaterialien: Neue Möglichkeiten und Techniken", *OP-J.* **2000**, 16, 294-298.

two natural bone samples are compared. The profiles clearly indicate the different crystalline character of the measured samples. The high sintering temperature for endobon[®] leads to a highly crystalline material. The other substitute material, "Kiel bone" shows a low crystallinity alike the two bone samples. Despite of its biomimetic crystallinity, the material is not in use any more, because of inflammatory adverse reaction to the residual antigenic components. Average crystallite sizes of the samples were determined by synchrotron X-ray diffraction employing the Scherrer equation⁹. Crystallites of endobon[®] are much bigger (> 62-71 nm) than the corresponding diameters for "Kiel bone" (7-22 nm) or natural bone samples (8-23 nm). The highly crystalline, sintered structure of endobon[®] significantly lowers the solubility and restricts the osteolytic potential of osteoclasts to be resorbed.

Fig.B.0-2 shows the contrasted residue of endobon[®] implanted into a human tibia four years after implantation. The material appears to be resistant to resorption and remodeling over a period of four years. This implies inhomogenities at the



Fig.B.0-2 X-ray photography of a human tibia treated with an endobon[®]-block - four years postoperatively¹⁰. Arrows pointing to the residual implant material. The contrast indicates the persistence of the bone substitute and an inhomogeneous implantation site.

implantation site and potential gradients and interfaces with respect to material integrity and stress-deviation trajectories.

Positive aspects of the endobon[®] implantation are the described rapid bone bonding

and integration (osteoconductivity) with resulting stability and the surface ingrowth of bone tissue¹¹. The material can be described as an integrated space-holder providing higher stability than an untreated defect. An active remodeling and the formation of new bone for the whole implant site is not achieved.

In context of the latest BSE discussion, general concerns were raised against implant materials of biogenic origin like e.g. endobon[®]. A tendency towards bone substitution with entirely synthetic materials (without risky components) can be expected to result from this discussion and public pressure.

Concerning CaP implant materials, hydroxyapatite (HAP, $\text{Ca}_{10}(\text{PO}_4)_6(\text{OH})_2$) and tricalcium phosphate (TCP, $\text{Ca}_3(\text{PO}_4)_2$) are the predominantly used phases. HAP as the archetype of the apatite family is predestined for implant design, because of the similar composition and the structural similarity to bone mineral. TCP has the advantage of a higher solubility¹².

Table B.0-1 gives a compilation of recently published composite combinations for biomedical purposes with calcium phosphates as basic substances.

No.	Reference
13	C. Doyle, E.T. Tanner, W. Bonfield "In vitro and in vivo evaluation of polyhydroxybutyrate and of polyhydroxybutyrate reinforced with hydroxyapatite ", <i>Biomaterials</i> 1991 , 12, 841-847.
14	M. Kikuchi, J. Tanaka, Y. Koyama, K. Takakuda "Cell culture test of TCP/CPLA composite", <i>J. Biomed. Mater. Res.</i> 1999 , 48, 108-110.
15	H. Tamai, H. Yasuda "Preparation of polymer particles coated with hydroxyapatite ", <i>J. Coll. Interf. Sci.</i> 1999 , 212, 585-588.
16	S. Li, Z. Zheng, Q. Liu, J.R. de Wijn, K. de Groot " Collagen/apatite coating on 3-dimensional carbon/carbon composite", <i>J. Biomed. Mater. Res.</i> 1998 , 40, 520-529.
17	D. Bakos, M. Soldan, I. Hernandez-Fuentes " Hydroxyapatite-collagen-hyaluronic acid composite", <i>Biomaterials</i> 1999 , 20, 191-195.
18	S.J. Peter, S.T. Miller, G. Zhu, A.W. Yasko, A.G. Mikos "In vivo degradation of a poly(propylene fumarate)/β-tricalcium phosphate injectable composite scaffold", <i>J. Biomed. Mater. Res.</i> 1998 , 41, 1-7.
19	A. Ignatius, K. Unterricker, K. Wenger, M. Richter, L. Claes, P. Lohse, H. Hirst "A new composite made of polyurethane and glass ceramic in a loaded implant model: a biomechanical and histological analysis", <i>J. Mater. Sci.: Mater. Med.</i> 1997 , 8, 753-756.

¹¹ K.A. Hing, S.M. Best, K.E. Tanner, W. Bonfield, P.A. Revell "Biomechanical assessment of bone ingrowth in porous hydroxyapatite", *J. Mater. Sci.: Mater. Med.* **1997**, 8, 731-736.

¹² S. Yamada, D. Heymann, J.-M. Bouler, G. Daculsi "Osteoclastic resorption of calcium phosphate ceramics with different hydroxyapatite/β-tricalcium phosphate ratios", *Biomaterials* **1997**, 18, 1037-1041.

20	N. Ignjatovic, S. Tomic, M. Dakic, M. Miljkovic, M. Plavsic, D. Uskokovic "Synthesis and properties of hydroxyapatite/poly-L-lactide composite biomaterials", <i>Biomaterials</i> 1998 , <i>20</i> , 809-816.
21	J.T. Heikkilä, A.J. Aho, I. Kangasniemi, A. Yli-Urpo "Polymethylmethacrylate composites: disturbed bone formation at the surface of bioactive glass and hydroxyapatite ", <i>Biomaterials</i> 1996 , <i>17</i> , 1755-1760.
22	L.-S. Liu, A. Y. Thompson, M. A. Heidarani, J.W.Poser, R.C. Spiro "An osteoconductive collagen/hyaluronate matrix for bone regeneration", <i>Biomaterials</i> 1999 , <i>20</i> , 1097-1108.
23	N. Sasaki, H. Umeda, S. Okada, R. Kojima, A. Fukuda "Mechanical properties of hydroxyapatite-reinforced gelatin as a model system of bone", <i>Biomaterials</i> 1989 , <i>10</i> , 129-132.
24	Y. Doi, T. Horiguchi, Y. Moriwaki, H. Kitago, T. Kajimoto, Y. Twayama "Formation of apatite-collagen complexes", <i>J. Biomed. Mater. Res.</i> 1996 , <i>31</i> , 43-49.
25	K.S. TenHuisen, P.W. Brown "The formation of hydroxyapatite-gelatin composites at 38°C", <i>J. Biomed. Mater. Res.</i> 1994 , <i>28</i> , 27-33.
26	A.C.A. Wan, E. Khor, G.W. Hastings "Preparation of a chitin-apatite composite by <i>in situ</i> precipitation onto porous chitin scaffolds", <i>J. Biomed. Mater. Res.</i> 1998 , <i>41</i> , 541-548.
27	J. Suwanprateeb, K.E. Tanner, S. Turner, W. Bonfield "Influence of sterilization by gamma irradiation and thermal annealing on creep of hydroxyapatite-reinforced polyethylene composites", <i>J. Biomed. Mater. Res.</i> 1998 , <i>39</i> , 16-22.
28	Y. Shikinami, M. Okuno "Bioresorbable devices made of forged composites of hydroxyapatite (HA) particles and poly-L-lactide (PLLA): Part I. Basic characteristics", <i>Biomaterials</i> 1999 , <i>20</i> , 859-877.

The growth, maintenance and adaptation of bone is mediated and executed by cells. The interplay of signal targeting and transduction, proliferation and differentiation is influenced by the spatial relative location of the cells itself as well as by the adherence to a scaffolding matrix²⁹. In bone, this task is fulfilled by the extracellular matrix (ECM), consisting mainly of collagen type I and several non-collagenous matrix molecules³⁰. Such a guiding host matrix is lacking pure calcium phosphate implants. Poly(α -hydroxy acids) are well established polymers in tissue engineering to allow cell adherence³¹ and retention of the differentiated phenotype, dynamic migration³², and

²⁹ M. Kantlehner, P. Schaffner, D. Finsinger, J. Meyer, A. Jonczyk, B. Diefenbach, B. Nies, G. Hölzemann, S.L. Goodman, H. Kessler "Surface coating with cyclic RGD peptides stimulates osteoblast adhesion and proliferation as well as bone formation", *Chem. Biochem.* **2000**, *1*, 107-114.

³⁰ Y. Ayukawa, F. Takeshita, T. Inoue, M. Yoshinari, M. Shimono, T. Suetsugu, T. Tanaka "An immunoelectron microscopic localization of noncollagenous bone proteins (osteocalcin and osteopontin) at the bone-titanium interface of rat tibiae", *J. Biomed. Mater. Res.* **1998**, *41*, 111-119.

³¹ A.G. Mikos, Y. Bao, L.G. Cima, D.E. Ingber, J.P. Vacanti, R. Langer "Preparation of poly(glycolic acid) bonded fiber structures for cell attachment and transplantation", *J. Biomed. Mater. Res.* **1993**, *27*, 183-189.

formation of three-dimensional cell/polymer constructs with biogenic ability³³. From that point of view, composites with polyesters represent an improvement of biocompatibility of calcium phosphates.

A prerequisite to express osteoinductive potential and to enable a three-dimensional remodeling process is an appropriate porosity. Cancellous bone has an interconnected pore system that allows cell migration and blood vessel ingrowth. Therefore implant development should aim to incorporate a porous network into the bulk material. The effects of surface structure and porosity on cell behavior are manifold and controversially discussed³⁴. However, pore diameters of 100-300 μm were shown to be optimal for the growth of bone³⁵.

The present chapter addresses the fabrication of PGA/calcium phosphate bodies. The composition of the composites is optimized for the external pH-value in aqueous solutions to avoid the problems associated with a non-physiological pH as discussed in chapter AII. Optimized composite bodies were subjected to a biocompatibility test with cell seeding murine osteoblasts over a period of four weeks. Cell proliferation and activity were characterized with diverse methods. The retrieved bodies were analyzed with SEM and XRD for morphological and crystallographic changes during incubation. Finally, two different approaches for an introduction of macroporosity are presented.

³² S. L. Ishaug, R. G. Payne, M.J. Yaszemski, T.B. Aufdemorte, R. Bizios, A.G. Mikos "Osteoblast migration on poly(α -hydroxy esters)", *Biotechnol. Bioeng.* **1996**, 50, 443-451.

³³ S.L. Ishaug, G.M. Crane, M.J. Miller, A.W. Yasko, M.J. Yaszemski, A.G. Mikos "Bone formation by three-dimensional stromal osteoblast culture in biodegradable polymer scaffolds", *J. Biomed. Mater. Res.* **1997**, 36, 17-28.

³⁴ R.G. Flemming, C.J. Murphy, G.A. Abrams, S.L. Goodman, P.F. Nealey "Effects of synthetic micro- and nano-structured surfaces on cell behavior", *Biomaterials* **1999**, 20, 573-588.

³⁵ R. Kuijjer, S.J.M. Bouwmeester, M.M.W.E. Drees, D.A.M. Surtel, E.A.W. Terwindt-Rouwenhorst, A.J. van der Linden, C.A. van Blitterwijk, S.K. Bulstra "The polymer PolyactiveTM as a bone-filling substance: an experimental study in rabbits", *J. Mater. Sci.; Mater. Med.* **1998**, 9, 449-455.

B.1 Results and discussion

Fabrication of composite bodies with calcium phosphate

Composite bodies were generally fabricated by mixing PGA from solid-state polycondensation (with and without included NaCl to produce compact or porous bodies after wash-out) with calcium phosphates in various mass ratios. The mixtures were compacted to pellets either by pressing at room temperature with a conventional IR-pellet press or at higher temperatures employing a melt-press. Designated compact samples were washed out prior to further processing, porous samples were washed out after the pressing step with NaCl included. Two different composite series were carried out with two different CaP phases.

In a first series HAP (for bioceramics) from Merck Biomaterials was used in various ratios to evaluate the external pH generated by the composites and the buffering capacity of this HAP with medium crystallinity (see **fig.B.0-1**).

The second series was carried out with a carbonated, low-crystalline apatite that was synthesized in the working-group to mimic bone mineral. The synthesis and the optimization process were carried out by Fabian Peters³⁶. The aim was to provide an amorphous calcium phosphate phase that exhibits all associated positive attributes, especially a high solubility (resorbability) and an excellent biocompatibility^{37,38,39}.

Bodies obtained from conventional pressing proved to be stable enough to be handled and stored. The conditions for melt-pressing (pressure, temperature, time) were optimized with respect to stability. For that purpose, the obtained pellets were fractured by hand. According to subjective stability impressions, conditions were varied to achieve the highest fracture stability. A pressure of 10 kN for 3 min at 150°C gave the most stable composite bodies.

³⁶ F. Peters, PhD thesis "Biologische Kristallisation von Calciumphosphaten - Untersuchung und Simulation", **2001**.

³⁷ A.S. Posner, F. Betts "Synthetic amorphous calcium phosphate and its relation to bone mineral structure", *Acc. Chem. Res.* **1975**, *8*, 273-281.

³⁸ B.R. Constantz, I.C. Ison, M.T. Fulmer, R.D. Poser, S.T. Smith, M. van Wagoner, J. Ross, S.A. Goldstein, J.B. Jupiter, D.I. Rosenthal "Skeletal repair by in situ formation of the mineral phase of bone", *Science* **1995**, *267*, 1796-1799.

³⁹ J. Barrelet, S. Best, W. Bonfield "Carbonate substitution in precipitated hydroxyapatite: An investigation into the effects of reaction temperature and bicarbonate concentration", *J. Biomed. Mater. Res.* **1998**, *41*, 79-86.

Adjustment of external pH-value of composite bodies

The pH-value generated by a material *in vivo* during implantation time plays a decisive role for the implant biocompatibility and the prospect of a successful healing process^{40,41}. The buffer systems of the human body provide stable pH-values at specific sites and compartments to ensure undisturbed cell biology and function⁶. Material integration, tissue and blood-vessel ingrowth and an active remodeling process as the ultimate goal strongly depend on vital cell activity at the implantation site. Therefore, a physiological pH in the range of 7.4 ± 0.2 should be achieved and maintained for the external pH of a degrading material. It can be deduced that at least the buffering capacity of surrounding body-fluid should not be exceeded. Although Martin et al.⁴² reported only a slight lowering of 0.2 pH units for degrading poly(DL-lactide-co-glycolide) in a tibial bone chamber and judged this drop as physiologically insignificant, other working-groups reported a decrease in cell proliferation⁴⁰, local production of cell-toxic solutions⁴¹, induction of inflammatory mononuclear cell migration⁴³ or encapsulation by fibrous tissue⁴⁴.

Agrawal et al.⁴⁵ combined PLA/PGA copolymers with three incorporated basic salts to compensate the decrease in pH in a degradation study in water over a period of 9 weeks (the pH of the control with pure polymer dropped to 3.0 after 9 weeks):

- calcium carbonate (42 wt%): pH drop from 7.4 to 6.3
- hydroxyapatite (44 wt%): pH drop from 6.9 to 4.3
- sodium bicarbonate (NaHCO₃) (35 wt%): pH drop from 8.2 to 4.5

The study concluded that the incorporation of basic salts can avoid a significant decrease of pH in the vicinity of degrading PLA/PGA copolymers. It has to be

⁴⁰ K.A. Athanasiou, G.G. Niederauer, C.M. Agrawal "Sterilization, toxicity, biocompatibility and clinical applications of polylactic acid/polyglycolic acid copolymers", *Biomaterials* **1996**, *17*, 93-102.

⁴¹ A.G. Mikos, G. Sarakinos, S.M. Leite, J.P. Vacanti, R. Langer "Laminated three-dimensional biodegradable foams for use in tissue engineering", *Biomaterials* **1993**, *14*, 323-330.

⁴² C. Martin, H. Winet, J.Y. Bao "Acidity near eroding polylactide-polyglycolide *in vitro* and *in vivo* in rabbit tibial bone chambers", *Biomaterials* **1996**, *17*, 2373-2380.

⁴³ S. Santavirta, Y.T. Konttinen, T. Saito, M. Grönblad, E. Partio, P. Kempainen, P. Rokkanen "Immune response to polyglycolic acid implants", *J. Bone Joint Sur.* **1990**, *72B*, 597-600.

⁴⁴ M. van der Elst, C.P.A.T. Klein, J.M. de Blicke-Hogervorst, P. Patka, H.J.T.M. Haarman "Bone tissue response to biodegradable polymers used for intra medullary fracture fixation: A long-term *in vivo* study in sheep femora", *Biomaterials* **1999**, *20*, 121-128.

⁴⁵ C.M. Agrawal, K.A. Athanasiou "Technique to control pH in vicinity of biodegrading PLA-PGA implants", *J. Biomed. Mater. Res. (Appl. Biomater.)* **1997**, *38*, 105-114.

commented that the chosen strategy appears to be a good idea, but that the resulting conditions would certainly lead to cell death in all examined cases.

In a first series, composites of PGA and HAP were fabricated (see materials and

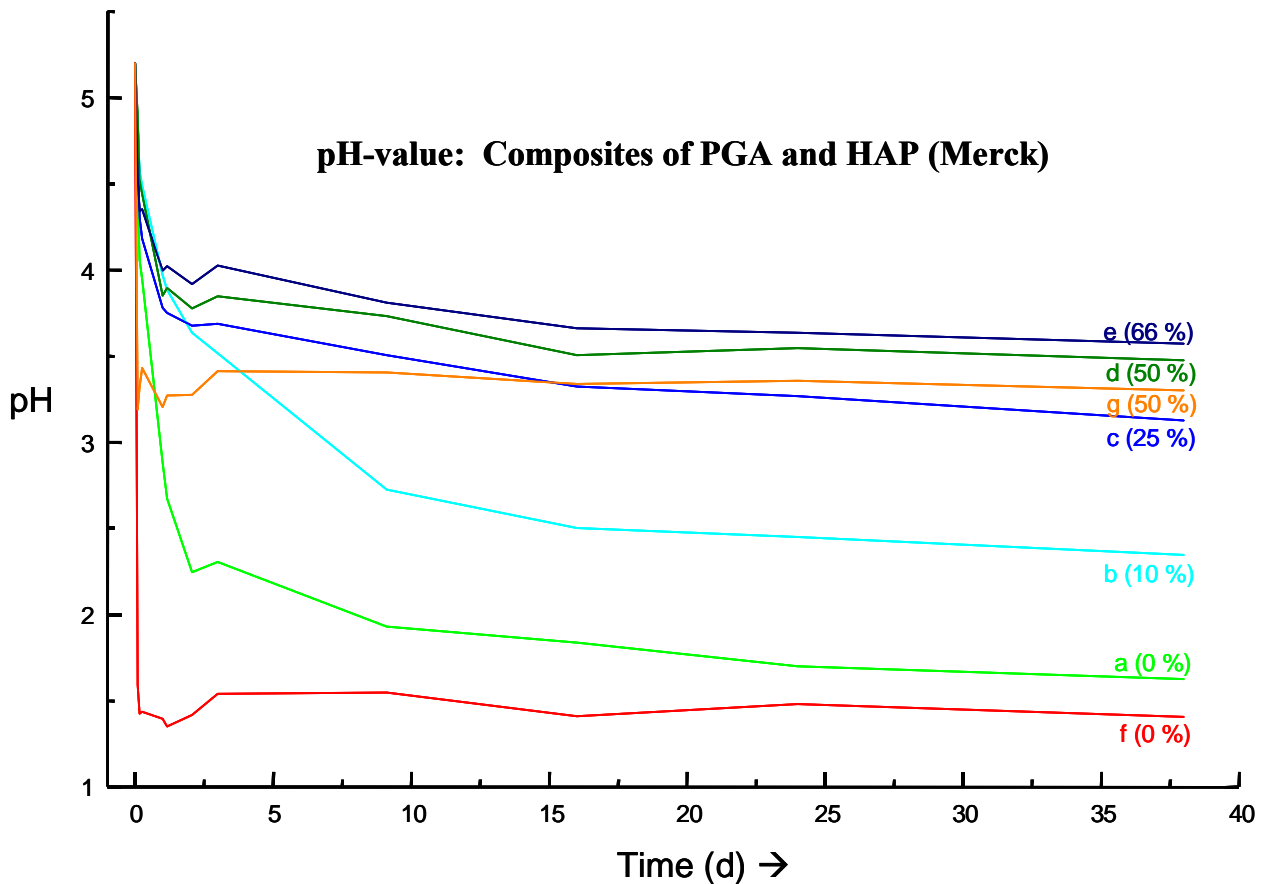


Fig.B.1-1 pH-development of water-incubated polymer samples and composites of PGA with HAP monitored over 38 days. a (PGA from solid-state reaction), b (10wt% HAP), c (25 wt%), d (50 wt%), e (66 wt%). The samples f and g were fabricated from commercially available PGA from Aldrich. f (0 wt% HAP), g (50 wt%).

methods) and subjected to incubation in water. The pH-value was measured over a period of 38 days. Porous pellets were fabricated with the following mass ratios of PGA and HAP for the washed-out bodies: **a** (0% HAP), **b** (10%), **c** (25%), **d** (50%), **e** (66%). For comparison, two samples were produced with commercially available PGA from Aldrich: **f** (0% HAP), **g** (50%).

Fig. B.1-1 shows the results of the pH-measurements for the water-incubated samples at 37°C. All samples show a rapid decrease of pH shortly after incubation ("acidic burst"). The pure polymer samples decrease to values below 2. The commercial PGA reaches a value of 1.5 within an hour and stays relatively constant for the whole period, the solid-state chemically prepared PGA decreases exponentially to a final value of about 1.7 after 38 days. The polymer samples show the expected behavior of

a strongly acidic reaction. The stronger and faster reaction of the commercial polymer is surprising if we consider the longer chains, a compact bulk structure and less endgroups.

The acidic burst at the beginning is ascribed to deprotonation of acid endgroups that may have formed by partial hydrolysis of the carboxylate groups. Surface reaction and mobilization of soluble oligomers can contribute to the observed decrease as well.

The addition of HAP to the degrading polymers clearly shows a buffering effect. The resulting values are shifted to higher values with increasing HAP content. With 66 wt% HAP incorporated, the pH still goes down to 3.8. Comparison of the two polymers of different origin with 50 wt% HAP shows the same results as for the pure compounds. The commercial PGA is slightly more acidic. The obtained values are in good agreement with the results reported by Agrawal et al.⁴⁵ (44 wt% HAP, pH = 4.3 after 63 days for degrading PLA/PGA (50:50) copolymer in water), keeping in mind that polyglycolide degrades much faster than polylactide and that PGA chains are intrinsically more acidic. Both studies clearly indicate that HAP is not capable to stabilize the pH in a physiological range in composite with degrading PGA/PLA polymers. The degradation of the polymer is, from a kinetic point of view, the dominating factor over the basic dissolution of the apatite. A compensation in the physiological range requires a more soluble, more basic calcium phosphate.

Carbonated apatite (CACP, B-type)⁴⁶ was prepared by fast precipitation from aqueous solution by mixing a solution of $\text{NH}_4\text{H}_2\text{PO}_4$ and K_2CO_3 with a solution of $\text{Ca}(\text{NO}_3)_2$ (see materials and methods). The amount of the incorporated carbonate is a function of the initial ratio of Ca and phosphate in the precipitation medium³⁶. The precipitate obtained is an X-ray amorphous carbonated apatite that is similar to the mineral in bone in structure and carbonate content^{37,38,39}. The CACP used was precipitated from a solution with carbonate in 20-fold excess over Ca concentration. Reflections of calcium carbonate were not detected in XRD analysis.

Composite pellets were fabricated in compact and porous form. Compact pellets were prepared by thoroughly mixing and grinding water-washed polyglycolide (i.e. without NaCl) with carbonated apatite in the w:w ratio 150 mg:60 mg (28.6 wt% CACP).

⁴⁶ J.C. Elliott "Structure and chemistry of the apatites and other calcium orthophosphates", in *Studies in inorganic chemistry*, 18, Elsevier, Amsterdam, London, New York, Tokyo, 1994.

Taking into account the release of 18.5 wt% water from the apatite phase during melt-pressing, the actual weight ratio of polyglycolide to apatite was 150 mg:49 mg (24.6 wt% CACP). Porous pellets were prepared by mixing untreated polyglycolide (i.e. with NaCl still in the pores) with carbonated apatite in the weight ratio (polyglycolide+NaCl):carbonated apatite 300 mg:60 mg. After melt-pressing the tablets were washed with cold water (8°C) for 4 h to remove NaCl (150 mg). This left a microporous composite with an actual weight ratio of polyglycolide to apatite of 150 mg:49 mg.

Fig.B.1-2 displays the pH-values monitored for the two components alone and as porous and compact composites in deionized water at 37°C. PGA shows the expected

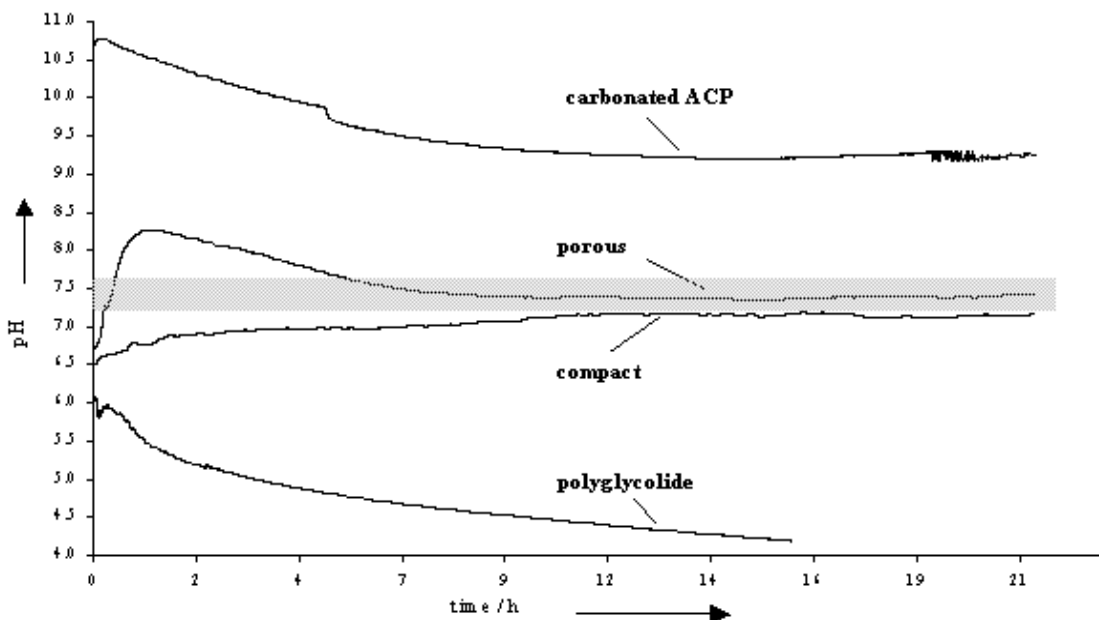


Fig.B.1-2 Monitoring of pH-value in unbuffered deionized water at 37°C for PGA, carbonated apatite and composites of the two components (porous and compact pellets) over a period of 21 hours. The physiological pH range (7.4 ± 0.2) is highlighted in gray.

decrease in pH, carbonated apatite reacts basic. The values for composite bodies lie in the range 6.5 to 8.3. After 12 hours, the pH is in the physiological range. The porous bodies show an initially alkaline pH, due to a large surface exposition of CACP to water, referred to the porous structure. The compact bodies exhibit a lower pH presumably due to a significantly smaller apatite/water interface during the first hours of incubation. It was concluded from these experiments that the fabricated composites are well suitable to maintain a physiological pH at a potential implantation site, at least

for an initial period. Note that the test medium was pure water without buffering constituents. The composites were immersed in water prior to cell contact to remove possible degradation products from melt-pressing, to avoid the negative implications of a non-physiological pH at the beginning and to allow a stable equilibrium.

Testing for biocompatibility with murine osteoblasts

To analyze the biocompatibility of the optimized composites, samples were incubated with murine calvarial osteoblasts in carbonate buffered α -MEM medium under

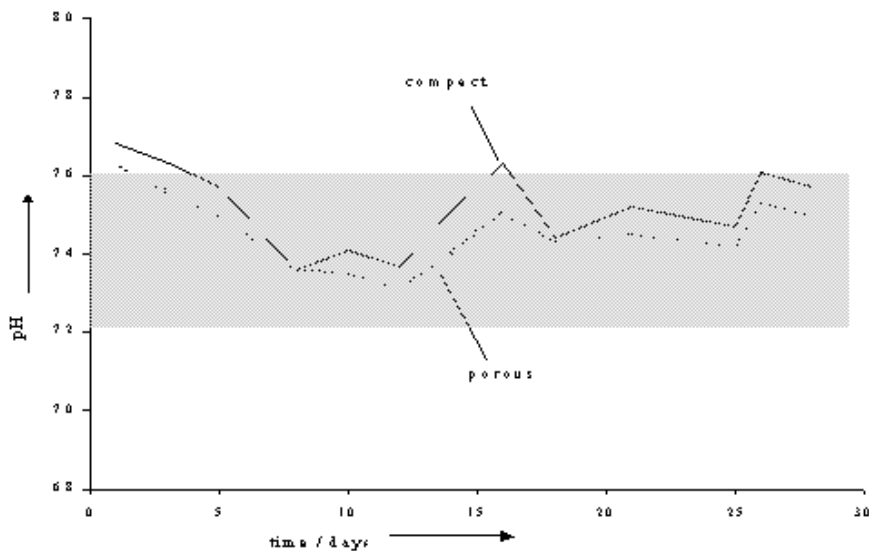


Fig.B.1-3 Monitoring of solution pH during cell culture experiments in α -MEM of the PGA-CACP composites. Medium was changed every other day. The pH is kept in the physiological range during the whole incubation period.

standardized culture conditions⁴⁷. Cell culture and staining experiments were carried out at the Department of Trauma Surgery, Hamburg University School of Medicine. The pH of the medium was recorded throughout the entire culture period of 4 weeks. The results of the water incubation were confirmed for buffered α -MEM medium. The pH is kept within the physiological range (**fig.B.1-3**) for the duration of the experiment. The adjustment of the external pH-value can be regarded as successful for the requirement of a physiological pH in a biomimetic medium.

Both types of pellets were immersed in pure water for 60 min before cell-seeding to

remove possible degradation products from melt-pressing, and to avoid the initial acidic or alkaline burst (**fig.B.1-2**). They were subsequently sterilized with pure ethanol and rinsed with sterile water.

Cell proliferation, activity and phenotype were characterized with established staining techniques. Undisturbed cell adhesion and proliferation until confluence were observed. The results of histobiochemical analysis are summarized in **fig.B.1-4**. Cells maintain their osteoblastic differentiation as determined by analysis of alkaline phosphatase and collagen expression as well as their ability to form mineralized nodules. The cells express alkaline phosphatase (B) as one of the marker molecules of osteoblast differentiation. Van Gieson stain (C and D) confirmed the formation of a dense, homogeneous collagen layer. The phenotype of osteoblasts was further determined by immunolabelling (E) for osteocalcin (green) and actin (red). Osteocalcin expression is currently regarded as the most specific marker for osteoblast phenotype. Cellular mineralization^{48,49} of the collagen matrix (nodule formation) is indicated by von Kossa (F) stain. CaP deposits are stained black.

Fig.B.1-5 presents a side-view on porous stained samples cut to 5 µm thick sections. A multilayer of cells on the surface is highlighted by van Gieson stain indicative for collagen. The thick cell layer is a direct proof for the biocompatibility of the composite material. The figure documents the heterogeneous nature of the pellet as well. CaP grains appear black in a von Kossa stain. The Toluidine blue stain (B) contrasts the cell layer in a light blue color.

In addition to the histological evaluation, recovered samples were dried with the critical point technique, sputtered with gold and subjected to SEM analysis. The SEM micrographs of porous and compact pellets from culture are displayed in **fig.B.1-6**. Picture A shows the covering cell layer partly detached from the composite surface. The micrograph shows a dense, continuous layer that is located on the surface of the sample only. Bundles of aligned collagen are visible in B. The pictures C and D allow

⁴⁷ W. Linhart, F. Peters, W. Lehmann, K. Schwarz, A.F. Schilling, M. Amling, J.M. Rueger, M. Epple "Biologically and chemically optimized composites of carbonated apatite and polyglycolide as bone substitution materials", *J. Biomed. Mater. Res.* **2001**, *54*, 162-171.

⁴⁸ M. Ahmad, M.B. McCarthy, G. Gronowicz "An in vitro model for mineralization of human osteoblast-like cells on implant materials", *Biomaterials* **1999**, *20*, 211-220.

⁴⁹ M.W. Squire, J.L. Ricci, R. Bizios "Analysis of osteoblast mineral deposits on orthopaedic/dental implant metals", *Biomaterials* **1996**, *17*, 725-733.

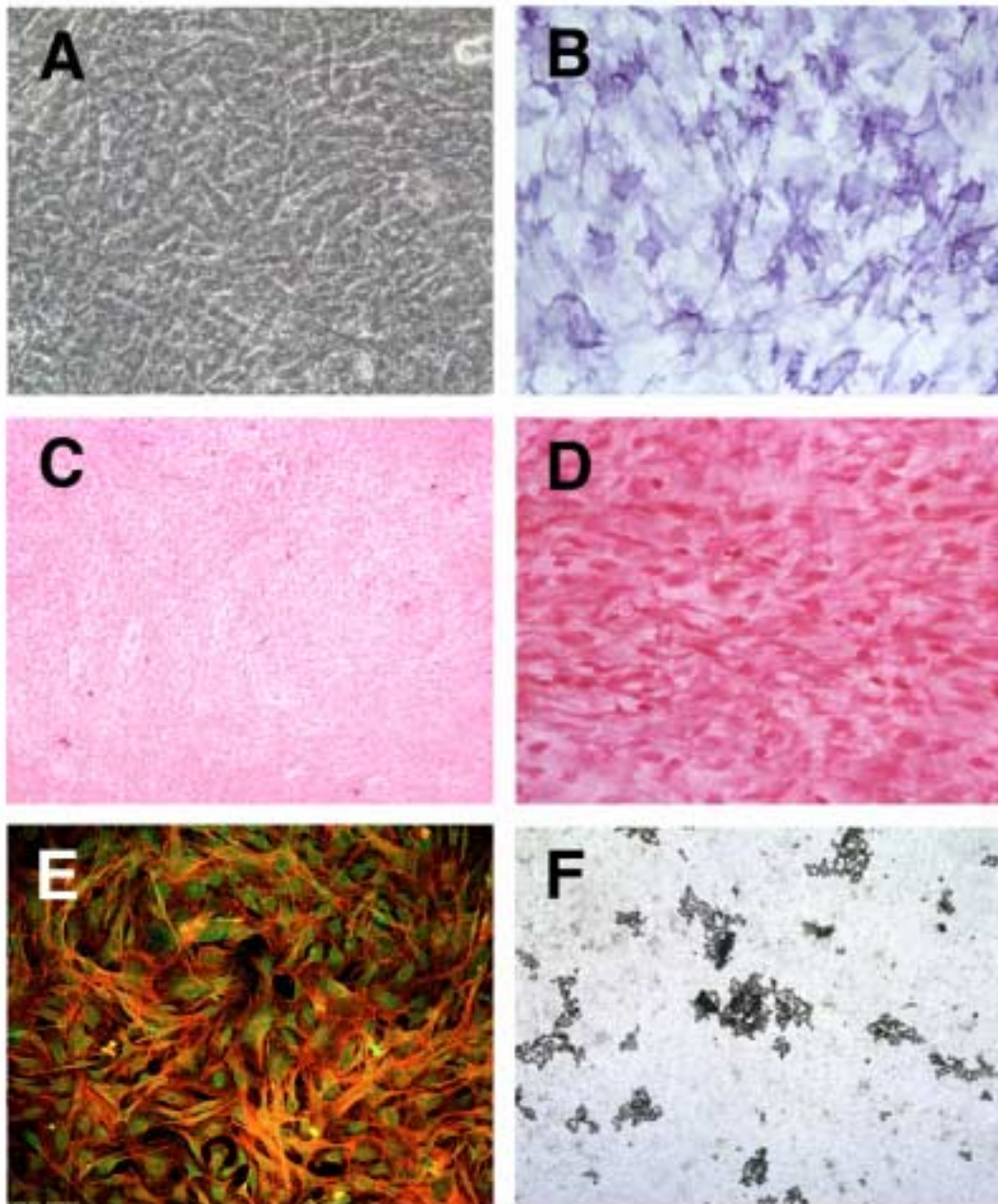


Fig.B.1-4 Characterization of osteoblasts maintained in culture for 4 weeks. (A) Confluent layer of osteoblasts (unstained, orig. magn. x100, 4 weeks). (B) High magn. (x200) of cells stained for alkaline phosphatase. (C) van Gieson staining for collagen (orig. magn. x100, 2 weeks). (D) Higher magn. of van Gieson staining (orig. magn. x100, 2 weeks). (E) Immunolabelling for osteocalcin (green) and actin (red) (confocal laser microscopy, orig. magn. x200, 2 weeks). (F) Von Kossa stain for calcium phosphate (mineralized bone matrix, black, orig. magn. x100, 4 weeks).

a closer look on the morphology of single osteoblasts anchored to the collagen matrix. Outstretched cells are visible with filopodia and numerous cell extensions interwoven with the matrix. The impressions from SEM analysis complement the data from histological characterization.

In a control experiment, pure porous polyglycolide pellets underwent the same procedure with respect to pH-monitoring (for 48 h) and cell seeding. The pH was in

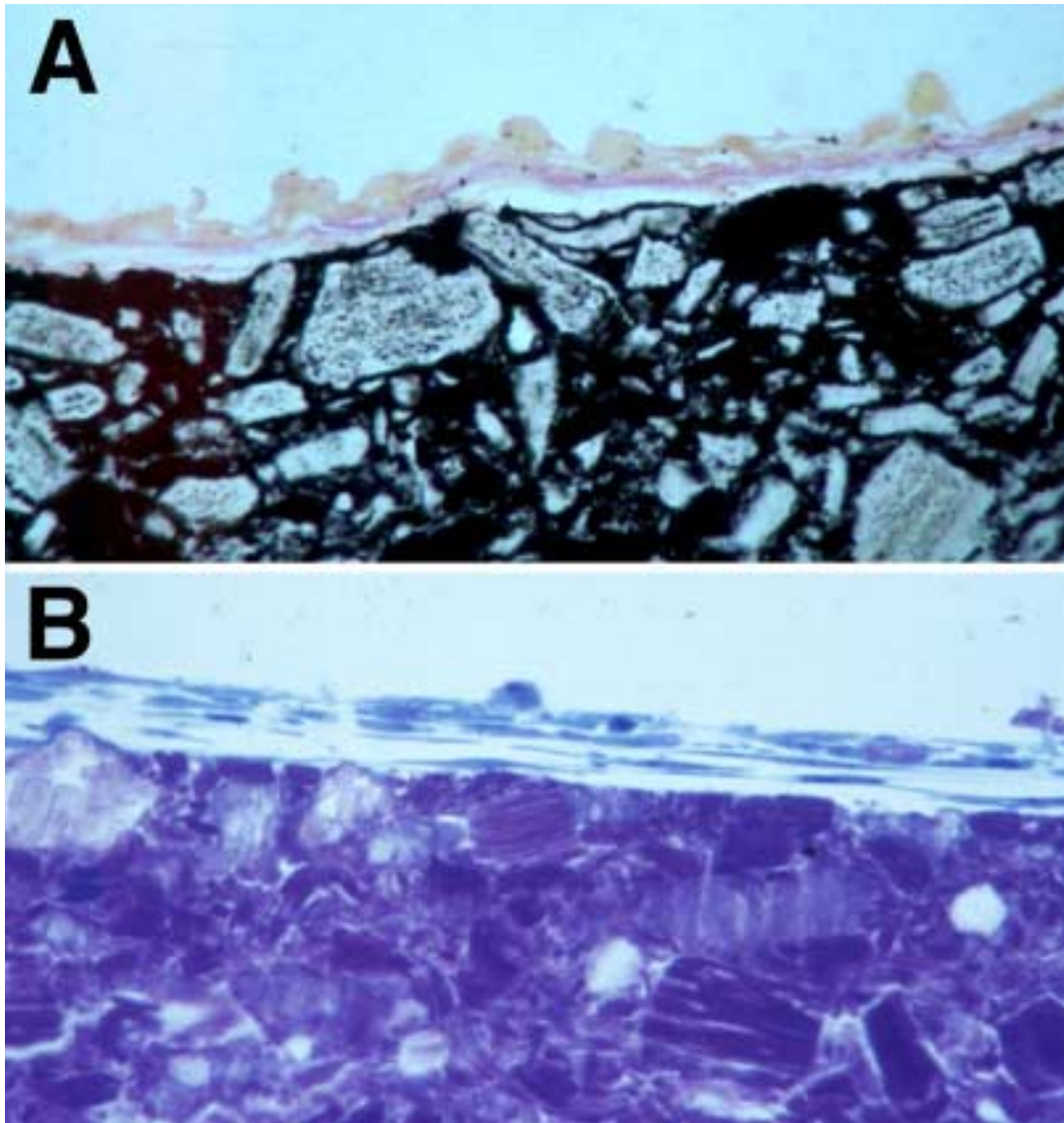


Fig.B.1-5 Undecalcified histology on porous pellets after 4 weeks. (A) von Kossa stain counterstained by van Gieson for appreciation of the cell layer. The heterogeneous texture of the composite is clearly visible (CaP appears black). (B) Toluidine blue stain. (orig. magn. A,B x400)

the range from 6.2 to 7. Cells did not form a confluent layer. Morphological changes (e.g., intracellular vacuoles, globular shape) indicated progressive cell death and detachment from the polymer substrate.

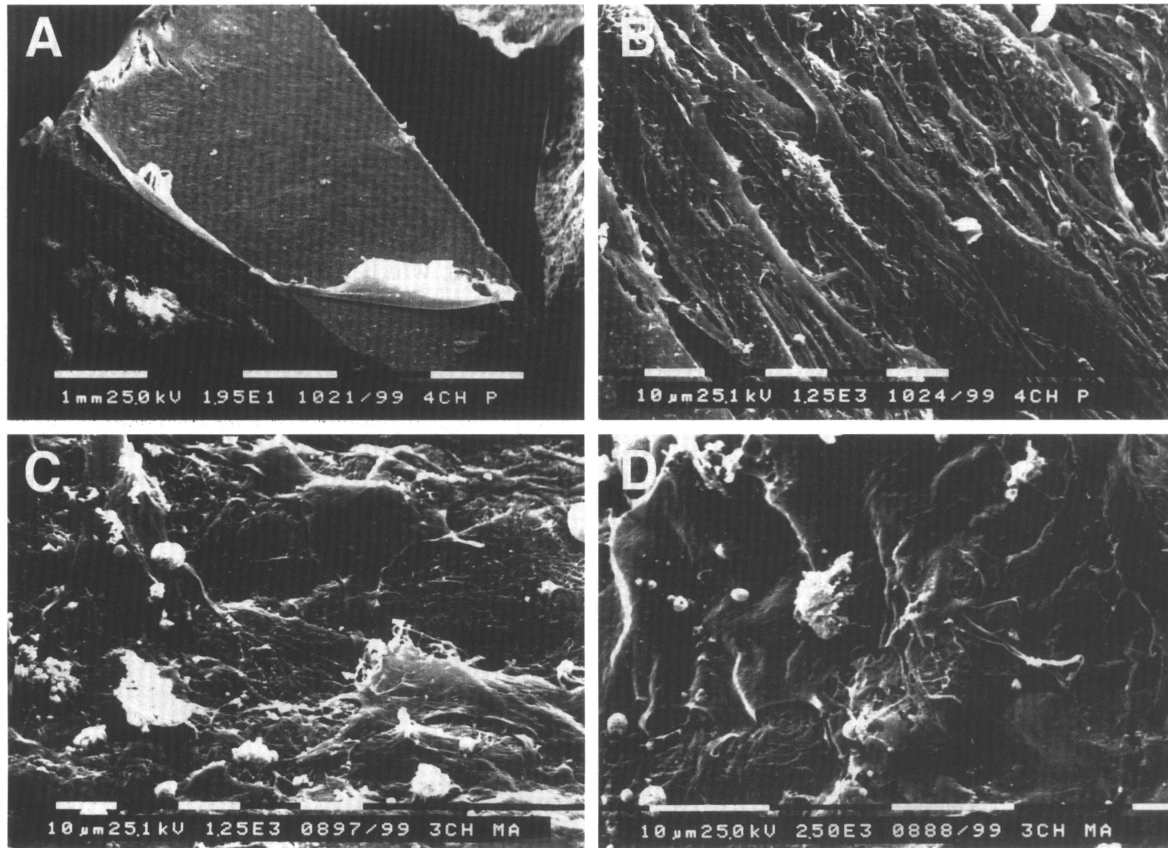


Fig.B.1-6 Scanning electron micrograph of osteoblasts that grew on the composites. (A) Confluent layer of osteoblasts covering the surface of the implant. Cells are capable of attaching, proliferating, and producing bone matrix at the surface of the implants (porous pellet, 4 weeks, orig. magn. $\times 19.5$). (B) Confluent layer of cells forming a close cellular sheet (4 weeks, porous pellet, orig. magn. $\times 1250$). (C and D) Viable cells with filopodia on a dense matrix of collagen (compact pellet, 3 weeks, orig. magn. $\times 1250$ (C), $\times 2500$ (D)).

Pellets were removed from the cell medium for XRD analysis after 1,2,3 and 4 weeks to monitor crystalline transformations inside the composites. **Fig.B.1-7** shows the results in comparison with the initial carbonate apatite and synthetic apatite to give a reference for apatite reflex positions and an impression of the respective crystallinities. The XRD diagram of the carbonated apatite indicates a highly amorphous material, showing only a weak halo in the range 25 to $35^\circ 2\theta$ (the first amorphous halo corresponds to the sample-holder). The calcium phosphate shows a very low tendency to crystallize during the four weeks of exposition to aqueous nutrition medium. This is a surprising observation, bearing in mind the thermodynamic instability of the CACP

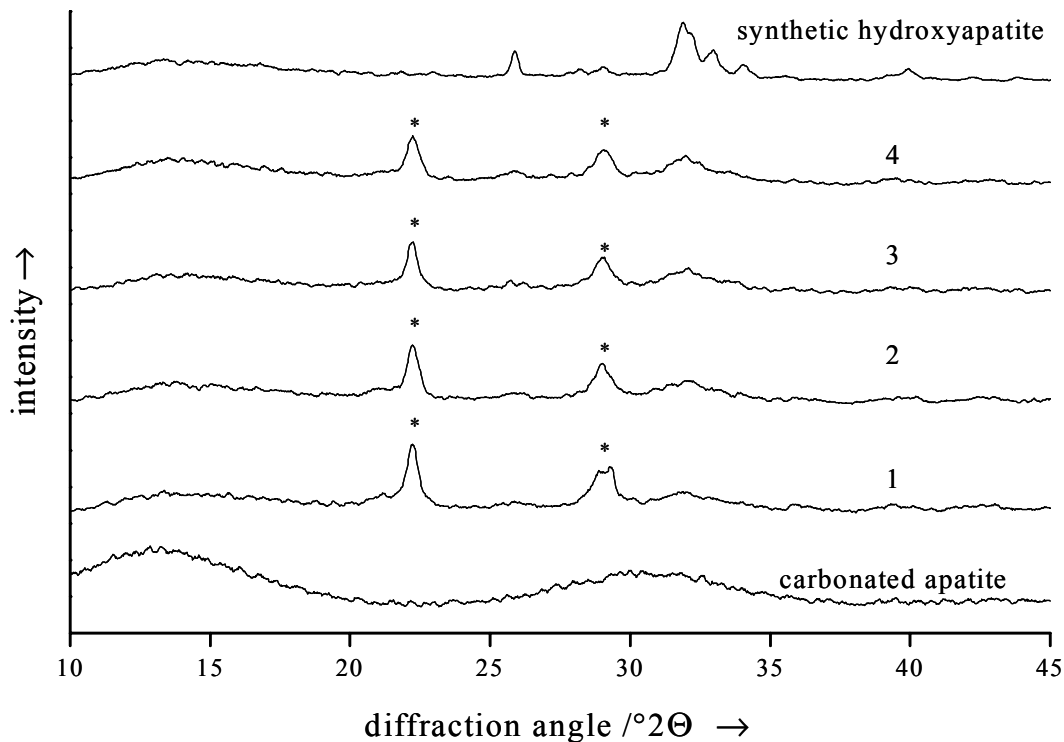


Fig.B.1-7 X-ray powder diffractometry of amorphous carbonated apatite (bottom) and of the incubated pellets after 1,2,3, and 4 weeks of immersion in cell nutrition medium (α -MEM) in the presence of osteoblasts. For comparison, synthetic hydroxyapatite (top) is shown. Reflections referring to polyglycolide are marked by asterisks (*). The crystallization of the CACP is significantly inhibited under the experimental conditions.

phase⁴⁶ that should cause a rapid crystallization at 37°C^{37,50,51}. Obviously, the intimate contact to PGA or medium components has an inhibiting effect on the crystallization process that stabilizes the CACP crystallites inside the composite. The phenomenon corroborates the biomimetic character of the developed composites. The kinetic inhibition of thermodynamically driven crystallization phenomena is one of nature's strategies in material functionalization to conserve and restore material properties^{52,53,54}.

⁵⁰ G. Williams, J.D. Sallis "Structural factors influencing the ability of compounds to inhibit hydroxyapatite formation", *Calcif. Tissue Int.* **1982**, 34, 169-177.

⁵¹ L. Chou, B. Marek, W.R. Wagner "Effects of hydroxylapatite coating crystallinity on biosolubility, cell attachment efficiency and proliferation in vitro", *Biomaterials* **1999**, 20, 977-985.

⁵² H.J. Höhling, S. Arnold, R.H. Backhaus, U. Plate, H.P. Wiesmann "Structural relationship between the primary crystal formations and the matrix macromolecules in different hard tissues. Discussion of a general principle", *Conn. Tissue Res.* **1995**, 33, 171-178.

⁵³ S. Weiner, L. Addadi "Design strategies in mineralized biological materials", *J. Mater. Chem.* **1997**, 7(5), 689-702.

Structuring of composite bodies

The SEM characterization of the pellets from cell culture in **fig.B.1-6** (A) is suitable to demonstrate the necessity of a macroporosity for composite implants. The cell layer is located on the surface of the material. The micropores of the porous polymer (sub-micron diameters) may provide a textured surface to promote cell adhesion⁵⁵, but they are by far too small to permit intrusion of medium with cells in the pre-confluent phase and the ingrowth of cells and tissue in later stages. Good examples for open structures with a porosity of up to 95% that allow complete wetting with cell medium are polyester foams⁵⁶. Injection of cells enables a homogeneous, three-dimensional distribution and adhesion to the scaffold.

Various processing techniques to create a porous structure are reviewed by Widmer and Mikos⁵⁷:

- Fiber bonding (partial thermal fusion of fibers leading to foams)
- Solvent-casting and particulate-leaching (inclusion of soluble particles, extraction)
- Melt molding, Extrusion
- Freeze-drying (CO₂ evaporation leads to hollow structures)
- Phase separation (solvent demixing leads to structured substrates)

The fact that the micropores of PGA from solid-state reaction can be generated by particulate-leaching of the included sub- μ m NaCl crystals in water suggests an extension of the principle to externally added NaCl of tunable grain sizes. The technique with spacers of different size is illustrated in **fig.B.1-8**.

In a test series⁵⁸ commercially available sodium chloride (average grain size \approx 300 μ m, approximated from SEM) was added to the precursor sodium chloroacetate before polymerization. The mass ratio precursor/external NaCl was 2:1, which equals the same mass and volume for micro- and macrocrystals. The polymerization mixture was

⁵⁴ A. Linde, A. Lussi, M.A. Crenshaw "Mineral induction by immobilized polyanionic proteins", *Calcif. Tissue Int.* **1989**, 44, 286-295.

⁵⁵ K. Matsuzaka, X.F. Walboomers, J.E. de Ruijter, J.A. Jansen "The effect of poly-L-lactic acid with parallel surface micro groove on osteoblast-like cells in vitro", *Biomaterials* **1999**, 20, 1293-1301.

⁵⁶ H.L. Wald, G. Sarakinos, M.D. Lyman, A.G. Mikos, J.P. Vacanti, R.Langer "Cell seeding in porous transplantation devices", *Biomaterials* **1993**, 14, 270-278.

⁵⁷ M. Widmer, A.G. Mikos "Fabrication of biodegradable polymer scaffolds for tissue engineering" in *Frontiers in tissue engineering*, Pergamon, Oxford, New York, Tokyo, **1998**, 107-120.

⁵⁸ K. Schwarz, M. Epple "Hierarchically structured polyglycolide - a biomaterial mimicking natural bone", *Macromol. Rapid Commun.* **1998**, 19, 613-617.

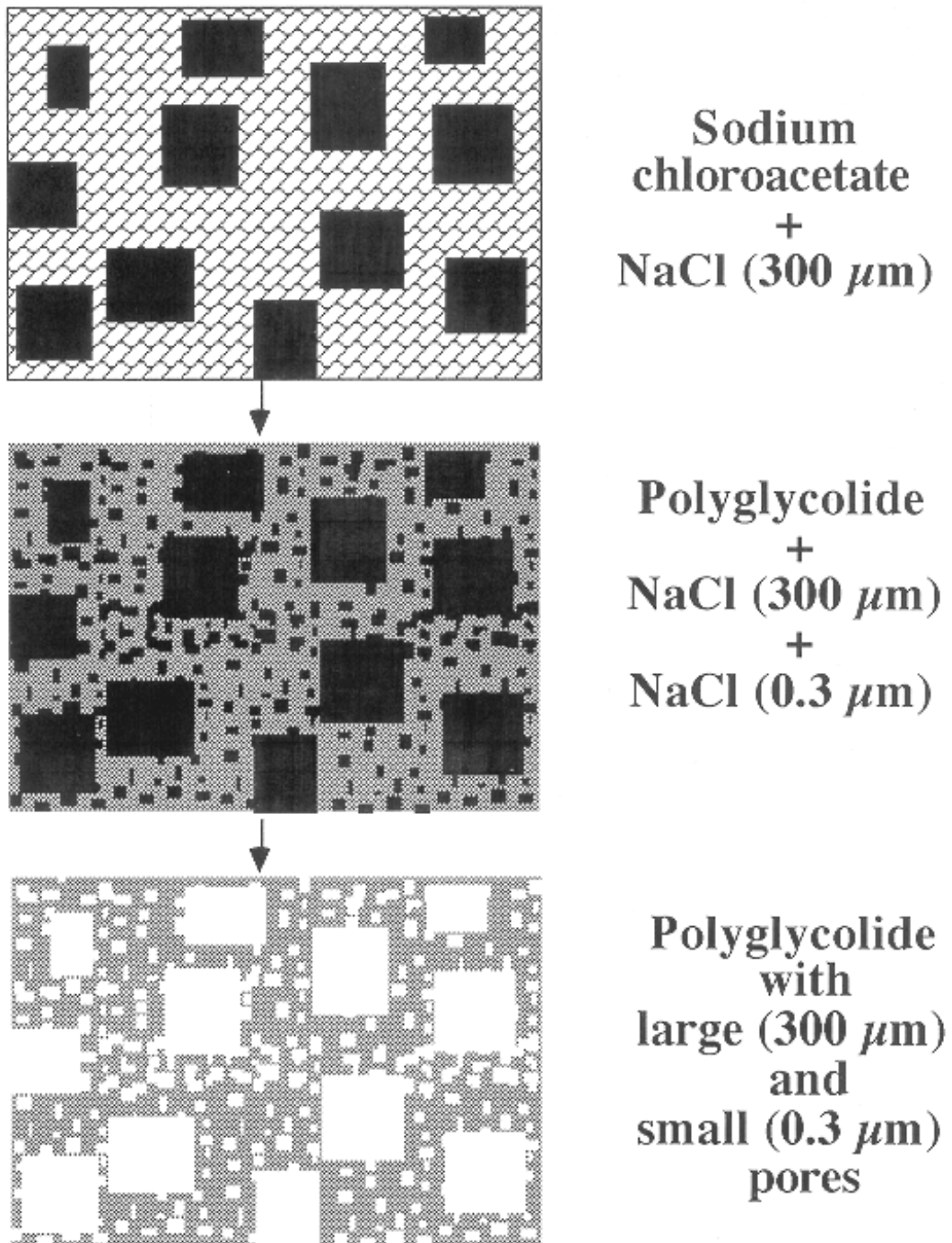


Fig.B.1-8 Schematic structuring of PGA with micro- and macropores

processed to pellets and washed out in cold water as described before. The obtained bodies were analyzed with SEM and compared to the natural structure of bovine spongiosa (**fig.B.1-9**). A certain similarity is obvious with respect to pore diameter and distribution. The natural original, however, possesses an interconnected pore system. This restriction to isolated cavities in the structured polymer is a logical consequence of the shape-isotropic nature of the porogen NaCl. This could only be avoided by very

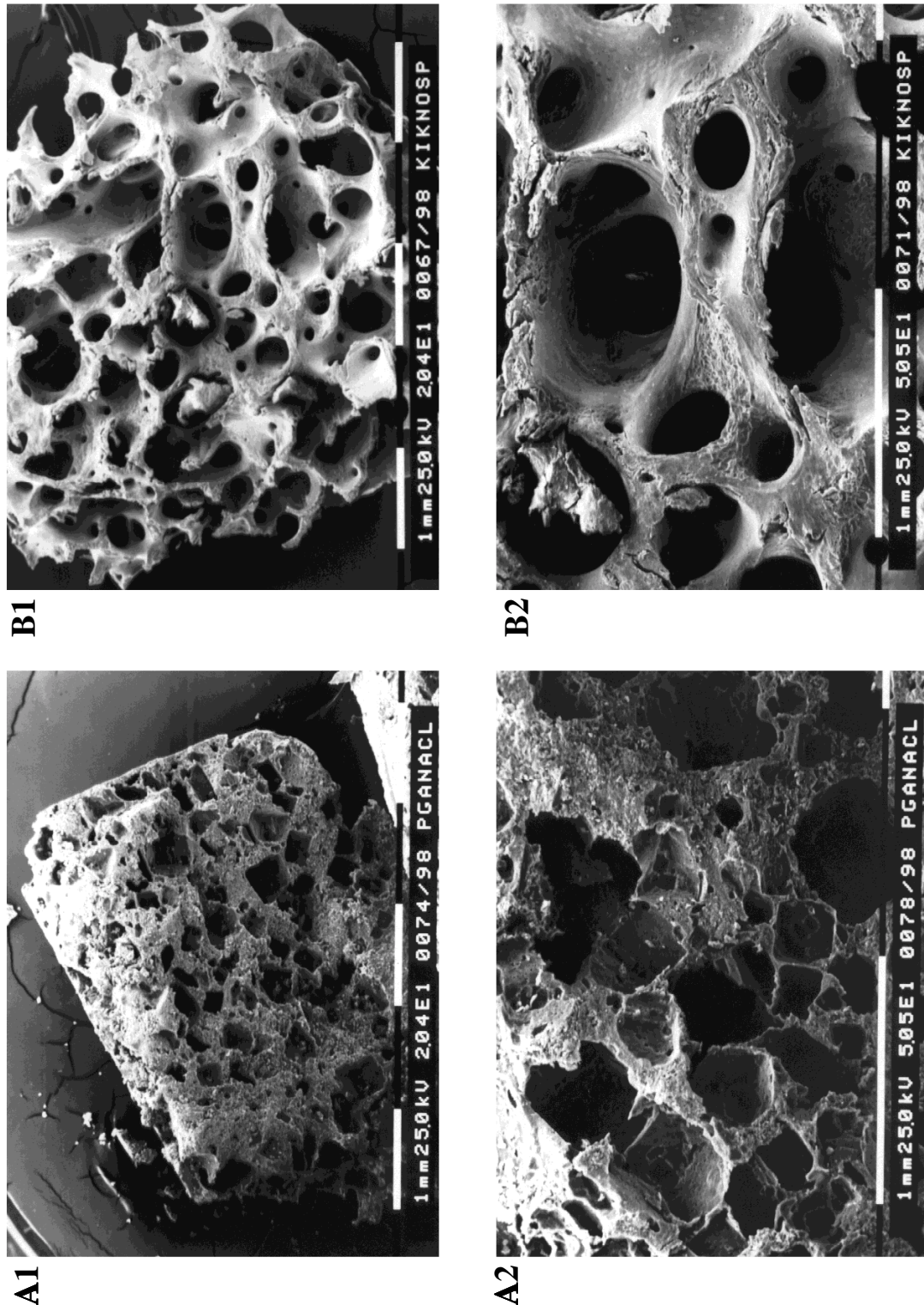


Fig.B.1-9 SEM micrographs of macroporous PGA (A1 and A2) after leaching of NaCl micro- and macrocrystals in comparison with bovine spongiosa (B1 and B2, “Kiel bone“). (magn.: A1 x20, A2 x50, B1 x20, B2 x50).

high loads of spacer crystallites to force the formation of cavity links on the expense of material stability. From this theoretical derivation, it was concluded to test an anisotropic, water-soluble fiber porogen with appropriate diameter. This strategy bears

the prospect of porous tubes and the option of a thermally-induced fiber bonding⁵⁹.

Fibers of polyvinylalcohol (PVA, "Kuralon K-II") were purchased from Kuraray and cut into pieces of 0.5 to 1.5 cm length. The diameter was ca. 100 μm (determined with SEM). DSC analysis revealed an weak endothermic melting signal (45 J g^{-1}) in the range 190 to 230°C indicating a nearly amorphous polymer.

The fibers (100 mg) were mixed with PGA (+NaCl, 300 mg) in a melt-press and compacted with a force of 10 kN for 5 min at 150°C. The temperature is not high enough for a partial liquefaction of the PVA, paying tribute to the thermal instability of PGA. The obtained samples were immersed in cold (4°C) water to remove both the NaCl and the PVA. **Fig.B.1-10** illustrates the results of the structuring attempt. The fibers are visible on the surface of the pellet (B). Contact with water, however, leads to

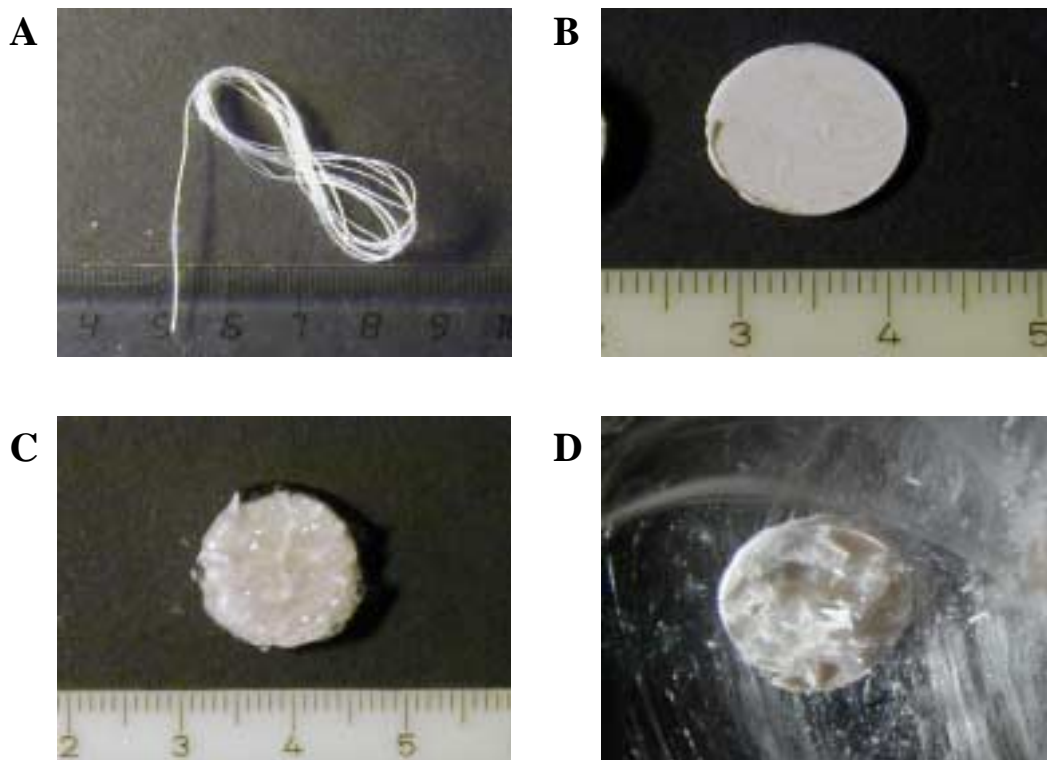


Fig.B.1-10 Structuring attempt with water-soluble PVA fibers (A). (B) Processed pellet with 25 wt% PVA. Fibers are outlined on the pellet surface. (C) Pellet after 1 hour in water. Swelling of PVA leads to gel formation around the pellet. (D) Fractured pellet after 12 hours immersion (placed on glass-wool).

swelling of the PVA and the formation of a gel-like layer around the pellet after one hour. Prolonged incubation and swelling result in a fractured pellet (D).

⁵⁹ A.G. Mikos, Y. Bao, L.G. Cima, D.E. Ingber, J.P. Vacanti, R. Langer "Preparation of poly(glycolic acid) bonded fiber structures for cell attachment and transplantation", *J. Biomed. Mater. Res.* **1993**, 27, 183-189.

The high swelling degree of the PVA leads to a progressing volume increase along the fibers from the ends that stick out of the pellet to the interior leading to cracks in the polymer pellet. It can be deduced from these results that a better fiber material should be water soluble with a lower swelling degree. Satisfying results were obtained with sugar crystals as porogen. The included sugar was washed out without a visible damage of the structured body. In conclusion, sugar fibers might be an ideal porogen to create a biomimetic porosity. Such a technique was published recently by Zhang and Ma⁶⁰.

B.2 Concluding remarks

Composites of polyglycolide from solid-state reaction and amorphous carbonated apatite were synthesized and processed to pellets as potential bone substitution materials with the following intentions concerning the composite properties:

- Polyglycolide allows cell attachment, migration and proliferation.
- The microporous structure enables an exchange of degradation products, thereby avoiding accumulation of acidic or harmful products. Supply with nutrients and oxygen is possible by diffusion through the porous network.
- The decrease in pH by degradation of the polyester is compensated by the basic calcium phosphate. The composites generate a sustainable physiological pH-value.
- The degradable character of the constituents should allow a replacement with new biogenic tissue.
- Carbonated apatite is similar to bone mineral in crystallite size, heterogeneity (carbonate content), crystallinity and solubility comprising the potential of a dynamic osteoclastic resorption.
- The intimate contact of polymer and CaP promotes an inhibitory stabilization of the apatite phase to prevent the conversion to a less active and higher crystalline hydroxyapatite.
- The material combination is expected to induce a cellular remodeling process.

An excellent biocompatibility was achieved and evidenced by cell culture experiments

⁶⁰ R. Zhang, P.X. Ma "Synthetic nano-fibrillar extracellular matrices with predesigned macroporous architectures", *J. Biomed. Mater. Res.* **2000**, 52, 430-438.

with murine osteoblasts. The cells shown a satisfying adhesion and proliferation on the composite material. They retained their osteoblastic phenotype throughout the culture experiment and express osteoblast-specific markers. Vital cell function was indicated by the formation of collagen multilayers and the subsequent formation of mineralized nodules.

Macropores were successfully incorporated into the composite material by particulate-leaching of externally added NaCl crystals. The introduction of an interconnected macroporous system failed with PVA fibers as an anisotropic porogen. Further optimization efforts are necessary to complement the biocompatibility of the composite materials with a biomimetic porosity and stability.

B.3 Materials and methods

Commercial PGA was purchased from Aldrich in the quality 99%+ and used as received. Hydroxyapatite (for bioceramics) was purchased from Merck in the quality 99%+. PVA fibers ("Kuralon KII", specification WN2) were obtained from Kuraray Co., LTD.

Polyglycolide

Porous polyglycolide was prepared by solid-state reaction from sodium chloroacetate as described in chapter **AI**.

Hydroxyapatite

HAP powder was ground in a mechanical mortar prior to use. The apatite was characterized by EA, IR and XRD.

EA: Ca: 37.92 % (theor. 39.89 % for stoichiometric hydroxyapatite $\text{Ca}_{10}(\text{PO}_4)_6(\text{OH})_2$), P: 17.75 % (theor. 18.50 %), O: 43.13 % (theor. 41.43 %), resulting Ca/P ratio 1.65 (theor. 1.67), IR (NaBr pellet): $\tilde{\nu}$ [cm^{-1}] = 3436 (m, O-H), 1417 (w, O-H), 1243, 1094, 1033 (s, PO_4), 963, 603, XRD ($\text{Cu K}_\alpha \lambda = 154.178 \text{ pm}$, Bragg-Brentano geometry): (main reflexes) diffraction angle [2θ] = 8.1, 10.6, 25.9, 31.8, 33.0, 34.1, 49.5.

Polyglycolide/hydroxyapatite composites

PGA (+NaCl), commercial PGA and HAP were previously ground in a mechanical mortar for 20 min. The powders were mixed to yield the following mass ratios after washing with cold water (4°C): 10 wt% HAP, 25 wt%, 50 wt%, 66 wt%, (50 wt% for commercial PGA). 300 mg of loaded PGA was weighed as a fixed mass, giving 150 mg polymer. Amounts of HAP were calculated according to the ratios given above. Pressing was carried out with a conventional IR-press (10 t, 5 min). Samples were washed in cold water to removed the included NaCl. pH measurements were carried out with bodies placed in 10 ml of deionized water (closed vessels) at 37°C.

Carbonated apatite

Carbonated apatite (CACP, B-type)^{36,46} was prepared by fast precipitation from aqueous solution by mixing a solution of $\text{NH}_4\text{H}_2\text{PO}_4$ and K_2CO_3 with a solution of $\text{Ca}(\text{NO}_3)_2$. It was filtered off after 2 min and dried at 80°C for 12 h. Its composition was established via X-ray powder diffraction (see **fig.B.1-7**). In addition to XRD analysis, carbonated apatite was characterized with IR, TG-DTA-MS and SEM.

IR (NaBr pellet): $\tilde{\nu}$ [cm^{-1}] = 1502, 1418 (s, CO_3), 1048 (m, PO_4), 863 (m, CO_3), 577 (PO_4). The sample contained 18.5 wt% water (released from 100 to 200°C) and 18 wt% carbon dioxide (released from 550 to 950°C). Both gases were identified by mass spectrometry. The largest grains as determined from scanning electron microscopy were polycrystals of irregular shape with 100 to 300 μm diameter. They were accompanied by many small grains of much smaller diameter (ca. 5 to 100 μm).

Polyglycolide/carbonated apatite composites

Composites of polyglycolide and carbonated apatite were prepared in two different ways leading to compact and microporous material, respectively, as described below. Compact pellets were prepared by thoroughly mixing (by grinding) water-washed polyglycolide (i.e. without NaCl) with carbonated apatite in the w:w ratio 150 mg:60 mg. This material was melt-pressed for 3 min at 150°C in a heated press under 10^8 MPa pressure to circular tablets of 13 mm diameter and 1.1 mm thickness. Afterwards, they were cooled to room temperature under the same pressure during 5 min. The pores in polyglycolide collapse under these conditions. The density of this material was 1.45 g cm^{-3} . Taking into account the release of 18.5 wt% water from the apatite

phase during melt-pressing, the actual weight ratio of polyglycolide to apatite was 150 mg:49 mg.

Porous pellets were prepared by mixing untreated polyglycolide (i.e. with NaCl still in the pores) with carbonated apatite in the weight ratio (polyglycolide+NaCl):carbonated apatite 300 mg:60 mg. Melt pressing was carried out under the same conditions as with compact material (resulting thickness: 1.6 mm). The NaCl crystals served as porogen (placeholder) in the composite (density 1.7 g cm^{-3}). After melt-pressing the tablets were washed with cold water (8°C) for 4 h to remove NaCl (150 mg). This left a microporous composite with an actual weight ratio of polyglycolide to apatite of 150 mg:49 mg, a pore volume of ca. 31 vol%, and an effective density of 1.0 g cm^{-3} .

Both types of pellets were immersed in pure water for 60 min before cell-seeding to remove possible degradation products from melt-pressing, and to avoid the initial acidic or alkaline burst (**fig.B.1-2**). They were subsequently sterilized with pure ethanol and rinsed with sterile water. Microporous pellets of pure polyglycolide (as controls) were prepared accordingly without addition of apatite.

Cell cultures

Mouse primary osteoblastic cells were obtained by sequential digestion of calvaria in a solution of 0.1 % clostridial collagenase Ia (Sigma Chemical Co., St. Louis, MO) and 0.2 % dispase (Boehringer Mannheim Biochemicals, Mannheim, Germany) from 3-day old mice and cultured in α -MEM containing 10 % fetal bovine serum (FBS), and 1 % penicillin-streptomycin (PS)^{61,62}. The cells were cultured in six-well plates (Falcon Labware, Oxnar, CA) on implants placed on glass coverslips at an initial density of $3 \cdot 10^5$ cells/well. The medium (5 ml per well) was changed after the first and the third day. Thereafter the medium was supplemented with 5 mmol β -glycerolphosphate, and $100 \mu\text{g ml}^{-1}$ ascorbic acid (mineralization medium) and replaced every other day. All cultures were maintained at 37°C under 95% air/5% CO_2 atmosphere. The pH of the culture was determined each time after medium replacement (pH-meter/pH 538, WTW, Weilheim, Germany). Samples were taken

⁶¹ P. Ducy, M. Starbuck, M. Priemel, J. Shen, G. Pinero, V. Geoffroy, M. Amling, G. Karsenty "A Cbfa-1-dependent genetic pathway controls bone formation beyond embryonic development", *Genes Devel.* **1999**, *13*, 1025-1036.

after 1, 2, 3, and 4 weeks of culture. The cultured cells on coverslips were fixed with 3.7 % formaldehyde in phosphate-buffered saline solution (PBS) for 10 minutes at room temperature and washed in PBS. Analysis for alkaline phosphatase and collagen synthesis (van Gieson staining), and for presence of a mineralized matrix (von Kossa staining) was done according to standard protocols^{61,62}. Cellular morphology was checked daily throughout the entire culture period.

The antibodies used in the detection of osteocalcin included a goat anti-mouse osteocalcin antibody (dilution 1:100) obtained from Biotrends and a secondary AlexaFluor 488 antibody from Molecular Probes. Rhodamine conjugated phalloidine from Molecular Probes was used for specific labeling of actin. For double-immunofluorescence analysis cultured cells plated on glass coverslips and on composite pellets were used. The cells were fixed with 3.7% formaldehyde in PBS for 10 minutes at room temperature and washed in PBS. All subsequent incubations were performed at room temperature with PBS containing 0.05% saponin, 0.1% BSA, and 5% normal goat serum (NGS). Samples were incubated in PBS-saponin-BSA-NGS for 30 minutes to block non-specific binding, and then for 2 h with the primary antibody. The samples were washed in PBS-saponin-BSA and all subsequent steps were performed in the dark. After washing the samples were incubated with the secondary antibody for 1 h. After washing actin was labeled by incubation with rhodamine conjugated phalloidine for 1 h. After final washing in PBS, the samples were mounted in FluorSave fluorescent mounting media (Calbiochem-Novabiochem Corp., La Jolla, CA). Samples were examined with a scanning laser confocal microscope (IX70 inverted Olympus microscope and Olympus Fluoview confocal imaging system) with a krypton/argon laser using an optical slice thickness of 2 μm . Computer images were collected on Zip-discs and computer enhanced with the Adobe Photoshop program.

A control experiment (secondary antibody without primary antibody) was negative.

For electron microscopy, the seeded implants were fixed with 3.5 % glutaraldehyde in PBS for 10 minutes at room temperature and washed in PBS. The samples were subsequently dehydrated in graded alcohol (ethanol-water mixtures of 40/60, 60/40, 80/20, 90/10, 100/0 (v:v)). Ethanol was then replaced in four steps by amylacetate.

⁶² J.D. Bancroft, A. Stevens "Theory and practice of histological techniques", Churchill Livingstone, New York.

The pellets were subjected to critical point drying with CO₂ (40°C, 100 bar) in a Balzers Union Critical Point Dryer. Scanning electron microscopy (SEM) was carried out on gold-sputtered samples with a Philips SEM 515 instrument operated at 25 kV.

Further Instruments

X-ray powder diffractometry (XRD) was carried out with an AXS Advance diffractometer (Nickel-filter; Cu K_α-radiation, $\lambda = 154.178$ pm; proportional detector) in Bragg-Brentano geometry. Differential scanning calorimetry (DSC) was carried out with a Mettler TA 4000 instrument in sealed aluminum crucibles. The heating rate was 5 K min⁻¹ and the average sample mass was 5-8 mg. Combined thermogravimetry-differential thermal analysis-mass spectrometry (TG-DTA-MS) was carried out with a Netzsch STA 409/Balzers QMS 421 system, employing dynamic air atmosphere (50 ml min⁻¹) and a heating rate of 5 K min⁻¹. Open alumina crucibles served as sample holders.

General conclusion

Poly(α -hydroxy acids) are polyesters with a long history in biomedical application. These polymers, with polylactide and polyglycolide as the main representatives, are chemically (by simple hydrolysis) and/or biologically degradable. The degradation products can be metabolized by cells and bacteria on regular pathways. Moreover, the material interface exhibits an initially excellent biocompatibility in contact with cellular host tissue. Adherence, proliferation and differentiation proved to be fulfilled for various cell phenotypes. These properties opened the entry of poly(α -hydroxy acid) homo- and copolymers into the biomedical materials field. Porous meshes of polyesters can serve as scaffolding matrix in tissue engineering, the young discipline of extracorporeal tissue and organ reconstruction. Pins, plates and screws are employed for bone fixation without the need for a second operation for material removal. Constructs are developed and designed to release drugs in a controlled manner by fine-tuning of the degradation behavior.

Complications can arise from local acidification and accumulation of degradation products during the degradation process as observed for degrading bulk devices. Such effects can lead to tissue necrosis, cell death or osteolysis of surrounding bone.

The thermally induced solid-state polycondensation of sodium chloroacetate (and other metal halogenoacetates) leads to polyglycolide with included sodium chloride crystals. The NaCl can be completely washed out with water, indicating an interconnected network. The resulting microporosity is, in terms of biocompatibility requirements, an additional qualification of the biomaterial polyglycolide.

The material performance of a biodegradable polyester *in vivo* is a function of multiple factors, among which the polyester type, molecular weight distribution, degree of crystallinity, structure (porosity), material properties and the degradation behavior are key factors on the material side.

Various parameters were monitored during the synthesis of polyglycolide from sodium chloroacetate to evaluate the character of the reaction itself and the properties of the formed product.

The reaction takes place as a one-step polycondensation without detectable intermediates. The reaction extent follows a sigmoidal time course and is strongly influenced by the reaction temperature. At 180°C, the reaction is completed after 2 h,

at 160° after about 15 h. The average degree of polymerization increases with reaction time, shows a maximum of ca. 40 monomer units and decreases subsequently due to thermal decomposition.

The degree of crystallinity increases with reaction time to reach a level of $55 \pm 10\%$, in good agreement with conventionally prepared polyglycolide. The porosity of the polymer is a consequence of the number, volume and shape of the formed NaCl crystallites. Some crystals grow at the expense of smaller ones during the reaction at elevated temperatures to a final diameter of 300-400 μm .

The limited achievable molecular weight and the difficulty to obtain controlled product properties from reproducible conditions are restrictions of the reaction, due to the complex influences of various parameters on the course of this solid-state reaction.

The *in vitro* degradation behavior was tested for porous and compact polymer bodies in water (unbuffered) and cell nutrition medium (buffered at pH 7.4) at physiological temperature over a period of eight weeks of incubation. Both media were changed weekly. The pH was in a constant range in the cell nutrition medium during the entire experiment. In water, however, a drop in pH was found down to 2.5 after 2 to 3 weeks. Repeated medium change resulted in values of 4 to 6, indicating a decrease in acidic potential due to mass loss of the samples. Porous bodies were more stable in both media. The incubation in physiologically buffered medium leads to a faster erosion and a lower geometric stability compared to acidic unbuffered aqueous medium. An inner/outer differentiation mechanism with a fast, autocatalytic degradation in the center leading to hollow structures as observed for bulk polyesters samples was not found. The crystallinity stayed at about 60% over the entire incubation time. Faster degradation of amorphous moieties is compensated by the parallel degradation of crystalline domains. As expected, average chain length, Young's modulus and fracture toughness decreased exponentially.

The degradation of the polyglycolide from solid-state reaction can be considered as fast compared to higher polyesters like polylactide or poly(hydroxybutyrate). The study demonstrated further the sustained acidity of the degrading polymer, which is incompatible with the requirement of a physiological pH at a potential implantation site.

With the prospect to obtain porous polyesters, Na and Ag 3-Cl-butyrates and Na Cl-

pivalate were analyzed for the occurrence of a polycondensation in the solid state. The respective polymers, poly(3-hydroxybutyrate) and poly(pivalolactone) are likely to be biocompatible, biodegradable and more stable towards hydrolysis than polyglycolide.

Substitution in the β -position was found to be susceptible to thermally induced elimination and the formation of an α/β -double bond. In the case of sodium 3-Cl-butyrate, the high onset-temperature of 130°C led to the formation of the unsaturated compounds crotonic acid and sodium crotonate as the main products. As a minor side-product, short chains of the desired poly(3-hydroxybutyrate) were detected.

The polycondensation/elimination reaction occurred simultaneously under liquefaction. The thermal events could not be separated employing different heating rates and final reaction temperatures. The reaction was accompanied by a one-step mass loss due to evaporation of the organic parts with sodium chloride and sodium crotonate as residues.

In the case of the higher reactive silver salt, the lower onset-temperature led to a different ratio of elimination and polycondensation. Poly(3-hydroxybutyrate) could be identified as the main product with crotonic acid as by-product. Liquefaction was not observed.

Heating Na Cl-pivalate led to a mixture of the desired polyester poly(pivalolactone) and unreacted precursor. The polycondensation is a separated phenomenon without mass loss during reaction. All investigated educts showed a tendency to solvate formation, thereby restricting a reproducible synthesis of pure precursor. The included solvent molecules can be removed by thermal pre-treatment in the case of the pivalate. The same efforts led to elimination of HCl in the case of the less stable butyrates.

These explorative studies showed a partially successful transposition of the solid-state reaction principle to the investigated systems.

In the second part of the thesis, the development of composites of polyglycolide from solid-state reaction and calcium phosphate is described. The composite concept mimics the composite character of human bone with polyglycolide as the collagen equivalent and calcium phosphate as the mineral phase.

The materials were analyzed with respect to the externally generated pH-value in aqueous media. Composites with commercially available hydroxyapatite were not capable to keep the pH in a physiological range. The acidic degradation of the polymer

was kinetically dominant over the alkaline dissolution of the apatite. In a second approach, an amorphous carbonated apatite was synthesized, which resembles the bone mineral in crystallinity, carbonate content and solubility.

Pellets of the composite material with this calcium phosphate were optimized in water and showed a sustainable physiological pH over a period of 4 weeks in buffered cell culture medium. This is a prerequisite to enable vital cell activity at a potential implantation site and a biological integration in the host bone tissue.

The optimized composites were subjected to biocompatibility testing with murine osteoblasts. Seeded cells showed a good adherence and proliferation to a confluent layer on the composite surface. The osteoblasts retained their differentiated phenotype over the entire culture experiment (4 weeks). Collagen was formed as a multilayer, covering the composite pellets. Another evidence for an undisturbed cell function was the formation of mineralized nodules, indicating an active cellular calcification process of the collagen fibers. The biocompatibility of the tested samples can be termed as excellent, leading to the *in vitro* formation of bone-like tissue on the implant material.

The chemical transformation of the carbonated apatite was analyzed with X-ray diffraction with respect to the degree of crystallinity on recovered samples from cell incubation medium. A conversion to higher crystalline hydroxyapatite was not detected, despite the thermodynamic instability of the carbonated apatite. Apparently, the polyglycolide matrix and/or the ingredients of the culture medium (e.g., serum albumin, amino acids, glucose) prevent the crystallization by inhibiting crystal-ripening and ordering. Such a kind of stabilization by coordination of macromolecules on crystallographic plains of calcium phosphate nuclei and nanometer sized crystallites preserves the unique nature of the mineral phase in bone and ensure a continual cellular remodeling process.

Regarding porosity, the structure of cancellous bone (spongiosa) is the ultimate model for implant design. The interconnected porous structure enables cell migration, supply and communication. The pores of polyglycolide from solid-state reaction (with diameters in the sub-micrometer range) are by far too small to meet these requirements. Therefore the introduction of a macroporosity was attempted for polymer bodies. Leaching of externally added NaCl crystals ($\approx 300 \mu\text{m}$) with water led to the formation of a macroporosity comparable to spongiosa in pore distribution and

diameters. The cavities were isolated, lacking an interconnected structure. Attempts with water soluble PVA fibers as porogen failed, due to swelling of the polymer in water. An ideal porogen would be a water soluble fiber material without significant change in volume during the wash-out step.

For conclusion, it has to be stated that bone is a highly optimized composite material that serves multiple functions. The production of a synthetic material with equivalent properties for bone substitution appears to be impossible. Instead, the approach of *in vitro* or *in vivo* (dynamic remodeling) tissue engineering seems to be a more prospectus strategy. The aim should be to provide an implant that can be converted to bone by cellular functions.

The rational concept of optimized polyglycolide/carbonated apatite composites was successful with respect to biocompatibility and the *in vitro* formation of bone-like tissue. Further research is necessary to evaluate an ideal material combination (i.e., variation of employed polyester) and to insert a biomimetic macroporosity under retainment of sufficient mechanical stability to complement the excellent biocompatibility.

victory - instinct over intellect
victory - erupts from deep inside
history - history is laughing at us
plotting its discoveries
victory, victory - blame it on the victory !
(G. Graffin)

Appendix

Zusammenfassung (summary in German)

Poly(α -hydroxycarbonsäuren) bilden eine Polyester-Stoffgruppe mit einer langen Geschichte im Bereich der biomedizinischen Anwendung. Die Polyester, allen voran Polyglycolid und Polylactid als deren wichtigste Vertreter, sind chemisch (durch einfache Hydrolyse) und/oder biologisch abbaubar. Die entstehenden Degradationsprodukte können durch Zellen und Bakterien aufgenommen und auf herkömmlichen Stoffwechselwegen metabolisiert werden. Die Materialien zeigen *in vivo* anfänglich eine exzellente Biokompatibilität im Kontakt mit Zellen und Geweben des Implantationsortes. Für verschiedene Zell-Phänotypen wurde eine gute Adhärenz, Proliferation und unveränderte Differentiation auf diesen Materialien bereits mehrfach nachgewiesen. Diese Eigenschaften qualifizieren Poly(α -hydroxycarbonsäuren) (Homo- und Copolyester) für den *in vivo* Einsatz und eröffneten den Einzug in das Feld der klinisch verwendeten Biomaterialien. Die bekanntesten Beispiele hierfür sind zum einen Matrices als Gerüstsubstanzen im Bereich des *Tissue Engineering*, einer neuen Disziplin innerhalb der molekularen Zellbiologie, zur *in vitro/in vivo* Rekonstruktion von Geweben und Organen. Degradierbare Nägel, Platten und Schrauben dienen der Fixierung und Verstärkung von Knochensegmenten. Im Gegensatz zu Metallen und anderen Permanentimplantaten erübrigt sich eine zweite Operation zur Entfernung der eingebrachten Materialien. Des weiteren dienen Polyester als Trägersubstanzen in der Entwicklung von Systemen zur kontrollierten Freisetzung von Arzneimitteln. Die Freisetzungsrates kann dabei als Funktion der Degradationsgeschwindigkeit eingestellt werden.

Komplikationen im klinischen Einsatz können im Zuge des fortschreitenden Degradationsprozesses auftreten. Die Akkumulation von Abbauprodukten und die damit einhergehende lokale Übersäuerung sind inkompatibel mit den Anforderungen eines physiologischen pH-Wertes. Beobachtete Konsequenzen sind Gewebeschädigungen, Zelltod oder die Auflösung von umgebendem Knochenmineral. Die thermisch initiierte Festkörper-Polykondensation von Natriumchloracetat (und anderer Metallhalogenacetate) führt zu Polyglycolid mit eingeschlossenen Kochsalz-Kristalliten. Das Kochsalz kann durch Waschen mit Wasser komplett ausgewaschen werden. Es resultiert eine interkonnektierte Porosität mit Porendurchmessern im

sub- μm -Bereich. Die inhärente Mikroporosität stellt (in Form einer Strukturierung) eine zusätzliche Qualifikation für das Biomaterial Polyglycolid dar.

Die Eignung und das Verhalten eines biodegradierbaren Polyesters *in vivo* hängt von einer Vielzahl von Faktoren ab, von denen die Art des Polyesters, das mittlere Molekulargewicht, der Grad der Kristallinität, die Porosität, die Materialeigenschaften und das Degradationsverhalten die Schlüsselp Parameter auf der Materialseite darstellen.

Die Synthese von Polyglycolid aus Natriumchloracetat wurde *ex situ* mit diversen Methoden verfolgt, um mehr über den Charakter der Reaktion selbst zu erfahren und das resultierende Produkt in seinen Eigenschaften zu charakterisieren.

Die Reaktion verläuft als Polycondensation ohne das Auftreten von detektierbaren Zwischenprodukten. Der Umsatz erweist sich als stark temperaturabhängig und kann mit einem sigmoidalen Verlauf beschrieben werden. Bei einer Temperatur von 180°C ist die Reaktion bereits nach zwei Stunden vollständig abgelaufen, während etwa 15 Stunden bei 160° nötig sind, um den gleichen Umsatz zu erzielen.

Der Polymerisationsgrad steigt bei beiden Temperaturen mit der Zeit an, erreicht ein Maximum von etwa durchschnittlich 40 Monomereinheiten pro Kette, um schließlich wieder zu sinken. Dieser Verlauf erklärt sich durch die Überlagerung von thermisch initiiertem Kettenwachstum und gleichzeitiger thermischer Zersetzung der entstandenen Ketten.

Der Kristallisationsgrad steigt ebenfalls im Laufe der Reaktion an und bewegt sich final bei Werten von $55 \pm 10 \%$ im Rahmen von konventionell hergestelltem Polyglycolid.

Die resultierende Porosität des Polymers ergibt sich aus der Anzahl, dem Volumen und der äußeren Form der Kochsalz-Kristallite. Durch die anhaltende thermische Aktivierung kommt es zu Reifungsprozessen (Minimierung von Oberflächenenergie), so dass größere Kristalle auf Kosten kleinerer Kristallite wachsen. Dieser Prozess endet bei Durchmessern von 300-400 μm .

Die auf dem beschriebenen Weg erzielbaren Molekulargewichte stellen eine Einschränkung des synthetische Potentials der Reaktion dar. Der Einfluss mehrerer Faktoren (wie z.B. Kristallinität, Reinheit und Korngrößen des Precursors, Wärmegradienten, Schüttdichte) auf die Reaktivität dieser Festkörperreaktion erschwert die reproduzierbare Synthese von Polyglycolid mit kontrollierten

Eigenschaften.

Das *in vitro* Degradationsverhalten von so erhaltenem Polyglycolid wurde an porösen und massiven Körpern in Wasser (ungepuffert) und Zell-Nährmedium (gepuffert bei pH 7.4) untersucht. Die Studie wurde bei 37°C über einen Zeitraum von acht Wochen durchgeführt. Die Medien wurden wöchentlich gewechselt, wobei die Pufferkapazität des Nährmediums ausreichte, ein Absinken des pH-Wertes zu verhindern. Im Wasser zeigte sich die saure Degradation in Werten von bis zu 2.5 nach 2-3 Wochen Inkubation. Zu späteren Zeitpunkten wurden höhere Werte im Bereich zwischen 4 und 6 gemessen, was mit dem Massenverlust der Proben (Verlust des aziden Potentials) und stetigem Medienwechsel erklärt werden kann. Poröse Tabletten erwiesen sich in beiden Medien als die stabileren Körper. In Nährmedium zeigte sich eine schnellere Erosion als im ungepufferten Wasser, in dem die Geometrie der Tabletten länger stabil erhalten blieb. Ein Degradationsgradient mit einer autokatalytisch beschleunigten Degradation im Inneren und einer langsameren in Randbereichen der Körper wurde nicht beobachtet. Ein solches Verhalten hatte in vergleichbaren Studien an massiven, voluminösen Polylactid-Körpern zu hohlen Strukturen geführt und gilt als anerkannter Mechanismus.

Die Kristallinität bewegte sich relativ konstant um einen Wert von 60 % herum. Der schnellere Abbau amorpher Anteile wird durch die parallele Degradation kristalliner Domänen kompensiert. Für die Parameter mittleres Molargewicht, Elastizitätsmodul und Bruchfestigkeit ergab sich erwartungsgemäß ein rapider exponentieller Abfall.

Verglichen mit Polylactid oder Poly(3-hydroxybuttersäure) verläuft die Degradation von Polyglycolid sehr schnell und ist verbunden mit einer nachhaltig sauren Wirkung. Letztere steht im Gegensatz zu der Anforderung eines möglichst physiologischen pH-Wertes an einem potentiellen Implantationsort.

In der Erwartung, das Reaktionsprinzip der Polykondensation im Festkörper auf höhere Analoga zu übertragen und poröse Polyester zu erhalten, wurden Natrium und Silber-3-chlorbutyrat sowie Natriumchlorpivalat auf das Auftreten dieser Reaktion hin untersucht. Die entsprechenden Polymere, Poly(3-hydroxybuttersäure) und Poly(pivalolacton), sollten biodegradierbar und biokompatibel sein. Zudem besitzen sie, verglichen mit Polyglycolid, eine höhere Stabilität bezüglich des hydrolytischen Abbaus.

Im Falle der Butyrate erwies sich die Halogenfunktion in der β -Position als empfindlich gegenüber der thermisch induzierten Eliminierung, welche zur Bildung einer α/β -Doppelbindung führt. Für das Natriumsalz wurden als Hauptprodukte bei einer Reaktionstemperatur von 130°C Natriumcrotonat und Crotonsäure erhalten. Als Nebenprodukt entstanden Oligomere der gewünschten Poly(3-hydroxybuttersäure). Bei dieser Temperatur überwiegt die Eliminierung von HCl gegenüber der intermolekularen Substitution. Eliminierung und Polykondensation treten parallel auf unter Verflüssigung des Reaktionsansatzes. Die Variation der Heizrate und der Endtemperatur führen nicht zu einer Trennung der thermischen Ereignisse. Die Reaktion wird begleitet von einem einstufigen Massenverlust, der dem Abgang organischer Molekülfragmente entspricht. Natriumchlorid und Natriumcrotonat verbleiben als Restsubstanzen.

Beim reaktiveren Silbersalz hingegen, das bei einer Temperatur von 100° umgesetzt wurde, ergab sich ein umgekehrtes Verhältnis. Poly(3-hydroxybuttersäure) konnte als Hauptprodukt identifiziert werden. Geringe Mengen an Crotonsäure wurden als Nebenprodukt gebildet. Der Ansatz zeigte keine Verflüssigung.

Das Erhitzen des Natriumchlorpivalats lieferte eine Mischung aus unreaktiertem Precursor und Poly(pivalolacton). Die Polykondensation trat isoliert von anderem Ereignissen auf und war von keinem Massenverlust begleitet. Die Precursor-Synthesen zeigten für beide Systeme eine starke Tendenz zur Solvatbildung. Die Lösungsmittelmoleküle können im Falle des Pivalats durch thermische Vorbehandlung entfernt werden. Beim Butyrat ist ein solches Vorgehen aufgrund der thermischen Instabilität ausgeschlossen. Die explorativen Studien zeigten eine teilweise erfolgreiche Übertragung des Reaktionsprinzips im Festkörper. Raum für Optimierung bilden die solvatreie Synthese und die Aufklärung der Beziehung zwischen Struktur und Reaktivität der Precursor.

Im zweiten Teil der Arbeit wird die Entwicklung von Kompositen aus Polyglycolid und Calciumphosphat als potentielle Knochenersatzmaterialien beschrieben. Das Konzept orientiert sich an dem Komposit-Charakter des natürlichen Knochens mit Polyglycolid als dem Kollagen-Analogen und Calciumphosphat als mineralischer Phase. Das Material wurde im Hinblick auf den erzeugten pH-Wert in destilliertem Wasser untersucht. Komposite mit synthetischem Hydroxylapatit waren nicht in der

Lage, den pH-Wert in einem physiologischen Bereich zu halten. Die saure Degradation des Polyesters überwog die basische Auflösung des Apatits. In einer zweiten Serie wurde ein amorpher carbonathaltiger Apatit verwendet, der dem Knochenmineral in Kristallinität, Carbonatgehalt und Löslichkeit sehr ähnelt.

Aus diesem Material hergestellte Tabletten wurden in destilliertem Wasser optimiert. Inkubiert in Zell-Nährmedium zeigten die optimierten Tabletten einen nachhaltig physiologischen pH-Wert. Damit ist eine wichtige Voraussetzung für eine vitale Zellaktivität am Implantationsort für eine biologische Integration des Materials in das Wirtsgewebe erreicht.

Die Komposit-Tabletten wurden einer Biokompatibilitäts-Testung mit murinen Osteoblasten unterzogen. Die kultivierten Zellen zeigten eine gute Adhärenz auf dem Material und proliferierten bis zur Bildung einer konfluenten Schicht. Die Osteoblasten erhielten ihren differenzierten Phänotyp über die vierwöchige Dauer des Experiments. Als Folge der Erhaltung der Zellfunktionen wurde ein mehrschichtiger Kollagenrasen auf der Kompositoberfläche von den Zellen gebildet. Darüber hinaus konnten mineralisierte Bereiche innerhalb des Kollagens nachgewiesen werden, die eine aktive Calcifikation anzeigen. Die Biokompatibilität der getesteten Komposite erwies sich als exzellent und führte im *in vitro* Experiment zur Bildung von knochenähnlichem Gewebe.

Die chemische Transformation des carbonathaltigen Apatits in Zellkultur wurde mit Hilfe der Roentgenpulverdiffraktometrie an den zurückgewonnenen Proben in Hinblick auf die Kristallinität untersucht. Trotz der thermodynamische Instabilität des amorphen Carbonatapatits konnte eine Konversion zu höher kristallinem Hydroxylapatit nicht nachgewiesen werden. Offensichtlich verhindern der Kontakt zum Polyglycolid und/oder die im Nährmedium gelösten Moleküle (z.B. Serumalbumin, Aminosäuren, Glukose) den Kristallisationsprozess durch Inhibierung des Kristallwachstums. Durch eine derartige Stabilisierung (Koordination von Makromolekülen an kristallographischen Flächen der Calciumphosphat-Kristallkeime) wird im Knochen die nanokristalline Natur der Mineralphase erhalten, um ein anhaltendes *Remodeling* durch zelluläre Aktivität zu ermöglichen.

In Bezug auf die anzustrebende Porosität eines Implantatmaterials ist der poröse Knochen (Spongiosa) das Idealbild. Die Knochenstruktur erlaubt Zell-Migration, -

Versorgung und Kommunikation. Das Porensystem des Polyglycolids aus Festkörperreaktion (mit Porendurchmessern im sub- μm -Bereich) ist für diese Aufgabe nicht geeignet. Aus diesem Grund wurde die Einführung einer Makroporosität für Polymer-Körper versucht. Das Auswaschen von extern zugeführtem Kochsalz mit größeren Kristallen ($\approx 300 \mu\text{m}$) führte zu einer Porosität, die in Porendurchmesser und -verteilung dem natürlichen Vorbild sehr ähnlich ist. Dieser Strukturierungsversuch liefert jedoch isolierte Poren und kein interkonnektiertes Porensystem. Die Verwendung von wasserlöslichen Fäden aus PVA als Porogen schlug aufgrund der starken Quellung in Wasser fehl. Das ideale Porogen sollte ein wasserlösliches Fadenmaterial sein, welches sich unter geringer Volumenveränderung auflöst.

Zusammenfassend muss festgehalten werden, dass der natürliche Knochen ein hochoptimiertes Kompositmaterial ist, welches zugleich mehreren Aufgaben erfolgreich dient. Die Erzeugung eines synthetischen Äquivalents mit vergleichbaren Eigenschaften für den Knochenersatz erscheint in seiner Komplexität unmöglich. Aussichtsreicher erscheint die Strategie, den natürlichen Funktionen im Körper ein Material anzubieten, das den zellulären Umbau zu Knochengewebe erlaubt und fördert. Diese Konvertierung kann im Rahmen des *Tissue Engineering* innerhalb oder außerhalb des Körpers erfolgen.

Das verfolgte Konzept der Komposite aus Polyglycolid und Carbonatapatit erwies sich als sehr erfolgreich und führte zur Bildung von knochenähnlichem Gewebe außerhalb des Körpers. Weitere Forschung ist notwendig zur Ermittlung der idealen Materialkombination (Wahl des am besten geeigneten Polyesters) und zur Einführung einer biomimetischen Makroporosität, die als Kompromiss noch genügend Stabilität des Implantats zulässt. Die Erreichung dieser Ziele würde die bewiesene Biokompatibilität des Materials abrunden.

Kurzzusammenfassung (short summary in German)**Biodegradable polyesters from solid-state precursors - basic components of a biomedical materials concept**

1. Gutachter: Prof. Dr. M. Epple 2. Gutachter: Prof. Dr. D. Rehder

Poly(α -hydroxycarbonsäuren) bilden eine Polyester-Stoffgruppe mit einer langen Geschichte im Bereich der biomedizinischen Anwendung. Polyglycolid, der kurzkettigste Vertreter dieser Polymere kann in poröser Struktur aus Halogenacetaten in einer Festkörper-Polykondensation erhalten werden. Ziel der vorliegenden Dissertation war die Charakterisierung dieser Festkörperreaktion, die Untersuchung des Degradationsverhaltens von so gewonnenem Polyglycolid, die Übertragung des Reaktionstypus auf höhere Homologe und die Entwicklung eines potentiellen Knochenersatzmaterials auf Basis von Polyglycolid im Komposit mit Calciumphosphaten.

Die Bildung von Polyglycolid aus Natriumchloracetat wurde unter Einsatz mehrerer Methoden *ex situ* bei verschiedenen Temperaturen untersucht. Die Reaktionsverfolgung diente der Ermittlung der Parameter Umsatz, mittleres Molekulargewicht, Kristallinität und Porosität des entstehenden Polyesters. Die Abhängigkeit dieser Charakteristika von Reaktionstemperatur und -zeit konnte aufgeklärt werden. Der Polykondensationsmechanismus (ohne nachweisbare Intermediate) wurde bestätigt.

Das Degradationsverhalten von Körpern aus so erhaltenem Polyglycolid wurde in einer Studie über acht Wochen bei 37°C in Wasser und in Zell-Nährmedium aufgezeichnet. Aspekte der Studie waren die Erhaltung der Körper-Geometrie, die Entwicklung des pH-Wertes, des mittleren Molekulargewichtes, der Kristallinität und der Probenmasse (Quellgrad und Erosion) sowie die mechanische Stabilität. Polyglycolid aus Festkörperreaktion weist eine schnelle Degradation innerhalb weniger Wochen unter nachhaltig saurer Wirkung auf.

In Erwartung einer Übertragung des Reaktionsprinzips auf höhere Homologe des Polyglycolids, wurden die Salze Natrium-3-chlorbutyrat, Silber-3-chlorbutyrat und Natriumchlorpivalat auf das Auftreten einer Polykondensation hin untersucht. Die jeweiligen Polymere Poly(3-hydroxybuttersäure) und Poly(pivalolacton) sollten ähnlich biokompatible Eigenschaften haben und stabiler hinsichtlich des

hydrolytischen Abbaus sein. Im Falle des Natrium-3-chlorbutyrats verhindern Nebenreaktion die gewünschte Bildung des Polymers. In den anderen beiden Fällen wurden die Polymere als Hauptprodukte erhalten.

Nach dem Vorbild von natürlichem Knochen, der als Komposit aus Kollagen und Calciumphosphat als mineralische Phase beschrieben werden kann, wurden Komposite aus Polyglycolid und amorphem Calciumphosphat als potentielle Knochenersatzmaterialien hergestellt. Das Material wurde im Hinblick auf den pH-Wert, den es in wässrigen Medien erzeugt, optimiert. In Zell-Nährmedium konnte ein nachhaltig physiologischer pH-Wert erreicht werden, eine Voraussetzung für eine integrative biologische Reaktion.

Die Biokompatibilität der optimierten Komposite wurde durch Zellbesiedlung mit murinen Osteoblasten (knochenbildende Zellen) getestet. Die Zellen zeigten eine gute Adhäsion und Proliferation auf dem Material. Sie erhielten ihren differenzierten Phänotyp über die Dauer des Experiments. Die Bildung von Kollagen und mineralisierten Bereichen bewiesen die ungestörte Zellaktivität. Auf dem Material wurde *in vitro* knochenähnliches Gewebe gebildet.

Die Einführung einer Makroporosität, um das Eindringen von Zellen und Blutgefäßen zu ermöglichen, wurde durch extern zugeführtes Natriumchlorid und anschließendes Auswaschen mit Wasser erreicht.

Sicherheit und Entsorgung (Toxicity)

Verbindung	Gefahrensymbol	R- und S-Sätze	Entsorgungsschlüssel
Aceton	leicht entzündlich	R: 11 S: 9-16-23-33	1
3-Chlorbuttersäure	-	-	4
Chloressigsäure	giftig; umweltgefährlich	R: 25-34-50 S: 23.2-37-45-61	4
Chloroform	gesundheitsschädlich	R: 22-38-40-48/20/22 S: 36/37	3
Chlorpivalinsäure	reizend	R: 36/37/38 S: 26-37/39	4
Crotonsäure	reizend	R: 36/37/38 S: 22-26	2
Dichlormethan	mindergiftig	R: 40 S: 23.2-24/25-36/37	3
Diethylether	hoch entzündlich	R: 12-19 S: 9-16-29-33	1
Ethanol	leicht entzündlich	R: 11 S: 7-16	1
Hexafluorisopropanol	gesundheitsschädlich	R: 22-26/27/28 S: 26-28A	3
Lithium-, Natrium-, Kaliumhydroxid	Ätzend	R: 35 S: 2-26-37/39	6
Methanol	giftig; leicht entzündlich	R: 11-23/25 S: 7-16-24-45	1
Monochloracetate	giftig	R: 25-34 S: 23-37-44	4
Natrium-3-chlorbutyrat	-	-	4
Natriumchlorid, -bromid, -iodid	-	-	7
Natriumchlorpivalat	-	-	4

Natrium- <i>tert.</i> -butylat	leichtentzündlich, ätzend	R: 11-14-34 S: 8-16-26-36/37/39 43.6-45	2
Penicillin/ Streptomycin	-	R: 20/21/22-42/43-61 S: 23-36/37/39	13
Pentan	leichtentzündlich	R: 11 S: 9-16-29-33	1
Polyglykolid	-	-	8
Salzsäure	ätzend	R: 34-37 S: 26-36/37/39-45	6
Silber-3-chlorbutyrat	-	-	5
Silberchlorid	--	--	5
Silbernitrat	ätzend	R: 34 S: 2-26	5
<i>tert.</i> -Butanol	leichtentzündlich, mindergiftig	R: 11-20 S: 9-16	1
Tetrahydrofuran	gesundheitsschädlich; leicht entzündlich	R: 11-19-36/37 S: 16-29-33	1

R-Sätze

- R 11: Leichtentzündlich
R 12: Hochentzündlich
R 14: Reagiert heftig mit Wasser
R 19: Kann explosionsfähige Peroxide bilden
R 20: Gesundheitsschädlich beim Einatmen
R 22: Gesundheitsschädlich beim Verschlucken
R 25: Giftig beim Verschlucken
R 26: Sehr giftig beim Einatmen
R 34: Verursacht Verätzungen
R 35: Verursacht schwere Verätzungen
R 36: Reizt die Augen
R 37: Reizt die Atmungsorgane
R 38: Reizt die Haut
R 40: Irreversibler Schaden möglich
R 41: Gefahr ernster Augenschäden
R 50: Sehr giftig für Wasserorganismen
R 61: Kann das Kind im Mutterleib schädigen
R 20/21/22: Gesundheitsschädlich beim Einatmen, Verschlucken und Berührung mit der Haut
R 23/25: Giftig beim Einatmen und Verschlucken

- R 23/24/25: Giftig beim Einatmen, Verschlucken und Berührung mit der Haut
 R 26/27/28: Sehr giftig beim Einatmen, Verschlucken und Berührung mit der Haut
 R 36/37: Reizt die Augen und die Atmungsorgane
 R 36/37/38: Reizt die Augen, Atmungsorgane und die Haut
 R 42/43: Sensibilisierung durch Einatmen und Hautkontakt möglich
 R 48/20/22: Gesundheitsschädlich: Gefahr ernster Gesundheitsschäden bei längerer Exposition durch Einatmen und durch Verschlucken

S-Sätze

- S 2: Darf nicht in die Hände von Kindern gelangen
 S 7: Behälter dicht geschlossen halten
 S 9: Behälter an einem gut gelüfteten Ort aufbewahren
 S 16: Von Zündquellen fernhalten - nicht rauchen
 S 22: Staub nicht einatmen
 S 23: Gas/Rauch/Dampf/Aerosol nicht einatmen. (Geeignete Bezeichnungen sind von Hersteller anzugeben)
 S 24: Berührung mit der Haut vermeiden
 S 26: Bei Berührung mit den Augen sofort mit Wasser abspülen und Arzt konsultieren
 S 28: Bei Berührung mit der Haut sofort abwaschen
 S 29: Nicht in die Kanalisation gelangen lassen
 S 33: Maßnahmen gegen elektrostatische Aufladung treffen
 S 36: Bei der Arbeit geeignete Schutzkleidung tragen
 S 37: Geeignete Schutzhandschuhe tragen
 S 43: Zum Löschen (geeignetes Löschmittel vom Hersteller anzugeben) verwenden
 S 45: Bei Unfall oder Unwohlsein sofort Arzt zuziehen
 S 61: Freisetzung in die Umwelt vermeiden. Besondere Anweisungen einholen/ Sicherheitsdatenblatt zu Rate ziehen
 S 24/25: Berührung mit den Augen und der Haut vermeiden
 S 36/37: Bei der Arbeit geeignete Schutzhandschuhe und Schutzkleidung tragen
 S 36/37/39: Bei der Arbeit geeignete Schutzhandschuhe, Schutzkleidung und Schutzbrille/Gesichtsschutz tragen
 S 37/39: Bei der Arbeit geeignete Schutzhandschuhe und Schutzbrille/Gesichtsschutz tragen

Entsorgungsschlüssel:

- 1 - In den Kanister für halogenfreie Lösemittelabfälle geben
- 2 - Als Lösung neutralisiert in den Kanister für halogenfreie Lösemittelabfälle geben
- 3 - In den Kanister für halogenhaltige Lösemittelabfälle geben
- 4 - Als Lösung neutralisiert in den Kanister für halogenierte Lösemittelabfälle geben
- 5 - Wiederaufbereiten und wiederverwenden, Reste angesäuert in den Behälter für Silberabfälle geben
- 6 - Neutralisieren und in den Behälter für anorganische Salzlösungen geben
- 7 - In Wasser lösen und in den Behälter für anorganische Salzlösungen geben
- 8 - In den Sammelbehälter für Feststoffabfälle geben

-
- 9 - Angesäuert in den Behälter für schwermetallhaltige Säureabfälle geben
 - 10 - Reduzieren, neutralisieren und in den Behälter für anorganische Salzlösungen geben
 - 11 - Reduzieren und die Lösung angesäuert in den Behälter für chromhaltige Säurelösungen geben
 - 12 - Oxidieren, neutralisieren und in den Behälter für anorganische Salzlösungen geben
 - 13 - Zell-Nährmedien und deren Zubereitungen wurden am Zentrum für Biomechanik des Universitätsklinikums Eppendorf (UKE) gesammelt, autoklaviert und entsorgt

Danksagungen (Acknowledgement)

Eine Reihe von Personen haben direkt oder indirekt zum Gelingen dieser Arbeit beigetragen. Im folgenden sei ihnen mein Dank ausgesprochen.

Professor Dr. Matthias Epple für die hervorragende wissenschaftliche Betreuung und den Rahmen für eine fachlich und persönlich interessante und lehrreiche Promotionszeit.

Meinen Kollegen Dr. Oliver Herzberg, Fabian Peters, Michael Siedler und Drazen Tadic für eine Zusammenarbeit und Freundschaft, die weit über das universitäre Engagement hinaus ging und geht.

Meinen Kollegen Bernd Hasse, Carsten Schiller und Markus Rehbein für die Zusammenarbeit und die stetige Hilfsbereitschaft.

Markus Brunnbauer für die freundschaftlichen fachlichen und privaten Diskussionen und die Einführung in die bayrische Kultur.

Dr. med. W. Linhart, Dr. med. M. Amling, Dr. med. W. Lehmann, Dr. med. A. Schilling und Prof. Dr. med. J.M. Rueger aus der Unfallchirurgie des UKE für die gute Kooperation im Bereich der Knochenersatzmaterialien.

Den Praktikanten Bernd Hasse, Michael Siedler, Matthias Wulf, Oliver Konrad, Markus Potthast, Malte Pflughoefft, Bruno Elzholz, Boris Kröplin, Alexander Prenzel, Matthias Hoff und Martin Wienke für die Anfertigung ihrer Arbeiten in der Arbeitsgruppe Epple und die Bereitschaft, sich von mir betreuen zu lassen.

Frau Warncke, Nina Schober, Dr. Frank Meyberg, Torborg Krugmann, Frau Ralya, Herrn Ludwig, Frau Heffter und den Glasbläsern T. Roth und J. Köster für die ausgeführten Messungen oder den freundlichen Service.

Ana Lagoa, Herminio Diogo und Manuel Minas da Piedade für die angenehme Zusammenarbeit und die Gastfreundschaft während des Aufenthalts in Lissabon.

Besonderer Dank geht an die Freunde Hauke Bols, Tobias Groß, Angela Keil-Zippermayr, Wolfgang Hattenkofer und Peter Vollmer, die es durch ihre Ermutigungen immer wieder ermöglichten, einen Schritt weiter zu gehen. Meiner Großmutter für die vielen kleinen Annehmlichkeiten. Meinem Bruder Hanjo für die innige Verbundenheit und den Zuspruch. Schließlich meinen Eltern für ihre Geduld, das Vertrauen und die finanzielle Unterstützung.

(Alle, die hier ungenannt bleiben, bitte ich um Nachsicht. Eine solche Liste kann wohl nie vollständig sein.)

List of publications

Regular papers in refereed journals

- 1) K. Schwarz, M. Epple "Biomimetic crystallization of apatite in a porous polymer matrix", *Chem. Eur. J.* **1998**, *4*, 1898-1903.
- 2) K. Schwarz, M. Epple "Hierarchically structured polyglycolide - a biomaterial mimicking natural bone", *Macromol. Rapid Commun.* **1998**, *19*, 613-617.
- 3) M. Epple, F. Peters, K. Schwarz "Composites aus Polyglycolid und Calciumphosphat als potentielle Knochenersatzmaterialien", in *Tagungsbände der Werkstoffwoche/Materialica 1998, IV, Symposium 4: Werkstoffe für die Medizintechnik*, Wiley-VCH **1999**, 233-237.
- 4) H. Ehrenberg, B. Hasse, K. Schwarz, M. Epple "Crystal structure determination of lithium chloroacetate, lithium bromoacetate, and lithium iodoacetate by powder diffraction", *Acta Cryst.* **1999**, *B55*, 517-524.
- 5) K. Schwarz, M. Epple "A detailed characterization of polyglycolide prepared by solid-state polycondensation reaction", *Macromol. Chem. Phys.* **1999**, *200*, 379-388.
- 6) M. Epple, O. Herzberg, F. Peters, K. Schwarz "Mikrostrukturiertes Polyglycolid als biomedizinischer Wirkstoff", in N.M. Meenen, A. Katzer, J.M. Rueger "Zelluläre Interaktion mit Biomaterialien", *Hefte zur Zeitschrift "Der Unfallchirurg"*, *278*, Springer, Berlin, Heidelberg, **2000**, 22-27.
- 7) F. Peters, K. Schwarz, M. Epple "The structure of bone studied with synchrotron X-ray diffraction, X-ray absorption spectroscopy and thermal analysis", *Thermochim. Acta* **2000**, *361*, 131-138.
- 8) W. Linhart, F. Peters, W. Lehmann, K. Schwarz, A.F. Schilling, M. Amling, J.M. Rueger, M. Epple "Biologically and chemically optimized composites of carbonated apatite and polyglycolide as bone substitution materials", *J. Biomed. Mater. Res.* **2000**, *54*, 162-171.
- 9) A.L.C. Lagoa, H.P. Diogo, M. P. Dias, M.E.M. da Piedade, L.M.P.F. Amaral, M.A.V.R. da Silva, J.A.M. simoes, R.C. Guedes, B.J.C. Cabral, K.Schwarz, M. Epple, "Energetics of C-Cl, C-Br, and C-I bonds in haloacetic acids. Enthalpies of formation of XCH₂COOH (X = Cl, Br, I) compounds and of the carboxymethyl radical", *Chem. Eur. J.* **2001**, *7*, 483-489.

Other publications

- 1) M. Epple, B. Hasse, K. Schwarz, H. Ehrenberg "Determination of the crystal structure of lithium bromoacetate from high-resolution X-ray powder diffraction data", *HASYLAB Jahresbericht* **1997**, 542-543.
- 2) M. Epple, B. Hasse, O. Herzberg, K. Schwarz, H. Ehrenberg, K.D.M. Harris, L. Elizabé, B.M. Kariuki, J.M. Thomas "Die Kristallchemie von Halogenacetaten: Ein Beitrag zur Reaktivität von Festkörpern", *Z. Krist.(Suppl.)* **1998**, 15, 84.
- 3) M. Epple, F. Peters, K. Schwarz, G. Delling "The structure of bone mineral and bone substituent materials probed by synchrotron X-ray diffraction", *HASYLAB Jahresbericht* **1998**, 591-592.
- 4) M. Epple, F. Peters, K. Schwarz, G. Delling "The structure of bone mineral and bone substituent materials probed by X-ray absorption spectroscopy", *HASYLAB Jahresbericht* **1998**, 825-826.
- 5) W. Linhart, W. Lehmann, K. Schwarz, F. Peters, M. Epple, J.M. Rueger "In vitro Charakterisierung der Biokompatibilität neuer Knochenersatzmaterialien aus Polyglycolid und definierten Calciumphosphaten", in: Hertel P., Rehm K. E. (Hrsg): *Hefte zu der Unfallchirurg*, 63. Jahrestagung der Deutschen Gesellschaft für Unfallchirurgie e. V., 17. – 20. November 1999, Berlin, Abstracts 275/**1999**; 242.
- 6) W. Linhart, F. Peters, W. Lehmann, K. Schwarz, M. Amling, M. Siedler, J. M. Rueger, M. Epple "New scaffolds for tissue engineering: biocompatible composites of carbonated apatite and biodegradable polyesters", *Cells Tissues Organs* **2000**, 166, 73.
- 7) W. Linhart, W. Lehmann, K. Schwarz, F. Peters, M. Siedler, M. Epple, M. Amling, J.M. Rueger "Entwicklung eines biodegradierbaren Knochenersatzmaterials aus Carbonatapatit und Poly-3-Hydroxybutyrat", *Osteologie Band 9/Supplement 1* **2000**; 2.
- 8) W. Linhart, W. Lehmann, D.W. Sommerfeldt, K. Schwarz, F. Peters, M. Epple, M. Amling, J.M. Rueger "Untersuchungen zur osteoblastenspezifischen Biokompatibilitätsprüfung unterschiedlicher Knochenersatzmaterialien", *Osteologie Band 9/Supplement 1* **2000**; 4.

Main oral presentations

- 1) Jahrestagung der Gesellschaft für Thermische Analyse (GEFTA), Berlin, 24.09.-26.09.1997, "Biomimetische Kristallisation in einer porösen Polymermatrix", mit O. Herzberg und M. Epple.
- 2) VIII. Tagung der Chirurgischen Arbeitsgemeinschaft für Biomaterialien der Deutschen Gesellschaft für Chirurgie: "Neue Biomaterialien in der Unfallchirurgie", Hannover, 05.12.1998, "Neue potentielle Biomaterialien: Poröse Komposit-Werkstoffe aus Polyglycolid und definierten Calciumphosphaten", mit M. Amling, G. Delling, F. Peters, A. Rücker, J.M. Rueger, D. v. Stechow und M. Epple.
- 3) Workshop "Grundlagen der Biomineralisation: Das Feststoffsystem Kollagen/Apatit", Sellamatt, Churfürsten, 01.03.-03.03.1999, "Das Composit Polyglycolid-Calciumphosphat als Modellsystem für natürlichen Knochen", mit F. Peters und M. Epple.
- 4) 2. Norddeutsches Doktoranden - Kolloquium, Hamburg, 08.10.-09.10.1999, "Festkörperchemie und Chirurgie: Kompositmaterialien aus biologisch abbaubaren Polyestern und körperähnlichem Calciumphosphat als Knochenersatzmittel", mit F. Peters, M. Epple, W. Linhart, W. Lehmann, M. Amling, J.M. Rueger.

Poster contributions

- 1) Jahrestagung der GDCh-Fachgruppe Umweltchemie und Ökotoxikologie: "Wege und Beiträge der Chemie zum Sustainable Development: Stoffe und Umwelt", Heidelberg, 03.11.-04.11.1997, "Mikroporöses Polyglycolid — ein verbesserter biologisch abbaubarer Polyester", mit O. Herzberg and M. Epple.
- 2) 6. Jahrestagung der Deutschen Gesellschaft für Kristallographie (DGK), Karlsruhe, 02.03.-05.03.1998, "Die Kristallchemie von Halogenacetaten: Ein Beitrag zur Reaktivität von Festkörpern", mit B. Hasse, O. Herzberg, M. Epple, H. Ehrenberg, K.D. M. Harris, L. Elizabé, B.M. Kariuki und J.M. Thomas.
- 3) Jahrestagung der Gesellschaft für Thermische Analyse (GEFTA), Stuttgart, 04.06.-05.06.1998, "Verbrennungskalorimetrische Untersuchungen an Halogenacetaten und an Magnesiumalkoholaten", mit O. Herzberg, M. Epple und S.M. Sarge.
- 4) 5th International Scientific Workshop on Biodegradable Plastics and Polymers, Stockholm, 09.06.-13.06.1998, "A solid-state chemical way to aliphatic polyesters", mit M. Epple.
- 5) 15th IUPAC Conference on Chemical Thermodynamics, Porto/Portugal, 26.07.-01.08.1998, "Standard molar enthalpy of formation of $\text{ClCH}_2\text{COONa}$ in the crystalline state", mit A.L.C. Lagoa, M.E. Minas da Piedade und M. Epple.

- 6) 9.Vortragstagung der GDCh-Fachgruppe Festkörperchemie: Syntheseprinzipien in der Festkörperchemie, Saarbrücken, 23.-25.09.1998, "Poröse Polymere: Neue Medien für diffusionskontrollierte Kristallisationsprozesse", mit F. Peters, B. Hasse und M. Epple.
- 7) 9.Vortragstagung der GDCh-Fachgruppe Festkörperchemie: Syntheseprinzipien in der Festkörperchemie, Saarbrücken, 23.-25.09.1998, "Rationales Design von Knochenersatzmaterialien in der Medizin: Beiträge der Festkörperchemie", mit F. Peters und M. Epple.
- 8) XVIIIth Congress and General Assembly of the International Union of Crystallography, Glasgow, UK, 04.-13.08.1999, "Biomimetic growth of calcium phosphates in and on porous polymers", mit F. Peters und M. Epple.
- 9) Deutscher Orthopäden-Kongreß 1999, Wiesbaden, 14.-17.10.1999, "Knochenersatzmaterialien: Neue Komposit-Werkstoffe aus Polyglycolid und definierten Calciumphosphatphasen", mit D. v. Stechow, A. Rücker, M. Amling, W. Linhart, G. Delling, F. Peters, M. Epple und J.M. Rueger.
- 10) 2nd BioValley Tissue Engineering Symposium", Freiburg i. Br., 25.-26.11.1999, "New scaffolds for tissue engineering: biocompatible composites of carbonated apatite and biodegradable polyesters", mit W. Linhart, W. Lehmann, M. Amling, J. M. Rueger, F. Peters, M. Epple und M. Siedler.
- 11) Sixth World Congress on Biomaterials, Hawaii, USA, 15.-20.05.2000, "Porous polyesters from solid-state reaction", mit M. Epple und M. Siedler.

Lebenslauf (Biography)***Persönliche Daten***

Name	Karsten Schwarz
Geburtsdatum	04.02.1972
Geburtsort	Marne
Familienstand	ledig
Staatsangehörigkeit	deutsch

Schulische Ausbildung

1978 - 1982	Besuch der Grundschule Süderhastedt
1982 - 1991	Besuch der Meldorfer Gelehrtenschule, Meldorf
08.06.1991	Abitur

Universitäre Ausbildung

01.10.1991	Beginn des Chemie-Studiums an der Universität Hamburg
20.10.1993	Diplomvorprüfung
Jan.-März 1994	Praktikumsaufenthalt an der University of Newcastle, Newcastle-upon-Tyne (GB), (Erasmus-Stipendium)
Nov. 1996	Mündliche Diplomhauptprüfungen
Dez. 1996 - Aug. 1997	Diplomarbeit „Thermisch initiierte Synthese von Polyestern aus Halogencarboxylaten und Füllung von porösem Polyglycolid mit Mineralien“, im Arbeitskreis Prof. Dr. Reller/ Dr. Epple, Institut für Allgemeine und Angewandte Chemie, Universität Hamburg
20.08.1997	Zuerkennung des Diploms
Aug. 1997	Aufnahme der Dissertation „Polyesters from solid-state precursors – basic components of a biomedical materials concept“, im Arbeitskreis Prof. Dr. Epple, Institut für Allgemeine und Angewandte Chemie, Universität Hamburg
Okt. 1997 - Dez. 1998	Wissenschaftlicher Mitarbeiter am Institut für Anorganische und Angewandte Chemie, Universität Hamburg
Seit Jan. 1999	Stipendiat im DFG-Graduiertenkolleg 476 "Molekularbiologie der Osteolyse"

Erklärungen (Declarations)

Hiermit versichere ich eidesstattlich, dass ich die vorliegende Arbeit selbständig verfasst und keine außer den angegebenen Hilfsmitteln und Quellen verwendet habe.

Hamburg, im April 2001

Karsten Schwarz

Hiermit erkläre ich eidesstattlich, dass ich keine weiteren Promotionsversuche unternommen habe.

Hamburg, im April 2001

Karsten Schwarz